



**Characterization of a novel phage-encoded  
actin-like protein and the function of the ChrSA  
two-component system in *Corynebacterium  
glutamicum***

A dissertation submitted to the  
Mathematisch-Naturwissenschaftliche Fakultät  
of the Heinrich-Heine-Universität Düsseldorf

presented by  
Antonia Heyer  
born in Neuss

Jülich, May 2013



The thesis in hand has been performed at the Institute of Bio- and Geosciences, IBG-1: Biotechnology, Forschungszentrum Jülich, from May 2010 until May 2013 under the supervision of Jun.-Prof. Dr. Julia Frunzke.

Printed with acceptance of the Mathematisch-Naturwissenschaftliche Fakultät  
of the Heinrich-Heine-Universität Düsseldorf.

Examiner: Jun.-Prof. Dr. Julia Frunzke  
Institute of Bio- and Geosciences,  
IBG-1: Biotechnology  
Forschungszentrum Jülich

Coexaminer: Prof. Dr. Rolf Wagner  
Department of Biophysics  
Heinrich-Heine-Universität Düsseldorf



Results described in this dissertation have been published in the following original publications:

**Heyer, A.**, Gärtner, K., Kalinowski, J., and Frunzke, J. **(2013)** Unveiling regulatory circuits of prophage CGP3 in *Corynebacterium glutamicum* – Characterization of the phage-encoded regulator Cg2040. **to be submitted.**

Donovan, C.\*, **Heyer, A.\***, Polen, T., Wittmann, A., Krämer, R., Frunzke, J., and Bramkamp, M. **(2013)** A prophage-encoded actin-like protein required for efficient viral DNA replication in bacteria. *Current Biology*, **submitted.**

Grünberger, A., Probst, C., **Heyer, A.**, Wiechert, W., Frunzke, J., and Kohlheyer, D. (2013) Microfluidic Picoliter Bioreactor for Microbial Single Cell Analysis: Fabrication, System Setup and Operation. *JoVE*, **accepted.**

**Heyer, A.**, Gätgens, C., Hentschel, E., Kalinowski, J., Bott, M., and Frunzke, J. **(2012)** The two-component system ChrSA is crucial for haem tolerance and interferes with HrrSA in haem-dependent gene regulation in *Corynebacterium glutamicum*. *Microbiology* **158**, 3020-3031.

Results of further projects not discussed in this thesis have been published in:

Lausberg, F., Chattopadhyay, A. R., **Heyer, A.**, Eggeling, L., and Freudl, R. **(2012)**. A tetracycline inducible expression vector for *Corynebacterium glutamicum* allowing tightly regulable gene expression. *Plasmid* **68**, 142-147.

\*The authors contributed equally to this work.



# Content

<b>1</b>	<b>Summary.....</b>	<b>1</b>
1.1	Summary English .....	1
1.2	Summary German .....	2
<b>2</b>	<b>Introduction .....</b>	<b>3</b>
2.1	Phages – a paradigm for gene regulation .....	3
2.1.1	Bistable switch between the lysogenic and the lytic state .....	4
2.1.2	Prophage induction upon stressful conditions .....	4
2.2	Phages in <i>Corynebacterium glutamicum</i> .....	5
2.2.1	<i>C. glutamicum</i> in biotechnology .....	5
2.2.2	Bacteriophages in corynebacteria .....	5
2.2.3	Prophage CGP3 of <i>C. glutamicum</i> ATCC 13032 .....	6
2.3	Cytoskeletal Proteins .....	7
2.3.1	Occurrence in eukaryotic and prokaryotic cells.....	7
2.3.2	Chromosome partitioning systems.....	8
2.3.3	Partitioning systems of mobile elements .....	8
2.3.4	Cytoskeletal proteins in <i>C. glutamicum</i> .....	9
2.4	Heme homeostasis in <i>C. glutamicum</i> .....	10
2.5	Aims of this work .....	11
<b>3</b>	<b>Results .....</b>	<b>12</b>
3.1	Unveiling regulatory circuits of prophage CGP3 in <i>Corynebacterium glutamicum</i> – Characterization of the phage-encoded regulator Cg2040 .....	14
3.2	A prophage-encoded actin-like protein required for efficient viral DNA replication in bacteria .....	25
3.3	Microfluidic Picoliter Bioreactor for Microbial Single Cell Analysis: Fabrication, System Setup and Operation .....	41
3.4	The two-component system ChrSA is crucial for haem tolerance and interferes with HrrSA in haem-dependent gene regulation in <i>Corynebacterium glutamicum</i> .....	57

<b>4</b>	<b>Discussion .....</b>	<b>70</b>
4.1	Prophage induction of CGP3.....	70
4.1.1	Activation of CGP3 upon induction of the SOS response .....	70
4.1.2	The Cro/Ci-type regulator Cg2040.....	72
4.2	The prophage-encoded actin-like protein AlpC.....	74
4.2.1	Filament formation of the actin-like protein AlpC.....	74
4.2.2	The putative adaptor protein AlpA.....	75
4.2.3	Influence of AlpA and AlpC on CGP3 life cycle.....	77
4.2.4	AlpAC in comparison to other phage-encoded cytoskeletal proteins.....	79
4.3	Heme homeostasis in <i>C. glutamicum</i> .....	81
4.3.1	Link between CGP3 induction and iron/heme homeostasis .....	81
4.3.2	Heme-dependent TCS.....	82
4.3.3	Interaction of ChrSA and HrrSA .....	82
<b>5</b>	<b>References .....</b>	<b>85</b>
<b>6</b>	<b>Appendix.....</b>	<b>93</b>
6.1	Additional Figures – AlpC.....	93
6.2	Supplemental Material – Cg2040 .....	95
6.3	Supplemental Material – AlpC.....	99
6.4	Supplementary Material – ChrSA .....	102
6.5	A tetracycline inducible expression vector for <i>Corynebacterium glutamicum</i> allowing tightly regulable gene expression .....	108

## Abbreviations

Amp <sup>R</sup>	Ampicillin resistance
ATCC	American Type Culture Collection
BHI(S)	Brain Heart Infusion (+ Sorbitol)
CFP	cyan fluorescence protein
ssDNA	single-stranded DNA
DNase	desoxyribonuclease
DTT	Dithiothreitol
EMSA	electrophoretic mobility shift assay
<i>et al.</i>	<i>et alii</i>
HTH	helix-turn-helix
IPTG	Isopropyl- $\beta$ -D-thiogalactopyranosid
Kan <sup>R</sup>	Kanamycin resistance
MBP	Maltose-binding protein
MIAME	minimum information about a microarray experiment
MmC	mitomycin C
OD <sub>600</sub>	optical density at 600 nm
PLBR	picoliter bioreactor
qPCR	quantitative polymerase chain reaction
RBS	ribosome binding site
Spec <sup>R</sup>	Spectinomycin resistance
TBE	Tris base – boric acid - EDTA
TCS	two-component system
TEV	Tobacco etch virus
TNI	Tris base – NaCl - imidazole
TSS	transcriptional start site
v/v	volume per volume
WT	wild type
w/v	weight per volume
eYFP	enhanced yellow fluorescent protein

Further abbreviations not included in this section are according to international standards, as for example listed in the author guidelines of *FEBS Journal*.



## Author contributions

### **Unveiling regulatory circuits of prophage CGP3 in *Corynebacterium glutamicum* – Characterization of the phage-encoded regulator Cg2040**

AH and JF designed the studies for characterization of Cg2040. KG was involved in construction of the expression vector and produced and purified the protein. She also performed first protein-DNA interaction studies supervised by AH and JF. RNA sequencing was conducted by JK. All remaining experiments were performed by AH. The manuscript was written by AH and JF.

### **A prophage-encoded actin-like protein required for efficient viral DNA replication in bacteria**

The biochemical characterization of AlpC, time-lapse imaging and co-localization studies was designed by CD and supervised by RK and MBr. The experimental work for this part was performed by CD and AW. CD and MBr wrote the respective parts of the manuscript. Transcriptome analysis of stressed cells, quantitative PCR of circular phage DNA as well as the characterization of AlpA were designed and performed by AH and supervised by JF. TP assisted in analysis of transcriptome data. AH and JF wrote the respective parts of the manuscript.

### **Microfluidic Picoliter Bioreactor for Microbial Single Cell Analysis: Fabrication, System Setup and Operation**

The design and fabrication of the microfluidic picoliter bioreactor was performed by AG, CP, supervised by DK. The cultivation of microbial strains in shake flasks in preparation for seeding was conducted by AH. Experimental setup, time-lapse imaging and analysis were performed by AG. The manuscript was written by AG and DK, assisted by CF, AH, JF and WW.

### **The two-component system ChrSA is crucial for haem tolerance and interferes with HrrSA in haem-dependent gene regulation in *Corynebacterium glutamicum*.**

AH and JF designed the study which was supervised by JF. The experimental work was performed by AH and CG and EH performed the studies with promoter fusions. JK conducted RNA sequencing. AH performed the analysis of the data and wrote the manuscript together with JF, assisted by EH and MBo.

### **A tetracycline inducible expression vector for *Corynebacterium glutamicum* allowing tightly regulable gene expression**

FL and RF designed the study and experimental work was performed by FL and AC. AH constructed a first tetR inducible vector in previous work and provided this vector for further constructions. The manuscript was written by FL and RF. AC, AH and LE assisted in writing the manuscript.

AH: Antonia Heyer, JF: Julia Frunzke, KG: Kim Gärtner, JK: Jörn Kalinowski, CD: Catriona Donovan, RK: Reinhard Krämer, MBr: Marc Bramkamp, AW: Anja Wittmann, TP: Tino Polen, AG: Alexander Grünberger, CP: Christopher Probst, DK: Dietrich Kohlheyer, WW: Wolfgang Wiechert, CG: Cornelia Gätgens, EH: Eva Hentschel, MBo: Michael Bott, FL: Frank Lausberg, RF: Roland Freudl, LE: Lothar Eggeling



# 1 Summary

## 1.1 Summary Englisch

Genome sequencing has revealed prophages or phage remnants in almost all organisms. However, only a fraction has been characterized to date. Upon infection of a bacterial host, temperate bacteriophages can either follow the lytic response, leading to the assembly of new virions, or the dormant, lysogenic response, in which the phage usually resides integrated into the genome of the host (prophage). In *Corynebacterium glutamicum* ATCC 13032, an important industrial amino acid producer, the prophage CGP3 was found to be spontaneously induced in a subpopulation, even in the absence of a specific trigger. However, nothing was known with respect to the stimulus triggering CGP3 induction and the regulatory proteins involved in this process. In this work, CGP3 induction was investigated and a novel prophage-encoded actin-like protein (AlpC) was characterized regarding its role in the phage life cycle. In an independent part of this work, the function of the two-component system (TCS) ChrSA in heme homeostasis in *C. glutamicum* was unraveled.

In the first part of this thesis, it was shown that the induction of the CGP3 prophage is linked to the host SOS response, as it has been reported for several phages. In the case of the model phage lambda of *Escherichia coli*, CI is the central regulator controlling the stable lysogenic state. In this work, the CGP3-encoded, transcriptional regulator Cg2040 of the Cro/CI family was characterized. EMSA studies and transcriptome analysis demonstrated that Cg2040 binds within the promoter region of *cg2040*, thereby, repressing its own expression and the transcription of the adjacent genes *cg2033-cg2040*, encoding mostly hypothetical proteins. However, deletion or overexpression of *cg2040* showed no significant influence on CGP3 induction. Therefore, it was proposed that Cg2040 does not represent the central phage repressor of CGP3, but may be involved in the downstream cascade.

A major focus of this work was the characterization of the novel actin-like protein Cg1890 (AlpC), which was identified in a phylogenetic study, and is, in fact, encoded by the first open reading frame next to CGP3 *attR*. A time-resolved transcriptome analysis revealed *alpC* among the early phage genes, highly induced upon prophage induction. In native concentrations, AlpC polymerizes by ATP/GTP hydrolysis into straight filaments pointing at varying angles to the cell membrane. The co-transcribed gene *alpA* (*cg1891*) has been proposed to code for a putative adaptor protein which couples phage DNA to AlpC filaments. EMSA studies revealed that AlpA binds in the promoter region of the operon *alpAC* (designated as *alpS*). *In vivo*, AlpA is often (87%) associated with an AlpC filaments. Thus, a first evidence for interaction of AlpC and AlpA was provided. In fluorescence microscopy studies using a strain with eYFP-labeled phage DNA, CGP3 DNA was detected at AlpC filaments or frequently close to the cell membrane. Deletion of *alpC* or *alpA* was shown to have a severe impact on phage DNA replication. Based on these data, a model has been postulated in which AlpC mediates efficient transport of CGP3 DNA to the cell membrane, where phage replication might take place.

Previous studies suggested a connection between CGP3 activity and iron homeostasis. Therefore, the function of the TCS ChrSA in heme homeostasis was studied in an independent part of this work. Transcriptome analysis of mutant strains and EMSA studies revealed the divergently located operon *hrtBA*, encoding a heme-detoxifying ABC transporter, as direct target activated by the response regulator ChrA. Consequently, deletion of *chrSA* or *hrtBA* resulted in an increased sensitivity towards heme. Furthermore, these studies revealed that ChrA autoregulates its own expression and, remarkably, represses the expression of the homologous response regulator *hrrA*. Altogether, the presented results provided evidence for a complex interaction of the TCS HrrSA and ChrSA in heme-dependent gene regulation in *C. glutamicum*.

## 1.2 Summary German

Durch Genomsequenzierungen konnten Prophagen und Phagenüberreste in fast jedem Organismus identifiziert werden, jedoch wurde bisher nur ein Bruchteil charakterisiert. Bei der Infektion eines Bakterienwirts, können temperente Bakteriophagen den lytischen Weg, der zur Assemblierung neuer Virionen führt, oder den inaktiven, lysogenen Weg verfolgen, bei dem der Phage meist integriert im Genom des Wirts (Prophage) verbleibt. In dem wichtigen Aminosäureproduzenten *Corynebacterium glutamicum* ATCC 13032 wurde der Prophage CGP3 in einer Subpopulation auch ohne einen spezifischen Auslöser spontan induziert vorgefunden. Über den Stimulus, der die CGP3 Induktion auslöst, und die an diesem Prozess beteiligten, regulatorischen Proteine war jedoch nichts bekannt. In dieser Arbeit, wurde die CGP3 Induktion untersucht und ein neues Prophagen-kodiertes Aktin-ähnliches Protein (AlpC) bezüglich seiner Funktion im Lebenszyklus des Phagen charakterisiert. In einem unabhängigen Teil dieser Arbeit wurde die Funktion des Zwei-Komponenten Systems (ZKS) ChrSA in der Häm-Homöostase in *C. glutamicum* aufgeklärt.

Im ersten Teil der Arbeit wurde gezeigt, dass die Induktion des Prophagen CGP3 mit der SOS Antwort verlinkt ist, wie es bereits für mehrere Phagen nachgewiesen wurde. Für den Phagen Lambda in *Escherichia coli* ist CI der zentrale Regulator, der den stabilen lysogenen Status kontrolliert. In dieser Arbeit wurde der CGP3-kodierte, transkriptionelle Regulator Cg2040 aus der Cro/CI Familie charakterisiert. Mittels EMSA Studien und Transkriptom-Analysen wurde gezeigt, dass Cg2040 in der Promotorregion von cg2040 bindet und dadurch seine eigene Expression und die Transkription der benachbarten Gene cg2033-cg2040 reprimiert, die überwiegend hypothetische Proteine kodieren. Allerdings zeigte die Deletion oder Überexpression von cg2040 keinen signifikanten Einfluss auf die CGP3 Induktion. Daher wurde angenommen, dass Cg2040 nicht den zentralen Repressor von CGP3 darstellt, aber in der nachfolgenden Kaskade involviert sein könnte.

Ein Schwerpunkt dieser Arbeit war die Charakterisierung des neuen Aktin-ähnlichen Proteins Cg1890 (AlpC), das in einer phylogenetischen Studie identifiziert wurde und durch den ersten offenen Leserahmen hinter CGP3 *attR* kodiert ist. Eine zeitlich aufgelöste Transkriptomanalyse zeigte, dass *alpC* zu den frühen Phagengenen gehört und nach der Prophagen Induktion stark induziert ist. AlpC polymerisiert in nativer Konzentration durch ATP/GTP Hydrolyse in gerade Filamente mit unterschiedlicher Ausrichtung zur Zellmembran. Es wurde vermutet, dass das gemeinsam transkribierte Gen *alpA* (cg1891) ein putatives Adapterprotein kodiert, das die Phagen DNA mit den AlpC Filamenten verbindet. Durch EMSA Studien wurde eine Bindung von AlpA in der Promotorregion des *alpAC* Operons nachgewiesen (als *alps* bezeichnet). AlpA ist *in vivo* oft (zu 87%) mit einem AlpC Filament assoziiert, was einen ersten Hinweis auf eine Interaktion zwischen AlpC und AlpA darstellt. Eine fluoreszenzmikroskopische Studie, bei der ein Stamm mit eYFP markierter Phagen DNA verwendet wurde, lokalisierte die CGP3 DNA an AlpC Filamenten oder häufig in der Nähe der Zellmembran. Es wurde nachgewiesen, dass die Deletion von *alpC* oder *alpA* einen bedeutenden Einfluss auf die Phagen Replikation hat. Aufgrund dieser Daten wurde ein Modell aufgestellt, in dem AlpC den effizienten Transport von CGP3 DNA zur Zellmembran vermittelt, an der die Replikation stattfinden könnte.

Vorherige Studien deuteten auf einen Zusammenhang zwischen CGP3 Aktivität und Eisen-Homöostase hin. Daher wurde die Funktion des ZKS ChrSA in der Häm-Homöostase in einem unabhängigen Teil dieser Arbeit untersucht. Durch Transkriptomanalysen von mutierten Stämmen und EMSA Studien wurde das divergent lokalisierte Operon *hrtBA*, das einen Häm-detoxifizierenden ABC Transporter kodiert, als direktes, durch den Antwortregulator ChrA aktiviertes Ziel identifiziert. Folglich führte die Deletion von *chrSA* oder *hrtBA* zu einer erhöhten Häm-Sensitivität. Des Weiteren zeigten diese Experimente, dass ChrA seine eigene Expression autoreguliert und außerdem die Expression des homologen Antwortregulators *hrrA* reprimiert. Die dargestellten Ergebnisse weisen insgesamt auf eine komplexe Interaktion der ZKS HrrSA und ChrSA in der Häm-abhängigen Genregulation in *C. glutamicum* hin.

## 2 Introduction

### 2.1 Phages – a paradigm for gene regulation

Viruses that infect bacteria (bacteriophages) represent a substantial and highly diverse majority of organisms. Due to horizontal gene transfer, phages and their hosts have evolved in close interaction with each other (Hatfull & Hendrix, 2011). Genome sequencing revealed phages or phage remnants in a majority of organisms (Casjens, 2003). In fact, the human genome contains about 8% retroviral genes (Lander *et al.*, 2001) and some bacterial genomes consist of up to 20% bacteriophage DNA (Casjens, 2003). The first bacteriophages were discovered by Frederick Twort (1915) and Felix D'Herelle (1917), who came up with the idea to administer bacteriophages therapeutically (Twort, 1915; D'Herelle, 2007). Nowadays, phage therapy displays a promising alternative to the therapeutic use of antibiotics (Lu & Koeris, 2011). Two different types of phages can be distinguished: Lytic phages assemble new phage progeny immediately after infection, which are then spread by cell lysis, whereas temperate phages can also reside as a prophage in a dormant state (lysogen or lysogenic response), integrated into the genome of their host or as heritable plasmids in the bacterial cell (Fig. 2.1) (Campbell, 1994).

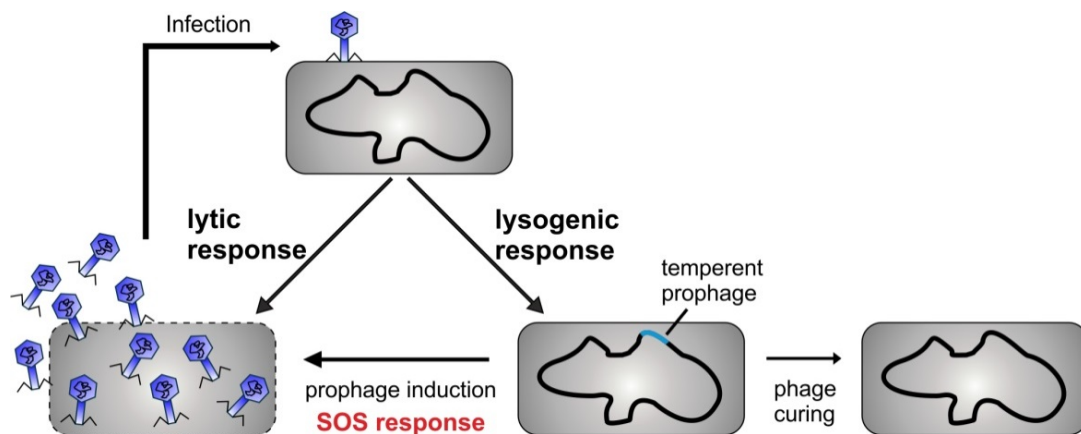


**Fig. 2.1 Infection by a temperate bacteriophage.** Upon infection the alternatives are integration of the phage DNA into the host genome (lysogenic response) or replication, virion assembly, and release of mature viruses (lytic response). Under stressful conditions, the lysogenic state can be switched to the lytic response. Adapted from (Oppenheim *et al.*, 2005).

A well characterized temperate phage that represents a model for studies of gene regulation is the phage  $\lambda$  of *Escherichia coli* (Lederberg, 1951). When the temperate phage  $\lambda$  infects *E. coli* cells, phage  $\lambda$  can choose the lytic response, in which the new virions are assembled accompanied by cell lysis, or the lysogenic response as described above. Each state is very stable (bistable switch) and the decision between both responses depends on the physiological state of the host (Dodd *et al.*, 2005). In rare

cases, the lytic or lysogenic response is abortive and phage DNA is lost (phage curing) (Oppenheim *et al.*, 2005).

### 2.1.1 Bistable switch between the lysogenic and the lytic state

Upon infection by phage  $\lambda$ , its DNA is introduced into the *E. coli* cell. First of all, early phage genes *N* and *cro* are expressed from the promoters  $P_L$  and  $P_R$ , respectively. Cro acts as a weak repressor for the promoters  $P_L$  and  $P_R$  and thereby supports the initial decision for the lytic pathway. An antitermination mediated by the protein N results in the expression of delayed early genes for the initiation of phage DNA replication, and late genes of the lytic pathway (Szambowska *et al.*, 2011; Hayes *et al.*, 2013; Friedman & Court, 1995). The gene *cII* is also among the delayed early genes and encodes a critical regulator of the lysogenic state. CII activates the expression of *ci* from the promoter  $P_{RE}$  (Kobiler *et al.*, 2005; Kobiler *et al.*, 2007; Rokney *et al.*, 2008). Furthermore, CII also activates the expression of the integrase, *int*, which is responsible for integration of  $\lambda$  DNA into the host genome at the attachment site. Due to its activating function of lysogenic genes, the level of CII is critical for the decision between the lytic state and lysogeny.

The phage repressor CI is required for stable maintenance of lysogeny (Benson *et al.*, 1988, Kaiser, 1957). CI can occupy three binding sites inside each operator  $O_R$  and  $O_L$  within the promoters  $P_R$  and  $P_L$ . Thereby CI represses the transcription at these two promoters (Hochschild & Lewis, 2009, Oppenheim *et al.*, 2005). Additionally, CI dynamically regulates its own expression level and ensures a stable lysogenic state. Interestingly, the regulator Cro recognizes the same three binding sites of the operators, but with opposing binding affinity (Benson & Youderian, 1989). Both regulators share a structural homology and belong to the same family of regulators (Pfam PF01381) (Ohlendorf *et al.*, 1983). The DNA-binding domain is located at the N-terminus of the proteins and the C-terminus is required for oligomerization. The role of Cro during development of the lytic state is not completely understood and controversially discussed (Oppenheim *et al.*, 2005; Schubert *et al.*, 2007; Svenningsen *et al.*, 2005). Nevertheless, when CI sufficiently represses the expression of promoter  $P_R$  and  $P_L$ , proteins favoring the lytic way are not produced and the lysogenic state is stable.

### 2.1.2 Prophage induction upon stressful conditions

Events that change the level of the lambda repressor CI can induce the prophage and switch the lysogenic state to lytic development. This switch is often directly or indirectly triggered by the SOS response, but can also occur in the absence of an external stimulus as spontaneous prophage induction. Exposure to UV radiation or treatment with antimicrobial agents such as mitomycin C (Tomasz, 1995) can lead to DNA double-strand breaks or single-stranded DNA (ssDNA). The appearance of ssDNA or stalled replication forks causes filament formation of RecA at the ssDNA in

an ATP-dependent process. Activated RecA\* catalyzes the autoproteolytic cleavage of the SOS master regulator LexA as a co-protease (Little, 1984; Little, 1991). In *E. coli*, LexA is involved in the repression of several genes encoding DNA repair proteins (e.g. UvrA, UvrB), by binding to an SOS box located in their respective promoter regions. Among the SOS targets are also genes for the cell cycle arrest (SulA or DivS) and genes for error-prone polymerases (UmuD, UmuC) (Ogino *et al.*, 2008; Little & Mount, 1982). Furthermore, RecA itself is involved in DNA repair and homologous recombination (Little & Mount, 1982). The RecA\* mediated autodigestion inactivates LexA and is followed by derepression of LexA target genes, which in turn initiates the SOS response. By different binding affinities of LexA to the SOS boxes, a cascade-like response is modulated (Courcelle *et al.*, 2001). Once the DNA damage is repaired, the SOS response is switched off. The expression of *lexA* and *recA* returns to basal level as the expression of these genes is regulated by LexA.

Upon induction of the SOS response, the phage lambda repressor CI represents another target of activated RecA\* filaments (Little, 1984; Galkin *et al.*, 2009). CI mimics the cleavage site of LexA, but the rate of cleavage is much slower than for LexA. Autoproteolytic degradation of CI leads to a derepression of the promoters P<sub>R</sub> and P<sub>L</sub>, the transcription of lytic genes is activated and the cell enters the lytic pathway. Once the prophage is induced, the lytic pathway cannot be reversed.

## 2.2 Phages in *Corynebacterium glutamicum*

### 2.2.1 *C. glutamicum* in biotechnology

The Gram-positive bacterium *C. glutamicum* was originally isolated during a screen for glutamate-producing bacteria (Kinoshita *et al.*, 1957). Nowadays, *C. glutamicum* represents a platform organism in white biotechnology for production of amino acids, such as L-glutamate (>2 million t/a) and L-lysine (1.5 million t/a) (Eggeling & Bott, 2005; Burkovski, 2008; Ajinomoto, 2011; Ajinomoto, 2012). By metabolic engineering, considerable amounts of other products such as organic acids can be produced (Wieschalka *et al.*, 2013; Bott & Eikmanns, 2013). Furthermore, *C. glutamicum* serves as a model organism for the close pathogenic relatives *Corynebacterium diphtheriae* and *Mycobacterium tuberculosis*.

### 2.2.2 Bacteriophages in corynebacteria

One beneficial feature of *C. glutamicum* for biotechnological processes is the fact that no phages have been reported to interfere with biotechnological processes based on strain *C. glutamicum* ATCC 13032 yet. In several other *C. glutamicum* strains, temperate phages were isolated after treatment with UV radiation (Moreau *et al.*, 1995; Pátek *et al.*, 1985). Most of the identified phages in corynebacteria are temperate phages and the phage particles consist of a polyhedral head and a long, non-contractile tail (Bukovska *et al.*, 2006). The bacteriophage BFK20 is an example for a lytic

phage which was identified in *Brevibacterium flavum* (the former designation for *C. glutamicum*) and characterized in several studies (Bukovska *et al.*, 2006; Koptides *et al.*, 1992; Halgasova *et al.*, 2012; Gerova *et al.*, 2011).

### 2.2.3 Prophage CGP3 of *C. glutamicum* ATCC 13032

In 2003, the genome of *C. glutamicum* ATCC 13032 was sequenced and revealed three integrated prophages (Kalinowski *et al.*, 2003). The two smaller prophages CGP1 (13.5 kbp) and CGP2 (3.9 kbp) are highly degenerated. The prophage CGP3 (187.3 kbp) is one of the largest known prophages and is integrated into a cluster of tRNA genes on the left border and encodes a putative phage integrase at the right border flanked by attachment sites (Fig. 2.2) (Kalinowski, 2005). Typical for phages, only a few genes share sequence similarity with genes of known functions, such as the putative phage integrase or a phage primase. The majority of CGP3 genes encode hypothetical proteins (Frunzke *et al.*, 2008; Kalinowski, 2005). Additionally, the genes encoding a restriction modification system are located in the genomic region of CGP3 (Schäfer *et al.*, 1997). A recent study of our group revealed, that CGP3 can excise from the genome and exists as circular phage DNA. The recombination takes place at the attachment sites flanking the prophage (Frunzke *et al.*, 2008). In a subpopulation of wild type cells (1-3%), a spontaneous induction of the prophage CGP3 was observed in the absence of any inducer, which was often accompanied by lysis of the respective cells. Population heterogeneity caused by prophages is a common phenomenon, however, its trigger and consequences thereof remain unclear (Smits *et al.*, 2006; Veening *et al.*, 2008; St-Pierre & Endy, 2008).

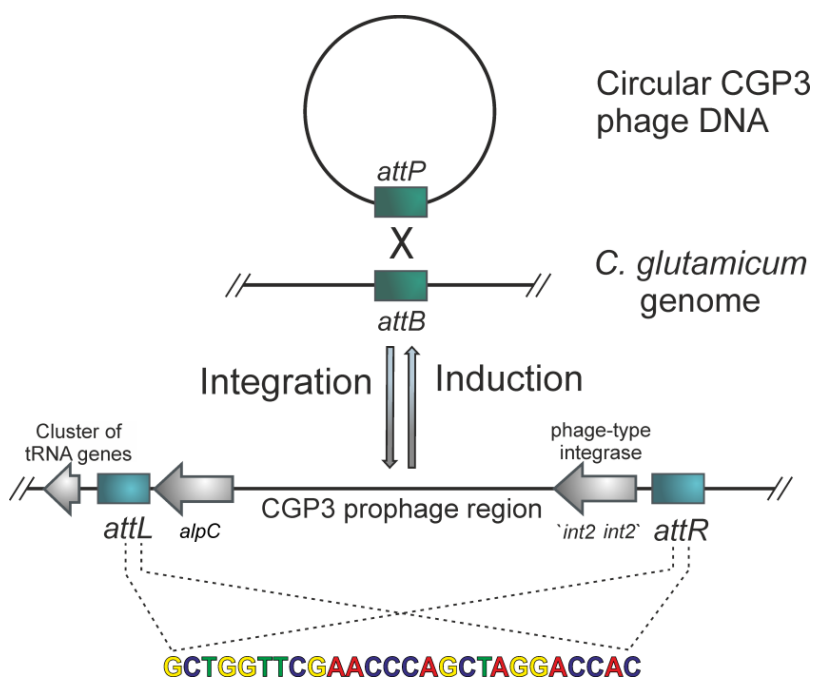


**Fig. 2.2 Model of CGP3 integration and induction in *C. glutamicum*.** The prophage CGP3 is integrated into the genome of *C. glutamicum* ATCC 13032. Upon prophage induction the recombination takes place at the flanking attachment site *attR* and *attL* (sequence is shown below) and CGP3 is excised from the genome. Adapted from (Frunzke *et al.*, 2008).

## 2.3 Cytoskeletal Proteins

### 2.3.1 Occurrence in eukaryotic and prokaryotic cells

The majority of species requires proteins to stabilize their cell membrane, define their cell shape, and coordinate dynamic movements of cellular components in the cell. In eukaryotic cells, the proteins actin, tubulin, and intermediate filaments are known as cytoskeletal proteins that characteristically form dynamic or stable filaments (Graumann, 2007). Actin polymerizes as a helical, right-handed filament and transports vesicles along the cell. Furthermore, actin filaments also facilitate cell movement by formation of pseudopods. Tubulin forms protofilaments that assemble into microtubules. Microtubules mediate the segregation of DNA during cell division, when they are attached to a centromere by kinetochores (Bloom & Joglekar, 2010). Furthermore, vesicles are transported along microtubules by motor proteins. The third group of cytoskeletal proteins, namely intermediate filaments, is involved in strengthening the cellular morphology and in organization and distribution of cell organelles (Herrmann *et al.*, 2009; Eriksson *et al.*, 2009).

For decades, cytoskeletal proteins were thought to be an exclusive feature of eukaryotic cells. However, homologs were also identified in prokaryotic cells and here they are involved in a variety of processes as well. The tubulin-like protein FtsZ promotes formation of a cytokinetic ring (Z-ring) in the middle of the cell by hydrolyzation of GTP. It is also required for recruiting other cell division proteins to form a divisome for septum formation (Lutkenhaus *et al.*, 1980; Lutkenhaus *et al.*, 2012; Huang *et al.*, 2013). FtsZ is highly conserved in bacteria and FtsZ ring formation is controlled by several proteins, such as FtsA and ZipA, which stabilize the ring, or SulA which inhibits FtsZ polymerization upon DNA damage. Interestingly, FtsA is a member of the actin family (Szwedziak *et al.*, 2012).

A well-studied actin-like protein, found in many prokaryotic species, is the membrane-associated protein MreB, which plays a major role in determining the cell shape and in the localization of proteins for cell wall synthesis (Jones *et al.*, 2001; van den Ent *et al.*, 2010). Similarities of MreB to actin are obvious; the crystal structure of MreB revealed conserved domains of two connecting regions, an adenosine motif and two phosphate regions important for ATP hydrolysis (Jones *et al.*, 2001; van den Ent *et al.*, 2001). In magnetotactic bacteria, the actin-like protein MamK organizes the positioning of magnetosomes, which contain magnetite ( $\text{Fe}_3\text{O}_4$ ) enclosed by a membranous cover (Ozyamak *et al.*, 2013). Magnetosomes are aligned in a straight line along the MamK filament and are required for the cell's orientation along the magnetic field (Draper *et al.*, 2011). Finally, crescentin encodes a bacterial intermediate filament-like protein which is essential for cell curvature in *Caulobacter crescentus* (Ausmees *et al.*, 2003).

### 2.3.2 Chromosome partitioning systems

The segregation of bacterial DNA is mediated by a tripartite partitioning system (Gerdes *et al.*, 2000). This system comprises two genes organized in a bicistronic operon, a DNA-binding protein (ParB) and a dynamic cytomotive protein, which can be a Walker A type ATPase (ParA, type I), an actin-like ATPase (ParM, type II), or a tubulin-like GTPase (TubZ, type III) (Schumacher, 2008). The DNA-binding protein ParB binds a centromere-like DNA-binding site (*par*-site) and interacts with ParA (Schumacher *et al.*, 2007; Graumann, 2007). The ParA protein forms helical, dynamic filaments and by interaction of the three components, the replicated chromosomes are segregated to the new cell poles before cell division (Gerdes *et al.*, 2010). The timing between replication, segregation, and cell division is crucial in this process. The ParA homolog Soj in *Bacillus subtilis* regulates the DNA replication initiation protein DnaA (Murray & Errington, 2008), while the corresponding ParB protein, Spo0J, recruits proteins for structural maintenance of chromosomes to the origin of replication (Sullivan *et al.*, 2009). In addition, the ParA-like protein MipZ in *C. crescentus* interacts with ParB and was found to inhibit polymerization of FtsZ, thereby linking segregation and cell division (Thanbichler & Shapiro, 2006).

### 2.3.3 Partitioning systems of mobile elements

Besides chromosomally-encoded partitioning systems, mobile genetic elements often encode their own partitioning systems for maintenance and segregation in similar composition to the chromosomal segregation system. The plasmid R1 encodes the ParMRC system for plasmid segregation during cell division (Fig. 2.3) (Salje *et al.*, 2010). ParM, an actin-like protein (type II plasmid segregation system), forms left-handed and twisted, double-stranded filaments by nucleotide hydrolysis of ATP and shows structural similarities to eukaryotic F-actin (Gayathri *et al.*, 2013). The actin-like polymers are highly dynamic, but can be stabilized by a complex of the *parC* DNA-binding site and ParR, an adaptor protein encoded in an operon with *parM*. ParR dimers polymerize at ten repeating binding motifs in the *parC* site located on the plasmid R1. Previously, models have suggested that the ParR-*parC* complex stabilizes the ParM filament by binding at both ends (Salje & Löwe, 2008; Salje *et al.*, 2010). However, a recent study revealed a bipolar spindle of antiparallel filaments for segregation, in which the ParR-*parC* complex is only bound to one end of ParM (Fig. 2.3) (Gayathri *et al.*, 2012). The other end of ParM is able to undergo degradation and by sliding of two filaments in a bidirectional way, the plasmids are separated and transported to the new cell poles.

Plasmids with a low copy number usually encode type I plasmid segregation systems with a Walker A type ATPase, for example the prophage P1, which is not integrated into the host genome, but remains in the cells as a circular DNA molecule. The ParAB system regulates the accurate distribution

of the plasmid phage P1 into both new daughter cells (Li & Austin, 2002; Sengupta *et al.*, 2010). In case of phage  $\phi 29$  in *B. subtilis*, replication of phage DNA is closely linked to the actin-like protein MreB (Muñoz-Espin *et al.*, 2009). MreB is required for the replication of phage  $\phi 29$  at the membrane. The phage protein p16.7 directly interacts with the membrane-associated MreB protein, thereby stimulating the replication of  $\phi 29$  DNA close to the cell membrane.

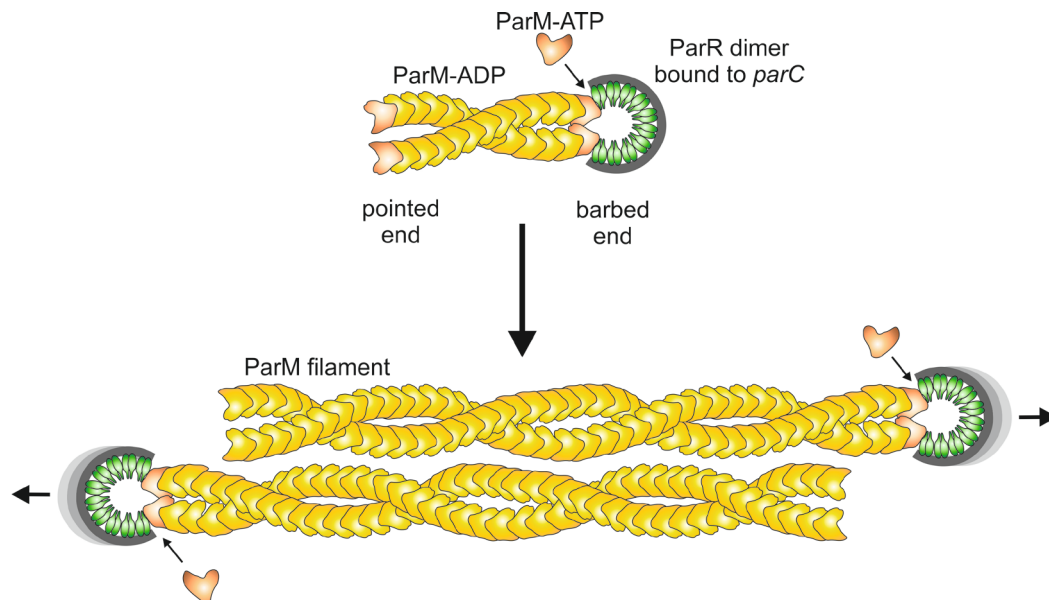


**Fig. 2.3 Bidirectional plasmid partitioning system ParMRC of plasmid R1 in *E. coli*.** ParM forms dynamic actin filaments by hydrolyzation of ATP (ParM-ATP filament state in orange, ParM-ADP in yellow) and is stabilized by a complex of ParR dimers (green) bound to the *parC* site (grey). The filaments are elongated when ParR-*parC* is bound to ParM and paired with a second ParM-ParR-*parC* filament in antiparallel orientation. By sliding of the filaments in a bipolar spindle, the plasmids are separated. Adapted from (Gayathri *et al.*, 2012).

### 2.3.4 Cytoskeletal proteins in *C. glutamicum*

In contrast to other rod-shaped bacteria, *C. glutamicum* lacks the cytoskeletal protein MreB (Letek *et al.*, 2008a). Instead of lateral growth, peptidoglycan is synthesized at the cell poles in *C. glutamicum* (Daniel & Errington, 2003). In cooperation with further cell division proteins, FtsZ assembles a divisome that is important for septum formation, but not necessarily formed in the middle of the cell in *C. glutamicum* (Ramos *et al.*, 2005). The partitioning of the newly synthesized chromosomes is accomplished by the ParAB system. The Walker A type ATPase ParA forms filaments and ParB, which is attached to a centromere-like DNA-binding site, segregates the chromosomes into the daughter cells (Donovan *et al.*, 2010). A further protein PldP was shown to play a role in division site selection. Furthermore, DivIVA is required for temporal coordination of divisome formation and the segregation of the chromosomes (Donovan *et al.*, 2013; Donovan *et al.*, 2012).

## 2.4 Heme homeostasis in *C. glutamicum*

An increased activity of CGP3 was often found in mutants of *C. glutamicum* that are impaired in iron or heme homeostasis, e.g. by deletion of DtxR, the master regulator of iron homeostasis (Frunzke *et al.*, 2008). Iron is an essential trace element in almost all organisms and is an important cofactor involved in major biological processes. However, iron implies also problems of poor solubility and toxicity due to its ability to form radical oxygen species (ROS). To meet this challenge, organisms have evolved sophisticated mechanisms to control the uptake and utilization of iron or heme. DtxR, the master regulator of iron homeostasis in *C. glutamicum*, controls about 60 genes involved in iron acquisition and storage depending on the iron availability (Wennerhold & Bott, 2006; Brune *et al.*, 2006). Among the target genes of DtxR, we identified *hrrA*, the response regulator of the two-component system (TCS) HrrSA. Prototypical TCSs consist of a sensor histidine kinase, which is usually membrane-associated and senses a specific (external) stimulus, and a cognate response regulator (Laub & Goulian, 2007; Gao & Stock, 2009). The regulator is activated by phosphorylation at a conserved aspartate residue and triggers a specific response to the stimulus by regulation of target genes upon binding to the upstream promoter region of the respective genes or operons.

The TCS HrrSA was shown to play a central role in heme homeostasis in *C. glutamicum* (Frunzke *et al.*, 2011). HrrA activates the expression of the heme oxygenase, *hmuO*, which is required for the utilization of heme as an alternative iron source, in a heme-dependent manner (Bibb *et al.*, 2007; Schmitt, 1997). The *hmuO* gene is also repressed by DtxR in its active, iron-bound form. Hence, under iron limiting conditions, the dissociation of DtxR from the promoter of *hrrA* enables utilization of heme as an alternative iron source. When iron is sufficient, the repression of *hmuO* by DtxR probably inhibits heme degradation. Besides *hmuO*, HrrA activates further genes encoding heme-containing proteins, such as the subunits I (*ctaD*) and III (*ctaE*) of cytochrome *aa<sub>3</sub>* and the three subunits of the cytochrome *bc<sub>1</sub>* complex (*qcrCAB*) of the respiratory chain (Niebisch & Bott, 2001; Niebisch & Bott, 2003). Genes of the heme biosynthetic pathway are repressed by HrrA, such as *hemA*, a glutamyl tRNA transferase, *hemE*, encoding an uroporphyrinogen decarboxylase, and the ferrochelatase gene *hemH*.

In *C. diphtheriae* a second TCS, ChrSA, is involved in the heme homeostasis together with HrrSA. ChrSA was shown to activate the expression of *hmuO* and represses *hemA* expression (Bibb *et al.*, 2005; Bibb *et al.*, 2007; Burgos & Schmitt, 2012). Additionally, ChrA activates the expression of *hrtBA* encoding a heme-detoxifying exporter (Bibb & Schmitt, 2010). In *C. glutamicum*, a second uncharacterized TCS, CgtSR8, was identified among the target genes of HrrA, but its function in heme homeostasis remains unclear.

## 2.5 Aims of this work

The first aim of this work was the identification of components belonging to the regulatory network involved in CGP3 induction. A previous analysis of CGP3 genes had revealed an uncharacterized regulator of the Cro/Ci family. Hence, the elucidation of a possible role of Cg2040 in the regulatory cascade controlling the activity of CGP3 was focused. Another aim was to identify the trigger(s) of CGP3 induction, in which the SOS response represented a prime candidate, and to determine early and late phage gene clusters involved in this process. A phylogenetic study revealed the protein Cg1890 (AlpC) of *C. glutamicum* to be an actin-like protein without mentioning that *alpC* is encoded in the prophage region. Therefore, the main focus of this work was the characterization of the actin-like protein AlpC and its role in the life cycle of CGP3. Initially, it had to be validated whether AlpC is induced upon prophage induction. Additionally, candidates that mediate the contact of AlpC and DNA had to be identified. The analysis will provide novel insights into the key question about the role of AlpC in segregation or replication of CGP3 DNA. A further topic of this work was motivated by the fact that CGP3 is induced by deletion of *dtxR* or *hrrA*; both mutants are impaired in the control of iron/heme homeostasis. To gain deeper insights into the complex regulatory network of these, the homologous system, ChrSA (previously CgtSR8), had to be characterized for target genes and the role in heme homeostasis. These studies are supposed to provide a detailed knowledge on how *C. glutamicum* manages the coordination of heme utilization and detoxification.

### 3 Results

The major topic of this PhD thesis was the investigation of the life cycle of prophage CGP3 in *C. glutamicum* as well as the role of the two-component system ChrSA in the regulation of heme homeostasis. The results allocated in this research have been summarized in two publications, one manuscript that was recently submitted, and a note (to be submitted).

In the note “Unveiling regulatory circuits of prophage CGP3 in *Corynebacterium glutamicum* – Characterization of the phage-encoded regulator Cg2040”, the Cro/CI regulator Cg2040 is described to repress its own transcription and the expression of genes adjacent to *cg2040* by binding within the promoter region of *cg2040*. The binding site of Cg2040 was identified and confirmed by mutational analysis. In addition, the influence of Cg2040 on the expression of prophage genes or prophage DNA replication was determined by transcriptome analysis and quantitative PCR.

The characterization of the phage-encoded actin-like protein AlpC (Cg1890) is described in the manuscript “A prophage-encoded actin-like protein required for efficient viral DNA replication in bacteria”, which is a joint project of our group in cooperation with Catriona Donovan and Marc Bramkamp, LMU Munich, and both groups contributed equally to this work: The biochemical characterization by our cooperation partners shows a nucleotide-dependent polymerization of AlpC into dynamic filaments. Transcriptome analyses of stressed cells were performed in our laboratory and the genes *alpA* and *alpC* were described to belong to the early response of prophage CGP3, upon prophage induction, triggered by the SOS response. Furthermore, our part was the characterization of the AlpA protein (cg1891), which represents a tempting candidate as adaptor protein for the connection of phage DNA and AlpC filaments. Fluorescence microscopy studies of our group found AlpA associated with AlpC. We investigate the impact of both proteins on efficient phage replication by quantitative PCR. In further microscopic studies by Catriona Donovan, CGP3 DNA was detected along AlpC filaments or close to the cell membrane. Based on these data, we developed a model of AlpC being required for efficient phage DNA transport to the place where replication occurs.

The development of microfluidic devices is required to allow insights into growth rate, morphology, or phenotypic heterogeneity in microcolonies over time. The optimization of a microfluidic picoliter bioreactor for single-cell analysis was performed by microfluidic experts (Alexander Grünberger and Dietrich Kohlheyer) in our institute. We supported the group by providing different *C. glutamicum* strains for cultivation in the microfluidic chambers. The design, production, and cultivation methods are described in the publication “Microfluidic Picoliter Bioreactor for Microbial Single Cell Analysis: Fabrication, System Setup and Operation”.

The characterization of the two-component system ChrSA and the role of ChrSA in regulation of heme tolerance are described in the publication “The two-component system ChrSA is crucial for haem tolerance and interferes with HrrSA in haem-dependent gene regulation in *Corynebacterium glutamicum*”. The response regulator ChrA acts as heme-dependent activator of *hrtBA* coding for a heme-detoxifying ABC transporter. Besides *hrtBA*, also the heme oxygenase gene *hmuO* and *hrrA* (encoding a homolog response regulator) were identified as direct target genes of ChrA. The two-component systems HrrSA and ChrSA share a high similarity and a complex interplay of both systems in the regulation of heme homeostasis was proposed.

## Unveiling regulatory circuits of prophage CGP3 in *Corynebacterium glutamicum* – Characterization of the phage-encoded regulator Cg2040

Antonia Heyer<sup>1</sup>, Kim Gärtner<sup>1</sup>, Jörn Kalinowski<sup>2</sup>, and Julia Frunzke<sup>1\*</sup>

<sup>1</sup> Institute of Bio- und Geosciences, IBG-1: Biotechnology, Forschungszentrum Jülich, Germany

<sup>2</sup> Centrum für Biotechnologie, CeBiTec, Universität Bielefeld, Germany

### Summary

\* Corresponding author

Dr. Julia Frunzke

Phone: +49 2461 61-5430

Fax: +49 2461 61-2710

Email: [j.frunzke@fz-juelich.de](mailto:j.frunzke@fz-juelich.de)

Keywords: bacteriophage, transcriptional regulation, phage repressor, EMSA

**Genome sequencing revealed prophage CGP3 in *Corynebacterium glutamicum*, but the regulatory network of this phage remained unclear. Here, we characterize the transcriptional regulator Cg2040, encoded by CGP3. Deletion of cg2040 had no influence on prophage gene expression or phage copy number. In contrast, overexpression of cg2040 resulted in a repression of the genes adjacent to cg2040 (cg2033 to cg2041). Further studies identified a binding site of Cg2040 close to the transcriptional start site (TSS) of cg2040, nevertheless, RNA sequencing revealed a complex regulation of these genes. In conclusion, Cg2040 is the first identified CGP3 encoded repressor, involved in the regulatory cascade of CGP3.**

Infections by lytic phages in fermentation processes cause substantial problems, *e.g.* in dairy fermentation (Jarocki *et al.*, 2013; Madera *et al.*, 2004). However, the spontaneous induction of temperate phages, residing as prophages in the genome of their host (lysogens), can also have a severe impact in fermentation processes (Jarocki *et al.*, 2013). Furthermore, spontaneous prophage induction was described to promote biofilm formation (Carrolo *et al.*, 2010; Gödeke *et al.*, 2011). The regulatory cascade controlling the lytic/lysogenic switch is well characterized for the example of *Escherichia coli* phage  $\lambda$ . Intensive studies during the last decades have established this complex regulatory network as a paradigm for gene regulation ((Kaiser, 1957) for reviews see (Campbell, 1994; Dodd *et al.*, 2005; Oppenheim *et al.*, 2005)). The lysogenic

state is predominantly maintained by the phage regulator  $\text{C}\lambda$ .  $\text{C}\lambda$  dimers bind at three binding sites at the operators  $O_L$  and  $O_R$ , cooperatively. In this way, the expression of lytic genes is blocked by transcriptional repression of the promoters  $P_R$  and  $P_L$ . Important for this step is the formation of an octameric complex of  $\text{C}\lambda$  dimers associated to two operator binding sites in each operator (Bell *et al.*, 2000; Révet *et al.*, 1999). Moreover,  $\text{C}\lambda$  functions not only as repressor, but acts also as an activator for its own transcription by direct interaction with the  $\sigma$  subunit of the RNA polymerase (Dove *et al.*, 2003; Jain *et al.*, 2004). Under stressful conditions, the lysogenic response can be switched to the lytic response. Upon DNA damage, RecA is activated by the formation of a complex with single-stranded DNA and ATP and mediates in its active form (RecA\*)

**Tab. 1** Strains and plasmids used in this study

Strains	Relevant characteristics	Source or Reference
<b><i>C. glutamicum</i> ATCC 13032</b>	Biotin-auxotrophic wild type strain	(Kinoshita <i>et al.</i> , 1957)
<b>ATCC 13032 <math>\Delta</math>cg2040</b>	In-frame deletion mutant of cg2040	This study
<b><i>E. coli</i> BL21(DE3)</b>	F <sup>-</sup> <i>ompT hsdS</i> (r <sub>B</sub> <sup>-</sup> m <sub>B</sub> <sup>-</sup> ) <i>gal dcm</i> $\lambda$ (DE3) ( $\lambda$ (DE3): <i>lacI</i> , <i>lacUV5-T7</i> gene 1, <i>ind1</i> , <i>sam7</i> , <i>nin5</i> )	(Studier & Moffatt, 1986)
<b>Plasmids</b>		
<b>pK19mobsacB</b>	Kan <sup>r</sup> ; vector for allelic exchange in <i>C. glutamicum</i> (pK18 <i>oriV<sub>E.c.</sub></i> <i>sacB lacZ<math>\alpha</math></i> )	(Schäfer <i>et al.</i> , 1994)
<b>pK19mobsacB-D2040</b>	Kan <sup>r</sup> , pK19mobsacB derivative for in-frame deletion of cg2040	This study
<b>pEKEx2</b>	Kan <sup>r</sup> , shuttle vector for regulated gene expression ( <i>P<sub>tac</sub></i> , <i>lacI<sup>d</sup></i> , pBL1 <i>oriV<sub>C.g.</sub></i> , pUC18 <i>oriV<sub>E.c.</sub></i> )	(Eikmanns <i>et al.</i> , 1994)
<b>pEKEx2-cg2040</b>	Kan <sup>r</sup> , pEKEx2 derivative containing cg2040 with artificial ribosome binding site under control of the inducible promoter <i>P<sub>tac</sub></i>	This study
<b>pET-TEV</b>	Kan <sup>r</sup> , vector for overproduction of proteins in <i>E. coli</i> , adding a N-terminal decahistidine tag and a TEV protease cleavage site to the target protein (pBR322, <i>oriV<sub>E.c.</sub></i> , <i>P<sub>T7</sub></i> , <i>lacI</i> )	(Bussmann <i>et al.</i> , 2010)
<b>pET-TEV-cg2040</b>	Kan <sup>r</sup> , pET-TEV derivative for overproduction of cg2040 with N-terminal decahistidine tag, cleavable by TEV protease	This study
<b>pMal-c</b>	Amp <sup>r</sup> , vector for overproduction of maltose binding protein (MBP) fusion proteins without signal peptide in <i>E. coli</i> , ( <i>P<sub>tac</sub></i> , <i>lacI<sup>d</sup></i> )	New England Biolabs
<b>pMBP-cg2040</b>	Amp <sup>r</sup> , pMal-c derivative containing cg2040, inserted downstream to <i>malE</i> (without signal sequence) with an additional TEV cleavage site, resulting in a MBP-Cg2040 fusion protein, the MBP can be cleaved off with TEV protease	This study

the autodigestion of LexA (Little, 1984). This leads to a derepression of the SOS response, controlled by LexA. Similarly, activated RecA\* also stimulates the autoproteolytic cleavage of the lambdaoid phage repressors (Galkin *et al.*, 2009; Little, 1984; Roberts *et al.*, 1978). Subsequently, the degradation of the phage repressor CI leads to prophage induction and expression of lytic genes. CI and the regulator Cro, which are able to repress the transcription of each other, regulate the bistable switch between lysogeny and phage induction. However, contrary results about the role of Cro in prophage induction were published (Atsumi & Little, 2006; Schubert *et al.*, 2007; Svenningsen *et al.*, 2005). Sharing a similar DNA-binding helix-turn-helix domain (HTH\_3, Pfam PF01381), the regulators CI and Cro belong to the same family of transcriptional

regulators. The HTH binding domain with two relevant  $\alpha$  helices is ordinarily located at the N-terminus of the repressors, while the C-terminus is important for oligomerization (Ohlendorf *et al.*, 1983; Pabo & Lewis, 1982). Further regulators involved in the cascade are the activator CII, stabilized by CIII and required for the maintenance of lysogeny (for review: (Oppenheim *et al.*, 2005)), and the anti-terminator proteins N and Q, which favor the lytic response (Friedman & Court, 1995).

In several *Corynebacterium* strains, exposure to UV radiation or the antibiotic agent mitomycin C led to the induction and isolation of several temperate phages present as prophages in the genomes of the respective strains (Koptides *et al.*, 1992; Moreau *et al.*, 1995; Pátek *et al.*, 1985; Sonnen *et al.*, 1990;

**Tab. 2** Transcriptome analysis of  $\Delta$ cg2040 in comparison to *C. glutamicum* wild type<sup>1)</sup>

Gene	Gene name	Annotation	Average	n	p-value
cg0230	<i>gltD</i>	Glutamine 2-oxoglutarate aminotransferase small SU	<b>0.72</b>	3	0.249
cg1584	<i>argF</i>	Ornithine carbamoyltransferase	<b>0.76</b>	3	0.341
cg1585	<i>argR</i>	Arginine repressor	<b>0.75</b>	3	0.321
cg2040		Putative transcriptional regulator	<b>0.00</b>	3	0.001
cg2184		ATPase component of peptide ABC-type transport system, contains duplicated ATPase domains	<b>0.28</b>	2	0.037
cg3226		Putative L-lactate permease	<b>0.27</b>	3	0.041
cg3227	<i>lldD</i>	Quinone-dependent L-lactate dehydrogenase	<b>0.29</b>	3	0.022

1) For transcriptome analysis,  $\Delta$ cg2040 and ATCC 13032 wild type were cultivated in a BHI preculture and transferred to a second preculture with CGXII minimal medium with 4% glucose. The main culture (CGXII) was inoculated from the second preculture to an OD<sub>600</sub> 1 and was harvested at an OD<sub>600</sub> of 5 in ice-filled tubes by centrifugation (6900 g, 10 min, and 4 °C). For preparation of RNA see (Möker *et al.*, 2004). The cDNA synthesis, labeling, and hybridization on 70-mer custom-made DNA microarray (Eurofins MWG Operon) were performed as described before (Frunzke *et al.*, 2008b). The normalized data were saved for further analysis in our in-house microarray database (Polen & Wendisch, 2004). The table shows the genes that matched a signal-to-noise ratio of  $\geq 5$  and  $\geq$  twofold altered mRNA level in at least two of the three independent DNA microarray experiments (*p*-value as indicated). The experiment was repeated in three biological replicates.

Trautwetter *et al.*, 1987). For the Gram-positive bacterium *Corynebacterium glutamicum* ATCC 13032, one of the most important platform organisms for the industrial production of amino acids (Kinoshita *et al.*, 1957), no infectious phages have been described so far. However, genome sequencing of this strain revealed three prophages (Kalinowski *et al.*, 2003). The prophage CGP1 (13.5 kbp) and CGP2 (3.9 kbp) are probably degenerated. Whereas, the largest prophage, CGP3 (187.3 kbp), accounts for 6% of the *C. glutamicum* DNA and was shown to excise from the genome and to exist as a circular phage DNA molecule (Frunzke *et al.*, 2008a). Spontaneous induction of the prophage in a small fraction of cells was observed even under non-stressful conditions and was often accompanied by lysis of the respective cell. However, the regulatory network controlling the lytic/lysogenic switch of CGP3 has not been studied yet. Hence, our studies aimed at identifying phage regulatory proteins involved in the control of CGP3 activity.

A screening of CGP3 genes revealed cg2040, coding for a putative transcriptional regulator in the prophage region. The protein Cg2040 contains a helix-turn-helix motif belonging to the HTH-3/HTH-XRE family (Pfam PF01381, Smart accession no. SM00530); this family also includes the phage regulators CI and Cro. Overall, the genome of *C. glutamicum* codes for 11 regulators of the HTH type 3 family, (CoryneRegNet, (Schröder & Tauch, 2010)). However, up to now only a few of the members of this family were characterized in *C. glutamicum*, e.g. the regulator CgIR, which is involved in controlling proteolysis and DNA repair genes (Engels *et al.*, 2004; Engels *et al.*, 2005). No other putative regulators of the HTH\_3 type were identified to be encoded in the prophage region, revealing cg2040 as a prime candidate for a central phage regulator.

To characterize the function of the putative transcriptional regulator, an in-frame deletion mutant of cg2040 was constructed (Tab. 1 & Tab S1). To investigate the effect of Cg2040 on global gene expression, the transcriptome of

$\Delta$ cg2040 was compared to the wild type (Tab. 2). When the cells were grown under standard conditions (CGXII medium with 4% glucose), no alteration in the mRNA level of prophage genes was observed in the  $\Delta$ cg2040 mutant. Interestingly, the expression of *argR*, encoding the arginine regulator ArgR, was slightly reduced, as well as the target genes of ArgR, *argF* and *gltD* (Lee *et al.*, 2010a; Lee *et al.*, 2010b). ArgR was proposed to influence the maintenance of phage P1 in *E. coli* (Paul & Summers, 2004), although further studies could not detect binding of ArgR at the *loxP* site of P1 (MacDonald *et al.*, 2008). A role of *C. glutamicum* ArgR on phage gene expression or the copy number of CGP3 has not been described, yet. The other genes with altered mRNA levels (*cg2184*, *cg3226*, and *lldD*, encoding an L-lactate dehydrogenase) were often detected in transcriptome analysis under varying conditions and, thus, are most likely not a specific response to the deletion of *cg2040* (unpublished data).

As the transcriptome analysis of  $\Delta$ cg2040 showed no effect on CGP3 genes, we tested the impact of *cg2040* overexpression on the expression of prophage genes. For this purpose, we performed a transcriptome analysis of the strain ATCC 13032/ pEKEx2-*cg2040* in comparison to the wild type containing the empty vector pEKEx2. Transcriptome analysis revealed a high expression level of *cg2040* upon induction by ITPG (Tab. S2). In the CGP3 region, the genes *cg2033*, *cg2036*, and *cg2039* adjacent to the gene *cg2040* showed a reduced mRNA level. The transcription of *cg2038* was also reduced, but was only detected with a signal to noise ratio of  $\geq 3$ . A motif search (SMART EMBL) revealed the presence of N-terminal signal peptides in *cg2033* and *cg2036*. The other proteins were annotated as hypothetical proteins and showed only low sequence homologies (below 30%) to other proteins from

*C. diphtheriae* and *C. bovis*. Furthermore, the prophage genes *cg2004* and *cg1935* were negatively influenced by overexpression of *cg2040*. *Cg2004* was annotated to be similar to the protein 232 of the temperate prophage *g1e* of *Lactobacillus*, but the function of protein 232 is unknown (Kodaira *et al.*, 1997). *Cg1935* encodes the gluconate responsive repressor *gntR2* (Frunzke *et al.*, 2008b). However, an effect on the regulon of GntR2 was not observed. In fact, previous studies of our institute indicated that the deletion of *gntR2* is complemented due to the presence of the equivalent regulator GntR1 (Frunzke *et al.*, 2008b). Overall, more than fifty genes were altered in the transcriptome analysis and the majority of them were reduced in gene expression. A highly increased mRNA level was observed for *cg1180* and the adjacent genes *cg1179* and *cg1181* (signal-to-noise ratio  $\geq 3$ ). This high induction is probably due to activity of transposases bordering the genes. Another group of genes with increased mRNA levels, *cg1292* to *cg1294*, are postulated as being under control of the oxidative stress regulator OxyR (CoryneRegNet ([www.coryneregnet.de](http://www.coryneregnet.de))). Remarkably, a role of OxyR in the maintenance of  $\lambda$  was described, as the oxygen sensitive regulator OxyR is able to bind at the CI controlled promoter  $P_M$  (Glinkowska *et al.*, 2010). Thereby OxyR influences the binding of CI to the three operator binding sites and stimulates the maintenance in the lysogenic state.

To identify direct target genes of Cg2040, we performed electrophoretic mobility shift assays with purified Cg2040 fused to a maltose-binding protein (MBP). This large tag was chosen in order to enhance the solubility of the protein, which ended up in inclusion bodies when produced in a His-tagged version. In EMSA studies, we tested the upstream region (500bp) of the genes *cg2033*, *cg2036*, *cg2038*,

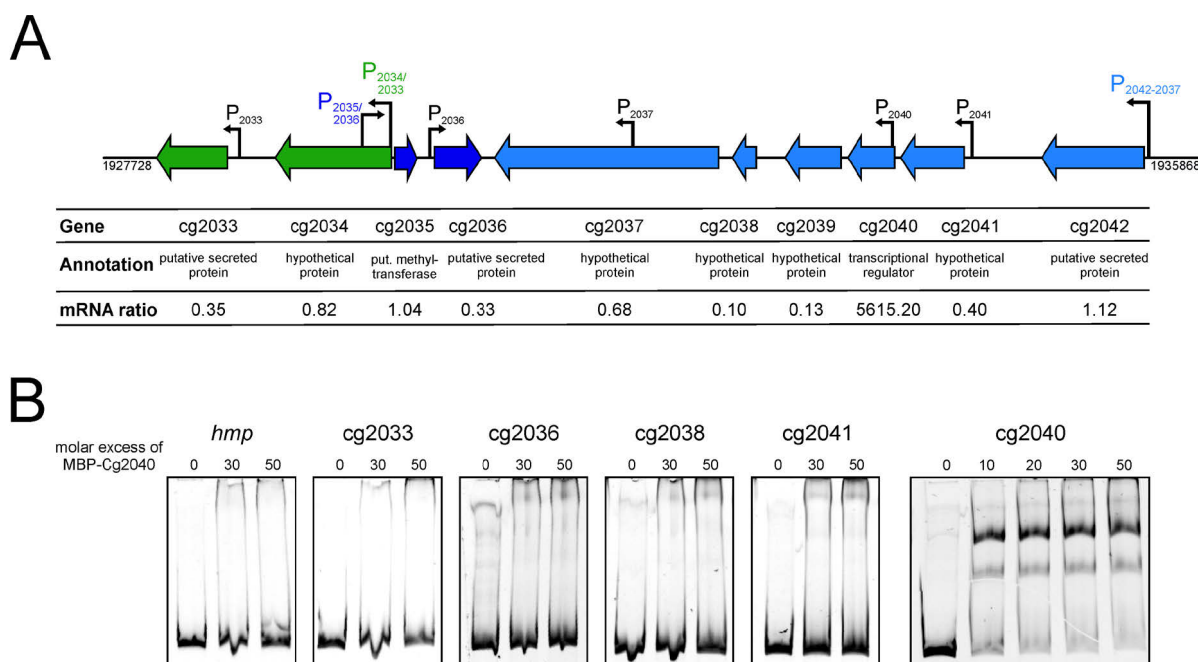


**Fig. 1 Identification of binding sites by electrophoretic mobility shift assays with purified MBP-Cg2040.** **(A)** Genomic organization of the genes cg2033 to cg2042, adopted from CoryneRegNet (Baumbach *et al.*, 2009; Pauling *et al.*, 2012). Below the mRNA ratios from the transcriptome analysis of the overexpression of cg2040 (signal-to-noise ratio  $\geq 3$  and ratio of medians  $> 0$ ) are given. Promoters (P) in this genomic region are indicated as arrows and have been identified by RNA sequencing. Larger arrows present the main promoters for transcription of more than one gene; internal promoters are indicated as smaller arrows. Color code indicates the operon structure of this locus **(B)** The putative target DNA, covering the upstream region of the genes cg2033, cg2036, cg2038, cg2039, cg2040 and cg2041 (500bp, 450bp upstream and 50bp downstream of the corresponding TSS), were amplified by PCR. For EMSA 100 ng of DNA were incubated with different amounts of MBP-Cg2040 for 20 minutes before loading onto a 10% non-denaturing polyacrylamide gel. The EMSA was performed as described previously (Heyer *et al.*, 2012). For overproduction of Cg2040 *E. coli* BL21 (DE3) was transformed with plasmid pMBP-cg2040 and grown in LB medium to an OD<sub>600</sub> of 0.6 to 0.8, before the expression of cg2040 was induced with 0.5 mM IPTG for 4 h. The purification of MBP-Cg2040 by an amylose affinity chromatography was performed as described in (Frunzke *et al.*, 2011). The buffer was exchange to bandshift buffer (20 mM Tris/HCl, pH 7.5, 50 mM KCl, 10 mM MgCl<sub>2</sub>, 5% (v/v) glycerol, 0.5 mM EDTA, 0.005% (w/v) Triton X-100) by using a PD10 desalting column (GE Healthcare).

cg2040, and cg2041 for binding of Cg2040 (Fig. 1). Binding of Cg2040 was only observed for the upstream region of cg2040 (Fig. 1B). For a proof of principle experiment, the maltose-binding protein of MBP-Cg2040 was cleaved by using TEV-protease (Bussmann *et al.*, 2010). An EMSA of Cg2040 without MBP protein demonstrated that the shift is specific to Cg2040 and is not influenced by the MBP-tag (data not shown).

In further experiments, the binding site of Cg2040 was narrowed down to position -22 to +8 (relative to the transcriptional start site, TSS) by testing smaller DNA fragments and

oligonucleotides covering the respective region (Fig. 2A and 2B). A motif prediction tool (MEME suite (meme.ncbr.net) predicted two putative palindromic repeats within the 30 bp binding region. For this reason, the nucleotides relevant for binding of Cg2040 were identified by testing oligonucleotides with an exchange of three nucleotides to the complementary ones (Fig. 3). Based on the mutational analysis and motif prediction, the imperfect direct repeat AGGATATAAGGTAA was deduced for Cg2040. A comparison with the consensus binding motif of Cl for the operator sites O<sub>L</sub> and O<sub>R</sub>, TATCACCGCGGTGATA, showed no significant

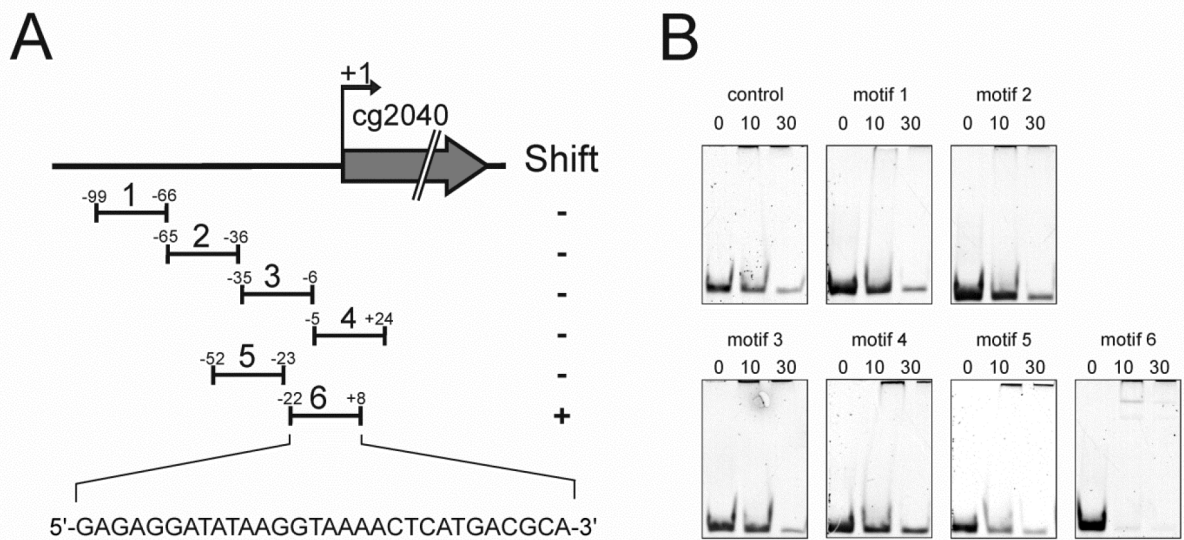


**Fig. 2 Search for the Cg2040 binding region. (A)** Tested subfragments. The positions are given relative to the TSS of cg2040, which was identified in this work by RNA sequencing (indicated as arrow +1). Binding of Cg2040 to the DNA fragment is indicated with +, fragments that were not shifted are indicated with -. **(B)** EMSA with the corresponding subfragments shown in A. The subfragments (30 bp) were obtained by hybridization of two complementary oligonucleotides at 95 °C for 5 min, followed by incubating on ice. As described in Fig. 1, 100 ng DNA were incubated with different amounts of Cg2040 (0, 10, or 30 molar excess) and subsequently separated on a non-denaturing 15% polyacrylamide gel, as describe previously (Heyer *et al.*, 2012).

similarities to the 17 bp asymmetric and palindromic motif (Benson *et al.*, 1988).

The described transcriptome studies revealed that Cg2040 acts as a repressor for its own gene expression (negative feedback) and as a repressor of the operons cg2033-cg2034, cg2035-cg2036 and cg2037-cg2040 adjacent to cg2040. The single binding site of Cg2040 suggested an organization of the genes in an operon. Determination of the promoter localization by RNA sequencing revealed a complex regulatory structure of this genomic region (personal communication J. Kalinowski). The promoter of the genes cg2037 to cg2041 is probably located upstream of cg2042, but additional promoters were found upstream of the genes cg2037, cg2040, and cg2041. An overview of the operon structure and location of promoters is given in Fig. 1A. The gene cg2040 is a leaderless transcript and the current annotation of the TSS is most likely wrong, as the transcript revealed by RNA sequencing starts 24 bp downstream of the initial TSS.

According to these results, the binding motif of Cg2040 is located at position -12 bp upstream of the TSS that was identified in this work. The localization of the identified binding site is in agreement with the proposed repressor function of Cg2040. At this position, Cg2040 most likely interferes with the binding of the RNA polymerase (Madan Babu & Teichmann, 2003).

Based on the fact, that we did not observe any effect on the CGP3 transcriptome in the  $\Delta$ cg2040 mutant, we assumed that Cg2040 might not be active under the tested conditions. In *C. glutamicum*, the transcription of a majority of prophage genes was highly increased when the SOS response was induced (Donovan *et al.*, 2013; Jochmann *et al.*, 2009). To investigate the impact of Cg2040 under stressful conditions, we determined the amount of circular phage DNA at several time points in  $\Delta$ cg2040 and the wild type after induction of the SOS response by treatment with mitomycin C. By quantitative PCR, the amount of circular

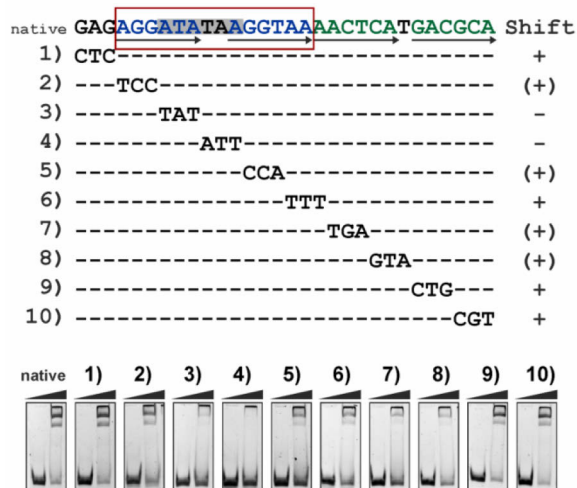


**Fig. 3 Mutational analysis of the Cg2040 binding site.** To identify relevant base pairs for binding of Cg2040, the oligonucleotide (30 bp) that was shifted by Cg2040 was mutated by an exchange of three nucleotides to the complementary bases, as indicated. The mutated fragments were analyzed by EMSA studies by incubating the hybridized oligonucleotides with different molar excesses of Cg2040 (0, 5, and 10-fold), as described in Fig. 1B and Fig. 2B. Fragments bound by Cg2040 are indicated as +, reduced binding affinity is indicated as (+), and a loss of binding is marked with -. The predicted motifs (MEME suite ([meme.ncbr.net/meme](http://meme.ncbr.net/meme))) are marked in blue (motif 1) and in green (motif 2), the background for relevant nucleotides is colored in grey and the identified motif is highlighted in the red box.

phage DNA was determined and a ratio of stressed versus unstressed cells was calculated. For a description of the experimental procedure see (Donovan *et al.*, 2013). In the wild type, the amount of circular phage DNA increased about 12-fold six hours after induction of the SOS response (Tab. 3). In  $\Delta$ cg2040, no significant difference to the wild type situation was observed. In conclusion, Cg2040 seems to have a minor impact on the phage copy number upon phage induction under the tested conditions.

Early studies demonstrated that mutations in the region of CI led to a strong decrease in the formation of lysogenic cells (Kaiser, 1957). In further studies different levels of CI were

analyzed with a temperature sensitive version of CI, where a decreased CI level subsequently led to the expression of lytic genes and cell lysis (Svenningsen *et al.*, 2005). In contrast,  $\Delta$ cg2040 showed no growth inhibition (data not shown). Altogether, our studies suggested that cg2040 might not act as a central phage repressor, but most likely acts further downstream in the cascade controlling prophage induction. Additionally, it has to be considered that Cg2040 might be regulated by further (phage-encoded) regulators. However, a mechanism of prophage induction differing from the  $\lambda$  model (based on CI-like phage repressor) has to be taken into account when studying the large prophage CGP3.

**Tab.3** Amount of circular CGP3 DNA in wild type and  $\Delta$ cg2040 upon induction of the SOS response.

Time point	Amount circular CGP3 DNA <sup>1)</sup>	
	Wild type	$\Delta$ cg2040
0 h	1.0 $\pm$ 0.1	0.8 $\pm$ 0.1
1 h	1.0 $\pm$ 0.1	1.0 $\pm$ 0.1
3 h	2.6 $\pm$ 0.3	2.6 $\pm$ 0.5
6 h	11.6 $\pm$ 1.3	9.4 $\pm$ 3.3
9 h	10.5 $\pm$ 2.6	7.6 $\pm$ 2.1
24 h	5.0 $\pm$ 0.8	4.9 $\pm$ 1.4

1) To measure the amount of circular phage DNA, the cells were cultivated in a CGXII preculture. The main culture (50 ml) was inoculated to an OD<sub>600</sub> 1. At an OD<sub>600</sub> of 3, the SOS response was induced by addition of the antibiotic agent mitomycin C (0.6  $\mu$ M). 3 to 5 ml of the culture were harvested at several time points (0 to 24 h after addition of mitomycin C) and genomic DNA was extracted from the samples (Eikmanns *et al.*, 1994). The determination of circular CGP3 DNA was performed as described recently (Donovan *et al.*, 2013; Frunzke *et al.*, 2008a). For each time point, the amount of CGP3 DNA in cells with mitomycin C was normalized to the amount of circular CGP3 DNA in non-induced cells of the same strain.

The induction of CGP3 by mitomycin C hints to an SOS-response-dependent induction mechanism and some CGP3 genes are, in fact, under direct control of LexA (Jochmann *et al.*, 2009). It was described that LexA regulates the expression of phage genes for the phage CTX of *Vibrio cholerae* in addition to the phage repressor (Kimsey & Waldor, 2009; Nickels, 2009; Quinones *et al.*, 2005). Thus, Cg2040 surely represents one part in a complex regulatory cascade controlling CGP3 activity, however, the key regulator maintaining the lysogenic state remains unknown.

### Acknowledgements

We thank Xenia Schuplezow for the kind gift of purified TEV-protease. This work was supported by Helmholtz Association (grant VH-NG-716) and by the priority program SPP1617 of the Deutsche Forschungsgemeinschaft.

### References

- Atsumi, S. & Little, J. W. (2006).** Role of the lytic repressor in prophage induction of phage lambda as analyzed by a module-replacement approach. *Proc Natl Acad Sci U S A* **103**, 4558-4563.
- Baumbach, J., Wittkop, T., Kleindt, C. K. & Tauch, A. (2009).** Integrated analysis and reconstruction of microbial transcriptional gene regulatory networks using CoryneRegNet. *Nat Protoc* **4**, 992-1005.
- Bell, C. E., Frescura, P., Hochschild, A. & Lewis, M. (2000).** Crystal structure of the lambda repressor C-terminal domain provides a model for cooperative operator binding. *Cell* **101**, 801-811.
- Benson, N., Sugiono, P. & Youderian, P. (1988).** DNA sequence determinants of lambda repressor binding *in vivo*. *Genetics* **118**, 21-29.
- Busmann, M., Baumgart, M. & Bott, M. (2010).** RosR (Cg1324), a hydrogen peroxide-sensitive MarR-type transcriptional regulator of *Corynebacterium glutamicum*. *J Biol Chem* **285**, 29305-29318.
- Campbell, A. (1994).** Comparative molecular biology of lambdoid phages. *Annu Rev Microbiol* **48**, 193-222.
- Carrolo, M., Frias, M. J., Pinto, F. R., Melo-Cristino, J. & Ramirez, M. (2010).** Prophage spontaneous activation promotes DNA release enhancing biofilm formation in *Streptococcus pneumoniae*. *PLoS One* **5**, e15678.
- Dodd, I. B., Shearwin, K. E. & Egan, J. B. (2005).** Revisited gene regulation in bacteriophage lambda. *Curr Opin Genet Dev* **15**, 145-152.
- Donovan, C., Heyer, A., Polen, T., Wittmann, A., Krämer, R., Frunzke, J. & Bramkamp, M. (2013).** A prophage-encoded actin-like protein required for efficient viral DNA replication in bacteria. *Curr Biol*, submitted.
- Dove, S. L., Darst, S. A. & Hochschild, A. (2003).** Region 4 of sigma as a target for transcription regulation. *Mol Microbiol* **48**, 863-874.
- Eikmanns, B. J., Thum-Schmitz, N., Eggeling, L., Lüdtke, K. U. & Sahm, H. (1994).** Nucleotide sequence, expression and transcriptional analysis of the *Corynebacterium glutamicum* *gltA* gene encoding citrate synthase. *Microbiology* **140**, 1817-1828.
- Engels, S., Schweitzer, J. E., Ludwig, C., Bott, M. & Schaffer, S. (2004).** *clpC* and *clpP1P2* gene expression in *Corynebacterium glutamicum* is controlled by a regulatory network involving the transcriptional regulators ClgR and HspR as well as the ECF sigma factor SigmaH. *Mol Microbiol* **52**, 285-302.
- Engels, S., Ludwig, C., Schweitzer, J. E., Mack, C., Bott, M. & Schaffer, S. (2005).** The transcriptional activator ClgR controls transcription of genes involved in proteolysis and DNA repair in *Corynebacterium glutamicum*. *Mol Microbiol* **57**, 576-591.
- Friedman, D. I. & Court, D. L. (1995).** Transcription antitermination: the lambda paradigm updated. *Mol Microbiol* **18**, 191-200.
- Frunzke, J., Bramkamp, M., Schweitzer, J. E. & Bott, M. (2008a).** Population Heterogeneity in *Corynebacterium glutamicum* ATCC 13032 Caused by Prophage CGP3. *J Bacteriol* **190**, 5111-5119.
- Frunzke, J., Engels, V., Hasenbein, S., Gätgens, C. & Bott, M. (2008b).** Co-ordinated regulation of gluconate catabolism and glucose uptake in *Corynebacterium glutamicum* by two functionally equivalent transcriptional regulators, GntR1 and GntR2. *Mol Microbiol* **67**, 305-322.
- Frunzke, J., Gätgens, C., Brocker, M. & Bott, M. (2011).** Control of Heme Homeostasis in

- Corynebacterium glutamicum* by the Two-Component System HrrSA. *J Bacteriol* **193**, 1212-1221.
- Galkin, V. E., Yu, X., Bielnicki, J., Ndjonka, D., Bell, C. E. & Egelman, E. H. (2009).** Cleavage of bacteriophage lambda cI repressor involves the RecA C-terminal domain. *J Mol Biol* **385**, 779-787.
- Glinkowska, M., łoś, J. M., Szambowska, A., Czyż, A., Calkiewicz, J., Herman-Antosiewicz, A., Wróbel, B., Węgrzyn, G., Węgrzyn, A. & łoś, M. (2010).** Influence of the *Escherichia coli oxyR* gene function on lambda prophage maintenance. *Arch Microbiol* **192**, 673-683.
- Gödeke, J., Paul, K., Lassak, J. & Thormann, K. M. (2011).** Phage-induced lysis enhances biofilm formation in *Shewanella oneidensis* MR-1. *ISME J* **5**, 613-626.
- Heyer, A., Gätgens, C., Hentschel, E., Kalinowski, J., Bott, M. & Frunzke, J. (2012).** The two-component system ChrSA is crucial for haem tolerance and interferes with HrrSA in haem-dependent gene regulation in *Corynebacterium glutamicum*. *Microbiology* **158**, 3020-3031.
- Jain, D., Nickels, B. E., Sun, L., Hochschild, A. & Darst, S. A. (2004).** Structure of a ternary transcription activation complex. *Mol Cell* **13**, 45-53.
- Jarocki, P., Podleśny, M., Pawelec, J., Malinowska, A., Kowalczyk, S. & Targónski, Z. (2013).** Spontaneous Release of Bacteriophage Particles by *Lactobacillus rhamnosus* Pen. *J Microbiol Biotechnol* **23**, 357-363.
- Jochmann, N., Kurze, A. K., Czaja, L. F., Brinkrolf, K., Brune, I., Hüser, A. T., Hansmeier, N., Pühler, A. Borovok, I. & Tauch, A. (2009).** Genetic makeup of the *Corynebacterium glutamicum* LexA regulon deduced from comparative transcriptomics and *in vitro* DNA band shift assays. *Microbiology* **155**, 1459-1477.
- Kaiser, A. D. (1957).** Mutations in a Temperate Bacteriophage Affecting its Ability to Lysogenize *Escherichia coli*. *Virology* **3**, 42-61.
- Kalinowski, J., Bathe, B., Bartels, D. & other authors (2003).** The complete *Corynebacterium glutamicum* ATCC 13032 genome sequence and its impact on the production of L-aspartate-derived amino acids and vitamins. *J Biotechnol* **104**, 5-25.
- Kimsey, H. H. & Waldor, M. K. (2009).** *Vibrio cholerae* LexA Coordinates CTX Prophage Gene Expression. *J Bacteriol* **191**, 6788-6795.
- Kinoshita, S., Udaka, S. & Shimono, M. (1957).** Studies on the amino acid fermentation: Part I. Production of L-glutamic acid by various microorganisms. *J Gen Appl Microbiol* **3**, 193-205.
- Kodaira, K. I., Oki, M., Kakikawa, M., Watanabe, N., Hirakawa, M., Yamada, K. & Taketo, A. (1997).** Genome structure of the *Lactobacillus* temperate phage phi g1e: the whole genome sequence and the putative promoter/repressor system. *Gene* **187**, 45-53.
- Koptides, M., Barák, I., Sisová, M., Baloghová, E., Ugorcaková, J. & Timko, J. (1992).** Characterization of bacteriophage BFK20 from *Brevibacterium flavum*. *J Gen Microbiol* **138**, 1387-1391.
- Lee, S. Y., Kim, Y. H. & Min, J. (2010a).** Conversion of phenol to glutamate and proline in *Corynebacterium glutamicum* is regulated by transcriptional regulator ArgR. *Appl Microbiol Biotechnol* **85**, 713-720.
- Lee, S. Y., Shin, H. S., Park, J. S., Kim, Y. H. & Min, J. (2010b).** Proline reduces the binding of transcriptional regulator ArgR to upstream of *argB* in *Corynebacterium glutamicum*. *Appl Microbiol Biotechnol* **86**, 235-242.
- Little, J. W. (1984).** Autodigestion of *lexA* and phage lambda repressors. *Proc Natl Acad Sci U S A* **81**, 1375-1379.
- MacDonald, A. I., Lu, Y., Kilbride, E. A., Akopian, A. & Colloms, S. D. (2008).** *PepA* and *ArgR* do not regulate Cre recombination at the bacteriophage P1 *loxP* site. *Plasmid* **59**, 119-126.
- Madan Babu, M. & Teichmann, S. A. (2003).** Functional determinants of transcription factors in *Escherichia coli*: protein families and binding sites. *Trends Genet* **19**, 75-79.
- Madera, C., Monjardín, C. & Suárez, J. E. (2004).** Milk contamination and resistance to processing conditions determine the fate of *Lactococcus lactis* bacteriophages in dairies. *Appl Environ Microbiol* **70**, 7365-7371.
- Möker, N., Brocker, M., Schaffer, S., Krämer, R., Morbach, S. & Bott, M. (2004).** Deletion of the genes encoding the MtrA-MtrB two-component system of *Corynebacterium glutamicum* has a

- strong influence on cell morphology, antibiotics susceptibility and expression of genes involved in osmoprotection. *Mol Microbiol* **54**, 420-438.M
- Moreau, S., Leret, V., Le Marrec, C., Varangot, H., Ayache, M., Bonnassie, S., Blanco, C. & Trautwetter, A. (1995).** Prophage distribution in coryneform bacteria. *Res Microbiol* **146**, 493-505.
- Nickels, B. E. (2009).** A New Twist on a Classic Paradigm: Illumination of a Genetic Switch in *Vibrio cholerae* phage CTX Phi. *J Bacteriol* **191**, 6779-6781.
- Ohlendorf, D. H., Anderson, W. F., Lewis, M., Pabo, C. O. & Matthews, B. W. (1983).** Comparison of the Structures of Cro and lambda Repressor Proteins from Bacteriophage lambda. *J Mol Biol* **169**, 757-769.
- Oppenheim, A. B., Kobilier, O., Stavans, J., Court, D. L. & Adhya, S. (2005).** Switches in Bacteriophage Lambda Development. *Annu Rev Genet* **39**, 409-429.
- Pabo, C. O. & Lewis, M. (1982).** The operator-binding domain of lambda repressor: structure and DNA recognition. *Nature* **298**, 443-447.
- Pátek, M., Ludvík, J., Benada, O., Hochmannová, J., Nesvera, J., Krumphanzl, V. & Bucko, M. (1985).** New bacteriophage-like particles in *Corynebacterium glutamicum*. *Virology* **140**, 360-363.
- Paul, S. & Summers, D. (2004).** ArgR and PepA, accessory proteins for XerCD-mediated resolution of Cole1 dimers, are also required for stable maintenance of the P1 prophage. *Plasmid* **52**, 63-68.
- Pauling, J., Röttger, R., Tauch, A., Azevedo, V. & Baumbach, J. (2012).** CoryneRegNet 6.0--Updated database content, new analysis methods and novel features focusing on community demands. *Nucleic Acids Res* **40**, D610-614.
- Polen, T. & Wendisch, V. F. (2004).** Genomewide expression analysis in amino acid-producing bacteria using DNA microarrays. *Appl Biochem Biotechnol* **118**, 215-232.
- Quinones, M., Kimsey, H. H. & Waldor, M. K. (2005).** LexA Cleavage Is Required for CTX Prophage Induction. *Mol Cell* **17**, 291-300.
- Révet, B., von Wilcken-Bergmann, B., Bessert, H., Barker, A. & Müller-Hill, B. (1999).** Four dimers of lambda repressor bound to two suitably spaced pairs of lambda operators form octamers and DNA loops over large distances. *Curr Biol* **9**, 151-154.
- Roberts, J. W., Roberts, C. W. & Craig, N. L. (1978).** *Escherichia coli* recA gene product inactivates phage lambda repressor. *Proc Natl Acad Sci U S A* **75**, 4714-4718.
- Sambrook, J., MacCallum, P. & Russell, D. (2001).** *Molecular Cloning: A Laboratory Manual*, 3rd ed. Ed. edn. New York: Cold Spring Harbor Laboratory Press.
- Schäfer, A., Tauch, A., Jäger, W., Kalinowski, J., Thierbach, G. & Pühler, A. (1994).** Small mobilizable multi-purpose cloning vectors derived from the *Escherichia coli* plasmids pK18 and pK19: selection of defined deletions in the chromosome of *Corynebacterium glutamicum*. *Gene* **145**, 69-73.
- Schröder, J. & Tauch, A. (2010).** Transcriptional regulation of gene expression in *Corynebacterium glutamicum*: the role of global, master and local regulators in the modular and hierarchical gene regulatory network. *FEMS Microbiol Rev* **34**, 685-737.
- Schubert, R. A., Dodd, I. B., Egan, J. B. & Shearwin, K. E. (2007).** Cro's role in the CI Cro bistable switch is critical for {lambda}'s transition from lysogeny to lytic development. *Genes Dev* **21**, 2461-2472.
- Sonnen, H., Schneider, J. & Kutzner, H. J. (1990).** Corynephage Cog, a virulent bacteriophage of *Corynebacterium glutamicum*, and its relationship to phi GA1, an inducible phage particle from *Brevibacterium flavum*. *J Gen Virol* **71 ( Pt 8)**, 1629-1633.
- Studier, F. W. & Moffatt, B. A. (1986).** Use of bacteriophage T7 RNA polymerase to direct selective high-level expression of cloned genes. *J Mol Biol* **189**, 113-130.
- Svenningsen, S. L., Costantino, N., Court, D. L. & Adhya, S. (2005).** On the role of Cro in lambda prophage induction. *Proc Natl Acad Sci U S A* **102**, 4465-4469.
- Trautwetter, A., Blanco, C. & Bonnassie, S. (1987).** Characterization of the corynebacteriophage CG33. *J Gen Microbiol* **133**, 2945-2952.

Name of the journal: to be submitted

Impact factor: -

Contribution of own work: 80%

1. Author: Experimental work and writing of the manuscript

# A prophage-encoded actin-like protein required for efficient viral DNA replication in bacteria

Catriona Donovan<sup>1,3,\*</sup>, Antonia Heyer<sup>2,\*</sup>, Tino Polen<sup>2</sup>, Anja Wittmann<sup>1</sup>, Reinhard Krämer<sup>1</sup>, Julia Frunzke<sup>2,‡</sup>, & Marc Bramkamp<sup>1,3‡</sup>

<sup>1</sup> Department of Biology I, Ludwig-Maximilians-University Munich, Großhaderner Str. 2-4, 82152 Planegg-Martinsried, Germany.

<sup>2</sup> Institut für Bio- und Geowissenschaften, IBG-1: Biotechnologie, Forschungszentrum Jülich, D-52425 Jülich, Germany.

<sup>3</sup> Institute for Biochemistry, University of Cologne, Zùlpicherstr. 47, 50674 Cologne, Germany.

## Highlights

- *Corynebacterium glutamicum* prophage CGP3 encodes actin-like protein AlpC
- AlpC is active and assembles into filamentous structures
- AlpC and the putative adaptor AlpA are required for phage replication
- AlpC mediates viral DNA transport to cell membrane

**Keywords:** AlpC, actin, phage, *Corynebacterium*, replication

---

\* These authors contributed equally

‡ Corresponding authors:

**Julia Frunzke**

Email: [j.frunzke@fz-juelich.de](mailto:j.frunzke@fz-juelich.de);

Phone: +49 2461 61-5430; Fax: +49 2461 61-2710

**Marc Bramkamp**

Email: [marc.bramkamp@lmu.de](mailto:marc.bramkamp@lmu.de);

Phone: +49 89 2180 74611; Fax: +49 89 -2180 74621

## Abstract

Active transport of DNA in bacteria is catalyzed by cytomotive structures. Mediators of subcellular plasmid positioning are Walker-type ATPases (ParA), actin-like proteins, or tubulin homologs. These motor proteins are coupled to the DNA via adaptor proteins that recognize specific DNA motifs. Here, we describe that a temperate phage, CGP3, integrated as a prophage into the genome of *Corynebacterium glutamicum* ATCC 13032 encodes an actin-like protein, AlpC. Biochemical characterization confirms that AlpC is a *bona fide* actin-like protein and cell biological analysis shows that AlpC forms dynamic filamentous structures upon prophage induction. The co-transcribed AlpA protein binds to a specific region upstream of the *alpAC* operon, possibly functioning as an adaptor protein that connects circular phage DNA to the tips of the AlpC filaments. Fluorescence microscopy studies suggested that AlpC filaments are likely involved in the transport of circular phage DNA. Furthermore, quantification of circular phage DNA in mutant strains revealed that both AlpA and AlpC are required for efficient phage replication. This is remarkably similar to actin-assisted membrane localization of eukaryotic viruses that use the actin cytoskeleton to concentrate virus particles at the egress sites.

## Introduction

Segregation of genetic material is mediated by cytoskeletal elements in eu- and prokaryotes [1, 2]. During mitotic segregation, eukaryotic chromosomes are moved by microtubules that attach to the centromere [1, 3]. In bacterial cells, mechanistically similar DNA segregation processes have been described in recent years [2, 4-11]. Best understood is the segregation of plasmid DNA via a tripartite *partitioning* system. The genetic organization of *par* loci is similar for both chromosome and plasmid encoded systems. In general, the *par* locus entails two *trans*-acting proteins encoded in an operon (*parA* and *parB*,

respectively) and *cis*-acting “centromere-like” elements. The centromere-binding protein (ParB) binds the centromere-like element (*parS*) forming a nucleoprotein complex [12-14]. The segrosomes are recognized and subsequently segregated by the action of dynamic cytomotive filaments, which, depending on the plasmid partitioning system, is either a Walker-A P loop ATPase (ParA, Type I), an actin-like ATPase (ParM, Type II) or a tubulin-like GTPase (TubZ, Type III) [9, 10, 15-17]. An active *parABS* partitioning system is present in the low copy plasmid P1 prophage from *E. coli*, thereby allowing its extremely efficient maintenance, despite often being present in as few as two copies prior to division [18-20]. Thus, apparently, similar to the eukaryotic chromosome segregation apparatus, a mitotic-like apparatus exists in bacteria.

Actin-like proteins such as ParM have not only been implicated in bacterial plasmid segregation, but play a major role in cell growth and shape determination. MreB is the archetype of the bacterial cytoskeletal proteins [21-23]. Solution of the MreB structure revealed its structural homology to actin [24]. The contemporaneous description of MreB filaments in bacterial cells [25] has changed our view on subcellular organization in bacteria. MreB and its homologs are now known to be involved in the positioning of cell wall synthesizing complexes [25-28]. However, recent reports challenge the idea that MreB forms continuous helical filaments similar to F-actin [27, 28]. It seems that MreB forms rather short dynamic filaments or patches that depend on the progressive force generated by the cell wall synthesizing proteins, *e.g.* the PBPs. Active participation of MreB in DNA segregation, in analogy to ParM, has also been suggested [29, 30], but is highly controversial [21]. However, MreB is involved in viral replication. Replication of the *B. subtilis* phage  $\phi$ 29 depends on the presence of all three MreB isoforms (MreB, Mbl, and MreBH) [31-33]. MreB apparently interacts with a phage-encoded membrane protein p16.7, suggesting that phage replication may occur at the membrane. As in eukaryotes, viral replication in prokaryotes appears to occur at specific intracellular locations, likely at the cell membrane [34]. The existence of an active segregation system in the *E. coli* P1 prophage suggested that phages in general may have segregation mechanisms based on cytomotive elements. It remains to be determined if

these phage segregation systems are necessary to transport phage DNA to the subcellular address where efficient replication occurs.

Prophages or temperate phages are found in almost all bacterial cells including the industrially relevant *Corynebacterium glutamicum* ATCC 13032. *C. glutamicum* harbors three prophages, CGP1-3, of which only CGP3 has been shown to replicate extra-chromosomally in a circularized form [35]. CGP3 encompasses with 187 kbp almost 6% of the entire *C. glutamicum* genome and belongs to the largest phages with known sequence [36]. Here, we describe that the first open reading frame in the CGP3 prophage-encodes an actin-like protein, AlpC and adjacent a phage DNA-binding protein, AlpA. Biochemical characterization reveals that AlpC has actin-like properties and our cell biological data show that AlpC and AlpA are necessary for efficient phage replication. Furthermore, using allelic replacement with fluorescently labeled AlpC and AlpA, we show that phage DNA molecules are bound by AlpA and transported to the membrane by the AlpC actin-like filament. The data fit best with a model where the phage is transported to the cell membrane where replication occurs. Thus, our model suggests that bacterial phages use an actin based transport system, analogous to vertebrate viruses such as the herpes virus [37, 38].

## Results

### A prophage-encoded cytoskeleton protein

In previous work our labs have shown that the *C. glutamicum* ATCC 13032 prophage CGP3 is able to excise from the chromosome and replicate autonomously [35]. The prophage insertion site is marked by a 26-bp flanking direct repeat, marking the core element of the attachment sites *attL* and *attR*. We noticed that the first open reading frame, cg1890, in the prophage shares weak sequence similarity with bacterial actins (Fig. 1). Recently, a phylogenetic analysis also identified cg1890 as a homolog of bacterial actin-like genes, not mentioning that it is in fact within a prophage region [39]. Alignment with other actin-like proteins reveals that the protein Cg1890 shares the actin signature motifs (Fig. 1B). Hence, consistent with the nomenclature suggested by the Pogliano lab [39], we renamed Cg1890 to AlpC (designated AlpC, for Actin-Like Protein Corynebacterium).

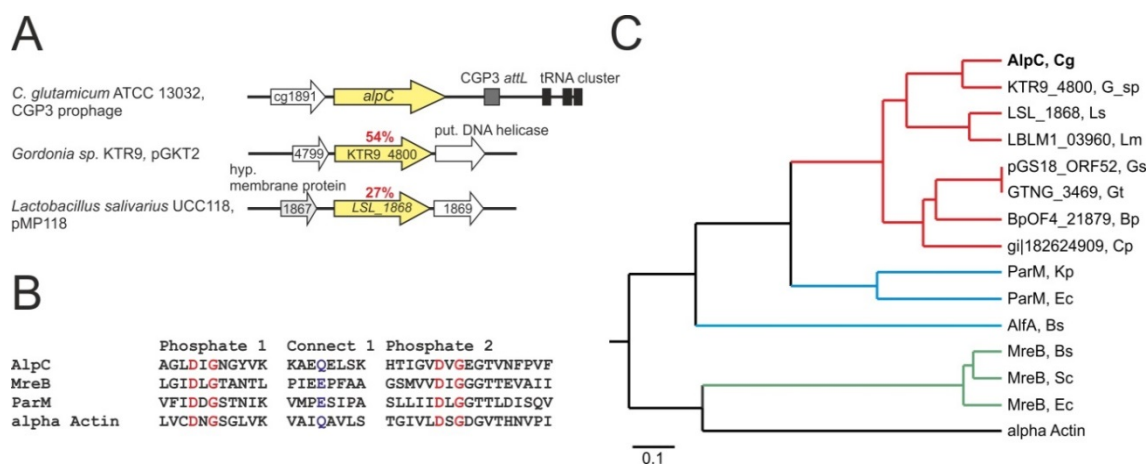


**Fig. 1. Genetic organization and phylogenetic analysis of AlpC.** (A) Genetic organization of *alpC* and close homologs (yellow). (B) Alignment of the phosphate 1, connect 1 and phosphate 2 regions [64]. Shown are the residues of *C. glutamicum* ATCC 13032 AlpC, *B. subtilis* MreB, *E. coli* ParM, and human alpha Actin. Highlighted residues correspond to alpha Actin D13 and G15 (red), Q139 (blue), and D156 and G158 (red). (C) Phylogenetic tree visualizing the relationship of AlpC homologs to bacterial actin-like proteins and human alpha actin. Amino acid sequences were aligned using the neighbor-joining method (ClustalW): AlpC Cg, *C. glutamicum* ATCC 13032 (gi|62390556), KTR9\_4800 G\_sp, *Gordonia* sp. KTR9 (gi|301321491), LSL\_1868 Ls, *Lactobacillus salivarius* UCC118 (gi|90962843), LBLM1\_03960 Lm, *Lactobacillus mucosae* LM1 (gi|377831150), pGS18\_ORF52 Gs, *Geobacillus stearothermophilus* (gi|169636508), GTNG\_3469 Gt, *Geobacillus thermodenitrificans* NG80-2 (gi|138898362), BpOF4\_21879 Bp, *Bacillus pseudofirmus* OF4 (gi|288557196), Cp, *Clostridium perfringens* D str. JGS1721 (gi|182624909), ParM Kp, *Klebsiella pneumonia* (gi|146150982), ParM Ec, *E. coli* (gi|385721336), MreB Bs, *B. subtilis* (gi|255767642), MreB Sc, *Streptomyces coelicolor* (gi|21221069), MreB Ec, *E. coli* (gi|377940072), alpha actin, *Homo sapiens* (gi|178029).

A phylogenetic analysis revealed that among actin-like proteins AlpC and homolog proteins are more closely related to plasmid partitioning system than to MreB-type cytoskeletal proteins (Fig. 1C). Protein homologs of *C. glutamicum* AlpC were found to be, in most cases, plasmid-encoded and were identified *via* Blast in a variety of Gram-positive bacteria such as *Lactobacillus* and *Bacillus* species as well as the pathogen *Clostridium perfringens* (Fig. 1C). Although they share considerably low sequence identity (mostly below 30%), the typical actin signature motif is conserved in these proteins (Fig. 1B). However, based on sequence analysis, it is not clear if AlpC shares similar properties to other actin homologs and related proteins, such as *in vivo* filament assembly and dynamics or nucleotide hydrolysis. A recent phylogenetic approach resulted in the identification of a large number of actin-like proteins, but only plasmid-encoded variants were studied in further detail [39]. Therefore, we set out to investigate the biochemical properties of AlpC and its cellular function.

### AlpC hydrolyzes both ATP and GTP

For *in vitro* characterization of the *C. glutamicum* actin-like protein, both the wild type AlpC and AlpC<sup>D301A</sup>, which lacks the conserved aspartic acid of the phosphate 2 motif, were heterologously

expressed and purified (see material and methods). Both proteins elute from the size exclusion column as mono-dispersed species in solution (not shown). However, at high concentrations, purified AlpC<sup>D301A</sup> had a tendency to aggregate, forming thick gel-like slurry (not shown).

In a nucleotide hydrolysis assay, the activity of 1  $\mu$ M of AlpC was measured with increasing concentrations of ATP or GTP (Fig. 2A). Similar to other characterized actin-like proteins, AlpC can hydrolyze both ATP and GTP, and exhibits Michaelis-Menten kinetics. In the presence of ATP, the maximum turnover rate is reached at slightly lower substrate concentrations compared to GTP. In the presence of GTP AlpC has a  $V_{max}$  of 4.3 mM min<sup>-1</sup>, compared to 3.75 mM min<sup>-1</sup> for ATP (Fig. 2A). The measured  $K_m$  is relatively low and does not differ significantly between ATP and GTP, 0.2 mM and 0.43 mM, respectively. However, *in vivo* ATP is much more abundant than GTP, and thus, ATP is probably the favored substrate. In comparison, nucleotide hydrolysis is abolished in the AlpC<sup>D301A</sup> mutant (Fig. 2A).

### AlpC polymerization is nucleotide-dependent, *in vitro*

To determine if AlpC requires nucleotides for polymerization, the purified protein was subjected

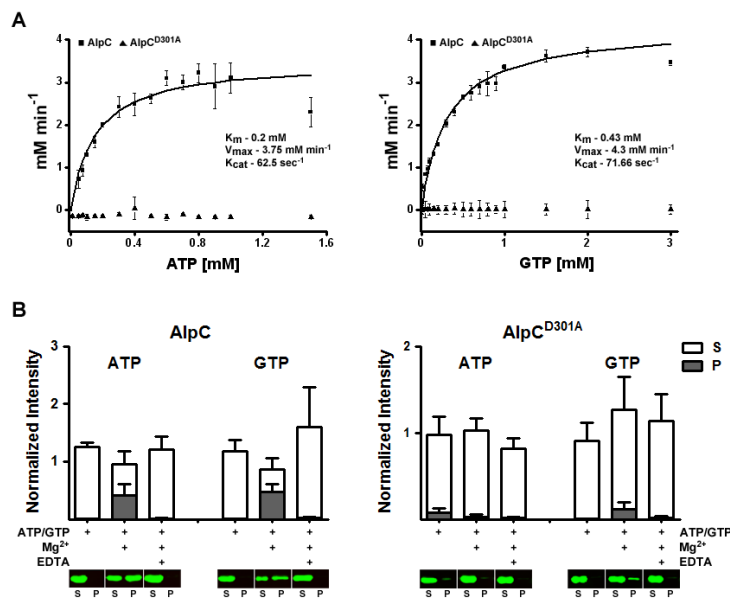


**Fig. 2. AlpC hydrolyses ATP and GTP, *in vitro*.**

(A) Shown is the turnover rate of 1  $\mu$ M of protein with increasing concentration of ATP and GTP. These plots are fitted for Michaelis-Menten kinetics. Mutation of the conserved aspartic acid of the phosphate 2 motif of AlpC abrogates nucleotide hydrolysis. Shown are the averages of three independent measurements. (B) Nucleotide dependent polymerization of AlpC. Polymerization of 2  $\mu$ M AlpC or AlpCD301A was assayed in the presence of 2 mM nucleotide (ATP or GTP), 2 mM Mg<sup>2+</sup> or 4 mM EDTA, as indicated, by means of sedimentation assays and quantitative Western blot. All values are normalized against the protein only fluorescence. Polymerization of AlpC is dependent on the presence of nucleotide and Mg<sup>2+</sup>. The hydrolytic inactive mutant does not exhibit nucleotide dependent polymerization. A montage of the immunoblotted samples is shown in the lower part of the figure. S - supernatant, P - pellet. Shown are the averages of three independent experiments.

to sedimentation assays (Fig. 2B). In the absence of nucleotides, purified AlpC did not sediment, thus, protein aggregation can be ruled out. AlpC polymerization was found to be dependent on the presence of nucleotide (ATP or GTP) and Mg<sup>2+</sup>. As a control, EDTA was additionally added to the reaction mixture, which abolished assembly of AlpC into filaments that sediment. However, contrasting to the wild type protein, AlpC<sup>D301A</sup> did not exhibit a nucleotide-dependent polymerization behavior.

### AlpC assembles into filaments, *in vivo*

One of the defining properties of actin and related cytoskeleton proteins is the ability to polymerize into filamentous structures *in vivo*. To determine if the novel *C. glutamicum* actin-like protein shares this characteristic, the subcellular behavior of AlpC was analyzed. Consequently, *alpC-cfp*, encoding a fusion protein of AlpC and CFP, was extra-chromosomally expressed from a pEKEx2 plasmid. Expression of *alpC-cfp* was induced with 0.5 mM IPTG and cells were grown in LB medium. In the vast majority of cells (97.2%, n = 870), AlpC-CFP assembled into numerous long and curved filaments, often extending from one pole to the other (Fig. 3A). However, some cells contained either a combination of filaments and foci or only discrete foci. To gain more insight into the distribution of the AlpC-CFP filaments within the cell, Z-stacks were carried out. As shown in figure 3B (and Movie S1), a number of long, curved filaments

extending the length of the cell were observed, some filaments appearing to elongate along the cell membrane. Thus, similar to actin and related cytoskeleton proteins AlpC can readily polymerize forming filamentous structures *in vivo*.

The catalytically inactive mutant AlpC<sup>D301A</sup> also assembled into filaments *in vivo* when overexpressed (Fig. 3A). However, the frequency of filament formation was significantly reduced (1.6%, n = 750) and the morphology of the AlpC<sup>D301A</sup> filaments was different from the wild type protein. Filaments were often at the membrane and some cells contained, what appeared to be, large aggregates often found near the cell pole (Fig. 3A).

### AlpC filament dynamics

*In vivo*, filaments assembled from ParM subunits are extremely dynamic, undergoing bursts of rapid growth and catastrophic decay [40]. Although such instability is not a distinguishing feature of actin and actin-like proteins, filament dynamics is essential for protein function. To ascertain if *C. glutamicum* AlpC is also dynamic, time lapse analysis was carried out. Images were acquired every 5 seconds over a period of 1 minute. It should be noted that due to bleaching effects an AlpC-CFP overexpression strain was used for the analysis. The time lapse analysis revealed that AlpC filaments are indeed dynamic (Fig. 3C and Movie S2). While some filaments appear to move along the membrane, other filaments curl into the cytoplasm.

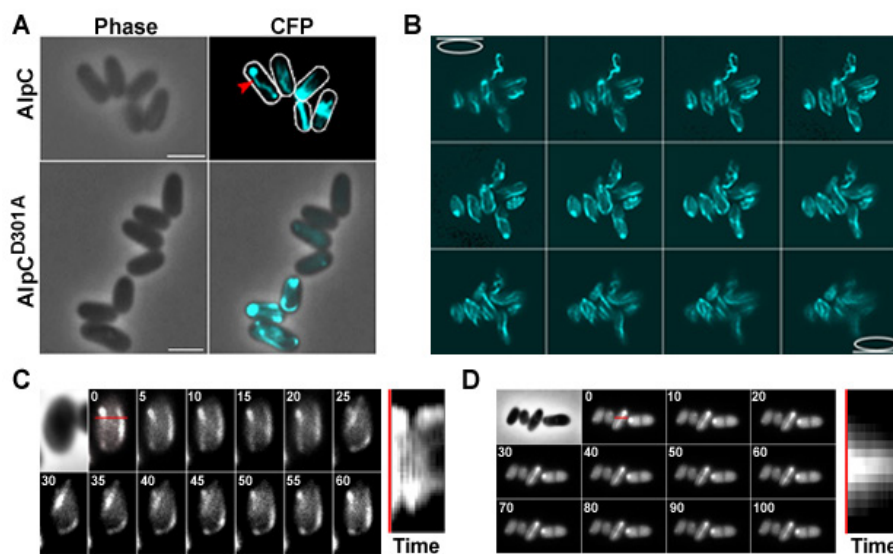


**Fig.3. AlpC assembles into filaments in *C. glutamicum*.** (A) AlpC-CFP assembles into long, curved filaments when overexpressed in *C. glutamicum*. Mutation of the conserved aspartic acid of the phosphate 2 motif of AlpC reduces filament assembly (lower panel). (B) Z-stack analysis of the subcellular distribution of AlpC-CFP filaments shows that cells contain numerous filaments of various orientation, curvature and length (Movie S1). (C) AlpC-CFP filaments are dynamic. Images were acquired at 5 second intervals (top left) for 1 minute (Movie S2). The red line denotes the position in the cell used to generate the kymograph (right). (D) AlpC<sup>D301A</sup>-CFP filaments are static. Images were acquired at 5 second intervals (top left) for 100 seconds (Movie S3). As in (C), a kymograph is shown on the right. Scale bar, 2  $\mu$ m.

*In vivo*, filament assembly of the catalytically inactive mutant (AlpC<sup>D301A</sup>) is not completely abolished, however the frequency of filament formation is greatly reduced (Fig. 3A). Time lapse analysis revealed that the AlpC<sup>D301A</sup> filaments are more stable and, hence less dynamic than wild type AlpC filaments (Fig. 3D, movie S3). This result would suggest that nucleotide hydrolysis is required for filament depolymerization or filament dynamics.

### Filament assembly of AlpC at physiological concentration

In order to study the behavior of AlpC at physiological concentration, the native *alpC* locus was replaced with an *ecfp-alpC* allele. The resulting strain has an N-terminal eCFP translational fusion to AlpC that is expressed from the native promoter. This strain exhibited medium-dependent expression and organization into filaments and foci. Under conditions of prophage induction eCFP-AlpC readily assembled into filaments (Fig. 6A). AlpC filaments or foci were observed in the vast majority of cells. The filaments were varying in length, straight and mostly found pointing to the cell membrane at different angles. These results suggest that AlpC expression and filament formation occurs in response to induction of the CGP3 prophage.

### Identification of an AlpC adaptor protein

The actin-like proteins studied to date are encoded on plasmids and are often co-transcribed with an adaptor protein, which connects the actin filament with the plasmid DNA. In many cases, the adaptor protein stimulates or stabilizes the actin filaments [15, 41-43]. Keeping with this line of thought, the behavior of AlpC was analyzed in a heterologous host. When produced in *E. coli*, AlpC-CFP was diffused in the cytoplasm, sometimes only forming irregularly sized foci (data not shown). The inability of AlpC to organize into filaments in a heterologous host suggests that filament assembly is not solely dependent on the intracellular concentration of AlpC-CFP. Thus, additional elements are required for production of AlpC-CFP filaments, most probably a factor found on the *C. glutamicum* CGP3 prophage.

AlpC is encoded in a putative operon together with Cg1891, a protein of unknown function (Fig. 1 A). We postulated that Cg1891 could be an adaptor that couples phage DNA to AlpC. To test whether Cg1891 binds to specific DNA regions, purified His<sub>10</sub>-Cg1891 protein was analyzed by electrophoretic mobility shift assays (EMSA). Previous studies of actin-like systems revealed that the binding region of these systems is often in close proximity of the respective operon [5]. Hence, we tested DNA

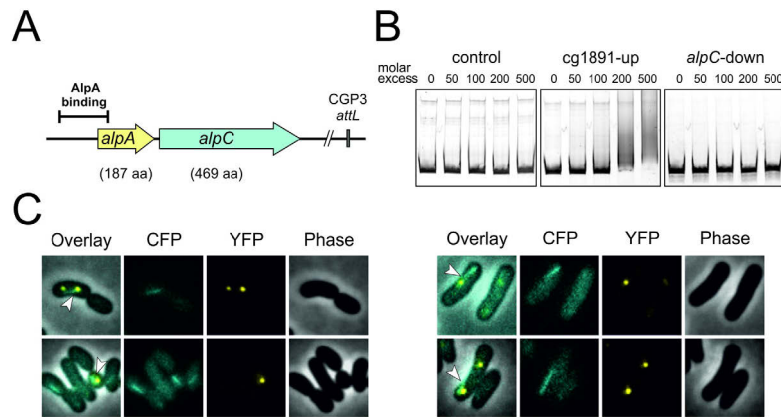


**Fig. 4. Characterization of the putative adaptor protein AlpA** (A) Genomic localization of the AlpA binding region. The DNA fragment tested for AlpA-binding is located upstream of *alpA*; 110 bp downstream of the transcriptional start site of *alpA*. (B) EMSA studies of AlpA with potential DNA target regions. For DNA-protein interaction studies, DNA fragments (500 bp) of the up- and downstream region of the putative operon *alpA-alpC* were incubated with different molar ratios of AlpA. The promoter region of *cg2036* served as control. (C) Co-visualization studies of eCFP-AlpC and AlpA-eYFP. The expression of both proteins was induced by the addition of mitomycin C before analysis.

fragments covering the up- and downstream region of the putative *cg1891-alpC* operon (Fig. 4A). The upstream region was specifically bound by Cg1891 (Fig. 4B), but a smear of shifted DNA rather than a clear band was observed. This suggested an oligomerization of the protein along the DNA, presumably at more than one binding site [44]. The downstream region and the control DNA fragment showed no binding of Cg1891. The specific DNA-binding in the upstream promoter region, in fact, revealed Cg1891 as a potential candidate for an adaptor protein. We therefore renamed *cg1891* to *alpA* (A for adaptor).

#### Co-localization of AlpA and AlpC *in vivo*

To verify our assumption of AlpA being the adaptor protein linking phage DNA to the AlpC filament, localization of both proteins was studied *in vivo*. For this purpose, an in-frame deletion of *alpA* was constructed in the background of strain CDC020, in which *alpC* was replaced by allelic exchange with *ecfp-alpC*. The deletion of *alpA* had no influence on the formation of eCFP-AlpC filaments (data not shown). For visualization of AlpA, the *alpA* gene was fused to *eyfp* and cloned into the vector pJC1 under control of the native promoter (in the  $\Delta alpA$  *alpC::ecfp-alpC* background). Fluorescence microscopy revealed small foci of AlpA-eYFP, which formed upon induction of CGP3 by addition of mitomycin C. Frequently, one to two foci of AlpA-eYFP per cell were observed at various positions; in a few cases up to four foci were detected in single cells. Remarkably, AlpA-eYFP foci were observed at

the tips or aligned with AlpC filaments (Fig. 4C). In 78% (n=37) of cells at least one AlpA focus was found to be associated with an AlpC filament. Nevertheless, the angle of the filaments and the position of the putative adaptor protein foci were, however, variable. These results provide first evidence for an interaction of AlpA and AlpC filaments.

#### Impact of AlpC on CGP3 replication

To investigate the physiological role of the actin-like protein AlpC and its role in the replication and/or segregation of the prophage CGP3, an in-frame deletion mutant lacking the *alpC* gene was constructed. Growth experiments in CGXII minimal medium showed no difference in growth phenotype compared to the wild type (data not shown). In order to analyze the impact of AlpC on CGP3 replication, *C. glutamicum* was treated with mitomycin C to induce prophage excision and replication. The intracellular amount of circular phage DNA significantly increased and reached about 10-fold induction in mitomycin C treated cells after six hours. Quantification of the intracellular amount of circular CGP3 DNA by qPCR in wild type and  $\Delta alpC$  strains revealed a similar progression (Fig. 5A). However, the maximal amount of circular CGP3 DNA was approximately two-fold reduced in  $\Delta alpC$  cells compared to wild type. As observed for  $\Delta alpC$ , the maximal amount of phage DNA was about two-fold reduced in a mutant strain lacking AlpA ( $\Delta alpA$ ).

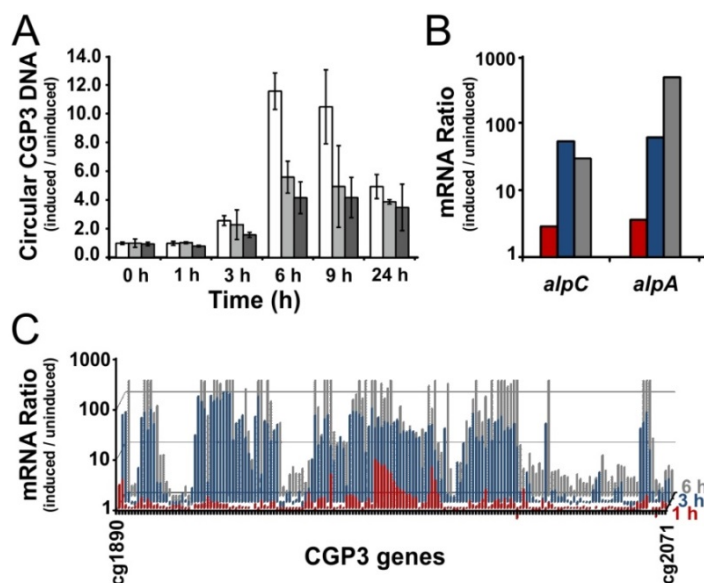


**Fig. 5. Impact of AlpC on CGP3 replication.** (A) The relative amount of circular phage CGP3 DNA was quantified by qPCR in *C. glutamicum* ATCC 13032 wild type (white) and  $\Delta alpC$  (light gray), and  $\Delta alpA$  (dark gray) upon treatment with 0.6  $\mu$ M mitomycin C. Cultivation was performed in CGXII minimal medium with 4% glucose (see material and methods). Shown are average values with standard deviation of three independent biological replicates. (B) Time course of *cg1890* (*alpC*) and *cg1891* (*alpA*) expression in *C. glutamicum* upon prophage induction triggered by the addition of 0.6  $\mu$ M mitomycin C. Shown is the mRNA ratio of cells treated with mitomycin C versus untreated cells one (red), three (blue), and six hours (gray) after mitomycin C addition analysed by DNA microarrays. (C) Time course of the mRNA ratio of the whole CGP3 gene region after addition of mitomycin C (as described in B).

Transcriptome analysis revealed that both genes, *alpC* and *alpA*, are among the early genes of CGP3 induced upon treatment with mitomycin C (Fig. 5B). The expression of *alpC* and *alpA* was 3-4-fold up-regulated one hour after induction, whereas the majority of CGP3 genes showed an increased mRNA level after 3-6 hours (Fig. 5C). Altogether, early expression of *alpC* and *alpA* in the course of CGP3 induction and the reduced level of circular CGP3 DNA in the two deletion mutants emphasizes the participation of AlpC and AlpA in the early stages of phage induction and/or synthesis, such as replication of phage DNA.

#### ***In vivo* co-visualization of the CGP3 viral DNA and AlpC filaments**

In light of the finding that several actin-like proteins are involved in segregation of plasmid DNA, an analogous role of AlpC was speculated. To test this idea, the CGP3 prophage and eCFP-AlpC were co-visualized *in vivo* by fluorescent microscopy. Visualization of CGP3 prophage DNA was carried out as described previously [35]. Basically, an array of *tetO* operator regions of transposon Tn10 was integrated into an intergenic region within the CGP3 prophage region. Co-expression of plasmid encoded *yfp-tetR* allowed direct visualization of the prophage region. The resulting strain, ATCC 13032 *alpC::ecfp-alpC/CGP3-YFP*, was grown and phage induction was triggered by mitomycin C addition. In many cells an increased number of foci corresponding to CGP3 DNA were visible [35]. In these cells, eCFP-AlpC

filaments or foci were readily observed. The eCFP-AlpC foci co-localized with the CGP3 prophage foci. Cells containing an AlpC filament in many cases had a phage particle at one tip of the filament. However, we did not observe two phage particles that were separated by an AlpC filament, thereby making it unlikely that AlpC filaments segregate two phage DNA molecules. Rather, we noticed that most AlpC filaments point at an angle to the membrane and seem to push the phage DNA towards the cell membrane. Indeed, phage DNA is mostly found at the cell membrane (Fig. 6B and C).

## **Discussion**

Segregation of genetic material by cytoskeletal elements is a common theme in eu- and prokaryotes. We describe here the identification and first characterization of an actin-like protein encoded by a prophage of the actinobacterium *C. glutamicum* ATCC 13032. Hence, contrary to the long-standing assumption, some *C. glutamicum* strains encode an actin homolog. So far, we have no evidence that AlpC influences cell growth and/or viability of *C. glutamicum*, however AlpC was shown to be a critical factor in phage replication.

#### **AlpC is a bona fide actin-like protein**

Actin and actin-related proteins share limited sequence and structural similarity [23, 24, 45, 46]. In general, to determine if candidate actin-like proteins, possessing the actin signature motif, are

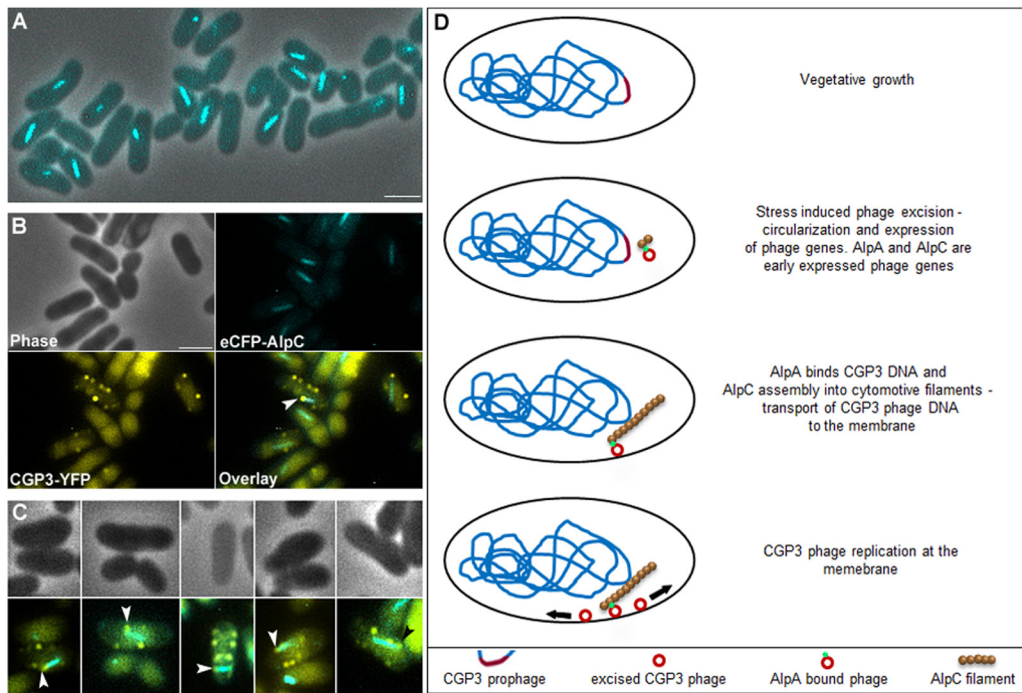


**Fig. 6.** (A) AlpC assembles into short, straight filaments when expressed at physiological concentration. (B-C) Co-visualization of eCFP-AlpC and induced CGP3 prophage (CGP3-YFP). In the example shown, the tip of an AlpC filament is connected to a phage particle. Further examples are shown in the lower panel. Scale bar, 2  $\mu$ m. (C) Proposed model for the role of AlpC as anterograde membrane transport of phage DNA. During vegetative growth the prophage is replicated with the host genome. Stress induced phage excision results in phage circularization and expression of phage genes. Via the adaptor protein AlpA, AlpC interacts with the excised phage DNA. AlpC assembles into cytomotive filaments that direct the phage DNA molecules to the cell membrane, where replication occurs.

cytoskeleton proteins a number of characteristic criteria must be met. These characteristics include assembly into dynamic filaments *in vivo* and *in vitro* binding and hydrolysis of nucleotides, in many cases both ATP and GTP. Although numerous bacterial actin-like proteins that contain the actin signature motif have been identified, relatively few have been characterized [39].

The formation of dynamic filamentous structures *in vivo* is common to both eukaryotic and prokaryotic homologs. In *C. glutamicum*, AlpC readily assembles into long curved filaments when overexpressed (Fig. 3A-B). At physiological concentration, AlpC assembled into short straight filaments, in addition to formation of compact foci (Fig. 6A). The dynamics of actin-like filaments varies and is often linked to the mode of subunit assembly, stability and function of the protein in question [47]. ParM, for example, exhibits extreme dynamic instability, displaying bursts of growth followed by rapid decay [40, 41, 48]. Stabilization of the ParM filament requires that the end of the ParM filament is capped with a ParR bound plasmid [42, 49]. Thus, the dynamic instability of the ParM filament is intrinsic to the mode of action of ParM in plasmid

segregation, where it searches the cytoplasmic environment for plasmids. Similarly, the mode of action of Alp7A filaments in plasmid segregation requires that both ends of the filament are capped with a plasmid [39]. Other actin-like proteins, such as AlfA, assemble into filaments by addition of subunits to one side of the filament only [43]. Alp7A filaments are more stable and long-lived. Although the mechanism by which Alp7A segregates plasmids is not well understood, it differs to ParM mediated segregation [15, 43].

The dynamics of AlpC filaments was analyzed in cells overexpressing *alpC-cfp*. This strain was used as the low concentration of AlpC expressed from the native promoter required longer exposure times which subsequently led to fluorophore bleaching. Z-stack analysis revealed numerous, long and curved AlpC-CFP filaments (Fig. 3B and movie S1). These filaments exhibited a dynamic behavior (Fig. 3C and movie S2), however unlike ParM and Alp7A dynamic instability was not observed [39, 40, 41, 48].

*In vitro*, AlpC can hydrolyze both ATP and GTP, with ATP being the more abundant and thus, likely the favored substrate (Fig. 2A). Mutation of one of the conserved residues in the phosphate 2 motif

(D301A) abolished nucleotide hydrolysis of AlpC (Fig. 2A). Additionally, filament assembly of AlpC<sup>D301A</sup> was severely reduced *in vivo* (1.6%, n = 750). In comparison, almost all cells expressing AlpC-CFP contained filaments (97.2%, n = 870). AlpC<sup>D301A</sup> filaments were often found close to the membrane and many cells contained large polar patches of aggregated protein (Fig 3A). According to the *in vitro* data, assemble of AlpC into filaments depends on the presence of nucleotide and Mg<sup>2+</sup> as a cofactor (Fig. 2B). On the contrary but in line with the *in vivo* data, assembly of purified AlpC<sup>D301A</sup> into filaments was greatly reduced *in vitro* (Fig 2B). It should however be noted that, unlike the wild type AlpC protein, the AlpC<sup>D301A</sup> hydrolysis mutant exhibited concentration dependent aggregation. Mutation of the conserved aspartic acid residue of the phosphate 2 motive also resulted in the formation of static filaments (Fig. 3D and movie S3).

### AlpC filaments are connected to circular phage DNA by the putative adaptor protein AlpA

Given the tripartite organization of chromosomal and plasmid segregation systems, we sought to identify an adaptor protein that connects the phage DNA with AlpC filaments. The upstream, co-transcribed *alpA* (cg1891) does not share any appreciable homology to known adaptor proteins of chromosome or plasmid segregation systems. *In vitro* EMSA assays showed that AlpA binds to DNA upstream of the *alpAC* operon (Fig. 5). *In vivo*, AlpA-YFP formed compact foci that often colocalized to the tips of AlpC filaments. However, filament assembly of AlpC was not altered in cells lacking AlpA, suggesting that AlpA does not necessarily induce or stabilize the actin-like filaments formation. Instead, we speculate that the role of AlpA is to connect phage DNA with AlpC filament which might be involved in the transport of phage DNA to the membrane. Nonetheless, the fact that AlpC does not assemble into filaments when expressed in *E. coli* would suggest that additional factors are required and assembly into filaments is not solely dependent on concentration, *in vivo*. Furthermore, filament assembly of eCFP-AlpC was severely reduced when expressed in a *C. glutamicum* strain that lacks most of the CGP3 prophage (data not shown). Thus, factors specific to the phage region are required for the formation of filaments.

### AlpC and AlpA are necessary for efficient prophage replication

Initially, we speculated that AlpC might function to actively segregate excised prophage DNA, akin to plasmid segregation systems. Interestingly, we found that AlpC filaments were sometimes absent in cells that contained multiple induced phage particles. In cells that contained multiple CGP3 foci and AlpC filaments, interaction between AlpC filaments and one phage particle was observed (Fig. 6B and C), arguing against a role in segregation of two phage genomes. In addition, as cell division is often halted under phage (or stress) inducing conditions (SOS response), AlpAC mediated segregation of phage particles into dividing daughter cells appears unlikely. However, the DNA of the induced prophage often accumulated at the cell membrane (Fig. 6B and C). There is an increasing amount of evidence suggesting that plasmid and phage replication occurs at the membrane [31, 33, 50]. We speculate that excised phage DNA is directed to the membrane where additional replication occur. Consistent with this idea, cells lacking AlpC have a 2-fold decrease in phage copy number. Additionally, the phage copy number in cells lacking AlpA is reduced (Fig. 5), highlighting a concerted role of the AlpAC in CGP3 phage replication.

### Mechanisms of phage-encoded cytoskeletal elements

During the preparation of this manuscript two interesting reports on phage-encoded tubulin homologs haven been published [51, 52]. Both reports describe that phage-encoded PhuZ [51] and TubZ [52] are required for correct phage particle placement in the infected host. Interestingly, the two reports arrive at different conclusions. PhuZ is encoded in the *Pseudomonas* phage 201φ2-1. PhuZ forms GTP hydrolysis dependent dynamic filaments *in vivo* and *in vitro* [51]. These filaments traverse the entire cell and are thought to assemble phage particles in the center of the cell. However, PhuZ was expressed from an inducible promoter. Here, we have observed a similar polymerization behavior of AlpC when it was overexpressed in *C. glutamicum*, but got a different picture when *alpC* was expressed from the native promoter. Phage replication was also impaired in PhuZ mutant background, suggesting that proper segregation is important for

phage replication. The authors arrive at the conclusion that PhuZ forms a spindle-like apparatus that positions the virus particles in the cell center [51]. Simultaneously, a TubZ homolog in the *Clostridium botulinum* phage c-st was shown to behave like a classical type II segregation system. TubZ binds, *via* the adaptor protein TubR, to the centromeric region of the phage DNA [52]. Superficially, the c-st TubZ and AlpC share a similar mechanism, in particular since both are encoded in prophages that replicate as plasmid-like entities. However, close inspection of the results that we describe here, make it unlikely that the short AlpC filaments observed after induction of phage replication would be suited to segregate plasmid particles into separating daughter cells. Rather, our data are consistent with AlpC guiding CGP3 DNA to the cell membrane, where replication likely occurs. Fluorescent co-localization of AlpC filaments and viral DNA show that phage DNA foci are often found in numerous copies at the membrane, while AlpC filaments only attach to single particles. In this aspect AlpC might resemble the role of eukaryotic F-actin in the anterograde transport of herpes-like viruses [37, 38, 53]. The anterograde transport brings virus particles to the cell membrane (Fig. 6). Actin plays, in fact, a prominent role as a host factor for viral replication in eukaryotes. Actin is not only required for retrograde transport, but also involved in uptake, retrograde transport to the nucleus, replication and long-range spread [38]. This is in line with observations that link the *B. subtilis* actin homolog MreB with replication of phages SPP1 and  $\phi$ 29 [33]. Proteins and DNA of  $\phi$ 29 localize in a punctuate pattern at the membrane where they co-localize with MreB. In absence of MreB phage polymerase and the putative membrane anchor p16.7 are delocalized. Consequently, phage replication was reduced. In this model MreB assists localization of the phage replication machinery, but is not involved in phage segregation analogous to ParM-driven plasmid segregation. It may, therefore, be advantageous for phages replicating in bacteria lacking an endogenous actin cytoskeleton to encode this cytoskeletal element within their own genome. A unifying theme is that phages with large genomes seem to rely on cytoskeletal filaments for intracellular movement. Thus, it seems plausible that the connection of actin and viral replication is

ancient [54] and that the general principle is well conserved even between bacteria and phages.

## Experimental Procedure

### Recombinant DNA work

Standard methods like PCR, restriction or ligation were carried out according to established protocols [55, 56]. Oligonucleotide synthesis and DNA sequencing was performed by Eurofins MWG Operon (Ebersfeld, Germany). Strain, plasmids and oligonucleotides are listed in Table S1.

In-frame deletion mutants of the *alpC* gene (cg1890) were constructed *via* the two-step homologous recombination procedure as described previously [57]. The *alpC* up- and downstream regions have been amplified using the oligonucleotide pairs DalpC-1/DalpC-2 and DalpC-3/DalpC-4. The resulting PCR products were used as template for an overlap extension PCR with the oligonucleotides DalpC-1/DalpC-4. The purified PCR product of ca. 1 kb was digested with EcoRI and BamHI and cloned into the vector pK19*mobsacB*. The resulting plasmid pK19*mobsacB*- $\Delta$ *alpC* was used for performing an allelic exchange by homologous recombination [57] in the chromosome of *C. glutamicum* ATCC 13032 resulting in the mutant strain *C. glutamicum*  $\Delta$ *alpC*.

To generate a strain overexpressing AlpC-CFP, *cfp*, including the stop codon, was amplified using primer pair CFP-SacI-F/*cfp* EX2 Eco R mS. The resulting PCR product was restriction digested with SacI and EcoRI and ligated into an identically treated pEKEx2 vector. Subsequently, *alpC*, lacking the stop codon, was amplified using primer pair AlpC-Sall-F/ AlpC-BamHI-os-R, restriction digested with Sall and BamHI and ligated into the pEKEx2-*cfp* vector. The resulting vector (pCD129) was transformation into *C. glutamicum* resulting in extrachromosomal, IPTG-inducible expression of *alpC*-*cfp* (CDC021). To generate a strain expressing *alpC*<sup>D301A</sup>-*cfp*, pCD129 was used as template and subjected to site directed mutagenesis using primer pair 1890-D301A-F/1890-D301A-R, giving rise to vector pCD130. Plasmids were verified by sequencing. The resulting vector was transformed in *C. glutamicum*, giving rise to strain CDC022.

The strain expressing *ecfp*-*alpC* at physiological concentration was generated by integrating *ecfp* upstream of and in-frame with *alpC*. As describe above, a two-step homologous recombination procedure was used [47]. The *ecfp* gene was PCR amplified using the primer pair eCFP-Sall-F/eCFP-XbaI-R. The resulting PCR product was restriction digested with Sall and XbaI and ligated into an identically digested pK19*mobsacB*

vector, placing *ecfp* in the middle of the multiple cloning site. The region upstream of the *alpC* start codon and the first 0.5 kb of *alpC* were amplified using primer pairs Alp-up-Hind-F/Alp-up-Sal-R and Alp-D-Xba-F/Alp-D-Bam-R, respectively. The resulting PCR products were digested with HindIII/SalI and XbaI/BamHI, respectively and sequentially ligated into a pK19*mobsacB-ecfp* vector. This vector was used for allelic replacement at the *alpC* locus, integrating *ecfp* at the 5' end of *alpC*, resulting in strain CDC020. Chromosomal integration was confirmed by PCR.

For an in-frame deletion of *alpA* (cg1891) the plasmid pK19*mobsacB-ΔalpA* was constructed using the oligonucleotides DalpA-1/DalpA-2 and DalpA-3/DalpA-4. For deletion of *alpA* in the strain CDC020, in which *alpC* is genomically replaced by *cfp-alpC*, the flanking downstream region of *alpA* was amplified with the oligonucleotides DalpA-3 and DalpA-cfp-alpC-4. As template DNA for this PCR served genomic DNA of strain CDC020. In an overlap extension PCR, the PCR products were combined by amplification with the oligonucleotides DalpA-1 and DalpA-4 or DalpA-cfp-alpA-4, respectively. After restriction with EcoRI and BamHI and ligation with pK19*mobsacB*, the plasmids pK19*mobsacB-ΔalpA* and pK19*mobsacB-ΔalpA-cfp-alpA* were obtained. The construction of an in-frame deletion mutant of *alpA* and the deletion of *alpA* in the strain CDC020 were performed as described for *ΔalpC* resulting in the mutant strains *ΔalpA* and *ΔalpA alpC::cfp-alpC*.

For co-visualization of eCFP-AlpC filaments and CGP3 prophage, strain CDC020 was used as the background strain and the CGP3 prophage was tagged as described previously [34].

For heterologous overexpression of His<sub>10</sub>-AlpC the *alpC* gene (cg1890) was PCR amplified using primers AlpC-et-F and AlpC-et-R, restriction digested with XhoI and BamHI and ligated into pET16b (Novagen). The resulting plasmid (pCD115) was transformed into BL21(DE3) pLysS for heterologous protein production. Site directed mutagenesis was employed to generate pCD116 (His<sub>10</sub>-AlpC<sup>D301A</sup>). For heterologous overexpression of AlpA the gene cg1891 (*alpA*) was amplified with the oligonucleotides alpA-fw and alpA-rv. The PCR product and the plasmid pET-TEV were digested with NdeI and EcoRI and ligated. Thereby the sequence of a His<sub>10</sub>-tag was fused to the 5'-end of *alpA*, resulting in the plasmid pET-TEV-*alpA*. Subsequently, *E. coli* BL21(DE3) was transformed with the plasmid for heterologous protein production.

To localize AlpA in single cells, an AlpA-eYFP protein fusion was used. For this purpose, the natural promoter P<sub>alpA</sub> and *alpA*, excluding the stop codon,

were amplified by PCR with the oligonucleotides pairs PalpA-BamHI-fw and alpA-link-rv. To amplify *eyfp* the oligonucleotides eyfp-link-fw and eyfp-SalI-rv were used, thereby adding the sequence 5'-GGCGCTGCTGGC-3' in front of *eyfp* as a linker sequence. Both PCR products were combined in an overlap-extension PCR with the oligonucleotides PalpA-BamHI-fw and eyfp-SalI-rv and digested with BamHI and SalI. Subsequently the product was ligated into pJC1, resulting in the plasmid pJC1-*PalpA-alpA-eyfp*. For co-localization studies the strain *ΔalpA alpC::cfp-alpC* was transformed with the plasmid.

#### Determination of circular phage DNA using quantitative PCR

The relative amount of circular phage DNA was determined via quantitative PCR (qPCR). Therefore, *C. glutamicum* wild type, the *alpC* deletion strain, and the *alpA* deletion strain were grown in 5 ml BHI (Brain Heart Infusion, Difco) for about 6 hours at 30°C. A second precultivation was performed in CGXII minimal medium containing 4% glucose as carbon source. From each preculture two main cultures were inoculated to an OD of 1 in CGXII minimal medium. At an OD of 3 mitomycin C (final concentration of 0.6 μM) was added to one culture to induce the SOS response; the second, untreated culture served as reference. 5 ml samples were harvested by centrifugation (4000 x g, 10 min and 4 °C) at different time points after induction (0-24 h). The preparation of genomic DNA was performed as described previously [58].

The determination of the relative amount of circular DNA of the phage CGP3 by quantitative PCR was conducted according to the protocol described in Frunzke *et al.* (2008) [35]. Briefly, each sample contained 1 μg total DNA as template for amplification. Amplification was performed using the DyNAmo Capillary SYBR Green qPCR Kit (Finnzymes Oy, Vantaa) and a LightCycler type 1.0 (Roche Diagnostics). The *ddh* gene (cg2900), which is present in one copy in the *C. glutamicum* genome, served as reference gene for normalization; the oligonucleotides *ddh*-LC-for and *ddh*-LC-rev were used for amplification. For the detection of circular CGP3 DNA, oligonucleotides (Phage-LC-for and Phage-LC-rev) were designed which anneal to the left and right border of CGP3, pointing into divergent directions. This arrangement was used to specifically amplify a 150 bp DNA fragment covering the attachment site (*attP*) of the excised circular CGP3 DNA molecule. For the calculation of the relative amount of the circular phage DNA the amount of the circular phage DNA in induced cells was normalized

with the amount of circular phage DNA in uninduced cells of the same strain at each time point.

### DNA microarrays

For transcriptome analysis cells were cultivated as described for the determination of circular CGP3 DNA (previous paragraph). Transcriptomes of *C. glutamicum* ATCC 13032 were comparisons of cells treated with or without 0.6 mM mitomycin C after one, three, six and nine hours after addition of mitomycin C. The custom DNA microarrays were obtained from Agilent Technologies (Waldbronn, Germany). Agilent's eArray platform was used to design oligonucleotide probes with the best probe methodology and assemble custom 4x44K 60mer microarray designs (<https://earray.chem.agilent.com/earray/>). The custom design included oligonucleotides for the annotated protein-coding genes and structural RNA genes of the four bacterial genomes from *C. glutamicum*, *Escherichia coli*, *Gluconobacter oxydans*, and *Bacillus subtilis* for genome-wide gene expression analysis. For *C. glutamicum*, the genome annotation NC\_006958 from NCBI was used listing 3057 protein coding genes and 80 structural tRNA and ribosomal RNA genes [36]. In the custom design, *C. glutamicum* genes are represented by one, two or three oligonucleotides which were used to determine relative RNA levels. The custom array design also included the Agilent's control spots.

Purified cDNA samples to be compared were pooled and prepared two-color samples were hybridized on 4x44K arrays at 65°C for 17 hours using Agilent's gene expression hybridization kit, Agilent's hybridization chamber, and Agilent's hybridization oven. After hybridization the arrays were washed using Agilent's wash buffer kit according to the manufacturer's instructions. Fluorescence of hybridized DNA microarrays was determined at 532 nm (Cy3-dUTP) and 635 nm (Cy5-dUTP) at 5 µm resolution with a GenePix 4000B laser scanner and GenePix Pro 6.0 software (Molecular Devices, Sunnyvale, CA, USA). Fluorescence images were saved to raw data files in TIFF format (GenePix Pro 6.0).

Quantitative TIFF image analysis was carried out using GenePix image analysis software and the Agilent's gene array list (GAL) file. The results were saved as GPR-file (GenePix Pro 6.0). For background correction of spot intensities, ratio calculation and ratio normalization, GPR-files were processed using the BioConductor R-packages *limma* and *marray* (<http://www.bioconductor.org>). For further analysis, the processed and loess-normalized data as well as detailed experimental information according to MIAME

[59] were stored in the in-house DNA microarray database [60]. To search the data for differentially expressed genes by the processed Cy5/Cy3 ratio reflecting the relative RNA level, the criteria flags  $\geq 0$  (GenePix Pro 6.0) and signal/noise  $\geq 5$  for Cy5 (F635Median/B635Median) or Cy3 (F532Median/B532Median) were used.

Array data were deposited in the GEO database ([ncbi.nlm.nih.gov/geo](http://ncbi.nlm.nih.gov/geo)) under accession number GSE45907.

### Heterologous protein expression and purification

His<sub>10</sub>-AlpC was heterologously overexpressed in *E. coli* BL21 (DE3) pLysS. Expression was induced with 0.4 mM IPTG. Cells were collected by centrifugation at 5000 *g* (4°C) for 10 min, resuspended in buffer A (100 mM Tris-HCl, pH 7.5, 150 mM KCl, 150 mM NaCl, 10 % glycerol and 10 mM imidazole), supplemented with DNase I and protease inhibitor. The cleared cell lysate was applied to a 1 ml HisTrap™ FF column, washed with 10 column volumes of buffer A and subsequently eluted by a step gradient of buffer B (buffer A supplemented with 490 mM imidazole). The affinity purified AlpC protein was further applied to a Superdex™ 200 10/300 gel filtration column and eluted in buffer C (buffer A lacking imidazole). Eluted fractions were analyzed by SDS-PAGE and immunoblotting. Heterologous overexpression and purification of AlpCD<sup>301A</sup> was identical.

The production of His<sub>10</sub>-AlpA in *E. coli* BL21 (DE3) pLysS was induced with 0.5 mM IPTG and harvested after 4 hours of expression as described for His<sub>10</sub>-AlpC. The disruption of the cells and purification of the protein with a Ni<sup>2+</sup>-NTA column (nickel-nitriloacetic acid) (Qiagen, Hilden) were performed as described previously [61]. The elution of AlpA was conducted with TN1400 buffer (20 mM Tris/HCl, 300 mM NaCl, 400 mM imidazole). The fractions of eluted protein were pooled and the buffer was exchanged to binding buffer (20 mM Tris/HCl, pH 7.5, 50 mM KCl, 10 mM MgCl<sub>2</sub>, 5% (v/v) glycerol, 0.5 mM EDTA, 0.005% (w/v) Triton X-100) with a PD10 desalting column (GE Healthcare) for DNA-Protein binding studies.

### Electrophoretic mobility shift assays

Studies of the DNA-Protein binding of AlpA and potential target DNA were performed according to [62]. The DNA (500 bp) of the upstream region of *alpA* and downstream region of *alpC* were amplified by PCR. The promoter region of *cg2036*, a gene encoded by the prophage CGP3 in *C. glutamicum*, was tested as control fragment. 100 ng DNA per lane were incubated with different molar ratios of purified AlpA for 20 minutes

before loading to a non-denaturing 10% polyacrylamide gel.

### Nucleotide hydrolysis assay

ATPase and GTPase activity was measured in a coupled enzyme assay constantly regenerating GTP [63]. Nucleotide hydrolysis rate of 1  $\mu\text{M}$  protein was measured in a total volume of 100  $\mu\text{l}$  containing varying nucleotide concentration, equimolar  $\text{MgSO}_4$ , 50 mM Tris-HCl, 200 mM NaCl, 10 % glycerol, 1 mM PEP, 0.6 mM NADH, 20 U/ml pyruvate kinase and 20 U/ml lactate dehydrogenase. The samples were setup in a 96-well microtiter plate and the absorbance of NADH was monitored at 340 nm for 1 hour at 30°C (Tecan Plate Reader, software: I-control). All data were obtained from triplicate determination and corrected for nucleotide autohydrolysis.

### Sedimentation assay

Prior to experimental setup, protein samples were subjected to centrifugation at 120,000  $g$  for 10 minutes to remove any aggregated protein. Purified protein (2  $\mu\text{M}$ ) was mixed with nucleotide (2  $\mu\text{M}$ ) in the presence or absence of 2  $\mu\text{M}$   $\text{Mg}^{2+}$  or 4  $\mu\text{M}$  EDTA. Volumes were adjusted to 100  $\mu\text{l}$  with buffer C. Reaction mixtures were incubated at 30°C for 30 minutes. Polymerized protein was then separated from non-polymerized protein by centrifugation at 120,000  $g$  for 10 minutes. Supernatant and pellet fractions were separated and quantitatively analyzed by immunoblot.

For quantitative Western blot analyses of polymerized His<sub>10</sub>-AlpC and His<sub>10</sub>-AlpC<sup>D301A</sup> from the sedimentation assays, samples were blotted onto an Immobilon-FL PVDF membrane (Millipore) and probed with anti-His antibody (Qiagen), followed by IRDye 800-conjugated goat anti-mouse IgG (H + L) antibodies (LI-COR) as secondary antibody. The IR fluorescence signals were quantified with the Odyssey<sup>TM</sup> IR fluorescence scanning system (LI-COR). Background values were automatically subtracted using the Odyssey software (LI-COR) (Median Top/Bottom method). Signals were normalized to a protein only sample.

### Fluorescence microscopy

For microscopic examination, expression from the pEKEx2 plasmid was induced by addition of 0.5 mM isopropyl- $\beta$ -D-thiogalactopyranoside (IPTG) to the growth medium, for approximately 60-90 min. For co-visualization of eCFP-AlpC filament and induced CGP3 prophage, cells were grown in CGXII medium supplemented with 4% glucose. Excision of the CGP3 prophage was induced by addition of mitomycin C (final

concentration 0.2  $\mu\text{g}$  / ml). Approximately 30 minutes prior to microscopic examination, 0.1 mM IPTG was added to induce synthesis of YFP-TetR.

For phase contrast and fluorescence microscopy, 1-3  $\mu\text{l}$  of a culture sample was placed on a microscope slide coated with a thin 1 % agarose layer and covered by a cover slip. Images were taken on a Zeiss AxioImager M1 equipped with a Zeiss AxioCam HRm camera or on a Zeiss AxioImager M2 equipped with a Zeiss AxioCam MRm camera. GFP fluorescence was monitored using filter set 38 HE eGFP, BG-430 fluorescence and CFP (eCFP) were monitored using filter 47 HE CFP, red fluorescence (membrane stain) was monitored by using filter 43 HE Cy3 or filter 63He and DAPI / Hoechst fluorescence was examined with filter set 49. An EC Plan-Neofluar 100x/1.3 Oil Ph3 objective was used. Digital images were acquired and analyzed with the AxioVision 4.6 software (Carl Zeiss). Final image preparation was done using Adobe Photoshop 6.0 (Adobe Systems Incorporated).

### Acknowledgements

The authors thank the Deutsche Forschungsgemeinschaft (priority program SPP1617) and the Helmholtz Association (Helmholtz grant VH-NG-716) for financial support.

### References

1. Bloom, K., and Joglekar, A. (2010). Towards building a chromosome segregation machine. *Nature* 463, 446-456.
2. Löwe, J., and Amos, L.A. (2009). Evolution of cytomotive filaments: the cytoskeleton from prokaryotes to eukaryotes. *Int J Biochem Cell Biol* 41, 323-329.
3. Yanagida, M. (2005). Basic mechanism of eukaryotic chromosome segregation. *Philos Trans R Soc Lond B Biol Sci* 360, 609-621.
4. Ptacin, J.L., Lee, S.F., Garner, E.C., Toro, E., Eckart, M., Comolli, L.R., Moerner, W.E., and Shapiro, L. (2010). A spindle-like apparatus guides bacterial chromosome segregation. *Nat Cell Biol* 12, 791-798.
5. Gerdes, K., Howard, M., and Szardenings, F. (2010). Pushing and pulling in prokaryotic DNA segregation. *Cell* 141, 927-942.
6. Schumacher, M.A. (2008). Structural biology of plasmid partition: uncovering the molecular mechanisms of DNA segregation. *Biochem J* 412, 1-18.
7. Hayes, F., and Barilla, D. (2006). The bacterial segrosome: a dynamic nucleoprotein machine for DNA trafficking and segregation. *Nat Rev Microbiol* 4, 133-143.
8. Ghosh, S.K., Hajra, S., Paek, A., and Jayaram, M. (2006). Mechanisms for chromosome and plasmid segregation. *Annu Rev Biochem* 75, 211-241.

9. Ebersbach, G., and Gerdes, K. (2005). Plasmid segregation mechanisms. *Annu Rev Genet* 39, 453-479.
10. Gerdes, K., Moller-Jensen, J., Ebersbach, G., Kruse, T., and Nordstrom, K. (2004). Bacterial mitotic machineries. *Cell* 116, 359-366.
11. Fogel, M.A., and Waldor, M.K. (2006). A dynamic, mitotic-like mechanism for bacterial chromosome segregation. *Genes Dev* 20, 3269-3282.
12. Schumacher, M.A., and Funnell, B.E. (2005). Structures of ParB bound to DNA reveal mechanism of partition complex formation. *Nature* 438, 516-519.
13. Funnell, B.E. (1988). Mini-P1 plasmid partitioning: excess ParB protein destabilizes plasmids containing the centromere *parS*. *J Bacteriol* 170, 954-960.
14. Salje, J., Gayathri, P., and Löwe, J. (2010). The ParMRC system: molecular mechanisms of plasmid segregation by actin-like filaments. *Nat Rev Microbiol* 8, 683-692.
15. Becker, E., Herrera, N.C., Gunderson, F.Q., Derman, A.I., Dance, A.L., Sims, J., Larsen, R.A., and Pogliano, J. (2006). DNA segregation by the bacterial actin Alfa during *Bacillus subtilis* growth and development. *Embo J* 25, 5919-5931.
16. Larsen, R.A., Cusumano, C., Fujioka, A., Lim-Fong, G., Patterson, P., and Pogliano, J. (2007). Treadmilling of a prokaryotic tubulin-like protein, TubZ, required for plasmid stability in *Bacillus thuringiensis*. *Genes Dev* 21, 1340-1352.
17. Donovan, C., Schwaiger, A., Krämer, R., and Bramkamp, M. (2010). Subcellular localization and characterization of the ParAB system from *Corynebacterium glutamicum*. *J Bacteriol* 192, 3441-3451.
18. Prentki, P., Chandler, M., and Caro, L. (1977). Replication of prophage P1 during the cell cycle of *Escherichia coli*. *Mol Gen Genet* 152, 71-76.
19. Abeles, A.L., Friedman, S.A., and Austin, S.J. (1985). Partition of unit-copy miniplasmids to daughter cells. III. The DNA sequence and functional organization of the P1 partition region. *J Mol Biol* 185, 261-272.
20. Li, Y., Dabrazhynetskaya, A., Youngren, B., and Austin, S. (2004). The role of Par proteins in the active segregation of the P1 plasmid. *Mol Microbiol* 53, 93-102.
21. Chastanet, A., and Carballido-Lopez, R. (2012). The actin-like MreB proteins in *Bacillus subtilis*: a new turn. *Front Biosci (Schol Ed)* 4, 1582-1606.
22. Carballido-Lopez, R., and Formstone, A. (2007). Shape determination in *Bacillus subtilis*. *Curr Opin Microbiol* 10, 611-616.
23. van den Ent, F., Amos, L., and Löwe, J. (2001). Bacterial ancestry of actin and tubulin. *Curr Opin Microbiol* 4, 634-638.
24. van den Ent, F., Amos, L.A., and Löwe, J. (2001). Prokaryotic origin of the actin cytoskeleton. *Nature* 413, 39-44.
25. Jones, L.J., Carballido-Lopez, R., and Errington, J. (2001). Control of cell shape in bacteria: helical, actin-like filaments in *Bacillus subtilis*. *Cell* 104, 913-922.
26. Daniel, R.A., and Errington, J. (2003). Control of cell morphogenesis in bacteria: two distinct ways to make a rod-shaped cell. *Cell* 113, 767-776.
27. Garner, E.C., Bernard, R., Wang, W., Zhuang, X., Rudner, D.Z., and Mitchison, T. (2011). Coupled, circumferential motions of the cell wall synthesis machinery and MreB filaments in *B. subtilis*. *Science* 333, 222-225.
28. Dominguez-Escobar, J., Chastanet, A., Crevenna, A.H., Fromion, V., Wedlich-Söldner, R., and Carballido-Lopez, R. (2011). Processive movement of MreB-associated cell wall biosynthetic complexes in bacteria. *Science* 333, 225-228.
29. Gitai, Z., Dye, N.A., Reisenauer, A., Wachi, M., and Shapiro, L. (2005). MreB actin-mediated segregation of a specific region of a bacterial chromosome. *Cell* 120, 329-341.
30. Soufo, H.J., and Graumann, P.L. (2003). Actin-like proteins MreB and Mbl from *Bacillus subtilis* are required for bipolar positioning of replication origins. *Curr Biol* 13, 1916-1920.
31. Munoz-Espin, D., Serrano-Heras, G., and Salas, M. (2012). Role of host factors in bacteriophage phi29 DNA replication. *Adv Virus Res* 82, 351-383.
32. Munoz-Espin, D., Holguera, I., Ballesteros-Plaza, D., Carballido-Lopez, R., and Salas, M. (2010). Viral terminal protein directs early organization of phage DNA replication at the bacterial nucleoid. *Proc Natl Acad Sci U S A* 107, 16548-16553.
33. Munoz-Espin, D., Daniel, R., Kawai, Y., Carballido-Lopez, R., Castilla-Llorente, V., Errington, J., Meijer, W.J., and Salas, M. (2009). The actin-like MreB cytoskeleton organizes viral DNA replication in bacteria. *Proc Natl Acad Sci U S A*.
34. Firshein, W. (1989). Role of the DNA/membrane complex in prokaryotic DNA replication. *Annu Rev Microbiol* 43, 89-120.
35. Frunzke, J., Bramkamp, M., Schweitzer, J.E., and Bott, M. (2008). Population Heterogeneity in *Corynebacterium glutamicum* ATCC 13032 caused by prophage CGP3. *J Bacteriol* 190, 5111-5119.
36. Kalinowski, J., Bathe, B., Bartels, D., Bischoff, N., Bott, M., Burkovski, A., Dusch, N., Eggeling, L., Eikmanns, B.J., Gaigalat, L., Goesmann, A., Hartmann, M., Huthmacher, K., Krämer, R., Linke, B., McHardy, A.C., Meyer, F., Möckel, B., Pfefferle, W., Pühler, A., Rey, D.A., Rückert, C., Rupp, O., Sahm, H., Wendisch, V.F., Wiegräbe, I., and Tauch, A. (2003). The complete *Corynebacterium glutamicum* ATCC 13032 genome sequence and its impact on the production of L-aspartate-derived amino acids and vitamins. *J Biotechnol* 104, 5-25.

37. Smith, G.A., Gross, S.P., and Enquist, L.W. (2001). Herpesviruses use bidirectional fast-axonal transport to spread in sensory neurons. *Proc Natl Acad Sci U S A* **98**, 3466-3470.
38. Taylor, M.P., Koyuncu, O.O., and Enquist, L.W. (2011). Subversion of the actin cytoskeleton during viral infection. *Nat Rev Microbiol* **9**, 427-439.
39. Derman, A.I., Becker, E.C., Truong, B.D., Fujioka, A., Tucey, T.M., Erb, M.L., Patterson, P.C., and Pogliano, J. (2009). Phylogenetic analysis identifies many uncharacterized actin-like proteins (Alps) in bacteria: regulated polymerization, dynamic instability and treadmilling in Alp7A. *Mol Microbiol* **73**, 534-552.
40. Garner, E.C., Campbell, C.S., and Mullins, R.D. (2004). Dynamic instability in a DNA-segregating prokaryotic actin homolog. *Science* **306**, 1021-1025.
41. Garner, E.C., Campbell, C.S., Weibel, D.B., and Mullins, R.D. (2007). Reconstitution of DNA segregation driven by assembly of a prokaryotic actin homolog. *Science* **315**, 1270-1274.
42. Salje, J., and Löwe, J. (2008). Bacterial actin: architecture of the ParMRC plasmid DNA partitioning complex. *Embo J* **27**, 2230-2238.
43. Polka, J.K., Kollman, J.M., Agard, D.A., and Mullins, R.D. (2009). The structure and assembly dynamics of plasmid actin AlfA imply a novel mechanism of DNA segregation. *J Bacteriol* **191**, 6219-6230.
44. Derman, A.I., Nonejuie, P., Michel, B.C., Truong, B.D., Fujioka, A., Erb, M.L., and Pogliano, J. (2012). Alp7R regulates expression of the actin-like protein Alp7A in *Bacillus subtilis*. *J Bacteriol* **194**, 2715-2724.
45. Amos, L.A., van den Ent, F., and Löwe, J. (2004). Structural/functional homology between the bacterial and eukaryotic cytoskeletons. *Curr Opin Cell Biol* **16**, 24-31.
46. van den Ent, F., Moller-Jensen, J., Amos, L.A., Gerdes, K., and Löwe, J. (2002). F-actin-like filaments formed by plasmid segregation protein ParM. *Embo J* **21**, 6935-6943.
47. Cabeen, M.T., and Jacobs-Wagner, C. (2010). The bacterial cytoskeleton. *Annu Rev Genet* **44**, 365-392.
48. Gayathri, P., Fujii, T., Namba, K., and Löwe, J. (2013). Structure of the ParM filament at 8.5Å resolution. *J Struct Biol*.
49. Gayathri, P., Fujii, T., Moller-Jensen, J., van den Ent, F., Namba, K., and Löwe, J. (2012). A bipolar spindle of antiparallel ParM filaments drives bacterial plasmid segregation. *Science* **338**, 1334-1337.
50. Firshein, W., and Kim, P. (1997). Plasmid replication and partition in *Escherichia coli*: is the cell membrane the key? *Mol Microbiol* **23**, 1-10.
51. Kraemer, J.A., Erb, M.L., Waddling, C.A., Montabana, E.A., Zehr, E.A., Wang, H., Nguyen, K., Pham, D.S., Agard, D.A., and Pogliano, J. (2012). A Phage Tubulin Assembles Dynamic Filaments by an Atypical Mechanism to Center Viral DNA within the Host Cell. *Cell* **149**, 1488-1499.
52. Oliva, M.A., Martin-Galiano, A.J., Sakaguchi, Y., and Andreu, J.M. (2012). Tubulin homolog TubZ in a phage-encoded partition system. *Proc Natl Acad Sci U S A* **109**, 7711-7716.
53. Greber, U.F., and Way, M. (2006). A superhighway to virus infection. *Cell* **124**, 741-754.
54. Villarreal, L.P. (2004). Are viruses alive? *Sci Am* **291**, 100-105.
55. Sambrook, J., Fritsch, E., and Maniatis, T. (1989). *Molecular Cloning. A Laboratory Manual*. 2<sup>nd</sup> Edition (New York: Cold Spring Harbor Laboratory Press).
56. Sambrook, J., MacCallum, P., and Russell, D. (2001). *Molecular Cloning. A Laboratory Manual*, 3<sup>rd</sup> Edition (New York: Cold Spring Harbor Laboratory Press).
57. Niebisch, A., and Bott, M. (2001). Molecular analysis of the cytochrome *bc<sub>1</sub>-aa<sub>3</sub>* branch of the *Corynebacterium glutamicum* respiratory chain containing an unusual diheme cytochrome *c<sub>1</sub>*. *Arch. Microbiol.* **175**, 282-294.
58. Eikmanns, B.J., Thum-Schmitz, N., Eggeling, L., Lüdtke, K.U., and Sahm, H. (1994). Nucleotide sequence, expression and transcriptional analysis of the *Corynebacterium glutamicum gltA* gene encoding citrate synthase *Microbiology* **140**, 1817-1828.
59. Brazma, A. (2009). Minimum Information About a Microarray Experiment (MIAME)--successes, failures, challenges. *ScientificWorldJournal* **9**, 420-423.
60. Polen, T., and Wendisch, V.F. (2004). Genomewide expression analysis in amino acid-producing bacteria using DNA microarrays. *Appl Biochem Biotechnol* **118**, 215-232.
61. Frunzke, J., Gätgens, C., Brocker, M., and Bott, M. (2011). Control of heme homeostasis in *Corynebacterium glutamicum* by the two-component system HrrSA. *J Bacteriol* **193**, 1212-1221.
62. Heyer, A., Gätgens, C., Hentschel, E., Kalinowski, J., Bott, M., and Frunzke, J. (2012). The two-component system ChrSA is crucial for haem tolerance and interferes with HrrSA in haem-dependent gene regulation in *Corynebacterium glutamicum*. *Microbiology* **158**, 3020-3031.
63. Ingerman, E., Perkins, E.M., Marino, M., Mears, J.A., McCaffery, J.M., Hinshaw, J.E., and Nunnari, J. (2005). Dnm1 forms spirals that are structurally tailored to fit mitochondria. *J Cell Biol* **170**, 1021-1027.
64. Bork, P., Sander, C., and Valencia, A. (1992). An ATPase domain common to prokaryotic cell cycle proteins, sugar kinases, actin, and Hsp70 heat shock proteins. *Proc Natl Acad Sci U S A* **89**, 7290-7294.

Name of the journal:	Current Biology
Impact factor:	9.647 (5-year: 10.881)
Contribution of own work:	40%
1. Author:	(equally contributed to this work with C. Donovan)  Experimental work and writing of the manuscript

# Microfluidic Picoliter Bioreactor for Microbial Single Cell Analysis: Fabrication, System Setup and Operation

Alexander Gruenberger, Christopher Probst, Antonia Heyer,

Wolfgang Wiechert, Julia Frunzke and Dietrich Kohlheyer\*

Institute of Bio- and Geosciences, IBG-1: Biotechnology,  
Forschungszentrum Jülich GmbH (Research Center Jülich), Jülich, Germany

**Keywords:** soft lithography, SU-8 lithography, picoliter bioreactor, single cell analysis, Polydimethyl-siloxane, *Escherichia coli*, *Corynebacterium glutamicum*

\*corresponding author:

E-Mail: [d.kohlheyer@fz-juelich.de](mailto:d.kohlheyer@fz-juelich.de)

Phone: +49 2461 61-2875

## Long abstract

In this protocol the fabrication, experimental setup and basic operation of the recently introduced microfluidic picoliter bioreactor (PLBR) is described in detail. The PLBR can be utilized for the analysis of single bacteria and microcolonies to investigate biotechnological and microbiological related questions concerning, *e.g.*, cell growth, morphology, stress response and metabolite or protein production. The device features continuous media flow enabling constant environmental conditions for perturbation studies, but in addition allows fast medium changes to mimic any desired situation as well as oscillating conditions. To fabricate the single use devices, a silicon wafer containing sub micrometer sized SU-8 structures served as the replication mold for rapid Polydimethylsiloxane casting. Chips were cut, assembled, connected and set up onto a high resolution and fully automated

## Short abstract

**In this protocol the fabrication, setup and basic operation of a microfluidic picoliter bioreactor (PLBR) for single cell analysis of prokaryotic microorganisms is introduced. Industrially relevant microorganisms were analyzed as proof of principle allowing insights into growth rate, morphology and phenotypic heterogeneity over certain time periods, hardly possible with conventional methods.**

microscope suited for time-lapse imaging, a powerful tool for spatio-temporal cell analysis. Here, the biotechnological platform organism *Corynebacterium glutamicum* was seeded into the PLBR and cell growth and intracellular fluorescence were followed over several hours unraveling time dependent population heterogeneity, not possible with conventional analysis methods such as flow cytometry. Besides insights into device fabrication, furthermore, the preparation of the pre-culture, loading, trapping of bacteria and the PLBR cultivation of single cells and colonies is demonstrated. These devices will add a new dimension in microbiological research to analyze time dependent phenomena with single cell resolution. Due to the simple and relatively short fabrication process the technology can be easily adapted at any microfluidics lab and simply tailored towards specific needs.

## Introduction

Time-lapse microscopy is a powerful tool for studying living cells under tightly controlled environmental conditions<sup>1</sup>. Meanwhile commercially available fully automated microscopy platforms including thermally induced focus drift compensation are commonly applied in biological research to study time-dependent phenomena, ranging from cancer and neuron cell research over tissue engineering and dynamic studies with single yeast or bacterial cells<sup>2-6</sup>.

Typically transparent well plates, agar-pads or simply microscopy slides are applied to provide cell culture environments during time-lapse imaging<sup>7</sup>. Although suitable for certain research these systems have very limited control over environmental conditions and do not allow for more complex perturbations or well defined and fast medium changes. Disposable microfluidic chip devices produced by mass production have been introduced to the market recently but are mostly tailored towards larger eukaryotic cell types<sup>4</sup>. Although growth can be studied, controlled growth investigations concerning, *e.g.*, precise cell trapping, colony size, growth direction and ability for cell removal is limited. Microfluidic habitats and reactors, where bacteria cells are cultured in 3D environments have been developed<sup>8-10</sup>, but have drawbacks when aiming for quantitative studies at the single cell level. Although cell-to-cell heterogeneity can be identified, many parameters such as morphology, fluorescence etc., cannot be determined accurately since growth is not restricted to monolayers.

This limitation triggered the development for micro systems enabling cultivation of cells in well-defined channels and geometries within monolayers and especially tight control over media supply and environmental conditions ultimately with single cell resolution<sup>6,11,12</sup>. Only few examples of microfluidic systems dealing with bacterial cells have been demonstrated<sup>12-14</sup>. This is mainly due to the fact that bacteria

typically exhibit very fast growth rates and require microfluidic structures in the range of few micrometers and below, especially when cell monolayers are desired for microscopy. Keymer *et al.* demonstrated growth and spreading of *E. coli* strains in microfabricated landscapes<sup>15,16</sup>. Since they were interested in population dynamics they did not investigate with single cell resolution.

We have developed the picoliter bioreactor (PLBR)<sup>13</sup>, which is currently applied to investigate various biotechnological performance indicators such as growth<sup>17</sup> and fluorescence coupled productivity analysis on single cell level<sup>18,19</sup>. Our microfluidic device allows environmental reactor control at a defined culture volume of approximately one picoliter and continuous single cell observation simultaneously. In comparison to open monolayer box systems<sup>11,14</sup>, where one or two sides are open to the media supply channel, the PLBR allows for controlled trapping and culturing. Our design allows for long term cultivation of bacteria without the risk of several adjacent colonies forming one large population. Furthermore, the system incorporates cultivation regions of 1  $\mu\text{m}$  height (in the order of the cell diameter) to restrict lateral bacteria growth to develop only 2D cell monolayers. In contrast, the supply channels are 10 fold deeper to minimize hydraulic resistance.

In comparison to miniaturized batch cultivation systems<sup>20</sup> our system allows cultivation under constant environmental parameters due to continuous media flow. Furthermore, environmental parameters such as medium composition, temperature, flow rates and gas exchange can be easily controlled and changed within seconds. This allows for the investigation of cellular response to changes in nutrient availability or stress stimuli using fluorescence dyes or proteins. The demand for reduced media volumes, namely in the range of few microliters only, enable researchers to

perform novel studies, *e.g.*, the perturbation of cells during time-lapse imaging with supernatant of large-scale experiments unraveling cell response under these specific environmental conditions<sup>17</sup>. The picoliter bioreactor provides researchers with a robust system that tightly controls biological as well as biophysical conditions and is operated using high precision syringe pumps and automated bright field and fluorescence microscopy for time-lapse imaging. Here, we report a complete protocol from device design, its fabrication and exemplary application.

## 1 Protocol

### 1.1 Wafer Fabrication

- 1.1.1) Design a drawing of the microfluidic device containing inlets, outlets, main channels and the PLBRs (Figure 1A).
- 1.1.2) The design presented in this protocol (Figure 2) consists of two seeding inlets, a gradient generator for mixing of two different substrates, one outlet, and six arrays of PLBRs. Each array contains 5 PLBRs, resulting in 30 parallel PLBRs for one microfluidic device.
- 1.1.3) Create a lithography photomask containing the desired chip layouts (Figure 1B). In our study the photomask was produced in house by electron beam writing with sub-micron resolution. The mask used was composed of a chromium layer on a 5 inch square glass plate.
- 1.1.4) Note: Perform all steps under clean room class 100 conditions (Overview see Figure 3A).
- 1.1.5) Clean a silicon wafer with piranha (10:1 ratio of sulfuric acid and hydrogen peroxide) and hydrofluoric acid for several minutes. Rinse with deionized (DI) water for approximately 10 s.
- 1.1.6) Dehydrate wafer for 20 minutes at 200°C.
- 1.1.7) Using a wafer spinner, spin-coat SU-8 2000.5 photoresist onto the wafer to aim to realize a height of 1  $\mu\text{m}$  (1st layer) (4 ml resist, spin 10 s with,  $v = 500$  rpm and  $a = 100$  rpm/s, spin 30 s with  $v = 1000$  rpm and  $a = 300$  rpm/s).
- 1.1.8) Place the wafer coated on a hotplate at 95 °C to drive off excess solvent (1.5 min at 65 °C, 1.5 min at 95 °C and 1 min at 65 °C; ideally use two hotplates).
- 1.1.9) Apply the photomask with the desired layout (here the trapping regions of the picoliter reactors) inside a wafer-mask aligner and expose to 350-400 nm (vacuum contact, 64 mJ/cm<sup>2</sup>,  $t = 3$  s,  $I = 7$  mW/cm<sup>2</sup>).
- 1.1.10) Perform post exposure bake on a hotplate at 95 °C to initiate the polymerization of SU-8 (1 min at 65 °C, 1 min at 95 °C and 1 min at 65 °C). During this step you already can see the structures in the SU-8 layer.
- 1.1.11) Place the wafer in a SU-8 developer bath for 1 min and transfer the wafer into a second container with fresh SU-8 developer for few seconds.
- 1.1.12) Rinse the wafer in isopropanol to remove SU-8 developer and dry wafer using nitrogen flow of wafer spin dryer.
- 1.1.13) Hard bake the wafer (10 min at 150 °C).
- 1.1.14) Spincoat 9  $\mu\text{m}$  SU-8 2010 photoresist onto the wafer (2nd layer). (dispense 4 ml resist, spin 10 s with  $v = 500$  rpm,  $a = 100$  rpm/s and spin 30 s with  $v = 4000$  rpm,  $a = 300$  rpm/s).
- 1.1.15) Place the wafer with SU-8 on a hotplate at 95 °C to drive off excess solvent (15 min at 65 °C, 45-60 min at 95 °C and 10 min at 65 °C). Attention has to be paid to wrinkles and bubbles. If the wafer is heated too fast to 95 °C, evaporated solvent may be encapsulated in tiny gas bubbles.
- 1.1.16) Place the mask with the desired layout (here main channels for nutrient supply) over the wafer and expose to 350-400 nm in a mask aligner (hard contact, 64 mJ/cm<sup>2</sup>,  $t = 10$  s ( $I = 7$  mW/cm<sup>2</sup>)).
- 1.1.17) Perform post exposure bake on a hotplate at 95 °C to finalize the polymerization of SU-8 (5 min at 65 °C, 3:30 min at 95 °C, 3 min at 65 °C). During this step you already can see the structures in the SU-8 layer.

- 1.1.18) Place the wafer in a SU-8 developer bath for 45 s and transfer the wafer in a second container with fresh SU-8 developer for 60 s.
- 1.1.19) Rinse the wafer 20 s in isopropanol to remove SU-8 developer and dry wafer using pressured nitrogen.
- 1.1.20) Finally hard bake the wafer at 150 °C. As a result the final structured wafer (Figure 1C) is obtained, which will be used as master mold for PDMS molding.
- 1.1.21) Perform profilometer measurements (Figure 3B), to ensure that parameters of wafer manufacturing resulted in trapping structures of 1 µm height and 9 µm main channels. Inaccuracies in structure height may results in inefficient cell trapping or loss of cells during cultivation.

## 1.2 Polydimethylsiloxane Chip Fabrication

**Note: All steps should be performed under laminar-flow conditions, to prevent that dust particles interfere within the fabrication procedure.**

- 1.2.1) Prepare a mixture of silicone based elastomer and curing agent in a 10:1 ratio. Stir and mix the polydimethylsiloxane (PDMS) carefully until a homogenous solution is achieved which looks opaque. Prepare as much as you need for adequate height (here 3 mm).
- 1.2.2) Degas the PDMS mixture for 30 minutes under slight vacuum until all bubbles have disappeared.
- 1.2.3) Prepare molding device (or petri dish) with appropriate SU-8 wafer and pour the PDMS mixture into it (Figure 1D).
- 1.2.4) Bake the PDMS for 3 hours at 80 °C in the oven.
- 1.2.5) Carefully peel off the PDMS slab from the wafer. Cut the slab into single chips using a sharp scalpel.
- 1.2.6) Wash the chips in an n-pentane bath for 90 minutes, followed by two acetone washing steps (90 min each). During the n-pentane wash, monomers and dimers are removed from the cured PDMS (chip size may double during washing procedure). Dry the chips overnight to remove any solvent. Perform the PDMS washing under a fume hood.
- 1.2.7) Store the microfluidic PDMS chips in close containers until the day of experiments.
- 1.2.8) Just before the experiment, punch the inlet and outlet holes using a needle (or hole-puncher) with a smaller diameter than the connectors that are used to connect tubing with PDMS chip.
- 1.2.9) Clean the microfluidic PDMS chip carefully with isopropanol and use scotch tape to remove any dust particles which might stick on the structured PDMS side. Use the scotch tape several times until no particle can be seen on the chip.
- 1.2.10) Clean a 170 µm thick glass slide with acetone and isopropanol successively. Finally clean with deionized water and dry with pressurized nitrogen.
- 1.2.11) Before plasma-activation, warm up the plasma cleaner and run the plasma for approximately 300 s. Plasma-oxidize glass slide and PDMS chip (Power 50 W, Time = 25 s, Oxygen flow rate = 20 sccm).
- 1.2.12) Align the PDMS chip and glass before bonding, using tweezers. Finally, place the PDMS chip carefully onto the glass slide (Figure 1E). PDMS and glass will bond within seconds.

**Note: Do not push with tweezers onto the top of the PDMS chip during the bonding process. This may lead to so called roof-collapsing of the channels and small structures.**
- 1.2.13) In order to strengthen the bond, bake the final PDMS-glass chip for 10 s at 80 °C.

## 1.3 Preparation of the Bacterial Culture

**Note: All cultivations should be prepared in sterile filtered medium to prevent accumulation of undesired particles, which might interfere during cultivation.**

- 1.3.1) Use a fresh agar plate containing your desired organisms (here, *C. glutamicum* ATCC 13032) and inoculate one colony into

- 20 ml of fresh BHI medium, incubate overnight ( $\approx$  8 -14 hours) at 30 °C on a rotary shaker (120 rpm).
- 1.3.2) Transfer 10  $\mu$ l of the preculture into the desired medium (here CGXII<sup>21</sup>) which will be used during microfluidic cell cultivation and grow the cells overnight at 30 °C on a rotary shaker (120 rpm).
  - 1.3.3) Transfer the desired amount of cells (between 10  $\mu$ l and 500  $\mu$ l, depending on the start of the experiment) into the desired medium (here CGXII<sup>21</sup>) which will be used during microfluidic cell cultivation. The best is to use cells from the early logarithmic phase for seeding. For our *C. glutamicum* culture the best optical density (OD<sub>600</sub>) for seeding was between 0.5 and 2.
  - 1.3.4) Transfer 1 ml of the bacterial culture into a sterile 2 ml tube. Note: This should be done right after the microfluidic PDMS chip was assembled to minimize transfer time between shake flask and microfluidic cultivation. Typically the transfer time is around 15 minutes and should be kept as small as possible to prevent impact on metabolism caused oxygen limitation and temperature changes.
- #### 1.4 Experimental Setup
- Note: All steps are performed with an inverted microscope, but can in general also be performed using upright microscope.**
- 1.4.1) Start incubator system 2 hours before the experiment to warm up the system. In our configuration we use an additional objective heater to minimize heat flux.  
**Note: The microscopy should be equipped with a full-size incubator to control temperature and if desired gas flow. Additional humidity control is not necessary since the chip system is continuously infused with media.**
  - 1.4.2) Open incubator system, select the 100x objective and add immersion oil to the objective.
  - 1.4.3) Mount the chip inside the chip holder and additionally fix the glass plate with adhesive tape in order to avoid chip any movement.
  - 1.4.4) Center the sample on the microscope and focus onto the PLBR arrays.
  - 1.4.5) Connect inlets(s) and outlet(s) with appropriate tubing (Figure 1F). Connect tubing to an appropriate waste reservoir. A representative chip can be seen in Figure 4 – left (B).
  - 1.4.6) Connect syringes with microfluidic pumps and start media flow. Use medium, buffer or if necessary coating solution and rinse the microfluidic channels for approximately 1 hour. Coating solution is used to coat channel walls to prevent unspecific cell adhesion.
  - 1.4.7) For *Escherichia coli*, 0.1 % solution of BSA is used to coat the channel walls. For *C. glutamicum* no coating is necessary. After the coating procedure, flush the chip with medium prior cell seeding.
  - 1.4.8) Before the cell seeding and cultivation, confirm that no leakage occurs and that the temperature is constant.
- #### 1.5 Seeding of Bacterial Cells into the Microfluidic Device
- 1.5.1) Make sure you have the desired bacteria solution ready in appropriate syringes connected to flexible plastic tubes.
  - 1.5.2) Disconnect buffer or coating solution and connect the cell suspension to the chip. To minimize death volume, undesired air bubbles and to reduce experimental time, change the complete needle as well as tubing, rather than only the syringes.
  - 1.5.3) Infuse the cell suspension into the channels at a volumetric flow rate of 200 nl/min until most of the PLBRs are filled with the desired amount of cells (Figure 5A).  
**Note: Optimal results depend on the bacterial strain, OD<sub>600</sub>, and growth medium of the preculture. These parameters have to be adapted to increase trapping efficiency and time until a sufficient number of cells are trapped in the reactor structures. For *C.***

***glutamciium*, typically a cell suspension of  $OD_{600}$  0.5-2 was used; for *E. coli* the  $OD_{600}$  was between 0.5 and 1.**

1.5.4) If only a small number of PLBRs are filled, increase the flow rate to 800-1200 nl/min.

1.5.5) Disconnect the cell suspension and connect the growth medium to the chip (Figure 5B). Make sure that no air bubble is introduced during the medium change. Perfuse with fresh growth media at 100 nl/min.

## 1.6 Time-Lapse Imaging

1.6.1) Select the PLBR of interest for time-lapse imaging. In our work PLBRs were chosen that contain a single cell at the beginning of an experiment. The number of spots that can be investigated in one experiment depends on the chosen frame rate and microscopic setup.

1.6.2) Select an appropriate frame rate depending of number of PLBRs. Make sure that the microscope can handle the desired amount of boxes in the desired time-interval.

1.6.3) Choose appropriate filter sets (here YFP). Automatically close the shutter during stage movement and after each time-lapse measurement to prevent chromophore bleaching.

1.6.4) Start the experiment.

1.6.7) After all PLBRs are filled, the experiment can be stopped and the microfluidic PDMS chip can be discarded and the experiment can be evaluated.

## 1.7 Analysis

**Note: The following steps or parts of the procedure can be performed manually or by (semi)-automated image analysis programs such as Image J etc.**

1.7.1) Determine PLBRs of interest, where cultivation fulfills all desired criteria, *e.g.*, number of mother cells, position of the mother cells etc.

1.7.2) To determine the growth rate of one microcolony count the number of cells in each time frame.

1.7.3) Calculate the maximum growth rate which represents one major parameter of bacteria cultures by plotting time vs.  $\ln(\text{cell number})$ . The slope of the plot represents the growth rate in [1/h] (see Figure 6).

1.7.4) Fluorescence data analysis strongly depends on the topic under investigation. In this report, an example was chosen to illustrate colony-to-colony and cell-to-cell heterogeneity between different isogenic microcolonies (see Figure 7)

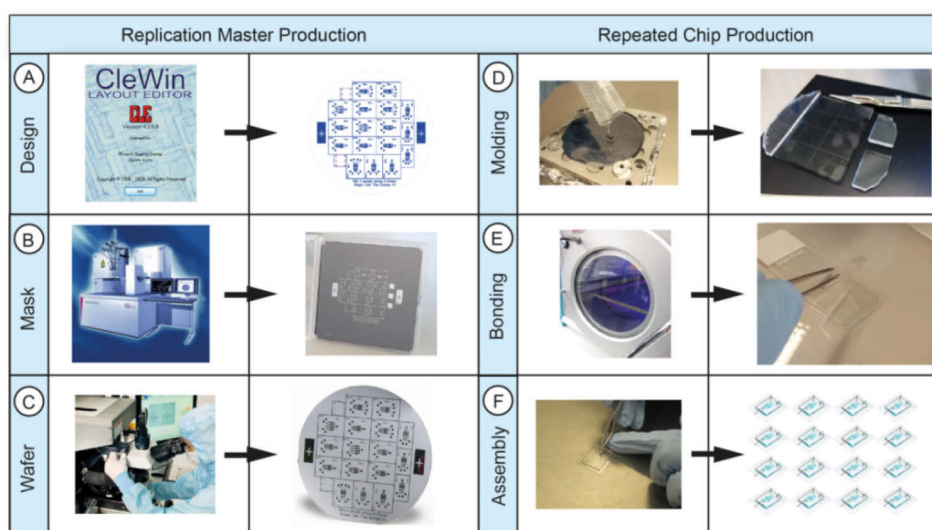


**Figure 1: Overview of PLBR chip production process.** (left) master mold fabrication: starting with (A) design, (B) lithography mask fabrication and (C) wafer production. (right) PDMS-glass chip production: starting with (D) of PDMS molding followed by (E) glass and PDMS bonding and (F) final chip assembly.

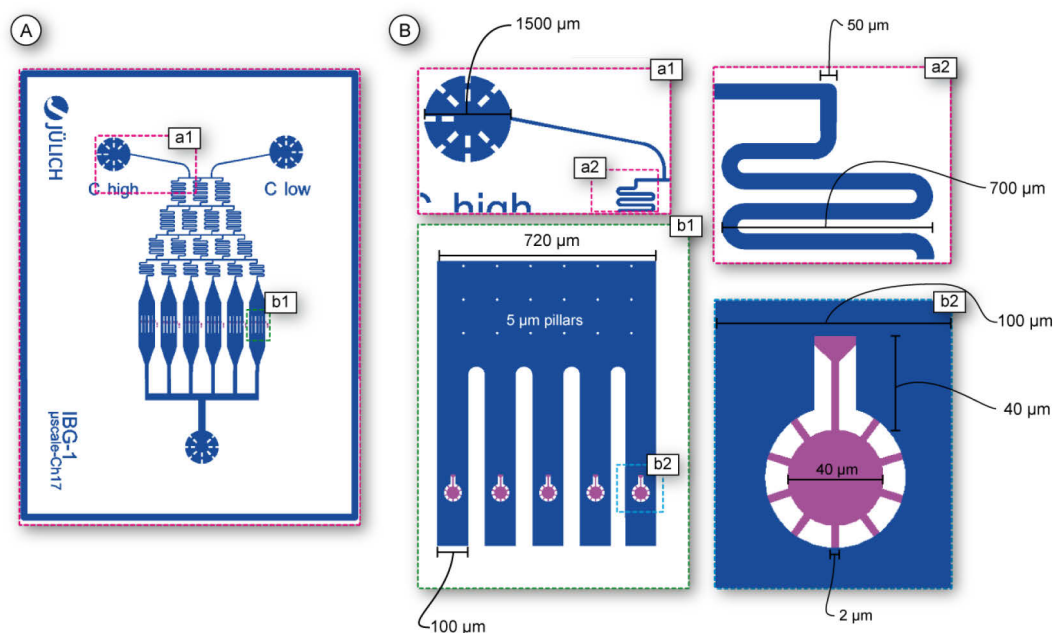


**Figure 2: Design of PLBR system.** (A) CAD drawing of the microfluidic system for single cell culturing (B) Magnification of selected layout positions. The layout contains two medium inlets (a1), a gradient generator (a2) and 6 parallel PLBR arrays (b1). Figure b2 shows one PLBR, which is embedded in a fluid channel with a width of 100  $\mu\text{m}$ . The PLBR has an inner diameter of 40  $\mu\text{m}$  and nutrient channels with 2  $\mu\text{m}$  in width. The seeding inlet has a length of 40  $\mu\text{m}$ . Pink color represents the first layer (trapping and cultivation region) and blue color represents the second layer (fluid transport).

## 2 Representative Results

### 2.1 Device Fabrication

The microfluidic PLBR system is a dual layer system, fabricated by two layers of PDMS bonded onto a glass chip. The fabrication consists of two main procedures: Firstly the fabrication of the replication master (Figure 1 A,B and C) and secondly the chip fabrication (Figure 1 D,E and F). According to the protocol, standard photolithographic microfabrication techniques are used to create the master mold. Laboratories without cleanroom facility can acquire the microfluidic master mold at a microfluidic vendor and do not need a clean room facility. Using repetitive PDMS molding (Figure 1 A,B and C) hundreds of disposable chips can be produced easily. PDMS molding and chip assembly can be done in any lab and do not require clean room facilities, however, filtered airflow workplaces are favorable.

The process starts with the design of the microfluidic chip system. We use a CAD software for microfluidic chip design (Figure

1A). After CAD, a mask is generated by an e-beam writer (Figure 1B) with submicron resolution. Here a 5" chromium mask was created which was used for the wafer lithography. The final wafer is used for PDMS molding (Figure 1D). After a baking step the PDMS slab is cut into chips which are irreversibly bonded onto microscopy cover slides (Figure 1E). Finally the tubing is connected (Figure 1F).

Figure 2 shows the design of the microfluidic system in detail. It consists of two seeding inlets (Figure 2 – a1), a gradient generator for mixing of different substrates (Figure 2 – a2), and one outlet. The main channels have a dimension of 50 x 10  $\mu\text{m}$  (W x H). Each device consists of six arrays (Figure 2 – b1) of PLBRs, containing 5 PLBRs (Figure 2 – b2) each. This results in 30 parallelized reactors in one microfluidic device.

Figure 3 illustrates the replication master production. As described in detail in the protocol, a first SU-8 layer is fabricated by SU-8 lithography (Figure 3A). A similar procedure is

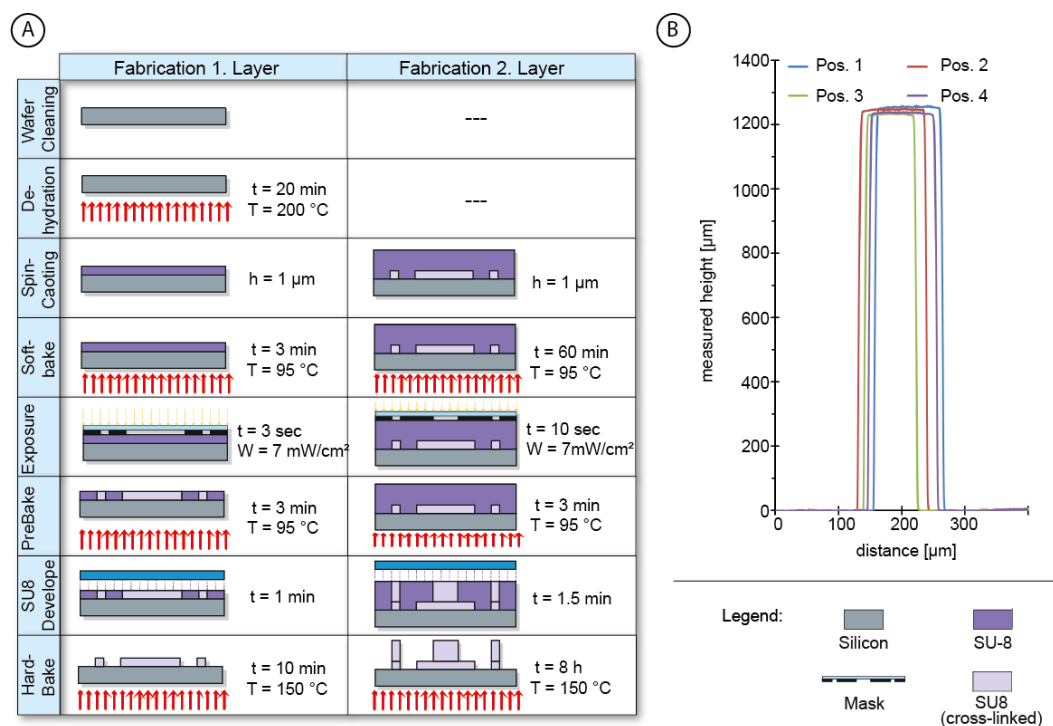


**Figure 3: Illustration of two layer wafer fabrication process.** (A) Fabrication of the first layer containing trapping structures; (B) Fabrication of the second layer containing fluid channels, inlets and outlets (C) representative surface profiles of the first layer. In this case the height of the first layer was 1200 nm and is used for the cultivation of *C. glutamicum* in complex medium.

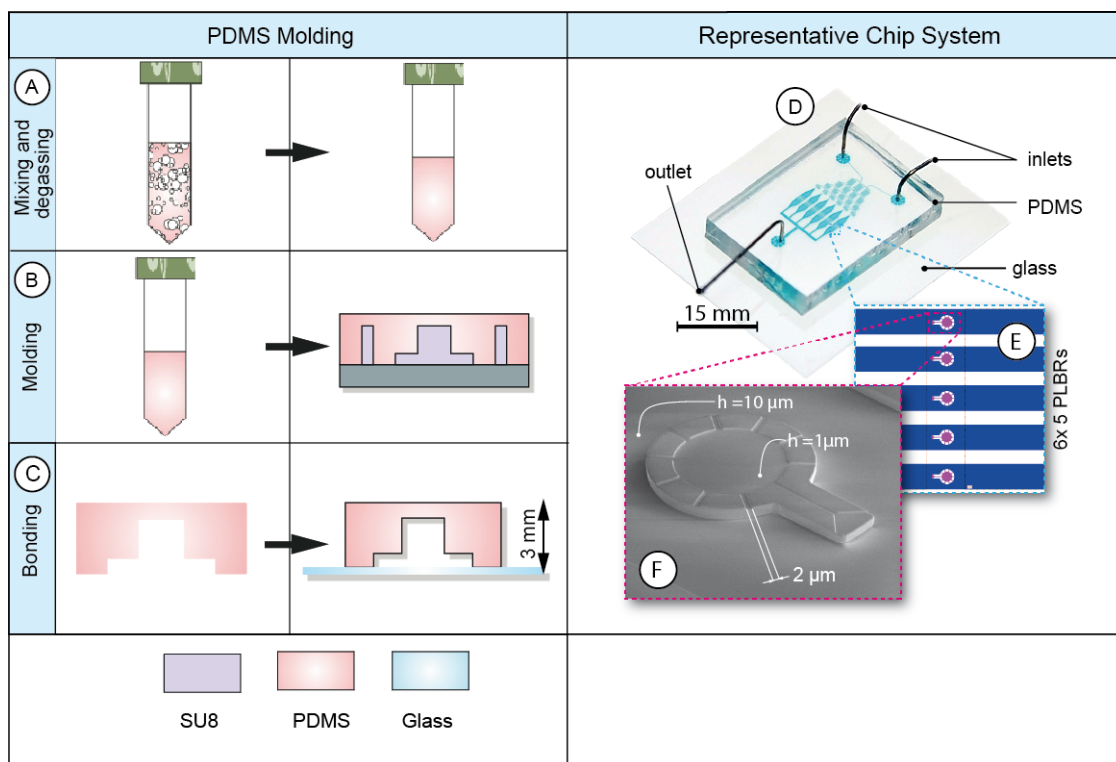
applied for the second layer (Figure 3B). To quantify and check the quality of the channel geometry we investigated the height of the PLBR and main channels with a profilometer. In the example shown in Figure 3 C, the first layer (the cultivation layer) was measured. Here the layer shows a consistent height of 1200 nm, suitable for the cultivation of *C. glutamicum* in BHI medium. As can be seen from the profile measurements, SU-8 is ideal to achieve straight channel walls.

Figure 4 illustrates the PDMS molding procedure starting with PDMS mixing (Figure 4A) followed by the molding process (Figure 4B) and eventually the final bonding step (Figure 4C). Figures 4 (right) shows the final microfluidic chip, incorporating the 170 μm thick glass plate, PDMS chip (3 mm in height) with inlets and outlets and steel needles connected to tubing. After the experiment the chip can be disposed and no extensive cleaning is necessary. Furthermore, it is easy to

assemble and handle. No complex and difficult filling procedure is necessary.

## 2.2 Device Principle

Figure 5 shows the working principle of the reactor system. Cells are infused into the microfluidic device and individual cells remain trapped inside the PLBR simply by cell-wall interactions. Due to the difference in hydrodynamic resistance of channel and PLBR, only minimal flow occurs inside the PLBR. After seeding of the PLBR (Figure 5A), the growth and observation phase is initiated with a change from bacteria solution to growth medium (Figure 5B). After the PLBRs are filled (Figure 5C) the experiment is typically stopped and time-lapse images can be analyzed. For the trapping mechanisms and flow profile within the PLBR the reader is referred to Grünberger *et al.*<sup>13</sup> for more details.



**Figure 4:** (left) Illustration of the PDMS molding process: (A) PDMS mixing and degassing; (B) PDMS molding; (C) mold release, cutting and chip bonding. (right) Final chip (Reproduced with permission of the Royal Society of Chemistry)<sup>13</sup>: (D) photograph of the PDMS chip with 2 inlets and 1 outlet; (E) CAD image of six parallel arrays containing 5 PLBRs each; (F) SEM image of one PLBR.

### 2.3 Growth Rate Analysis

Our system can be applied to study various bacterial species with respect to different biological parameters such as growth or production of fluorescence proteins (as protein or promoter fusions). In a first example *C. glutamicum*, an industrially relevant production organism was cultured under standard

cultivation conditions ( $T = 30\text{ }^{\circ}\text{C}$ , CGXII medium<sup>21</sup>). Figure 6A shows the growth curves derived from three isogenic microcolonies. Exponential growth is maintained until the PLBRs are filled indicating that no nutrient limitations occur. Figures 6B shows four DIC microscopy images of a growing *C. glutamicum* colony at selected time points.

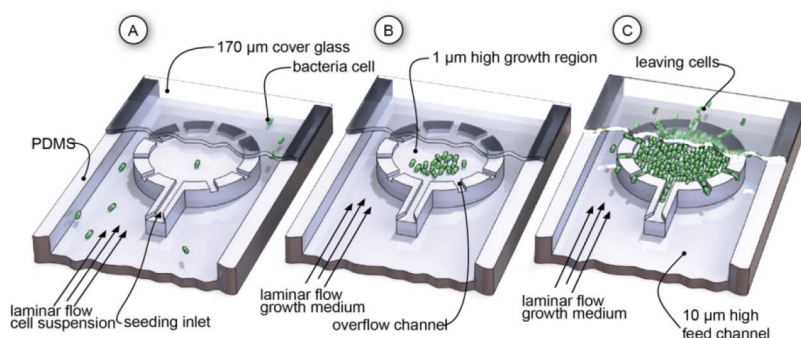


**Figure 5: Working principle of the PLBR system.** (A) Seeding phase (B) Growth phase of the bacterial microcolonies (C) Overflow phase. Excess bacteria are pushed out of the system. Reproduced with permission of the Royal Society of Chemistry<sup>13</sup>

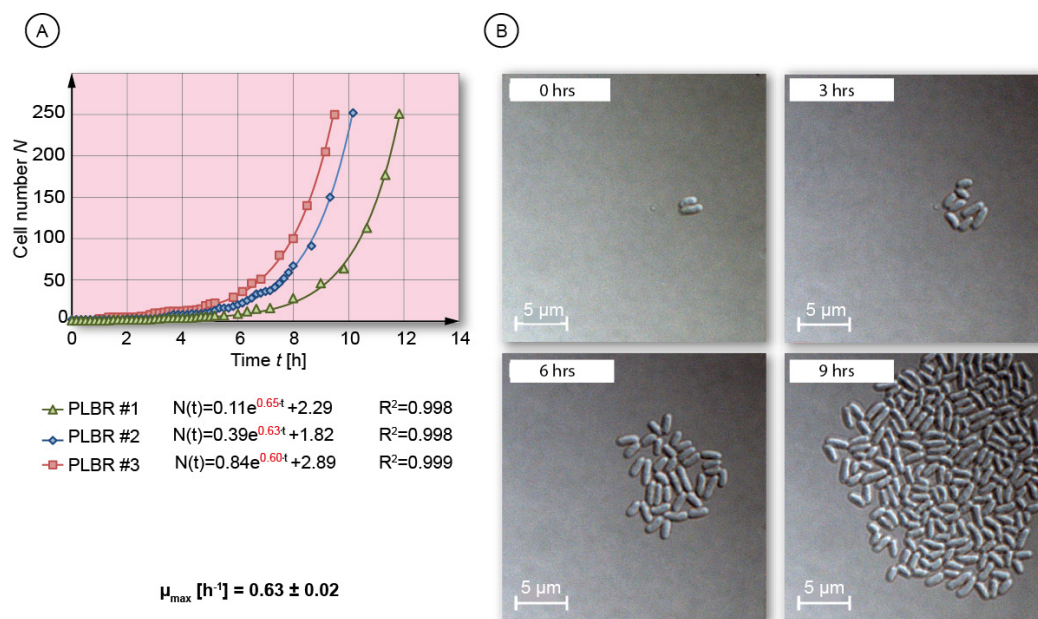


**Figure 6: Growth rate determination of *C. glutamicum* WT microcolonies.** (A) Isogenic growth of three PLBR cultivations (Parts reproduced with permission of the Royal Society of Chemistry)<sup>13</sup> (B) Time-lapse pictures of a growing *C. glutamicum* colony.

## 2.4 Fluorescence Analysis

For single cell fluorescence microscopy studies researchers often make use of specific fluorescence dyes or proteins, such as GFP or derivatives, to couple a measurable output to a specific phenotype of interest. To demonstrate the applicability of the PBLR for fluorescence based time-lapse studies, we investigated fluorescence emission of a *C. glutamicum* strain producing a plasmid-encoded YFP-TetR fusion protein under control of the  $P_{tac}$  promoter (pEKEEx2-*yfp-tetR*)<sup>18,22</sup>. In the presence of low inducer (IPTG) concentrations, expression from  $P_{tac}$  is known to lead to significant cell-to-cell variation in isogenic bacterial populations. Starting from one preculture, the growth and single cell fluorescence was followed for several isogenic microcolonies. As it can be seen in Figure 7, we observed phenotypic heterogeneity between different microcolonies as well as at the single cell level in colonies starting from one common ancestor cell. One colony (PLBR 1) showed almost no fluorescence emission, whereas cells of PLBR 2 exhibited a low fluorescence

emission due to basal *yfp-tetR* expression from the  $P_{tac}$  promoter. In PLBR 3 fluorescence emission was considerable strong, compared to the other colonies and a broad distribution of the population was observed (see PLBR 3 histogram). This example demonstrates the suitability of the PBLR for time-lapse fluorescence microscopy studies. In comparison to flow cytometry, where the fluorescence distribution of single cells can be determined at one timepoint, our systems allows the tracking of cells and the study of single cell fluorescence in real time over many generations.

## 3 Discussion

We have described the fabrication, experimental setup and related operation procedures of a microfluidic PDMS device containing several (PLBRs) for single cell analysis of bacteria. Microfabrication using soft lithography techniques allows easy manipulation of device dimensions for various

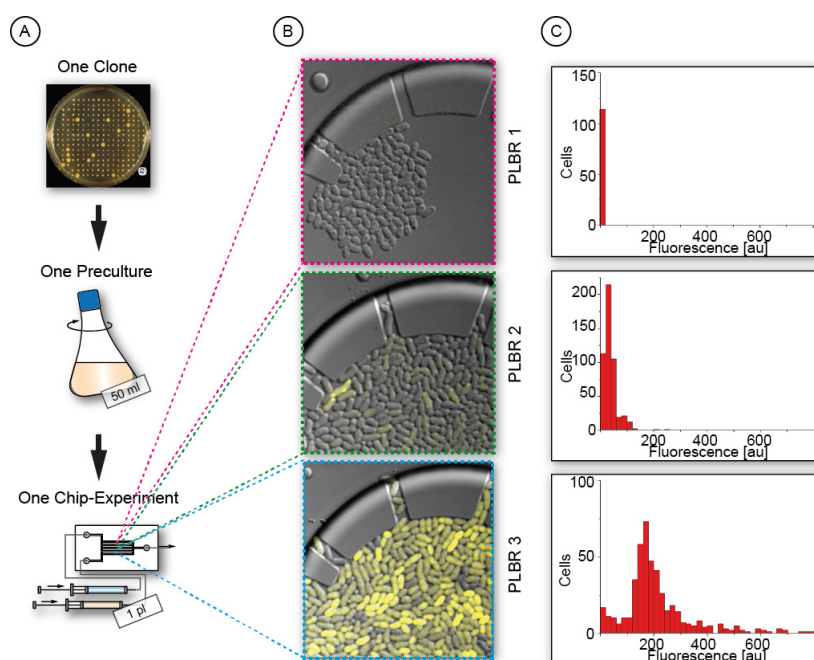


**Figure 7: PBLR-based analysis of population heterogeneity.** Shown is *C. glutamicum* expressing an *yfp-tetR* fusion under the control of the  $P_{tac}$  promoter ( $pEKEx2-yfp-tetR$ ) in the absence of the inducer IPTG. (A) Experimental workflow; (B) three isogenic microcolonies, showing colony-to-colony heterogeneity and cell-to-cell heterogeneity; (C) distribution of single cell fluorescence within the respective microcolonies.

sizes and bacteria morphologies. We continue to optimize the picoliter bioreactor and extend its utility, especially for the cultivation of different microbial organisms and regarding (high) throughput. In order to increase the trapping efficiency, currently the reactor geometry is still under optimization. Figure 8 shows four new PLBRs which are currently under investigation to improve trapping efficiency. In all cases the seeding channel was “reduced” to a seeding inlet, which is varied in width and shape. A consideration of this approach lies in the enlargement of the inlets. In practice, this seems to have an effect on the number of cells that are trapped, but needs further investigations.

Significant improvements on the trapping efficiency are also reached by the addition of more overflow channels leading to higher convective flow through the reactor and more cells being trapped. However, at the same time one increases the risk to wash out cells during cultivation. Although future designs

will alter and continuous optimization will be performed, the basic principle and thus this protocol remains essentially the same.

The device is an interesting alternative to macroscale cultivations that have been used for decades to investigate growth and production processes. However, it has some important requirements: For parallel monitoring of several picoliter bioreactors a high resolution and fully motorized microscopic setup with focus drift compensation is mandatory. In addition an incubation system is needed to maintain the desired cultivation temperature constant throughout the measurements.

We achieve a 95 % success rate in device fabrication. Main problems are related to inefficient PDMS-glass bonding, PDMS roof collapse or fluid leakage (See Table 1 for troubleshooting of most occurring problems). Although the experimental work is done partially under non-sterile conditions, we rarely see contamination during experiments, due to the closed fluidic system. PDMS microfluidic

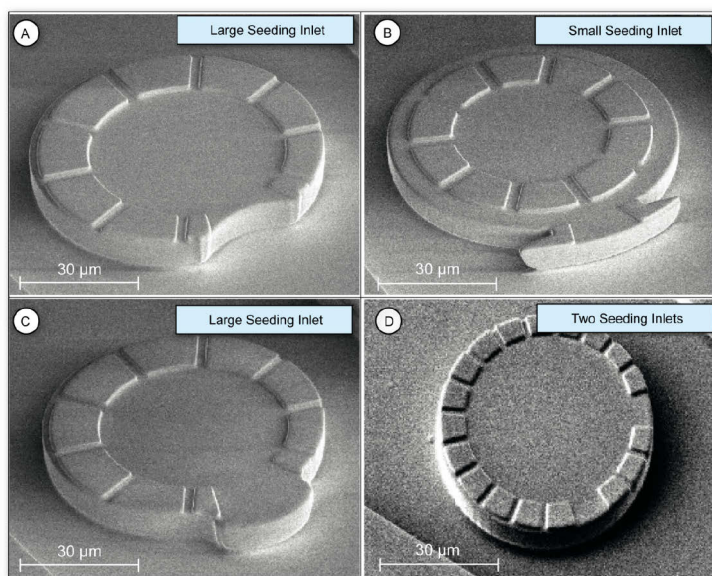


**Figure 8: Scanning electron images of different PLBRs with seeding inlets for optimization of trapping efficiency which are currently under investigations. (A) Larger seeding inlets (B) Smaller seeding inlets (C) Larger "open" seeding inlets (D) Two seeding inlets**

devices are optically transparent, therefore, can be used for high resolution *in vivo* imaging. Although PDMS seems to be perfect for the application, it has a high affinity for hydrophobic molecules, making the use of solvents which are widely used in whole cell biocatalytic processes, limited. However suitable coatings are available to adapt the protocol to these kinds of applications.

Our PLBR is well suited for spatio-temporal analysis of cellular and even sub-cellular events of various kinds of bacteria. A major advantage of our approach lies in the ability to quantify microcolony growth directly in contrast to conventional methods. Furthermore, the PLBR allows for culturing under defined and constant conditions. Because the system facilitates the use of small amounts of reagents or materials it carries the advantages of being inexpensive, customizable and amenable to high throughput. In traditional methods average values of the whole population are considered when analyzing microbial cultivation. Furthermore, existing methods need manual sampling which can lead to degradation of samples and thus to errors in the measurement. The picoliter bioreactor offers new perspectives for bioprocess development

and population heterogeneity analysis in microbiology. The PLBR is a promising tool for various applications within bioprocess development.

Main fields of application could be:

- 1) Analysis of cell-to-cell heterogeneity at constant environmental conditions
- 2) Analysis of specific cell clusters within cell-lineages
- 3) Screening of environmental factors with respect to growth and productivity of microbial production strains
- 4) Qualitative and quantitative real-time investigation of cell phenotypes

#### 4 Disclosure

The authors declare that they have no competing financial interests.

#### 5 Acknowledgements

The authors would like to thank the technician Agnes Mueller-Schroerer for her significant contribution to the development of this protocol. We furthermore would like to thank the Helmholtz Nanoelectronic Facility (HNF) for the possibility to fabricate the master molds in their facilities.

**Table 1:** Summary of problems during PDMS chip fabrication, assembly and microfluidic single cell culturing.

Step	Problem	Possible Reason	Solution
<b>Wafer fabrication</b>	Trapped air bubbles in SU-8 during soft bake	Increase of temperature to fast	Switch back from 95°C to 65°C several times
<b>Wafer fabrication</b>	Disappearing and broken SU-8 structures	Not optimal fabrication procedure; mechanical stress in SU-8 structures	Optimize parameter such as baking time, exposure time
<b>Wafer fabrication</b>	SU-8 layers too low or high or uneven layer thickness	Problem during spin coating	Check spin-coater parameters and chuck
<b>Chip Bonding and assembly</b>	Collapsing PLBRs	Bonding parameters not optimal	Adjust power, oxygenation time and baking time after bonding
<b>Chip Bonding and assembly</b>	Dirty structures and particles in the PLBRs	Chip was not properly cleaned	Intensify scotch-tape cleaning steps
<b>Chip Bonding and assembly</b>	No bonding	Bonding parameters not optimal or not properly cleaned	Check settings of oxygen plasma
<b>Microfluidic Experiment</b>	Leakage	Inlet/outlet hole was not properly punched	Optimize hole punching process
<b>Microfluidic Experiment</b>	Many small PDMS particles during filling	Hole was not properly punched	Optimize hole punching process
<b>Microfluidic Experiment, biological aspect</b>	No cell growth	Potentially remaining solvent from cleaning procedure	Flush chip more extensively prior cell loading or let solvent evaporate prior bonding
<b>Microfluidic Experiment, biological aspect</b>	Changing growth rates	Various reasons	Check pre-culture and temperature
<b>Microfluidic Experiment, biological aspect</b>	Cell morphology changes during cultivation	Nutrient limitations or temperature shift	Check incubator and flow
<b>Microfluidic Experiment, technical aspect</b>	Time-lapse series loses focus	Oil between glass plate and stage	Prevent touching of oil film with microscopic stage
<b>Microfluidic Experiment, technical aspect</b>	Drift in position	No equilibrium in temperature	Check temperature profile prior experiments until no oscillation
<b>Microfluidic Experiment, technical aspect</b>	Loss of cells during cultivation	Slightly too high reactor height through fabrication tolerance in SU-8 height	Use new wafer/ other chip position
<b>Microfluidic Experiment, technical aspect</b>	No trapping	Too low reactor height through fabrication tolerance in SU-8 height	Use new wafer/ other chip position

## 6 Materials

Name	Company	Catalog Number	Comments
<u>Material</u>			
Wafer	Si-MAT		P/BOR <100>
SU-8 2000,5	MicroChem		
SU-8 2010	MicroChem		
SU-8 Developer	Micro Resist Technology		mr DEV- 600
Polydimethylsiloxane (PDMS)	Dow Corning		Sylgard 184 Silicone Elastomer Kit
Needles	Nordsen EFD		Precision Tips 27 GA; ID = 0.2 mm, OD = 0.42 mm
Glass plates	Schott AG, Germany		D263 T eco, 30 mm 6 25 mm 6 0.17 mm
Hole puncher	Harris Uni-Core		AKA 5130-B-90
Tubing	Tygon		Tygon S-54-HL, ID = 0.25 mm, OD = 0.76 mm
Syringes	Braun	552-183143	Disposable Syringes – Omnifix Spritzen BRAUN Omnifix 40 Duo, 1 ml
Syringes	ILS		1ml sterile glass syringes
<u>Chemicals</u>			
(NH <sub>4</sub> ) <sub>2</sub> SO <sub>4</sub>	ROTH		
Urea	ROTH		
KH <sub>2</sub> PO <sub>4</sub>	ROTH		
K <sub>2</sub> HPO <sub>4</sub>	ROTH		
MgSO <sub>4</sub> x 7 H <sub>2</sub> O	ROTH		
MOPS	ROTH		
FeSO <sub>4</sub> x 7 H <sub>2</sub> O	ROTH		
MnSO <sub>4</sub> x H <sub>2</sub> O	ROTH		
ZnSO <sub>4</sub> x 7 H <sub>2</sub> O	ROTH		
CuSO <sub>4</sub>	ROTH		
NiCl <sub>2</sub> x 6 H <sub>2</sub> O	ROTH		
CaCl <sub>2</sub>	ROTH		
Biotin	ROTH		
Procatechuic acid	ROTH		
Glucose-Monohydrate	ROTH		
BHI	Becton, Dickinson		
<u>Cells</u>			
<i>Corynebacterium glutamicum</i>	DSMZ		ATTC 13032
<i>Escherichia coli</i>	DSMZ		MG 1655
<u>Equipment</u>			
Wafer Cleaner	Solid State Equipment LLC		SSEC 3300
Spin Coater	SPS Europe B.V.		SPIN150 -NPP
Mask Aligner	Karl Suess		Karl Suess, MA-6
Hot Plate	Torrey Pines Scientific		HP30A - 2
Oven	Memmert		UN 200
Plasma Cleaner	Diener Electronics		Femto Plasma Cleaner
Syringe pumps	Cetoni GmbH		neMESYS Syringe pumps
Magnetic stirrer	Stuart	VWR 442-0304	CB 162
Microscope	Nikon		Nikon Eclipse Ti
Centrifuge	Eppendorf	9776501	Minispin plus “black line”
Photometer	Eppendorf	6132000008	Eppendorf BioPhotometer plus
Incubator	GFL		Incubatorsystem 3031
Profilometer	Veeco		Dektak 150 Stylus Profiler

## 7 References

- 1 Muzzey, D. & van Oudenaarden, A. Quantitative Time-Lapse Fluorescence Microscopy in Single Cells. *Annual Review of Cell Dev Biol* **25**, 301-327, doi:doi:10.1146/annurev.cellbio.042308.113408 (2009).
- 2 Wei, P. *et al.* Bacterial virulence proteins as tools to rewire kinase pathways in yeast and immune cells. *Nature* **488**, 384–388, doi:Doi 10.1038/Nature11259 (2012).
- 3 Park, S. *et al.* Influence of topology on bacterial social interaction. *Proc Natl Acad Sci U S A* **100**, 13910-13915, doi:10.1073/pnas.1935975100 (2003).
- 4 Lee, P. J., Helman, N. C., Lim, W. A. & Hung, P. J. A microfluidic system for dynamic yeast cell imaging. *BioTechniques* **44**, 91-95 (2008).
- 5 Kobel, S. A. *et al.* Automated analysis of single stem cells in microfluidic traps. *Lab Chip* **12**, 2843-2849 (2012).
- 6 Carlo, D. D., Wu, L. Y. & Lee, L. P. Dynamic single cell culture array. *Lab Chip* **6**, 1445-1449 (2006).
- 7 Locke, J. C. W., Young, J. W., Fontes, M., Jimenez, M. J. H. & Elowitz, M. B. Stochastic Pulse Regulation in Bacterial Stress Response. *Science* **334**, 366-369, doi:DOI 10.1126/science.1208144 (2011).
- 8 Boedicker, J. Q., Li, L., Kline, T. R. & Ismagilov, R. F. Detecting bacteria and determining their susceptibility to antibiotics by stochastic confinement in nanoliter droplets using plug-based microfluidics. *Lab Chip* **8**, 1265-1272, doi:Doi 10.1039/B804911d (2008).
- 9 Fritzsche, F. S. O. *et al.* Picoliter nDEP traps enable time-resolved contactless single bacterial cell analysis in controlled microenvironments. *Lab Chip* **13**, 397-408, doi:Doi 10.1039/C2lc41092c (2013).
- 10 Groisman, A. *et al.* A microfluidic chemostat for experiments with bacterial and yeast cells. *Nat Methods* **2**, 685-689, doi:Doi 10.1038/Nmeth784 (2005).
- 11 Mather, W., Mondragon-Palomino, O., Danino, T., Hasty, J. & Tsimring, L. S. Streaming Instability in Growing Cell Populations. *Phys Rev Lett* **104**, doi:Doi 10.1103/Physrevlett.104.208101 (2010).
- 12 Wang, P. *et al.* Robust growth of Escherichia coli. *Curr Biol* **20**, 1099-1103, doi:10.1016/j.cub.2010.04.045 (2010).
- 13 Grünberger, A. *et al.* A disposable picolitre bioreactor for cultivation and investigation of industrially relevant bacteria on the single cell level. *Lab Chip* **12**, 2060-2068, doi:10.1039/c2lc40156h (2012).
- 14 Walden, M. & Elf, J. Studying transcriptional interactions in single cells at sufficient resolution. *Curr Opin Biotech* **22**, 81-86, doi:DOI 10.1016/j.copbio.2010.10.004 (2011).
- 15 Keymer, J. E., Galajda, P., Lambert, G., Liao, D. & Austin, R. H. Computation of mutual fitness by competing bacteria. *Proc Natl Acad Sci U S A* **105**, 20269-20273, doi:DOI 10.1073/pnas.0810792105 (2008).
- 16 Keymer, J. E., Galajda, P., Muldoon, C., Park, S. & Austin, R. H. Bacterial metapopulations in nanofabricated landscapes. *Proc Natl Acad Sci U S A* **103**, 17290-17295, doi:DOI 10.1073/pnas.0607971103 (2006).
- 17 Grünberger, A. *et al.* Beyond growth rate 0.6: *Corynebacterium glutamicum* cultivated in highly diluted environments. *Biotechnol Bioeng* **110**, 220-228, doi:Doi 10.1002/Bit.24616 (2013).
- 18 Binder, S. *et al.* A high-throughput approach to identify genomic variants of bacterial metabolite producers at the single-cell level. *Genome Biol* **13**, doi:Doi 10.1186/Gb-2012-13-5-R40 (2012).
- 19 Mustafi, N., Grünberger, A., Kohlheyer, D., Bott, M. & Frunzke, J. The development and application of a single-cell biosensor for the detection of L-methionine and branched-chain amino acids. *Metab Eng* **14**, 449-457, doi:DOI 10.1016/j.ymben.2012.02.002 (2012).
- 20 Huber, R. *et al.* Robo-Lector - a novel platform for automated high-throughput cultivations in microtiter plates with high information content. *Microb Cell Fact* **8**, doi:Doi 10.1186/1475-2859-8-42 (2009).
- 21 Keilhauer, C., Eggeling, L. & Sahm, H. Isoleucine synthesis in *Corynebacterium glutamicum*: molecular analysis of the *ilvB-ilvN-ilvC* operon. *J Bacteriol* **175**, 5595-5603 (1993).
- 22 Frunzke, J., Bramkamp, M., Schweitzer, J. E. & Bott, M. Population Heterogeneity in *Corynebacterium glutamicum* ATCC 13032 caused by prophage CGP3. *J Bacteriol* **190**, 5111-5119, doi:10.1128/JB.00310-08 (2008).

Name of the journal: Journal of Visualized Experiments (JoVE)

Impact factor: 2-year: 1.19 (unofficial)

Contribution of own work: 20%

3. Author: Experimental work and assistance in writing of the manuscript

## The two-component system ChrSA is crucial for haem tolerance and interferes with HrrSA in haem-dependent gene regulation in *Corynebacterium glutamicum*

Antonia Heyer,<sup>1</sup> Cornelia Gätgens,<sup>1</sup> Eva Hentschel,<sup>1</sup> Jörn Kalinowski,<sup>2</sup> Michael Bott<sup>1</sup> and Julia Frunzke<sup>1</sup>

Correspondence  
Julia Frunzke  
j.frunzke@fz-juelich.de

<sup>1</sup>Institut für Bio- und Geowissenschaften, IBG-1: Biotechnologie, Forschungszentrum Jülich, Germany

<sup>2</sup>Centrum für Biotechnologie, CeBiTec, Universität Bielefeld, Germany

We recently showed that the two-component system (TCS) HrrSA plays a central role in the control of haem homeostasis in the Gram-positive soil bacterium *Corynebacterium glutamicum*. Here, we characterized the function of another TCS of this organism, ChrSA, which exhibits significant sequence similarity to HrrSA, and provide evidence for cross-regulation of the two systems. In this study, ChrSA was shown to be crucial for haem resistance of *C. glutamicum* by activation of the putative haem-detoxifying ABC-transporter HrtBA in the presence of haem. Deletion of either *hrtBA* or *chrSA* resulted in a strongly increased sensitivity towards haem. DNA microarray analysis and gel retardation assays with the purified response regulator ChrA revealed that phosphorylated ChrA acts as an activator of *hrtBA* in the presence of haem. The haem oxygenase gene, *hmuO*, showed a decreased mRNA level in a *chrSA* deletion mutant but no significant binding of ChrA to the *hmuO* promoter was observed *in vitro*. In contrast, activation from  $P_{hmuO}$  fused to *eyfp* was almost abolished in an *hrrSA* mutant, indicating that HrrSA is the dominant system for haem-dependent activation of *hmuO* in *C. glutamicum*. Remarkably, ChrA was also shown to bind to the *hrrA* promoter and to repress transcription of the paralogous response regulator, whereas *chrSA* itself seemed to be repressed by HrrA. These data suggest a close interplay of HrrSA and ChrSA at the level of transcription and emphasize ChrSA as a second TCS involved in haem-dependent gene regulation in *C. glutamicum*, besides HrrSA.

Received 26 July 2012  
Revised 28 September 2012  
Accepted 1 October 2012

### INTRODUCTION

Haem plays an important role as a cofactor for proteins of various functions and is used as an alternative source of iron by many bacterial species (Andrews *et al.*, 2003; Nobles & Maresso, 2011; Skaar, 2010). To ensure sufficient Fe<sup>2+</sup> supply but also avoid toxic intracellular levels, iron uptake and utilization is usually tightly regulated at the transcriptional level (Andrews *et al.*, 2003; Hantke, 2001; Skaar, 2010). Classical two-component systems (TCSs), composed of a sensor histidine kinase and a cognate response regulator, represent a typical regulatory module to sense extracellular environmental stimuli and transduce

the information via protein phosphorylation to the level of gene expression (Krell *et al.*, 2010; Mascher *et al.*, 2006; Stock *et al.*, 2000). Upon stimulus perception, the sensor kinase undergoes autophosphorylation of a conserved histidine residue; this phosphoryl group is subsequently transferred to an aspartate residue of the response regulator, which modulates gene expression by binding to the promoter region of target genes (Laub & Goulian, 2007; Stock *et al.*, 2000; West & Stock, 2001).

The Gram-positive soil bacterium *Corynebacterium glutamicum* represents an important platform organism in industrial biotechnology (Burkovski, 2008; Eggeling & Bott, 2005). In total, 13 TCSs are encoded in the *C. glutamicum* genome (Kocan *et al.*, 2006), several of which have been studied in more detail (Brocker *et al.*, 2011; Bott & Brocker, 2012; Schaaf & Bott, 2007; Schelder *et al.*, 2011). In a recent study, we demonstrated that the TCS HrrSA exhibits a central function in the control of haem homeostasis and haem utilization in *C. glutamicum*. In

Abbreviations: EMSA, electrophoretic mobility shift assay; TCS, two-component system; TSS, transcription start site.

Three supplementary tables and a more detailed method for the cloning techniques used here are available with the online version of this paper.

The normalized and processed microarray data from this study are available in the GEO database under accession no. GSF37327.

the presence of haem, the response regulator HrrA directly represses haem biosynthesis genes and activates haem oxygenase (*hmuO*) as well as genes encoding haem-containing components of the respiratory chain (Frunzke *et al.*, 2011). Expression of *hrrA* itself underlies control by the global iron regulator DtxR, which represses transcription from the promoter  $P_{hrrA}$ , downstream of *hrrS*, under conditions of sufficient iron supply (Wennerhold & Bott, 2006). Under iron-limiting conditions, DtxR dissociates from the *hrrA* promoter, thereby enabling the utilization of alternative iron sources such as haem. Besides *hrrA*, DtxR directly regulates the transcription of about 60 genes involved in iron uptake and storage in response to iron availability (Boyd *et al.*, 1990; Frunzke & Bott, 2008; Wennerhold *et al.*, 2005; Wennerhold & Bott, 2006).

For haem utilization, *C. glutamicum*, as well as its pathogenic relative *Corynebacterium diphtheriae*, depends on a haem uptake apparatus composed of the ABC transporter HmuTUV, several cell surface haem-binding proteins (Allen & Schmitt, 2009, 2011; Drazek *et al.*, 2000; Frunzke *et al.*, 2011) and a haem oxygenase (HmuO), which catalyses the intracellular degradation of the tetrapyrrol ring to  $\alpha$ -biliverdin, free iron ( $\text{Fe}^{3+}$ ) and carbon monoxide (Kunkle & Schmitt, 2007; Schmitt, 1997; Wilks & Schmitt, 1998). Acquisition of haem, however, exposes the respective organism to the toxicity associated with high levels of haem. It was shown in a recent study that the haem-regulated ABC transport system, HrtAB, is crucial for *C. diphtheriae* to cope with elevated haem concentrations (Bibb & Schmitt, 2010). The HrtAB system consists of the permease HrtB and the ATPase HrtA and is widespread among Gram-positive bacteria (Stauff *et al.*, 2008; Stauff & Skaar, 2009a, b). In *C. diphtheriae*, *hrtBA* expression was shown to be activated in the presence of haem by the TCS ChrSA (Bibb *et al.*, 2005; Bibb & Schmitt, 2010). In previous studies, the ChrSA system was described to activate expression of *hmuO* and repress expression of the *hemAC* operon encoding haem biosynthesis enzymes (Bibb *et al.*, 2007). Both targets, *hmuO* and *hemAC*, are also controlled by the second haem-dependent TCS, HrrSA, in *C. diphtheriae* (Bibb *et al.*, 2005, 2007).

Previous studies in *C. glutamicum* and *C. diphtheriae* revealed the TCSs HrrSA and ChrSA to have a global function in the control of haem homeostasis; however, no studies concerning the interplay of the two systems on the transcriptional level have been performed so far. In this report, we used genome-wide transcriptome analyses, protein–DNA interaction studies and promoter fusions to identify direct target genes of ChrSA (previously named CgtSR8) and study the interaction with the homologous system HrrSA in *C. glutamicum*. Our data reveal that HrrSA is the dominant system for the haem-dependent activation of haem oxygenase in *C. glutamicum*, whereas ChrSA plays a crucial role in haem tolerance mediated by the HrtBA haem transport system. Furthermore, we provide evidence for cross-regulation of both systems, HrrSA and ChrSA, at the level of transcription.

## METHODS

**Bacterial strains, media and growth conditions.** The bacterial strains used in this study are shown in Table S1 (available with the online version of this paper). For growth experiments, a 20 ml preculture of CGXII minimal medium containing 4% (w/v) glucose (Keilhauer *et al.*, 1993) was inoculated from a 5 ml BHI (brain heart infusion, Difco) culture after washing the cells with 0.9% (w/v) NaCl. Cells were incubated overnight at 30 °C and 120 r.p.m. in a rotary shaker. The trace element solution with or without iron as well as the  $\text{FeSO}_4$  or haemin (protoporphyrin IX with  $\text{Fe}^{3+}$ ) solution were added from stock after autoclaving, as indicated. Standard CGXII minimal medium contains 36  $\mu\text{M}$   $\text{FeSO}_4$ . For the haemin stock solution, haemin (Sigma Aldrich) was dissolved in 20 mM NaOH to 250  $\mu\text{M}$ . The main culture was inoculated from the second preculture to  $\text{OD}_{600}$  1 in CGXII minimal medium containing 4% (w/v) glucose and either  $\text{FeSO}_4$  or haemin as iron source. For cloning purposes *Escherichia coli* DH5 $\alpha$  was used; for overproduction of ChrA *E. coli* BL21(DE3) (Studier & Moffatt, 1986). *E. coli* was cultivated in Luria–Bertani (LB) medium at 37 °C or on LB agar plates. When necessary, kanamycin was added at an appropriate concentration (50  $\mu\text{g ml}^{-1}$  for *E. coli* and 25  $\mu\text{g ml}^{-1}$  for *C. glutamicum*). For growth experiments on agar plates the strains were grown in a 5 ml BHI culture overnight. The stationary culture was diluted to  $\text{OD}_{600}$  1 and dilution series (3  $\mu\text{l}$  each,  $10^0$  to  $10^{-7}$ ) were spotted on CGXII agar plates containing 4% (w/v) glucose and either 2.5 or 36  $\mu\text{M}$   $\text{FeSO}_4$  with or without haemin. Pictures of the plates were taken after incubation for 24 h at 30 °C.

Growth experiments in microtitre scale were performed in the BioLector system (m2p-labs). Therefore, 750  $\mu\text{l}$  CGXII containing 2% glucose (w/v) and different concentrations of  $\text{FeSO}_4$  (2.5 or 36  $\mu\text{M}$ ) or haemin (2.5–20  $\mu\text{M}$ ) were inoculated with cells from a 20 ml CGXII preculture with iron-starved cells (0  $\mu\text{M}$   $\text{FeSO}_4$ ) to  $\text{OD}_{600}$  1 and cultivated in 48-well flowerplates (m2p-labs) at 30 °C, 1200 r.p.m. and a shaking diameter of 3 mm. The production of biomass was determined as the backscattered light intensity of sent light with a wavelength of 620 nm (signal gain factor of 10); measurements were taken in 10 min intervals. The average backscatter of non-growing wild-type cells (first 2 h of the wild-type in CGXII minimal medium with 15  $\mu\text{M}$  haemin) was used for referencing. High fluctuations of low backscatter signals (non-growing cells, Fig. 1) are due to technical limitations. For promoter fusion studies, the eYFP chromophore was excited with 510 nm and emission was measured at 532 nm (signal gain factor of 50). The specific fluorescence (au) was calculated by the eYFP fluorescence signal per backscatter signal (Kensy *et al.*, 2009).

**Cloning techniques.** Routine methods were performed according to standard protocols (Sambrook *et al.*, 2001). Chromosomal DNA of *C. glutamicum* ATCC 13032 was prepared (Eikmanns *et al.*, 1994) and utilized as template for PCR. DNA sequencing and oligonucleotide synthesis were performed by Eurofins MWG Operon (Ebersberg, Germany). Plasmids and oligonucleotides used in this work are listed in Tables S1 and S2, respectively. A detailed description of the construction of strains and plasmids is given in the supplementary material.

**DNA microarrays.** The transcriptome of the deletion mutant  $\Delta\text{chrSA}$  grown on haem or  $\text{FeSO}_4$  was compared with the wild-type using whole-genome-based DNA microarrays. For this purpose, cells of a BHI preculture were used for inoculation of a second preculture in CGXII medium containing 1  $\mu\text{M}$   $\text{FeSO}_4$ . For main culture, cells were cultivated in CGXII minimal medium with 4% glucose (w/v) containing either 2.5  $\mu\text{M}$   $\text{FeSO}_4$  or haemin as iron source and harvested at  $\text{OD}_{600}$  5–6 in pre-cooled (–20 °C) ice-filled tubes via centrifugation (6900 g, 10 min, 4 °C). The cell pellet was subsequently frozen in liquid nitrogen and stored at –70 °C until RNA

A. Heyer and others

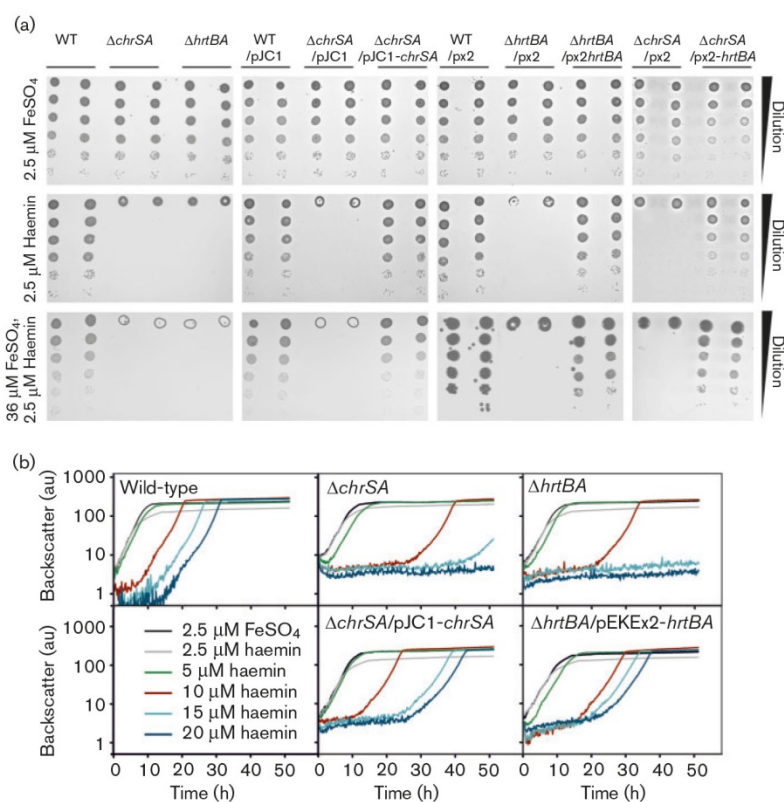


**Fig. 1.** Growth phenotype of *C. glutamicum* ATCC 13032 wild-type,  $\Delta chrSA$  and  $\Delta hrtBA$  mutants. (a) For growth on agar plates, cells were spotted on CGXII minimal medium plates in serial dilutions containing either 2.5  $\mu M$  FeSO<sub>4</sub>, 2.5  $\mu M$  haemin or 36  $\mu M$  FeSO<sub>4</sub> plus 2.5  $\mu M$  haemin. (b) For growth in liquid culture, cells were resuspended in 750  $\mu l$  CGXII minimal medium containing 2.5  $\mu M$  FeSO<sub>4</sub> or haemin (2.5–20  $\mu M$ ) and cultivated in 48-well flowerplates in a BioLector system (see Methods). Growth was monitored as backscattered light (620 nm). Without iron, the cells reached a final backscatter value of about 50 (data not shown). Please note that the high fluctuations of backscatter values below 10 are due to technical limitations. Growth curves show one representative experiment of three biological replicates.

preparation. The preparation of total RNA was performed as described previously (Möker *et al.*, 2004). For cDNA synthesis, 25 ng total RNA from each sample was used. Labelling and hybridization was performed with a 70-mer custom-made DNA microarray purchased from Eurofins MWG Operon, as described previously (Frunzke *et al.*, 2008). All DNA microarray experiments were repeated in three biological replicates. The normalized and processed data were saved in the in-house microarray database (Polen & Wendisch, 2004) for further analysis and in the Gene Expression Omnibus (GEO) database under accession no. GSE37327.

**Overproduction and purification of ChrA.** For the overproduction of ChrA, *E. coli* BL21(DE3) was transformed with the vector pET28b-*chrA* and cultivated in 200 ml LB medium. At OD<sub>600</sub> 0.6–0.8, the expression of *chrA* was induced by addition of 1 mM IPTG. After 4 h of expression at 30 °C, the cells were harvested by centrifugation (4000 g at 4 °C, 10 min). The cell pellet was stored at –20 °C until further use. For protein purification, the cell pellet was resuspended in 3 ml TNI5 buffer (20 mM Tris/HCl pH 7.9, 300 mM NaCl and 5 mM imidazole) containing Complete protease inhibitor cocktail (Roche). Cells were disrupted by passing through a French pressure

cell (SLM Aincos, Spectronic Instruments) twice at 207 MPa. The cell debris was removed by centrifugation (6900 g, 4 °C, 20 min), followed by ultracentrifugation of the cell-free extract for 1 h (150 000 g, 4 °C). ChrA was purified from the supernatant via Ni<sup>2+</sup>-NTA (nickel-nitriloacetic acid) affinity chromatography as described for *C. glutamicum* HrrA (Frunzke *et al.*, 2011). ChrA was eluted from the column with TNI100 buffer (containing 100 mM imidazole) and analysed on a 12% SDS-polyacrylamide gel. Protein concentration was determined with Bradford reagent (Bradford, 1976). Elution fractions of ChrA were pooled and the buffer was exchanged to bandshift buffer [20 mM Tris/HCl, pH 7.5, 50 mM KCl, 5 mM ATP, 10 mM MgCl<sub>2</sub>, 5% (v/v) glycerol, 0.5 mM EDTA, 0.005% (w/v) Triton X-100] using a PD10 desalting column (GE Healthcare). The protein was stored in aliquots at –20 °C.

**Electrophoretic mobility shift assay (EMSA).** EMSAs were performed with purified ChrA protein and DNA fragments of the putative target genes. Promoter regions (500 bp) of the putative target genes were amplified via PCR and purified by using the Qiagen PCR purification kit. As a negative control, the promoter region of the *gntK* gene was used. DNA (100 ng per lane) was incubated with

different molar excesses of the purified ChrA protein at room temperature for 30 min in bandshift buffer. For phosphorylation of ChrA, 50 mM of the small phosphate donor phosphoramidate was incubated with the protein before the DNA was added. After incubation, sample buffer [0.1% (w/v) xylene cyanol dye, 0.1% (w/v) bromophenol blue dye, 20% (v/v) glycerol in 1 × TBE (89 mM Tris base, 89 mM boric acid, 2 mM EDTA)] was added and samples were separated on a non-denaturing 10% polyacrylamide gel with 170 V in 1 × TBE buffer. DNA was stained using SYBR Green I (Sigma-Aldrich). For verification of the ChrA binding motif, 30 bp double-stranded oligonucleotides were assembled by hybridization of two complementary oligonucleotides. The amount of shifted DNA was quantified by using the ImageQuant TL software (GE Healthcare).

**Identification of transcription start sites (TSSs) and promoter regions by RNA-Seq.** A 5'-end enriched RNA-Seq library was constructed according to the following procedures. 1) Depletion of stable rRNA and enrichment of mRNA molecules were performed using the Ribo-Zero rRNA removal kit for Gram-positive bacteria (Epicentre Biotechnologies). 2) The enriched mRNA was fragmented by magnesium oxalacetate (MgKOAc) hydrolysis. Four vols RNA solution were mixed with one vol. MgKOAc solution (100 mM KOAc and 30 mM MgOAc in 200 mM Tris/HCl, pH 8.1) and the mixture was incubated for 2.5 min at 94 °C. The reaction was stopped by adding an equal volume of 1 × TE (10 mM Tris, 1 mM EDTA, pH 8) and chilling on ice for 5 min. 3) The fragmented RNA was precipitated by addition of three vols 0.3 M NaAc in ethanol with 2 µl glycogen and incubation overnight at -20 °C. 4) The precipitated RNA fragments were dissolved in water and the 5'-end RNA fragments were enriched by using Terminator 5'-phosphate-dependent exonuclease (Epicentre Biotechnologies). 5) After RNA precipitation (as above), the triphosphates were removed using RNA 5'-polyphosphatase (Epicentre Biotechnologies). 6) After RNA precipitation (as above), the 5'-enriched, monophosphorylated RNA fragments were used to construct a cDNA library by using the Small RNA Sample Prep kit (Illumina).

The fragmentation of RNA molecules (fragment sizes were 200–500 bp) and RNA concentration were monitored using the RNA 6000 Pico Assay on an Agilent 2100 Bioanalyser (Agilent). Sequencing of the cDNA library was carried out on the GA IIX platform (Illumina). Resulting reads were aligned to the *C. glutamicum* genomic sequence using the mapping software SARUMAN (Blom *et al.*, 2011). TSS and promoter regions were deduced by combining published information about promoter regions in *C. glutamicum* (Pátek & Nešvera, 2011) with 5'-end enriched RNA-Seq data.

## RESULTS

### The TCS ChrSA (previously CgtSR8): sequence similarities and genomic organization

In a previous study the TCS HrrSA was reported to play a central role in the control of haem homeostasis in *C. glutamicum* (Frunzke *et al.*, 2011). *In vitro* DNA binding studies with purified HrrA protein provided evidence that the response regulator HrrA binds to the upstream promoter region of an operon encoding another TCS, *chrSA* (cg2201–cg2200) (Kocan *et al.*, 2006). This system consists of the genes cg2200 (*chrA*, previously *cgtR8*), encoding the response regulator ChrA, and cg2201 (*chrS*, previously *cgtS8*), encoding the sensor kinase ChrS. Sequence analysis revealed considerable similarity of ChrSA to the recently described system HrrSA of *C. glutamicum*. The

sensor kinases, ChrS and HrrS, share a sequence identity of about 35%, whereas the response regulators, ChrA and HrrA, exhibit a sequence identity of about 58% at the protein level (Table 1). Both systems also share significant similarities with HrrSA and ChrSA of *C. diphtheriae*. A pairwise comparison is given in Table 1. In terms of consistency with the previously described orthologous system of *C. diphtheriae*, we renamed CgtSR8 to 'ChrSA' for *C. glutamicum*.

RNA sequencing experiments indicated that, in contrast with the *hrrSA* operon, where a second promoter is located upstream of *hrrA*, the genes *chrSA* form a classical operon with one promoter upstream of *chrS* (Table S3). The start codon of *chrA* overlaps with the stop codon of *chrS*. Divergently from *chrSA* (intergenic region of 110 bp) the operon *hrtBA* is located, encoding the permease (HrtB) and ATPase (HrtA) components of an ABC-type transport system. Microsynteny is observed at this genomic locus consisting of a classical TCS and an operon encoding a 'haem-regulated transport system', which is highly conserved in Gram-positive bacteria. The transporter HrtAB has been described to be involved in export of haem or degradation products thereof (Stauff & Skaar, 2009a). These findings suggest that the TCS ChrSA might interfere in the control of haem homeostasis with the recently reported system HrrSA in *C. glutamicum*.

### Deletion of *chrSA* leads to increased haem sensitivity

To characterize the role of the TCS ChrSA in haem utilization, we constructed an in-frame deletion mutant lacking the genes *chrA* and *chrS*. In first experiments, we analysed the haem tolerance of the deletion mutant  $\Delta$ *chrSA* and the *C. glutamicum* wild-type. Growth of the strains was compared on agar plates or in liquid culture containing either haemin or FeSO<sub>4</sub> as iron source. Growth in liquid culture (2.5 µM FeSO<sub>4</sub> or 2.5–20 µM haemin) was performed in microtitre plates (48-well flowerplates, see

**Table 1.** Sequence identities of the TCSs ChrSA and HrrSA of *C. glutamicum* and *C. diphtheriae*

	Amino acid sequence identity (%)			
	1	2	3	4
<b>Response regulators</b>				
ChrA_Cg2200 (1)	100	–	–	–
ChrA_DIP2327 (2)	44	100	–	–
HrrA_Cg3247 (3)	58	52	100	–
HrrA_DIP2267 (4)	55	50	86	100
<b>Sensor kinases</b>	<b>5</b>	<b>6</b>	<b>7</b>	<b>8</b>
ChrS_Cg2201 (5)	100	–	–	–
ChrS_DIP2326 (6)	29	100	–	–
HrrS_Cg3248 (7)	35	25	100	–
HrrS_DIP2268 (8)	35	25	51	100

A. Heyer and others

Methods) where *C. glutamicum* exhibits similar growth properties as in shake flasks.

When cultivated with FeSO<sub>4</sub> as an iron source, both wild-type and  $\Delta chrSA$  showed the same growth phenotype on agar plates and in liquid minimal medium (Fig. 1). Grown on 2.5  $\mu$ M haemin,  $\Delta chrSA$  revealed a strong growth defect on plates (Fig. 1a). Under iron-replete conditions, the same phenotype was observed in the presence of haem (36  $\mu$ M FeSO<sub>4</sub> and 2.5  $\mu$ M haemin), indicating that the observed phenotype is a result of the elevated haem concentration and is not influenced by the iron concentration (Fig. 1a). In liquid culture, the presence of 2.5  $\mu$ M haemin resulted in a decelerated growth rate and a lower final backscatter signal for both strains. The addition of 5  $\mu$ M haemin extended the lag phase and resulted in a higher final backscatter compared with cells grown on 2.5  $\mu$ M haemin, indicating that iron is a limiting factor under the chosen conditions. Higher haemin concentrations (10–20  $\mu$ M) led to a proportional extension of the lag phase after which cells started to grow again with a growth rate comparable to cells grown on iron (Fig. 1b). Again, the mutant strain  $\Delta chrSA$  exhibited a higher sensitivity towards elevated haemin concentrations (10–20  $\mu$ M haemin). This delayed growth of the tested strains and the fact that the cells resume growth after the lag phase with an unaltered growth rate or final density led to the assumption that the added haemin is degraded in the culture medium over time until the concentration drops under a certain threshold. This tolerable limit would then be higher for the wild-type than for  $\Delta chrSA$ . The observed phenotype of the  $\Delta chrSA$  mutant was complemented by transformation with the plasmid pJC1-*chrSA*, expressing *chrSA* under the control of its native promoter (Fig. 1). Overall, these findings emphasize a central role of ChrSA in haem detoxification.

### The HrtBA transporter confers resistance towards haem toxicity

Growth experiments revealed a significant haemin sensitivity of the  $\Delta chrSA$  mutant. As outlined in the Introduction, the genes *hrtBA*, located divergently to *chrSA*, encode a putative 'haem regulated transporter' (Bibb & Schmitt, 2010; Stauff & Skaar, 2009b). Thus, a lowered expression of *hrtBA* in the  $\Delta chrSA$  mutant could be a reason for the observed haem sensitivity of the  $\Delta chrSA$  mutant. In order to investigate the function of the putative transport system HrtBA in *C. glutamicum*, an in-frame deletion mutant of the genes *hrtB* and *hrtA* was constructed. As observed for  $\Delta chrSA$ , the growth of  $\Delta hrtBA$  was not affected when FeSO<sub>4</sub> was added as sole iron source. In the presence of haemin,  $\Delta hrtBA$  exhibited a significant growth defect, both on agar plates and during liquid cultivation (Fig. 1). This phenotype was complemented by transformation of  $\Delta hrtBA$  with the plasmid pEKEx2-*hrtBA* carrying the *hrtBA* operon under the control of the IPTG-inducible P<sub>tac</sub> promoter, which allows a basal gene expression even in the absence of IPTG. The strain  $\Delta hrtBA$ /pEKEx2-*hrtBA* showed wild-type-like tolerance towards high

haemin concentrations (Fig. 1). Induction of *hrtBA* expression by addition of IPTG led to a strong growth defect (data not shown). In the next step, we tested our hypothesis that reduced expression of *hrtBA* might be the reason for the observed growth phenotype of the  $\Delta chrSA$  mutant and examined whether plasmid-driven expression of *hrtBA* in  $\Delta chrSA$  could restore wild-type-like growth. In fact, the cross-complemented strain  $\Delta chrSA$ /pEKEx2-*hrtBA* exhibited wild-type-like growth on agar plates containing 2.5  $\mu$ M haemin (Fig. 1a). These data indicate that HrtBA plays a key function in haem detoxification in *C. glutamicum* and suggest a role of ChrSA in the control of *hrtBA* expression.

### Transcriptome analysis of a $\Delta chrSA$ mutant strain

To identify additional potential target genes of ChrSA we assessed the influence of ChrSA on global gene expression via comparative transcriptome analysis of the  $\Delta chrSA$  mutant and *C. glutamicum* wild-type grown in CGXII minimal medium with 4% glucose and either 2.5  $\mu$ M FeSO<sub>4</sub> or 2.5  $\mu$ M haemin as iron source. Genes whose mRNA level showed a more than twofold alteration in either experiment (FeSO<sub>4</sub> or haemin) are listed in Table 2. In cells grown on FeSO<sub>4</sub>, the deletion of *chrSA* had no significant influence on global gene expression. When cultivated with haemin as an iron source, the relative expression level of *hrtBA* (coding for the putative haem transport system HrtBA) was two- to threefold decreased in the  $\Delta chrSA$  mutant.

Likewise, the expression of *hmuO*, encoding the haem oxygenase, was nearly sevenfold decreased in the presence of haemin, but showed no difference on iron as well. Expression of *hmuO* is also described as being under control of the global iron regulator DtxR in *C. glutamicum* (Wennerhold & Bott, 2006). In our studies, the  $\Delta chrSA$  mutant showed a slightly reduced expression (1.3- to 2-fold) of several DtxR target genes (Table 2) composing the typical iron starvation response. Among those, we found the operon *hmuTUV* encoding a haem uptake system as well as *htaA*, *htaC* and *htaD* encoding putative haem-binding proteins. However, *hmuO* expression was significantly decreased even more than the other DtxR targets.

Remarkably, the mRNA level of *hrrA* encoding the response regulator of the TCS HrrSA was slightly increased (approx. 1.5-fold) in the  $\Delta chrSA$  mutant. Together with the observed derepression of *chrSA* in a  $\Delta hrrA$  mutant (Frunzke *et al.*, 2011) these data hint at a cross-regulation of both systems at the level of transcription. Further genes exhibiting an altered mRNA level include a regulator of unknown function (cg3303) and the redox-sensing regulator *qorR*, whose DNA-binding activity was reported to be affected by oxidants (Ehira *et al.*, 2009).

### Identification of direct target genes of the response regulator ChrA

To test for direct binding of the response regulator ChrA to putative target promoters, we performed *in vitro* EMSA

**Table 2.** Comparative transcriptome analysis of  $\Delta chrSA$  and *C. glutamicum* wild-type

This table shows all genes that revealed a  $\geq$  twofold altered relative mRNA ( $P$ -value  $\leq 0.06$ ) level in at least two of three independent DNA microarrays of *C. glutamicum*  $\Delta chrSA$  versus wild-type grown on CGXII minimal medium with 4% (w/v) glucose and 2.5  $\mu$ M FeSO<sub>4</sub> or haem as iron source.

Gene ID	Gene	Annotation	Ratio 2.5 $\mu$ M FeSO <sub>4</sub> *	Ratio 2.5 $\mu$ M haem*
<b>TCSs</b>				
cg3247	<i>hrrA</i>	TCS, response regulator	1.03	1.45
cg3248	<i>hrrS</i>	TCS, signal transduction histidine kinase	1.01	0.86
<b>Haem homeostasis-related genes</b>				
cg2202	<i>hrtB</i>	ABC-type transport system, permease component	1.05	0.64
cg2204	<i>hrtA</i>	ABC-type transport system, ATPase component	1.17	0.33
cg2445	<i>hmuO</i>	Haem oxygenase	0.96	0.16
cg0466	<i>htaA</i>	Secreted haem transport-associated protein	0.97	0.48
cg0467	<i>hmuT</i>	Haemin-binding periplasmic protein precursor	0.89	0.68
cg0468	<i>hmuU</i>	Haemin transport system, permease protein	1.03	0.66
cg0469	<i>hmuV</i>	Haemin transport system, ATP-binding protein	0.98	n.d.
<b>Others</b>				
cg0018		Hypothetical membrane protein	1.02	2.02
cg1552	<i>qorR</i>	Redox-sensing transcriptional regulator	1.00	2.07
cg2518		Putative secreted protein	1.01	2.03
cg2845	<i>pstC</i>	ABC-type phosphate transport system, permease component	0.93	2.17
cg3303		Transcriptional regulator, PadR-like family	0.95	2.20

\*The mRNA ratio represents the mean value of three independent DNA microarray experiments.

studies with purified ChrA. To this end, ChrA was overproduced in *E. coli* containing an N-terminal hexahistidine tag and purified by affinity chromatography. Purified ChrA was phosphorylated by the addition of the small-molecule phosphate donor phosphoramidate, which led to an approximately two- to threefold increased affinity of ChrA~P to the tested DNA fragments.

In our assays, a clear binding of ChrA to the intergenic region of *chrSA* and *hrtBA* was detected (Fig. 2a). A complete shift was observed upon addition of a 30- to 50-fold molar excess of phosphorylated ChrA. Under these conditions neither the negative control (*gntK*, cg2732) nor the promoter region of *htaA* was bound by ChrA (data not shown). Binding of ChrA to a DNA fragment covering the promoter of *hrrA* was also observed, however, with a lower affinity than binding to *hrtBA*–*chrSA*. Notably, the promoter region of *hmuO* whose expression level was significantly decreased (sevenfold) in the  $\Delta chrSA$  mutant was not bound by ChrA in this assay.

In further EMSA assays, the binding region of ChrA to the promoters of *hrtBA*–*chrSA* and *hrrA* was narrowed down to DNA fragments of about 30 bp. Positive subfragments covering the binding motif of ChrA showed a comparable shift from the originally tested fragments (Fig. 2b). For the *hmuO* promoter region EMSA assays with a subfragment covering the region upstream of the DtxR-binding region (–45 bp upstream of the TSS) showed a slightly different picture to the negative control, suggesting

very low affinity binding of ChrA *in vitro*. Whether this binding is of physiological relevance has to be verified in further studies.

### Mutational analysis of the ChrA-binding motif

Sequence analysis of the 30 bp DNA fragment in the intergenic region of *hrtBA* and *chrSA* revealed a small inverted repeat (CGACcaaaGTCG). To assess the relevance of this repeat for ChrA binding we performed mutational analysis of the whole 30 bp fragment. For this purpose, three to four nucleotides were exchanged for the complementary ones and the mutated fragments were tested in gel retardation analysis. The exchange of small inverted repeats abolished ChrA binding, whereas the exchange of adjacent nucleotides or the four nucleotides in between the repeat led to reduced ChrA affinity towards the particular DNA fragment (Fig. 3). Mutations outside of the motif did not affect ChrA binding. Overall, the mutational analysis supported the relevance of the inverted repeat for binding of ChrA and revealed the sequence AgTaCGACcaaaGTCGgAtT as binding motif in the intergenic region of *hrtBA*–*chrSA*. A motif with considerable sequence identity was also found in the promoter region of *hrrA* (Fig. 4). A 30 bp fragment covering this predicted motif exhibited a clear binding by ChrA in EMSA assays (Fig. 2b).

Fig. 4 illustrates the position of the ChrA binding sites in relation to the TSS of the respective target gene. The TSS

A. Heyer and others

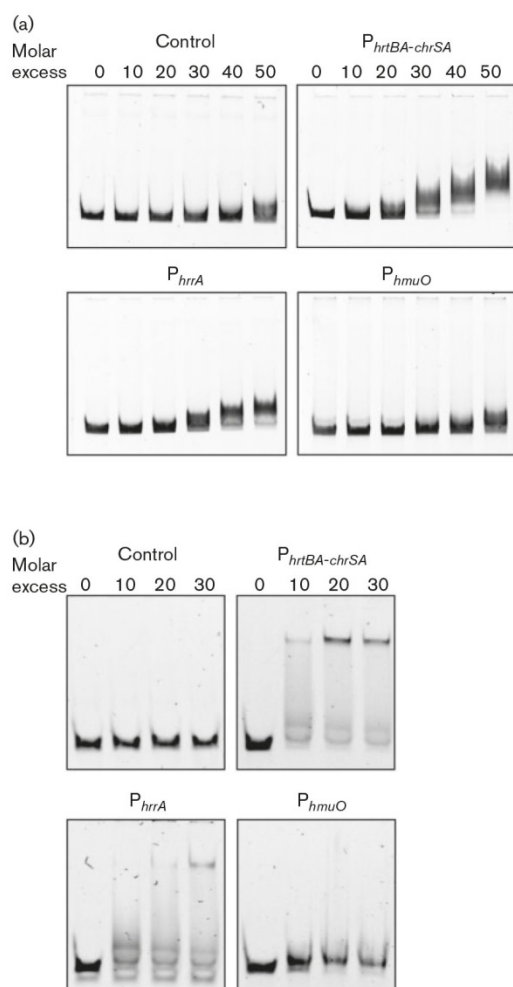


**Fig. 2.** DNA–protein interaction studies of ChrA and putative target promoters. (a) For gel retardation assays, 500 bp DNA fragments covering the promoter regions of *hrtBA-chrSA*, *hrrA* and *hmuO* were incubated without or with different molar excesses of phosphorylated ChrA (0- to 50-fold). The promoter region of *gntK* served as control fragment. For phosphorylation, purified ChrA protein was preincubated with 50 mM phosphoramidate (see Methods). Samples were separated on a 10% non-denaturing polyacrylamide gel and stained with SYBR green I. (b) As described in (a), 30 bp DNA fragments covering the putative binding site of ChrA. Samples were separated on a 15% non-denaturing polyacrylamide gel.

has been determined by RNA sequencing of the *C. glutamicum* transcriptome (see Table S3). In the *hrtBA-chrSA* intergenic region the ChrA motif is located in between the  $-35$  regions of *hrtBA* and *chrSA*, a position that would be in agreement with ChrA having an activating

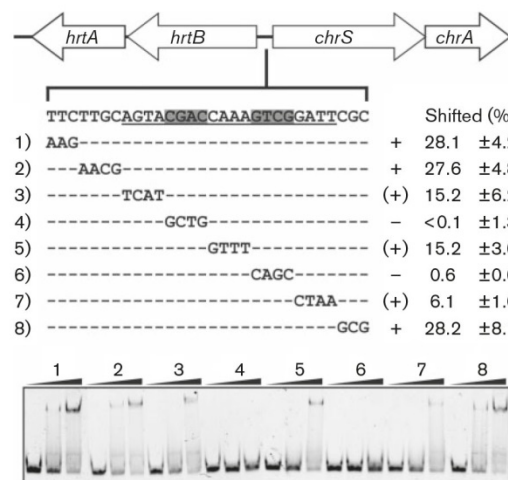


**Fig. 3.** Mutational analysis of the ChrA binding site in the intergenic region of *hrtBA-chrSA*. To analyse the relevance of different nucleotides for ChrA binding, a 30 bp DNA fragment covering the putative ChrA binding site in the *hrtBA-chrSA* intergenic region was mutated by an exchange of 3 to 4 bp to the complementary base pairs, as indicated, and analysed via EMSA studies. After incubation, the samples were separated on a 15% non-denaturing polyacrylamide gel and stained with Sybr Green I. +, Fragments that were shifted with unaltered affinity; (+), a shift with lower affinity; -, fragments that were not shifted. The amount of shifted DNA is given as a percentage and was quantified by using ImageQuant TL (GE Healthcare) from three experimental replicates (mean ± SD).

function on the expression of both operons. In the case of *hrrA*, which showed a slightly increased mRNA level in the  $\Delta chrSA$  mutant, the ChrA binding site is located close to the TSS and would support a proposed repressor function of ChrA interfering at this locus with the binding of the RNA polymerase (Madan Babu & Teichmann, 2003).

### HrrSA and ChrSA interfere in haem-dependent gene regulation

Previous studies revealed binding of the response regulator HrrA to the *hrtBA-chrSA* intergenic region. In view of the data reported in this study, HrrA and ChrA likely interfere in the transcription control of *hrtBA* and/or *chrSA*. To study the influence of both TCSs *in vivo* we constructed promoter fusions of the intergenic region of *hrtBA-chrSA* fused to *eyfp* in both possible directions ( $P_{chrSA}$  and  $P_{hrtBA}$ ). While the wild-type containing the reporter plasmids (WT/pJCI- $P_{hrtBA-eyfp}$ , WT/pJCI- $P_{chrSA-eyfp}$ ) exhibited no fluorescence when grown on iron, cells grown on haem showed a significantly increased fluorescence signal in the lag and early exponential phase (Fig. 5a). The  $\Delta chrSA$  strain transformed with the promoter fusion plasmids ( $\Delta chrSA/pJCI- $P_{hrtBA-eyfp}$ ,  $\Delta chrSA/pJCI- $P_{chrSA-eyfp}$ ) showed no$$

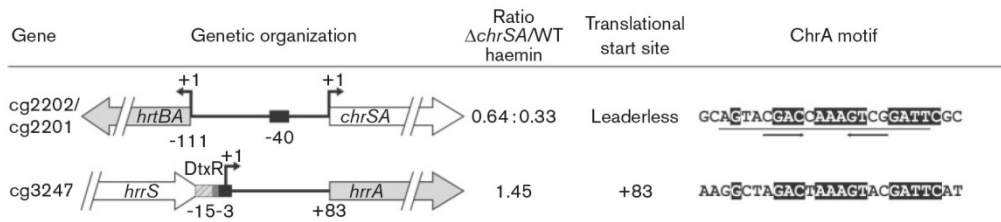


**Fig. 4.** Localization of ChrA binding sites in the *hrtBA*–*chrSA* intergenic region and the *hrrA* promoter. Promoters were derived from RNA sequencing experiments; the corresponding –10 and –35 regions are given in Table S3. The TSS is indicated as +1 and the ChrA binding sites are shown as a black box, the DtxR binding site is shown as shaded box. The number below the ChrA box indicates the distance to the TSS. The mRNA ratios were obtained from DNA microarray analysis [ $\Delta chrSA$  mutant versus wild-type (WT) grown on 2.5  $\mu\text{M}$  haemin, see also Table 2]. Nucleotides conserved in both motifs are shaded in black.

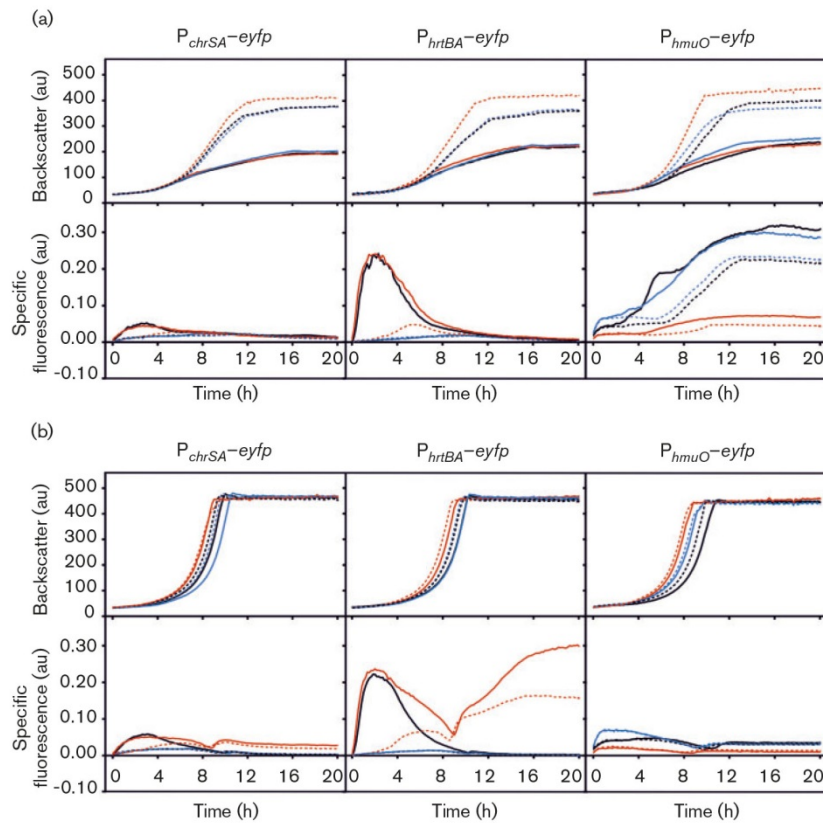


**Fig. 5.** Promoter studies of  $P_{chrSA}$ ,  $P_{hrtBA}$  and  $P_{hmuO}$  in wild-type and TCS mutants. For promoter studies, the promoters of *chrSA*, *hrtBA* and *hmuO* were fused to *eyfp*. *C. glutamicum* wild-type (black),  $\Delta chrSA$  (blue), and  $\Delta hrrSA$  (red) were cultivated in CGXII minimal medium with 2% glucose in microtitre plates (a) with 2.5  $\mu\text{M}$   $\text{FeSO}_4$  (dotted lines) or 2.5  $\mu\text{M}$  haemin (solid lines) as iron source or (b) with 36  $\mu\text{M}$   $\text{FeSO}_4$  with (solid lines) or without (dotted lines) 2.5  $\mu\text{M}$  haemin. In the BioLector system, the growth (backscatter signal of 620 nm light) and eYFP fluorescence (excitation 510 nm/emission 532 nm) were monitored over 10 min intervals. The specific fluorescence was calculated as fluorescence signal per backscatter signal (given in arbitrary units, au). Shown are representative experiments of three to four independent replicates.

A. Heyer and others

significant fluorescent signal (Fig. 5a), indicating that ChrSA is crucial for the haem-dependent activation of both promoters. A similar response was observed under iron-excess conditions (36  $\mu\text{M}$   $\text{FeSO}_4$ ) in the presence of haem (Fig. 5b). These data are in line with a positive autoregulation of *chrSA* and a ChrA-dependent activation of *hrtBA* in haem-grown cells. In a  $\Delta\text{hrrSA}$  strain, lacking the genes *hrrA* and *hrrS* of the TCS HrrSA, a higher signal was detected for both promoters ( $P_{\text{hrtBA}}$  and  $P_{\text{chrSA}}$ ) under iron limitation in comparison with the wild-type, supporting the postulated repressor function of HrrA on *chrA* (Fig. 5). Remarkably, under iron-replete conditions, the activity of  $P_{\text{hrtBA}}$  and  $P_{\text{chrSA}}$  in the  $\Delta\text{hrrSA}$  strain remained high throughout the exponential and stationary growth phase and did not decline to the background level.

### HrrSA is crucial for the haem-dependent activation of *hmuO*

Transcriptome analysis of the  $\Delta\text{chrSA}$  mutant revealed a significant reduction of the *hmuO* mRNA level in the mutant strain when cultivated on haem. However, no significant binding of ChrA was observed to the *hmuO* promoter. In the following experiment we used a promoter fusion of  $P_{\text{hmuO}}$  to *eyfp* to further study the impact of the TCSs HrrSA and ChrSA on *hmuO* expression *in vivo*. In contrast with  $P_{\text{hrtBA-eyfp}}$  and  $P_{\text{chrSA-eyfp}}$  whose expression peaked in the early exponential phase, the wild-type containing the  $P_{\text{hmuO-eyfp}}$  construct showed an increasing signal during the exponential phase in cells grown on haem as an iron source. In iron-grown cells (2.5  $\mu\text{M}$   $\text{FeSO}_4$ ), *hmuO* expression showed an increase later in the mid-exponential phase, which correlates with the derepression of the iron starvation response controlled by DtxR (Wennerhold & Bott, 2006). Under iron-replete conditions (36  $\mu\text{M}$   $\text{FeSO}_4$ ) the activity of  $P_{\text{hmuO}}$  was reduced to an almost background level (Fig. 5b). In the absence of *chrSA*, a similar course was observed during cultivation on iron, whereas the increase of  $P_{\text{hmuO}}$  activity on haem-grown cells was slightly delayed in the exponential phase (Fig. 5a) but reached wild-type levels in the stationary phase. Remarkably, the fluorescent signal was strongly diminished in a mutant lacking *hrrSA* ( $\Delta\text{hrrSA/pJC1-P}_{\text{hmuO-eyfp}}$ ). These data emphasize a central role of HrrSA in haem-dependent activation of *hmuO* expression in *C. glutamicum*.

## DISCUSSION

Many bacterial species rely on haem or haem proteins as alternative sources of iron. Here, we showed that the TCS ChrSA is the crucial regulatory system for resistance towards haem toxicity in the non-pathogenic soil bacterium *C. glutamicum*. We identified the putative haem exporter *hrtBA* and *hrrA*, which encodes the response regulator HrrA of the homologue TCS HrrSA, as direct target genes of the response regulator ChrA. The highest binding affinity of purified ChrA was observed in the

presence of the phosphate donor phosphoramidate, indicating that ChrA follows the classical model and is active in its phosphorylated state (Gao *et al.*, 2007; Stock *et al.*, 2000). This is consistent with recent studies where the phosphotransfer from the soluble kinase domain of ChrS to the response regulator ChrA was described for the *C. diphtheriae* ChrSA system (Burgos & Schmitt, 2012). The autophosphorylation of ChrS was shown to occur in the presence of haemin in purified *E. coli* proteoliposomes, indicating a direct interaction of ChrS with haem (Ito *et al.*, 2009).

The results described in this study support the prediction that *C. glutamicum* ChrSA has a key function in activating the expression of the divergently located operon *hrtBA* in the presence of haem. In fact, this function of ChrSA was expected due to the conserved microsynteny of this genomic locus where an operon of a TCS system is found in divergent orientation to *hrtBA* encoding a putative 'haem-regulated' ABC-transport system. This genomic organization is highly conserved among Gram-positive bacteria and homologous HrtAB transport systems were described as being required for coping with toxic haem concentrations for the species *C. diphtheriae*, *Staphylococcus aureus* and *Bacillus anthracis* (Bibb & Schmitt, 2010; Stauff *et al.*, 2008). So far, this transport system has mainly been described in pathogenic species where it is of major importance during host infection, when the bacteria are exposed to high haem concentrations in the blood. The presence of *hrtBA* in the genome of the non-pathogenic soil bacterium *C. glutamicum* might be a relic of evolution, as *C. glutamicum* is closely related to several pathogenic *Corynebacteria*, such as *C. diphtheriae* or *Corynebacterium ulcerans* (Yukawa *et al.*, 2007). However, high haem tolerance might also be of benefit in the soil, where haem is present in decaying organic material and represents an attractive alternative iron source for aerobic bacteria (Andrews *et al.*, 2003). An alternative regulatory mechanism of transcriptional regulation of *hrtBA* has recently been reported for the Gram-positive commensal bacterium *Lactococcus lactis*. Here, the cytoplasmic one-component regulator HrtR was described as a crucial factor for the haem-dependent activation of *hrtBA* (Lechardeur *et al.*, 2012). This mechanism is conserved among different Gram-positive commensals and contrasts with the TCS-mediated control described for several pathogenic species as well as *C. glutamicum*.

By using gel retardation assays and mutational analysis, we identified an imperfect inverted repeat (AgTaCGACcaaaGTCGgAtT) as a ChrA binding site within the *hrtBA-chrSA* intergenic region. Five of the eight nucleotides composing the inverted repeat are conserved in the binding site in the *hrrA* promoter. A genome-wide motif search did not reveal candidates for additional, putative binding sites of haem-relevant genes, probably due to the poor conservation of the motif. The motif revealed only weak similarities to the identified ChrA binding motif upstream of *C. diphtheriae hrtBA* (CatATCAACCagtcGGTTGATggG) or with the motif of the ChrA orthologues HssR from *S. aureus* and *B.*

*anthracis* (Bibb & Schmitt, 2010; Burgos & Schmitt, 2012; Stauff & Skaar, 2009b). However, our data reveal differences in the network composition of *C. glutamicum* ChrSA and HrrSA in comparison to what is known for the *C. diphtheriae* systems. An adequate example therefore is the haem-dependent gene regulation of the haem oxygenase (*hmuO*). Whereas ChrSA was reported to be the prominent system involved in haem-dependent *hmuO* activation in *C. diphtheriae* (Bibb *et al.*, 2005, 2007), promoter fusion studies in this work emphasize HrrSA to hold this function in *C. glutamicum*, since almost no signal of the  $P_{hmuO}$ -*eyfp* construct was observed in a  $\Delta$ *hrrSA* mutant. Reduced *hmuO* expression was also observed in a  $\Delta$ *chrSA* mutant by transcriptome analysis, but promoter fusion studies suggested that this effect might rather be due to delayed *hmuO* expression in the early and mid-exponential phase. Whether this effect is directly mediated by ChrA is currently unclear as no significant binding of ChrA to the *hmuO* promoter was observed in our *in vitro* studies. A potential binding motif that shares slight similarity to the *C. diphtheriae* motif is located upstream of the DtxR binding site in the *hmuO* promoter (−45: TCCAACCTAAGGGACTA). A binding motif for HrrA has not been reported so far but binding of HrrA is also likely to be located in this promoter region (upstream of −35). As the two response regulators ChrA and HrrA share significant sequence identity (62% sequence identity in the DNA-binding helix–turn–helix motif), it can be speculated whether both regulators might bind to overlapping or even identical regions with different affinities – a question which will be addressed in following studies.

Although the HrrSA and ChrSA systems share high sequence similarity, the genomic organization differs. In contrast with *chrSA*, *hrrA* expression is repressed by the global iron regulator DtxR under iron sufficiency and is derepressed when iron becomes limiting (Wennerhold & Bott, 2006) (Fig. 6). This control of *hrrA* by DtxR seems not to be present in *C. diphtheriae* (Bibb *et al.*, 2007). Variations in the regulatory network composition in these closely related species may be surprising; however, sequence analysis revealed striking differences between *Corynebacterium* species regarding their TCS equipment (Bott & Brocker, 2012). With respect to HrrSA and ChrSA, several corynebacterial genomes contain only one of the two systems; both systems together were identified in the *C. glutamicum* species *C. diphtheriae*, *C. pseudotuberculosis* and *C. lipophiloflavum* (Bott & Brocker, 2012; Cerdeño-Tárraga *et al.*, 2003; Kalinowski *et al.*, 2003; Trost *et al.*, 2010; Yukawa *et al.*, 2007). These findings indicate significant variation at the species level and suggest an individual network constitution meeting the requirements of each particular species.

The fact that both TCSs HrrSA and ChrSA are involved in haem-dependent gene regulation already suggests that the two systems might interact with each other. Here, we provided evidence for a cross-regulation of HrrSA and ChrSA at the level of transcription. In our previous studies, we observed a weak binding of HrrA to the intergenic region of *hrtBA*–*chrSA* (Frunzke *et al.*, 2011). This result is further

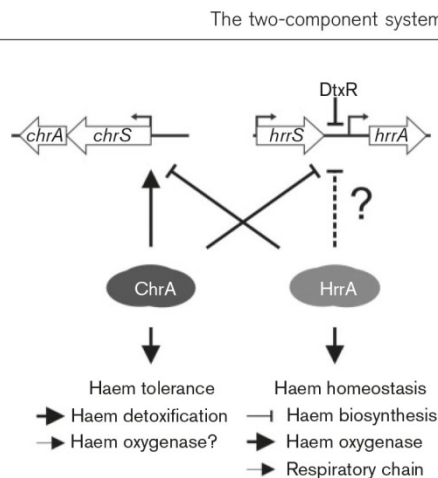


**Fig. 6.** The current model of ChrSA and HrrSA cross-regulation in *C. glutamicum*. Based on current insights, ChrSA is the prominent system required for dealing with haem toxicity and activates *hrtBA* expression in the presence of haem. Under iron limitation, *chrSA* is repressed by HrrA to avoid haem export when haem is required as an alternative iron source. As a balancing counterpart, *hrrA* itself, but not *hrrS*, is repressed by ChrA. Altogether, the current results emphasize a high level of regulatory network linkage to balance haem detoxification and the use of haem as a protein cofactor and alternative iron source.

supported by the finding that expression from  $P_{chrSA}$  is increased in a  $\Delta$ *hrrSA* mutant indicating repression of *chrSA* by the homologous system (Fig. 5). This effect is especially obvious under iron limitation where HrrSA seems to be the dominating system ensuring additional iron supply from haem by the activation of haem oxygenase (Fig. 5). Additionally, our data suggest haem-dependent repression of *hrrA* by ChrA. Our current model shown in Fig. 6 emphasizes that this cross-regulation acts as a balancing act to avoid toxic levels on the one hand and ensure iron acquisition on the other hand. Remarkably, this cross-regulation only affects the expression of *hrrA* and not *hrrS*, which seems to be expressed at a constitutively low level; no significant difference in the level of *hrrS* mRNA was observed in transcriptome comparisons of  $\Delta$ *chrSA* and wild-type. A further level of interaction was suggested in previous studies of the *C. diphtheriae* systems, which provided evidence for *in vivo* cross-talk by phosphoryl transfer of HrrSA and ChrSA (Bibb *et al.*, 2005, 2007). Altogether, these data provide striking evidence for a close link between the HrrSA and ChrSA systems and further studies are required to understand the interplay between these TCSs and the physiological relevance thereof.

## ACKNOWLEDGEMENTS

We thank Melanie Brocker and Christina Mack for providing us with the  $\Delta$ *hrrSA* strain and for vital discussions, Arun Nanda for critical reading of this manuscript and Tino Polen for support of DNA microarray analysis. The RNA sequencing work received valuable help

A. Heyer and others

from Katharina Pfeifer and Christian Rückert (CeBiTec, Bielefeld University). This work was supported by the Helmholtz Association (grant VH-NG-716 to J.F.) and by a grant from the Ministry of Innovation, Science, Research and Technology of the German Federal State Northrhine-Westfalia (grant 280371902 to J.K.).

## REFERENCES

- Allen, C. E. & Schmitt, M. P. (2009). HtaA is an iron-regulated heme binding protein involved in the utilization of heme iron in *Corynebacterium diphtheriae*. *J Bacteriol* **191**, 2638–2648.
- Allen, C. E. & Schmitt, M. P. (2011). Novel heme binding domains in the *Corynebacterium diphtheriae* HtaA protein interact with hemoglobin and are critical for heme iron utilization by HtaA. *J Bacteriol* **193**, 5374–5385.
- Andrews, S. C., Robinson, A. K. & Rodríguez-Quiriones, F. (2003). Bacterial iron homeostasis. *FEMS Microbiol Rev* **27**, 215–237.
- Bibb, L. A. & Schmitt, M. P. (2010). The ABC transporter HrtAB confers resistance to heme toxicity and is regulated in a hemin-dependent manner by the ChrAS two-component system in *Corynebacterium diphtheriae*. *J Bacteriol* **192**, 4606–4617.
- Bibb, L. A., King, N. D., Kunkle, C. A. & Schmitt, M. P. (2005). Analysis of a heme-dependent signal transduction system in *Corynebacterium diphtheriae*: deletion of the *chrAS* genes results in heme sensitivity and diminished heme-dependent activation of the *hmuO* promoter. *Infect Immun* **73**, 7406–7412.
- Bibb, L. A., Kunkle, C. A. & Schmitt, M. P. (2007). The ChrA-ChrS and HrrA-HrrS signal transduction systems are required for activation of the *hmuO* promoter and repression of the *hemA* promoter in *Corynebacterium diphtheriae*. *Infect Immun* **75**, 2421–2431.
- Blom, J., Jakobi, T., Doppmeier, D., Jaenicke, S., Kalinowski, J., Stoye, J. & Goesmann, A. (2011). Exact and complete short-read alignment to microbial genomes using Graphics Processing Unit programming. *Bioinformatics* **27**, 1351–1358.
- Bott, M. & Brocker, M. (2012). Two-component signal transduction in *Corynebacterium glutamicum* and other corynebacteria: on the way towards stimuli and targets. *Appl Microbiol Biotechnol* **94**, 1131–1150.
- Boyd, J., Oza, M. N. & Murphy, J. R. (1990). Molecular cloning and DNA sequence analysis of a diphtheria toxin iron-dependent regulatory element (*dtxR*) from *Corynebacterium diphtheriae*. *Proc Natl Acad Sci U S A* **87**, 5968–5972.
- Bradford, M. M. (1976). A rapid and sensitive method for the quantitation of microgram quantities of protein utilizing the principle of protein-dye binding. *Anal Biochem* **72**, 248–254.
- Brocker, M., Mack, C. & Bott, M. (2011). Target genes, consensus binding site, and role of phosphorylation for the response regulator MtrA of *Corynebacterium glutamicum*. *J Bacteriol* **193**, 1237–1249.
- Burgos, J. M. & Schmitt, M. P. (2012). The ChrA response regulator in *Corynebacterium diphtheriae* controls hemin-regulated gene expression through binding to the *hmuO* and *hrtAB* promoter regions. *J Bacteriol* **194**, 1717–1729.
- Burkovski, A. (2008). *Corynebacteria: Genomics and Molecular Biology*. Norfolk, UK: Caister Academic Press.
- Cerdeño-Tarraga, A. M., Efstratiou, A., Dover, L. G., Holden, M. T., Pallen, M., Bentley, S. D., Besra, G. S., Churcher, C., James, K. D. & other authors (2003). The complete genome sequence and analysis of *Corynebacterium diphtheriae* NCTC13129. *Nucleic Acids Res* **31**, 6516–6523.
- Drazek, E. S., Hammack, C. A. & Schmitt, M. P. (2000). *Corynebacterium diphtheriae* genes required for acquisition of iron from haemin and haemoglobin are homologous to ABC haemin transporters. *Mol Microbiol* **36**, 68–84.
- Eggeling, L. & Bott, M. (editors) (2005). *Handbook of Corynebacterium glutamicum*. Boca Raton, FL: Academic Press.
- Ehira, S., Ogino, H., Teramoto, H., Inui, M. & Yukawa, H. (2009). Regulation of quinone oxidoreductase by the redox-sensing transcriptional regulator QorR in *Corynebacterium glutamicum*. *J Biol Chem* **284**, 16736–16742.
- Eikmanns, B. J., Thum-Schmitz, N., Eggeling, L., Lütke, K. U. & Sahm, H. (1994). Nucleotide sequence, expression and transcriptional analysis of the *Corynebacterium glutamicum* *glTA* gene encoding citrate synthase. *Microbiology* **140**, 1817–1828.
- Frunzke, J. & Bott, M. (2008). Regulation of iron homeostasis in *Corynebacterium glutamicum*. In *Corynebacteria: Genomics and Molecular Biology*, pp. 241–266. Edited by A. Burkovski. Norwich, UK: Horizon Scientific Press.
- Frunzke, J., Engels, V., Hasenbein, S., Gätgens, C. & Bott, M. (2008). Co-ordinated regulation of gluconate catabolism and glucose uptake in *Corynebacterium glutamicum* by two functionally equivalent transcriptional regulators, GntR1 and GntR2. *Mol Microbiol* **67**, 305–322.
- Frunzke, J., Gätgens, C., Brocker, M. & Bott, M. (2011). Control of heme homeostasis in *Corynebacterium glutamicum* by the two-component system HrrSA. *J Bacteriol* **193**, 1212–1221.
- Gao, R., Mack, T. R. & Stock, A. M. (2007). Bacterial response regulators: versatile regulatory strategies from common domains. *Trends Biochem Sci* **32**, 225–234.
- Hantke, K. (2001). Iron and metal regulation in bacteria. *Curr Opin Microbiol* **4**, 172–177.
- Ito, Y., Nakagawa, S., Komagata, A., Ikeda-Saito, M., Shiro, Y. & Nakamura, H. (2009). Heme-dependent autophosphorylation of a heme sensor kinase, ChrS, from *Corynebacterium diphtheriae* reconstituted in proteoliposomes. *FEBS Lett* **583**, 2244–2248.
- Kalinowski, J., Bathe, B., Bartels, D., Bischoff, N., Bott, M., Burkovski, A., Dusch, N., Eggeling, L., Eikmanns, B. J. & other authors (2003). The complete *Corynebacterium glutamicum* ATCC 13032 genome sequence and its impact on the production of L-aspartate-derived amino acids and vitamins. *J Biotechnol* **104**, 5–25.
- Keilhauer, C., Eggeling, L. & Sahm, H. (1993). Isoleucine synthesis in *Corynebacterium glutamicum*: molecular analysis of the *ilvB-ilvN-ilvC* operon. *J Bacteriol* **175**, 5595–5603.
- Kensy, F., Zang, E., Faulhammer, C., Tan, R. K. & Büchs, J. (2009). Validation of a high-throughput fermentation system based on online monitoring of biomass and fluorescence in continuously shaken microtiter plates. *Microb Cell Fact* **8**, 31.
- Kocan, M., Schaffer, S., Ishige, T., Sorger-Herrmann, U., Wendisch, V. F. & Bott, M. (2006). Two-component systems of *Corynebacterium glutamicum*: deletion analysis and involvement of the PhoS-PhoR system in the phosphate starvation response. *J Bacteriol* **188**, 724–732.
- Krell, T., Lacal, J., Busch, A., Silva-Jiménez, H., Guazzaroni, M. E. & Ramos, J. L. (2010). Bacterial sensor kinases: diversity in the recognition of environmental signals. *Annu Rev Microbiol* **64**, 539–559.
- Kunkle, C. A. & Schmitt, M. P. (2007). Comparative analysis of *hmuO* function and expression in *Corynebacterium* species. *J Bacteriol* **189**, 3650–3654.
- Laub, M. T. & Goulian, M. (2007). Specificity in two-component signal transduction pathways. *Annu Rev Genet* **41**, 121–145.
- Lechardeur, D., Cesselin, B., Liebl, U., Vos, M. H., Fernandez, A., Brun, C., Gruss, A. & Gaudu, P. (2012). Discovery of intracellular heme-binding protein HrtR, which controls heme efflux by the

- conserved HrtB-HrtA transporter in *Lactococcus lactis*. *J Biol Chem* **287**, 4752–4758.
- Madan Babu, M. & Teichmann, S. A. (2003)**. Functional determinants of transcription factors in *Escherichia coli*: protein families and binding sites. *Trends Genet* **19**, 75–79.
- Mascher, T., Helmmann, J. D. & Unden, G. (2006)**. Stimulus perception in bacterial signal-transducing histidine kinases. *Microbiol Mol Biol Rev* **70**, 910–938.
- Möker, N., Bocker, M., Schaffer, S., Krämer, R., Morbach, S. & Bott, M. (2004)**. Deletion of the genes encoding the MtrA-MtrB two-component system of *Corynebacterium glutamicum* has a strong influence on cell morphology, antibiotics susceptibility and expression of genes involved in osmoprotection. *Mol Microbiol* **54**, 420–438.
- Nobles, C. L. & Maresso, A. W. (2011)**. The theft of host heme by Gram-positive pathogenic bacteria. *Metalomics* **3**, 788–796.
- Pátek, M. & Nešvera, J. (2011)**. Sigma factors and promoters in *Corynebacterium glutamicum*. *J Biotechnol* **154**, 101–113.
- Polen, T. & Wendisch, V. F. (2004)**. Genomewide expression analysis in amino acid-producing bacteria using DNA microarrays. *Appl Biochem Biotechnol* **118**, 215–232.
- Sambrook, J., MacCallum, P. & Russell, D. (2001)**. *Molecular Cloning: a Laboratory Manual*, 3rd edn. Cold Spring Harbor, NY: Cold Spring Harbor Laboratory.
- Schaaf, S. & Bott, M. (2007)**. Target genes and DNA-binding sites of the response regulator PhoR from *Corynebacterium glutamicum*. *J Bacteriol* **189**, 5002–5011.
- Schelder, S., Zaade, D., Litsanov, B., Bott, M. & Bocker, M. (2011)**. The two-component signal transduction system CopRS of *Corynebacterium glutamicum* is required for adaptation to copper-excess stress. *PLoS ONE* **6**, e22143.
- Schmitt, M. P. (1997)**. Transcription of the *Corynebacterium diphtheriae hmuO* gene is regulated by iron and heme. *Infect Immun* **65**, 4634–4641.
- Skaar, E. P. (2010)**. The battle for iron between bacterial pathogens and their vertebrate hosts. *PLoS Pathog* **6**, e1000949.
- Stauff, D. L. & Skaar, E. P. (2009a)**. The heme sensor system of *Staphylococcus aureus*. *Contrib Microbiol* **16**, 120–135.
- Stauff, D. L. & Skaar, E. P. (2009b)**. *Bacillus anthracis* HssRS signalling to HrtAB regulates haem resistance during infection. *Mol Microbiol* **72**, 763–778.
- Stauff, D. L., Bagaley, D., Torres, V. J., Joyce, R., Anderson, K. L., Kuechenmeister, L., Dunman, P. M. & Skaar, E. P. (2008)**. *Staphylococcus aureus* HrtA is an ATPase required for protection against heme toxicity and prevention of a transcriptional heme stress response. *J Bacteriol* **190**, 3588–3596.
- Stock, A. M., Robinson, V. L. & Goudreau, P. N. (2000)**. Two-component signal transduction. *Annu Rev Biochem* **69**, 183–215.
- Studier, F. W. & Moffatt, B. A. (1986)**. Use of bacteriophage T7 RNA polymerase to direct selective high-level expression of cloned genes. *J Mol Biol* **189**, 113–130.
- Trost, E., Ott, L., Schneider, J., Schröder, J., Jaenicke, S., Goesmann, A., Husemann, P., Stoye, J., Dorella, F. A. & other authors (2010)**. The complete genome sequence of *Corynebacterium pseudotuberculosis* FRC41 isolated from a 12-year-old girl with necrotizing lymphadenitis reveals insights into gene-regulatory networks contributing to virulence. *BMC Genomics* **11**, 728.
- Wennerhold, J. & Bott, M. (2006)**. The DtxR regulon of *Corynebacterium glutamicum*. *J Bacteriol* **188**, 2907–2918.
- Wennerhold, J., Krug, A. & Bott, M. (2005)**. The AraC-type regulator RipA represses aconitase and other iron proteins from *Corynebacterium* under iron limitation and is itself repressed by DtxR. *J Biol Chem* **280**, 40500–40508.
- West, A. H. & Stock, A. M. (2001)**. Histidine kinases and response regulator proteins in two-component signaling systems. *Trends Biochem Sci* **26**, 369–376.
- Wilks, A. & Schmitt, M. P. (1998)**. Expression and characterization of a heme oxygenase (HmuO) from *Corynebacterium diphtheriae*. Iron acquisition requires oxidative cleavage of the heme macrocycle. *J Biol Chem* **273**, 837–841.
- Yukawa, H., Omumasaba, C. A., Nonaka, H., Kós, P., Okai, N., Suzuki, N., Suda, M., Tsuge, Y., Watanabe, J. & other authors (2007)**. Comparative analysis of the *Corynebacterium glutamicum* group and complete genome sequence of strain R. *Microbiology* **153**, 1042–1058.

Edited by: J. Cavet

Name of the journal:	Microbiology
Impact factor:	3.061
Contribution of own work:	75%
1. Author:	Experimental work and writing of the manuscript

## 4 Discussion

### 4.1 Prophage induction of CGP3

Bacteriophages discovered to date are highly diverse and very abundant in nature (Hatfull & Hendrix, 2011). Genomes are often interspersed with phage DNA, prophages or phage remnants, accounting for up to 20% of the bacterial genome (Casjens, 2003). After the discovery of bacteriophages in the 1920s, it took many decades until the regulatory networks of a few selected model phages have been unraveled (Casjens, 2003; Lwoff, 1953). Nowadays, the regulatory circuit controlling the bistable switch between lysogeny and lysis of the model phage lambda has become a paradigm for gene regulation.

We focused on the prophage CGP3 in the genome of *C. glutamicum*, which was assumed to be inactive, as successful prophage induction or plaque formation had not been reported for the *strain* ATCC 13032 (Kalinowski, 2005). However, studies by Frunzke *et al.* revealed a spontaneous induction of CGP3 even under non-stressful conditions, and showed increased expression of phage genes in a mutant lacking the master regulator DtxR ( $\Delta dtxR$ ) of iron homeostasis (Frunzke *et al.*, 2008). Nevertheless, the mechanism of prophage induction of CGP3 has not yet been characterized in detail.

In this work, the regulatory processes leading to CGP3 prophage induction were further explored. The regulator Cg2040 was identified as a phage-encoded transcriptional regulator, but is, however, not the central phage repressor of CGP3. The activation of CGP3 was shown to be at least partially dependent on the SOS response. In further studies, a novel phage-encoded actin-like protein was identified and characterized *in vitro* and *in vivo*. Furthermore, based on the increased activity of the prophage CGP3 in  $\Delta dtxR$ , the connection between DtxR and the two-component systems (TCS) HrrSA and ChrSA, involved in heme homeostasis, came into focus (Wennerhold & Bott, 2006; Frunzke *et al.*, 2008). The response regulator HrrA, which is a target of DtxR, was found to regulate the expression of *chrSA*, encoding a second TCS. Thus, the role of ChrSA in heme homeostasis and resistance was also characterized during this thesis.

#### 4.1.1 Activation of CGP3 upon induction of the SOS response

For phage  $\lambda$  and other lambdoid-like phages, prophage induction is generally linked to the SOS response of the host. In these temperate phages, genes of the lytic pathway are repressed by a phage repressor during lysogeny. Nevertheless, it is beneficial for phages to enter the lytic pathway upon stressful conditions, *e.g.* DNA damage, to secure their propagation over time (Hatfull & Hendrix, 2011; Casjens, 2003).

This work demonstrated a strong dependence of CGP3 prophage induction on the activation of the SOS response in *C. glutamicum*. The SOS response was induced by the addition of mitomycin C (MmC), an antibiotic agent that leads to the formation of single-stranded DNA strands by crosslinking the DNA (Tomasz, 1995). Time-resolved transcriptome analysis of *C. glutamicum* cells treated with MmC revealed not only the activation of LexA target genes (Jochmann *et al.*, 2009), but also strongly increased expression of CGP3 genes. The time-resolved data provide basal information about the involvement of specific genes in the early or the late response of prophage induction, and represent an important basis for preliminary classification of phage genes into functional groups. In analogy, the life cycle of phage  $\lambda$  is organized in modules, such as early or delayed early genes for the establishment of lysogeny or phage replication, and late genes for virion assembly and cell lysis (Oppenheim *et al.*, 2005). However, only a few CGP3 genes exhibit similarities to known phage genes, which impede the identification of key components for CGP3 induction (Kalinowski, 2005; Frunzke *et al.*, 2008).

The SOS response is involved in several processes, such as DNA recombination and repair and the inhibition of cell division (Little & Mount, 1982). In *C. glutamicum*, the SOS response and the LexA regulon are similar to the SOS response in *E. coli* to some extent (Jochmann *et al.*, 2009). However, 17 out of 48 genes of the LexA regulon encode proteins of unknown function. The CGP3 prophage genes cg1977, cg2026, and cg2034 were found to be directly repressed by LexA (Fig. 4.1) (Jochmann *et al.*, 2009). Since these phage genes also encode hypothetical proteins, a detailed amino acid sequence analysis and a domain search by SMART analysis were performed (Blast (NCBI) <http://blast.ncbi.nlm.nih.gov/Blast.cgi>, SMART (EMBL Heidelberg) <http://smart.embl-heidelberg.de/>, (Letunic *et al.*, 2012; Bouchard *et al.*, 2002)). Whereas Cg2026 revealed affiliations to a group of uncharacterized proteins conserved in bacteria (Pfam09954), Cg1977 showed a low sequence identity to Na<sup>+</sup>/H<sup>+</sup> antiporters in *Vibrio* species (30%- 36%). Cg2034 inherits few similarities to a putative anti-sigma factor in *Sphingobacterium spiritivorum* (37%) and an abort lactococcal phage infection protein AbiTii from *Lactococcus lactis* (38%), which is involved in resistance to phage infections (Bouchard *et al.*, 2002). The restriction-modification system is encoded by genes cg1996-cg1998 in the CGP3 prophage region and is part of the LexA regulon (Schäfer *et al.*, 1997). Nonetheless, the function of these genes in the *C. glutamicum* SOS response remains unclear.

In *C. glutamicum*, the sigma factor  $\sigma^H$  influences the SOS response and plays a central role in regulating heat-stress related genes and genes involved in disulfide stress response (Ehira *et al.*, 2009; Busche *et al.*, 2012). It was shown that  $\sigma^H$  directly controls the SOS target genes *uvrA* (cg1560) and *uvrC* (cg1795), encoding an excinuclease important for nucleotide-excision repair, as well as *uvrD3* (cg1555), coding for a helicase, and a cluster of DNA repair related genes (cg0184-cg0186). Interestingly, LexA controls *uvrA* and  $\sigma^H$ , which additionally links  $\sigma^H$  to the SOS response and presents

$\sigma^H$  as a central regulator of this regulatory network in *C. glutamicum* (Busche *et al.*, 2012). In *Staphylococcus aureus*, the alternative sigma factor  $\sigma^H$  was found to influence the rate of spontaneous prophage induction by modulating the integration of prophages (Tao *et al.*, 2010). The sigma factor  $\sigma^H$  binds to the promoter of *int* encoding the integrase in *S. aureus*, and a deletion of  $\sigma^H$  reduced the expression of *int* and the rate of prophage excision. Additionally,  $\sigma^H$  altered the rate of spontaneous lysis and was proposed to have a stabilizing effect on lysogeny. This suggested a novel regulatory mechanism of prophage integration controlled by a host-encoded sigma factor (Tao *et al.*, 2010). However, no CGP3 prophage genes were detected as direct targets of  $\sigma^H$  in *C. glutamicum* (Busche *et al.*, 2012). A starting point for further studies would be the phenotype of deletion mutants lacking the LexA-regulated phage genes under stressful conditions, which would provide first insights regarding their impact on the SOS response and on CGP3 prophage induction.

#### 4.1.2 The Cro/CI-type regulator Cg2040

In this work, we started to uncover regulatory circuits of the prophage CGP3. A key element for maintenance of prophage lysogeny is the presence of a central phage repressor (Campbell, 1994). For phage  $\lambda$ , the phage regulator CI is a central factor for the retention of the lysogenic state during the phage life cycle (Kaiser, 1957). Moreover, further regulators participate in the complex regulatory network for the bistable balance between the lysogenic and lytic state (Dodd *et al.*, 2005; Oppenheim *et al.*, 2005). During this work, the CGP3-encoded regulator Cg2040 of the HTH\_3 family (including CI and Cro regulators, also named Cro/CI family, Pfam PF01381) was identified (Pabo & Lewis, 1982; Ohlendorf *et al.*, 1983). Cg2040 was shown to repress its own expression (autorepression) and the expression of the adjacent genes (Fig. 4.1). However, a significantly altered CGP3 gene expression, as it was observed upon treatment with MmC, did not result from *cg2040* deletion or overexpression. In addition, Cg2040 has almost no impact on CGP3 replication after phage induction. Consequently, Cg2040 does not occupy the role as central phage regulator of CGP3 in analogy to CI in phage  $\lambda$ .

Notably, the amino acid residues alanine and glycine, which are important for LexA and CI autoproteolytic cleavage, were not only conserved in LexA of *C. glutamicum*, but also in Cg2040 at position alanine-33 and glycine-34 (new annotation of *cg2040* defined in this work). Furthermore, a sequence comparison (Clustal Omega (Sievers *et al.*, 2011)) of LexA,  $\lambda$  repressor CI, and Cg2040 revealed conservation of the residues serine-119 and lysine-156, which are also relevant for autocleavage in LexA<sub>C.g.</sub> and CI. Due to the smaller size of Cg2040 (119 aa, new annotation) compared to CI or LexA (253 aa in *C. glutamicum*), direct conservation of these residues were not observed in Cg2040, although Cg2040 contains a lysine residue at the C-terminal end (position 115) as well as

several serine residues. To examine whether Cg2040 still undergoes an autodigestion, which might be mediated by RecA, is an interesting point for further studies.

In *C. glutamicum*, only three out of 11 HTH\_3 type regulators were characterized in detail, namely RamB, ClgR, and PrpR (Engels *et al.*, 2004; Gerstmeir *et al.*, 2004; Plassmeier *et al.*, 2012). RamB is a master regulator in the coordinated control of carbon metabolism and controls expression of more than 50 genes particularly involved in acetate metabolism (Gerstmeir *et al.*, 2004; Schröder & Tauch, 2010). Whereas PrpR acts as a specific activator of propionate catabolism (Plassmeier *et al.*, 2012), ClgR was shown to modulate the expression of genes encoding proteins that are involved in DNA repair and proteolysis (Engels *et al.*, 2004; Engels *et al.*, 2005). Furthermore, two HTH\_3 type regulators, namely cg1292 and cg3230, showed similarity to toxin/antitoxin systems. These systems were found to be involved in phage resistance, but have so far not been described to play a role in prophage induction (Makarova *et al.*, 2009; Sberro *et al.*, 2013).

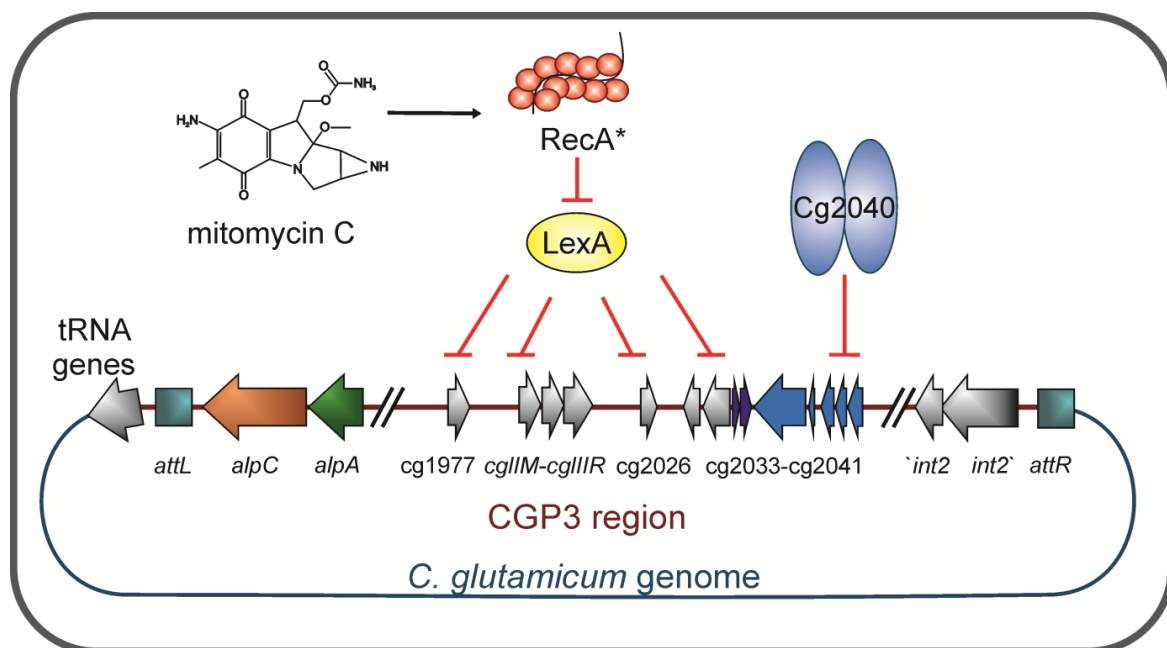


**Fig. 4.1 Factors influencing CGP3 activity in *C. glutamicum*.** Upon induction of the SOS response by treatment with mitomycin C, RecA is activated and catalyzes the autoproteolytic cleavage of LexA. The cleavage of LexA leads to derepression of CGP3 target genes, such as cg1977, cg2026, and cg2034, encoding hypothetical genes, and the operon cg1996-cg1998, coding for the restriction-modification system *cglIM-cglIR-cglIIR*. The LexA box is located upstream of cg1996 (grey arrows as indicated). The transcriptional phage-encoded regulator Cg2040 was found to be autoregulated and controls the transcription of the downstream genes cg2033, cg2035, and cg2037-cg2040. The gene c2035 encodes a putative methyltransferase; the other genes are annotated as hypothetical or putative secreted proteins (blue arrows). Although Cg2040 belongs to the Cro/Ci family, Cg2040 does not possess the role of a central phage regulator like Ci in the regulatory network of phage  $\lambda$ . The illustrated components are not drawn to scale.

Generally, a mechanism of prophage induction differing from phage  $\lambda$  can be assumed as well. For example, the prophage CTX $\phi$ , which is important for virulence by cholera toxin production, revealed differences to the regulatory network of the phage  $\lambda$  family (Nickels, 2009; Waldor & Friedman, 2005). The CTX $\phi$  prophage holds the phage regulator RstR, which represses genes required for replication and virion production in cooperation with LexA (Kimsey & Waldor, 2009; Quinones *et al.*, 2005). Upon induction of the SOS response, RstR blocks its own transcription by binding to a further operator site that was occupied by LexA before. The decline in RstR level allows the transcription and production of virions (Nickels, 2009). As discussed above, four targets for LexA binding were identified in the CGP3 gene region in *C. glutamicum*. However, the relevance of these genes and LexA as an additional regulator in prophage induction will be object of future studies. In addition, attempts to identify the regulatory components are required to explore the regulatory mechanism of CGP3 prophage induction in more detail. Further regulators could be identified by DNA affinity chromatography studies with promoter regions of early phage genes. For example, the first operon at the left attachment site, encoding cg1890 and cg1891, was identified to be involved in the early response of the phage. In this work, these two genes were proposed to encode an actin-like protein as well as an adaptor protein for transport of CGP3 DNA. Hence, the identification of regulators that bind within the promoter region of the putative operon will provide details about the early regulatory processes of CGP3, and will be part of prospective experiments.

## 4.2 The prophage-encoded actin-like protein AlpC

A phylogenetic approach by Derman *et al.* (Derman *et al.*, 2009) identified more than 35 new families of bacterial actin-like proteins. Among them Cg1890 of *C. glutamicum* was identified as a putative actin-like protein, without mentioning that the gene is localized in the CGP3 prophage region (Derman *et al.*, 2009). In this work, Cg1890 was characterized and renamed to AlpC (designated AlpC for actin-like protein Corynebacterium). Thus, *C. glutamicum* AlpC represents the first phage-encoded actin-like protein that was characterized in detail *in vitro* and *in vivo*. Based on our data, a model was proposed in which AlpC mediates the transport of phage DNA towards the cell membrane for an efficient replication upon induction of the CGP3 prophage.

### 4.2.1 Filament formation of the actin-like protein AlpC

More than 35 families of actin-like proteins were disclosed by a phylogenetic approach (Derman *et al.*, 2009). The majority of the genes were discovered on mobile elements, such as plasmids, integrating conjugative elements or phage genomes. Among the highly divergent families of actin-like proteins, Cg1890 was classified into family Alp29. In fact, cg1890 encodes the first gene of CGP3 close to the left attachment site. Thus, we were interested in characterizing the relevance of actin-like protein Cg1890 for the activity of phage CGP3.

An initial phylogenetic comparison revealed low sequence conservation of AlpC to other bacterial actins, such as the cytoskeleton protein MreB. Nevertheless, the phosphate region for nucleotide hydrolyzation of actin-like proteins was highly conserved. Low sequence conservation but high functional homology is a common phenomenon for actin-like proteins or tubulin-like proteins encoded on mobile elements in bacteria (Derman *et al.*, 2009). In contrast, chromosomally-encoded actins and tubulins, such as MreB and FtsZ, respectively, usually display high sequence conservation as the proteins are essential for almost all bacteria (Derman *et al.*, 2009; Derman *et al.*, 2012). In *C. glutamicum*, the tubulin-like cell division protein FtsZ mediates the formation of the Z-ring, but can be inhibited by DivS in response to DNA damage (Ogino *et al.*, 2008; Ramos *et al.*, 2005). However, *C. glutamicum* lacks the actin-like protein MreB. Instead, DivIVA inherits a central role for polar cell growth and cell division site selection (Donovan *et al.*, 2013; Letek *et al.*, 2008b; Letek *et al.*, 2012).

The ability of AlpC to hydrolyze ATP or GTP and the nucleotide-dependent polymerization to filaments are typical features of actin-like proteins. Remarkably, the morphology of AlpC filaments was concentration-dependent *in vivo*. While the filaments were long and curved when *alpC* was overexpressed from  $P_{tac}$  promoter, AlpC filaments in native concentrations (under control of the native promoter) appeared short and straight in varying angles to the cell membrane. In *E. coli*, AlpC filaments were not observed, indicating the involvement of further phage- or bacterial-encoded components for polymerization. In the study of Derman *et al.*, the actin-like protein Alp7A from plasmid pLS20 in *B. subtilis* was shown to form filaments in *E. coli* and the function of Alp7A in plasmid partitioning was characterized (Derman *et al.*, 2009). Furthermore, the phage-encoded actin-like protein Alp6A, identified by phylogenetic studies in phage 0305 $\phi$ 8-36 of *B. thuringiensis*, forms filaments in *E. coli*, in contrast to AlpC (Derman *et al.*, 2009; Haeusser & Margolin, 2012). Although Alp6A exhibits a conserved phosphate region characteristic for actins, the detailed cellular function of Alp6A is still unknown (Derman *et al.*, 2009).

#### 4.2.2 The putative adaptor protein AlpA

Actin-like plasmid partitioning systems like ParMRC usually comprise an additional component to facilitate the attachment of the plasmid DNA to actin-filaments for segregation (Gerdes *et al.*, 2000). Adaptor proteins are often located in an operon with the gene encoding the actin-like protein and recognize a binding site located in the vicinity of the respective operon (Gerdes *et al.*, 2010). Therefore, the gene *cg1891*, encoded in a putative operon with *alpC*, was characterized and renamed to *alpA*. AlpA contains a relatively high amount of charged amino acids residues (26%) (Appendix Fig. 6.1.1), which is comparable to the adaptor protein ParR containing 28% charged residues (Derman *et al.*, 2009). In this work, a DNA-binding region of AlpA was localized upstream of the *alpAC*

operon (designated to *alpS* for AlpA binding site), suggesting that AlpA represents a tempting candidate as adaptor protein to mediate the connection of AlpC filaments and phage DNA.

In an additional sequence comparison, AlpA shows weak identity (38%) to surface adhesion proteins and to the gene KTR9\_4799 from *Gordinia sp.* KTR9 (36%), as indicated in Appendix Fig. 6.1.2. The adjacent gene KTR9\_4800 shares the highest sequence identity (54%) to AlpC. These two genes, KTR9\_4799 and KTR9\_4800, are located on the large plasmid pGKT2 (182 kbp) in *Gordinia sp.* KTR9 (Indest *et al.*, 2010). Interestingly, the adjacent gene KTR9\_4798 shares similarities to the Orf8 containing *oriV* for plasmid maintenance of the large plasmid pKB-1 (101 kbp) in *Gordinia westfalica* (Indest *et al.*, 2010; Bröker *et al.*, 2003). Although these genes from *Gordinia sp.* KTR9 were not characterized for their role in plasmid maintenance, they represent a homolog system to the AlpAC system.

### Binding sites of AlpA

The binding studies with AlpA suggested an oligomerization of AlpA along the binding region, which is a common feature of plasmid-partitioning adaptors. For example, the DNA-binding protein ParR of the ParMRC system binds as a dimer at ten repeats in the *parC* binding site (Breüner *et al.*, 1996; Dam & Gerdes, 1994). Remarkably, a motif search (MEME suite, <http://meme.nbcr.net/meme/>) revealed five highly similar, putative binding motifs in the binding region of AlpA (*alpS*). In further experiments, included in the appendix of this work, the binding region of AlpA was narrowed down to two binding sites in the upstream region of *alpAC* by testing subfragments in EMSA studies (Appendix Fig. 6.1.3). However, binding studies with 30 bp oligonucleotides containing the predicted putative motifs revealed only one shifted motif. Thus, AlpA might possess a different binding motif or requires adjacent regions for cooperative polymerization along the binding sites.

### Genomic organization of *alpAC*

The genomic organization of the phage-encoded *alpAC* system in *C. glutamicum* differs in comparison to other systems, as *alpA* is located upstream of *alpC*. This genetic organization was often found in partitioning systems with a relatively small actin-like protein (Gerdes *et al.*, 2010). In contrast, the gene for the DNA-binding protein, *alp7R*, is located downstream of *alp7A*, coding for the actin-like protein of plasmid pLS20 in *B. subtilis* (Derman *et al.*, 2012). A similar assembly was found for the ParMRC system of plasmid R1 in *E. coli* (Salje *et al.*, 2010). In all loci, the DNA-binding site was located upstream among the promoter region of the presumed operons. Moreover, the DNA-binding protein was often described to act as a transcriptional regulator of the particular plasmid partitioning system. For example, the DNA-binding protein Alp7R negatively regulates the transcription of the gene *alp7A* (Derman *et al.*, 2012). Whether AlpA additionally acts as

transcriptional regulator for the putative operon *alpAC*, could be elucidated by transcriptome analysis in further studies.

### **Evidence for interaction of AlpC and AlpA**

N-terminal protein fusions of AlpA with the fluorescent protein YFP and chromosomally integrated AlpC, fused to the cyan-fluorescent protein CFP, were used for co-localization studies of AlpC and AlpA. In almost 80% of the cells, which displayed both AlpA foci and AlpC filaments, an AlpA focus was found adjacent to an AlpC filament. These findings suggested an interaction of both proteins *in vivo*. The verification of a direct interaction of AlpA and AlpC proved to be difficult. Using a LexA-based two hybrid system in *E. coli* (Dmitrova *et al.*, 1998), interaction of AlpA and AlpC could not be detected (data not shown). Further experiments with surface plasmon resonance techniques revealed only weak interactions (data not shown). Finally, the impact of AlpC on the binding-affinity of AlpA to the upstream region of the operon *alpAC* was tested by EMSA studies (Appendix Fig. 6.1.4). No difference was observed by incubation of target DNA with AlpA in the presence of AlpC. However, when AlpC filament formation was induced by addition of ATP, differences in the shift were observed. Thus, providing a first evidence for an interaction of AlpC filaments and AlpA in the presence of DNA. However, AlpC polymerization seems to be necessary for interaction of the three components. To further demonstrate interaction between these components, a co-purification of AlpC and AlpA from crude-extract of stressed cells might represent a promising approach.

### **4.2.3 Influence of AlpA and AlpC on CGP3 life cycle**

Since plasmid-encoded actin-like proteins and their adaptor proteins are crucial elements for plasmid maintenance, a role for AlpC and AlpA in phage maintenance was presumed. Fluorescent labeling of the actin-like protein AlpC and CGP3 DNA showed that the phage DNA is located close to the AlpC filaments under stressful conditions. Furthermore, the CGP3 DNA was frequently localized close to the cell membrane. Hence, we supposed in our current model that the AlpA-bound phage DNA is transported along AlpC filaments to the membrane upon prophage induction.

In this work, quantitative PCR demonstrated a ten-fold increase of circular CGP3 DNA upon induction of the SOS response. Furthermore, deletions of *alpC* or *alpA* reduced the amount of circular phage DNA after prophage induction in comparison to the wild type. These findings indicate an influence of AlpC and AlpA on prophage replication upon induction. Strikingly, the prophage induction and maintenance was not completely abolished and still led to a five-fold increase of circular phage DNA in the deletion mutants. The residual increase indicated an impact on the efficiency of phage DNA propagation by AlpC or AlpA rather than an essential role in phage

replication or segregation. Although the expression of the *alpAC* system is relatively low under conventional cultivation conditions, *alpA* and *alpC* belong to the early and strongly induced genes of CGP3 upon induction of the prophage by the SOS response. However, expression of *divS*, encoding an inhibitor of cell division, is also part of the SOS response and arrests the cell cycle upon stressful conditions (Jochmann *et al.*, 2009; Ogino *et al.*, 2008). Accordingly, a segregation of phage DNA molecules into separating cells would not be required under these conditions. This makes an involvement of AlpAC on phage replication more likely than a role in the segregation of phage DNA.

In eukaryotic cells, viruses frequently exploit the host cell cytoskeleton for their own transfer within the cell. For viruses, it is helpful to use a transport system to ensure an efficient transfer rather than undirected free diffusion to the place of replication, which is often the nucleus in eukaryotic cells (Greber & Way, 2006). This can accelerate the propagation of virus infections by a directional transfer to the nucleus (retrograde) or back to the cell periphery as new assembled virus progeny to exit the cell (anterograde) (Greber & Way, 2006). The transport of a virus along microtubules is a common phenomenon. For example, herpes viruses or HIV as well as vaccinia viruses were found to exploit the transport mechanism of microtubules to get to the microtubule-organizing center close to the nucleus (Greber & Way, 2006; Fackler & Kräusslich, 2006). Herpes viruses are known for their latency, and interact not only with microtubules, but also with actin and presumably with intermediate filaments (Roberts & Baines, 2011; Hertel, 2011, Smith, 2012). Although the function of actins and phage replication are different in eukaryotic and prokaryotic cells, it probably is an advantage for a large phage to encode its own cytoskeletal proteins for transport.

### **Transport function of AlpAC**

A function of the AlpAC system might be the transport of phage DNA to the host membrane for assembly and secretion of phage particles or phage-encoded substances. However, to date, CGP3 virions or secreted phage particles have not been described. In fact, filamentous phages are often released from their host by secretion instead of cell lysis (Rakonjac *et al.*, 2011). For example, the phage CTX $\phi$ , which is related to filamentous coliphages such as M13, uses a host-encoded secretin (EpsD) of an extracellular protein (*eps*) type II secretion system to secrete cholera toxin and phage virions (Davis *et al.*, 2000; Davis & Waldor, 2003). Furthermore, integrating and conjugative elements (ICE) were characterized as a new class of mobile elements (Juhas *et al.*, 2009; Wozniak & Waldor, 2010). In a subpopulation (3-5%) of *Pseudomonas knackmussii* B13, the ICE*clc* element induces a transfer competence (*tc*) for horizontal transfer to new host recipient cells (Gaillard *et al.*, 2010; Reinhard *et al.*, 2013). To analyze the ability for horizontal gene transfer or re-infection by CGP3, CGP3 DNA in a donor strain (CGP3+) and a recipient strain (CGP3-) could be tagged by insertion of

genes coding for different fluorescent proteins. A transfer of phage DNA from the donor into recipient cells would result in a transfer of the donor-tag into the recipient cell. A useful tool to monitor the transfer events by time-lapse fluorescence microscopy is presented by the microfluidic picoliter bioreactor. The general cultivation of *C. glutamicum* strains in this microfluidic system was tested, in this work. Furthermore, the supernatant of stressed cells could be enriched and examined for phage virions by transmission electron microscopy.

#### 4.2.4 AlpAC in comparison to other phage-encoded cytoskeletal proteins

To date, only a few examples of an interaction of cytoskeletal proteins with phages or even phage-encoded proteins have been described in detail, but they reveal interesting features of phage life cycles. An overview of the phage-encoded cytoskeletal proteins, which have been characterized to date and their proposed mode of action, is given in Fig. 4.2.

##### Phage $\phi$ 29 interacts with bacterial MreB

In *B. subtilis*, the replication of phage  $\phi$ 29 takes place close to the membrane and is connected to the host cytoskeleton (Bravo *et al.*, 2005; Muñoz-Espin *et al.*, 2012). The phage primarily exploits the membrane-associated cytoskeleton protein MreB for replication (Salje *et al.*, 2011; Carballido-López, 2006; Muñoz-Espin *et al.*, 2009). The phage-encoded membrane protein p16.7 interacts directly with MreB, thereby attaching phage DNA to the cell membrane and organizing the replication under contribution of  $\phi$ 29 DNA polymerase at the cell membrane (Muñoz-Espin *et al.*, 2009; Meijer *et al.*, 2001). Consequently, not only the phage protein p16.7, but also an intact cytoskeleton of the bacterial MreB protein, and its isoforms Mbl and MreBH are required for efficient viral DNA replication (Carballido-López & Errington, 2003; Carballido-López *et al.*, 2006). In contrast to other rod-shaped bacteria, *C. glutamicum* does not encode MreB proteins (Letek *et al.*, 2008b; Daniel & Errington, 2003). In *C. glutamicum*, selection of the division site and growth behavior is controlled by chromosome segregation, which is mediated by the ParAB partitioning system and polar localized DivIVA (Donovan *et al.*, 2010; Donovan *et al.*, 2013). Interaction between DivIVA and ParB at the cell poles enables segregation of the chromosomes (Donovan *et al.*, 2012). In analogy to phage  $\phi$ 29, AlpC might interact with other membrane-associated proteins for replication in *C. glutamicum*.

##### Phage-encoded tubulin-like proteins

Recently, it has been reported that relatively large phages encode their own tubulin-like cytoskeleton to organize localization of phage virions or segregation of phage plasmids (Haeusser & Margolin, 2012). The size of phages is highly diverse and ranges for example from  $\sim$ 3.4 kbp ssRNA phages in *E. coli* or 11.7 kbp of the dsDNA phage P1 of *Mycoplasma*, up to an almost 500 kbp phage in *Bacillus megaterium* (Friedman *et al.*, 2009; Tu *et al.*, 2001; Hatfull & Hendrix, 2011). The size of

CGP3 (187 kbp) is comparable to the phage c-st from *Clostridium botulinum* (186 kbp), whereas the phage 201  $\phi$ 2-1 from *Pseudomonas chlororaphis* is two-times larger (316 kbp) (Kalinowski *et al.*, 2003; Kraemer *et al.*; 2012; Oliva *et al.*, 2012). Both phages encode tubulin/FtsZ-like proteins, which are important for phage transport and positioning of phage DNA within the host cell (Oliva *et al.*, 2012; Kraemer *et al.*, 2012).

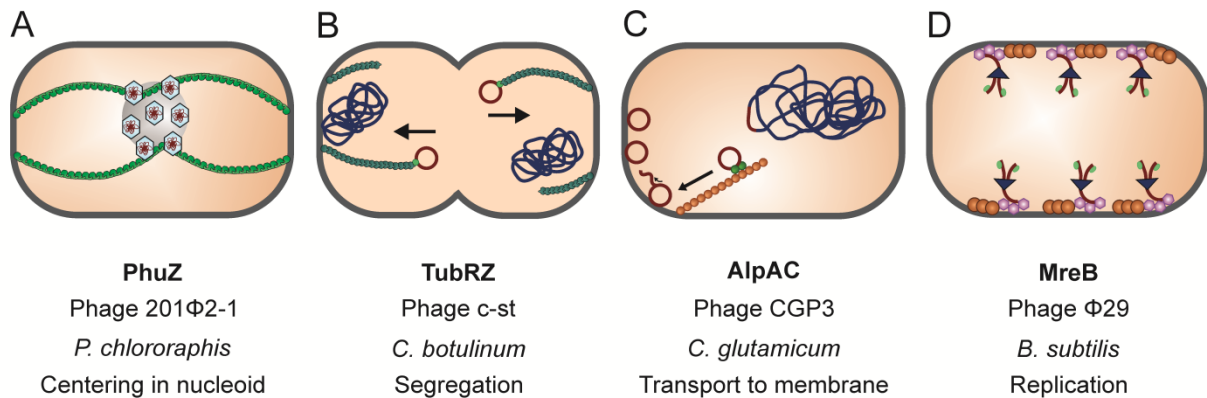


**Fig. 4.2 Overview of phage-encoded cytoskeletal proteins.** (A) The tubulin-like protein PhuZ (green) of phage 201 $\phi$ 2-1 in *P. chlororaphis* is required for positioning of encapsulated DNA at the center of the cell to form a rosette infection nucleoid. (Kraemer *et al.*, 2012) (B) TubZ of phage c-st in *C. botulinum* shows high similarity to plasmid encoded TubZ of *B. thuringiensis*, where TubZ (dark green) and the DNA-binding protein TubR (light green) facilitate segregation of the plasmid pBtoxis. An analogous mechanism was suggested for TubZ of c-st. (Oliva *et al.*, 2012, Larsen *et al.*, 2007) (C) The actin-like protein AlpC (orange) and the DNA-binding protein AlpA (green) of phage CGP3 in *C. glutamicum* were characterized in this work. This system was proposed to mediate the transport of circularized CGP3 DNA (red) excised from the genome (blue) to the cell membrane under stressful conditions. (D) Phage  $\phi$ 29 in *B. subtilis* utilizes bacterial MreB (brown) for replication close to the membrane (DNA polymerase indicated as triangle (dark blue), terminal proteins (green)), by direct interaction with the phage protein p16.7 (purple) (Muñoz-Espin *et al.*, 2009; Muñoz-Espin *et al.*, 2010). Adapted from (Kraemer *et al.*, 2012) and (Haeusser & Margolin, 2012).

### Phage c-st encodes type II segregation system TubZ-R-S-Y

The phage c-st remains in the cell as a plasmid-like element. Comparison of crystal structures of the tubulin-like protein TubZ from plasmid phage c-st to the plasmid-encoded TubZ of *Bacillus thuringiensis* revealed high structural homology (Aylett *et al.*, 2010; Oliva *et al.*, 2012). Based on the homology and biochemical characterizations, TubZ might represent a type III plasmid segregation system for the phage, together with the DNA-binding protein TubR that binds the *tubS* binding region and interacts with the C-terminus of TubZ (Ni *et al.*, 2010; Larsen *et al.*, 2007). Furthermore, this system comprises an additional fourth component, TubY, facilitating complex formation of TubZ-R-S (Oliva *et al.*, 2012). In contrast, the CGP3 prophage is integrated into the genome of *C. glutamicum*, and due to the lack of an AlpC crystal structure, no functional comparison to other actin-like protein could have been performed yet.

## PhuZ positions encapsulated phage DNA centrally in the cell

A second tubulin/FtsZ-like protein, PhuZ, encoded by phage 201 $\phi$ 2-1 of *P. chlororaphis*, revealed a conserved tubulin fold, but exhibited differences to the phage-encoded TubZ by displaying an acidic knuckle at the C-terminus required for polymerization (Kraemer *et al.*, 2012). *In vivo*, PhuZ, fused to the fluorescent protein GFP, showed a diffuse localization by expressing *phuZ-gfp* at low concentrations. At higher concentrations, PhuZ assembled into long filaments. During the lytic response, PhuZ filament formation could be visualized by additional production of plasmid-borne PhuZ-GFP. Under these conditions, PhuZ formed filaments, which conducted encapsulated phage DNA to the center of the cell to model a rosette infection nucleoid (Kraemer *et al.*, 2012). The function of PhuZ under native concentrations during lytic growth was not evaluated. In comparison to phage 201 $\phi$ 2-1, CGP3 DNA was rarely positioned at the center of the cell, rather CGP3 DNA was found close to the membrane. However, the concentration-dependent differences in filament formation of AlpC, observed in this work, highlight the importance of investigating filament formation at native levels.

A further sequence comparison of tubulin-like proteins identified further phage-encoded tubulin-like proteins and noted a strong conservation in the 3-dimensional structure (Aylett *et al.*, 2013). Hence, the characterization of both phage-encoded actin-like proteins (AlpC and Alp6A) as well as tubulin-like proteins will remain in the focus of research. For further detailed analysis of AlpC, microscopic analysis as well as crystallization of AlpC filaments would help to understand AlpC polymerization and to verify our current model in comparison to the proposed action of other phage-encoded or plasmid-originated cytoskeletal proteins. Additionally, FRAP studies (fluorescent recovery after photo bleaching) of AlpC in native concentration could provide an insight into the dynamics of AlpC filament formation. Future studies will focus on the interaction of AlpC filaments and AlpA to understand the mechanism of CGP3 DNA partitioning.

## 4.3 Heme homeostasis in *C. glutamicum*

### 4.3.1 Link between CGP3 induction and iron/heme homeostasis

Previously, a mutant lacking the master regulator of iron homeostasis DtxR showed increased expression of CGP3 prophage genes (Brune *et al.*, 2006; Frunzke *et al.*, 2008; Wennerhold & Bott, 2006). The deletion of *dtxR* probably increases the intracellular level of iron by derepression of DtxR-regulated iron uptake systems. Subsequently, high concentrations of iron promote the formation of reactive oxygen species (ROS), like hydroxyl radicals, *via* the Fenton reaction. ROS causes lipid peroxidation or DNA damage by formation of strand breaks, leading to the activation of the oxidative stress. In *C. glutamicum*, the sigma factor  $\sigma^H$  connects oxidative stress and the SOS response, as the

regulon of  $\sigma^H$  comprises several genes involved in both responses (Lee *et al.*, 2013; Busche *et al.*, 2012). An increased level of SOS response in  $\Delta dtxR$  could explain the increased induction of CGP3. However, the level of SOS response in  $\Delta dtxR$  seemed not to be elevated in transcriptome analyses (Wennerhold & Bott, 2006). A further analysis of the stress level in  $\Delta dtxR$  could be enabled by application of promoter fusions of central SOS targets.

### 4.3.2 Heme-dependent TCS

Deletion mutants that were impaired in iron homeostasis often showed an increased CGP3 phage activity. Due to this connection, a focus in this thesis was also set on the regulatory network of iron and heme homeostasis. DtxR regulates the expression of *hrrA*, encoding the response regulator of the TCS HrrSA which is involved in the regulation of heme homeostasis and which was shown to be crucial for the utilization of heme as an alternative iron source (Frunzke *et al.*, 2011). Among the target genes of HrrA, we identified the genes *chrSA* of a second TCS. ChrSA inherits an essential role in heme detoxification, as ChrA activates the expression of the heme exporter system *hrtBA*, located divergently to the operon of *chrSA*. The genomic organization is highly conserved, and homologs of the ABC transporter system HrtBA were primarily found in pathogenic bacteria such as *C. diphtheriae* or *S. aureus* (Bibb & Schmitt, 2010; Stauff *et al.*, 2008). Although HrtBA is crucial for protection against high heme concentrations (Bibb, Schmitt 2010), the mechanism of heme toxicity is not completely understood. On the one hand, it was described that heme itself can lead to DNA damage in the cells (Nir *et al.*, 1991; Anzaldi & Skaar, 2010). On the other hand, heme degradation products or by-products might be toxic for cells (Anzaldi & Skaar, 2010). To validate these hypotheses of heme toxicity, chemically modified heme variants, *e.g.* heme without the central iron ion, can be used in further experiments.

### 4.3.3 Interaction of ChrSA and HrrSA

The TCS's ChrSA and HrrSA share a high amino acid sequence identity. Hence, an overlap in regulation of both systems is likely. Indeed, we observed a cross-regulation on several levels: First, both systems are responsive to heme. Whether the signal is sensed intracellular or extracellular has still to be validated in further studies. Second, a cross-talk between the kinases ChrS and HrrS by phosphoryl transfer might represent a further level of interaction. In *C. diphtheria*, evidence for a phosphor-transfer between the orthologous systems was postulated (Bibb *et al.*, 2005, Bibb *et al.*, 2007). To test for cross-phosphorylation between the *C. glutamicum* systems, genetic analysis with mutant strains lacking the kinases would be a promising approach. Further evidence could be provided by *in vitro* phosphotransfer studies or bacterial two-hybrid assays. A third level of interaction is a cross-regulation of both response regulators at the transcriptional level by controlling the transcription of each other. The regulators ChrA and HrrA were shown to bind in the mutual

promoter region, thereby regulating the transcription of each other (Frunzke *et al.*, 2011). At last, the regulons of ChrA and HrrA revealed an overlap in target genes representing a further level of interaction. In protein-DNA-binding studies, the promoter regions of all identified target genes were recognized by ChrA, but also by HrrA with different affinities. For example, the affinity of ChrA to the promoter of *hmuO* was marginal, unlike HrrA which has a strong affinity to the *hmuO* promoter. This represents a prominent difference to the regulation of heme homeostasis in *C. diphtheriae*, where ChrSA is the primary regulator of *hmuO* for heme degradation (Bibb *et al.*, 2005; Bibb *et al.*, 2007).

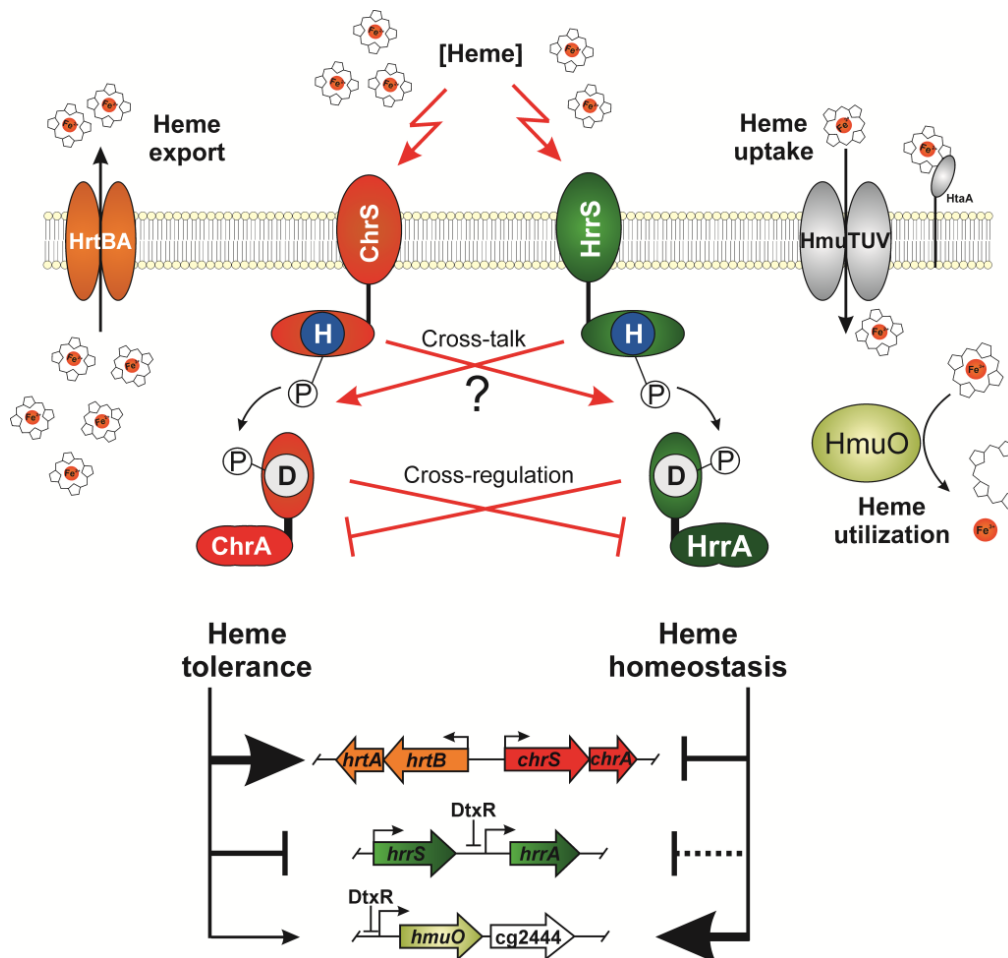


**Fig. 4.3 The TCS HrrSA and ChrSA potentially interact on multiple levels.** ChrSA represents the prominent system for heme resistance and detoxification by activation of the heme exporter *hrtBA* in the presence of heme. HrrSA is required for utilization of heme as alternative iron source. HrrA activates the heme oxygenase *hmuO* for heme degradation and represses *chrSA* to avoid export of heme under iron limiting conditions. Contrarily, ChrA represses also the expression of *hrrA*. Adapted from (Heyer *et al.*, 2012) and (Bott & Brocker, 2012).

The complex interactions between the two systems on multiple levels (Fig. 4.3) underline the importance for *C. glutamicum* to inherit two systems, but raise the question of their physiological relevance. In *C. glutamicum*, the presence of two TCS's seems to be physiologically important for tight regulation of the optimal intracellular heme level. Whereas ChrSA is crucial for resistance

towards elevated heme concentrations, HrrSA is important for heme utilization as an alternative iron source. Accordingly, HrrSA is not only heme-dependent, but is also regulated in dependency of iron availability by DtxR. Interestingly, the iron-dependent regulation of *hrrA* by DtxR seems not to be present in *C. diphtheriae* (Bibb *et al.*, 2007).

This complex regulation has to be investigated in further studies to establish its impact in more detail, *in vivo*. For this purpose, the expression level of key target genes has to be analyzed in deletion mutants lacking the components of both TCSs in combination with different iron and heme concentrations. This will provide a profound knowledge about the role of each component in the complex network of heme homeostasis.

## 5 References

- Ajinomoto, (2011) Feed-use amino acid business. In. <http://www.ajinomoto.com/en/ir/pdf/Feed-useAA-Oct2011.pdf>.
- Ajinomoto, (2012) Food products business. In. <http://www.ajinomoto.com/en/ir/pdf/Food-Oct2012.pdf>.
- Anzaldi, L.L. & E.P. Skaar, (2010) Overcoming the Heme Paradox: Heme Toxicity and Tolerance in Bacterial Pathogens. *Infect Immun* **78**: 4977-4989.
- Ausmees, N., J.R. Kuhn & C. Jacobs-Wagner, (2003) The bacterial cytoskeleton: an intermediate filament-like function in cell shape. *Cell* **115**: 705-713.
- Aylett, C.H., T. Izoré, L.A. Amos & J. Löwe, (2013) Structure of the Tubulin/FtsZ-Like Protein TubZ from *Pseudomonas* Bacteriophage PhiKZ. *J Mol Biol*: In Press.
- Aylett, C.H., Q. Wang, K.A. Michie, L.A. Amos & J. Löwe, (2010) Filament structure of bacterial tubulin homologue TubZ. *Proc Natl Acad Sci U S A* **107**: 19766-19771.
- Benson, N., P. Sugiono & P. Youderian, (1988) DNA sequence determinants of lambda repressor binding *in vivo*. *Genetics* **118**: 21-29.
- Benson, N. & P. Youderian, (1989) Phage lambda Cro protein and *cl* repressor use two different patterns of specific protein-DNA interactions to achieve sequence specificity *in vivo*. *Genetics* **121**: 5-12.
- Bibb, L.A., N.D. King, C.A. Kunkle & M.P. Schmitt, (2005) Analysis of a Heme-Dependent Signal Transduction System in *Corynebacterium diphtheriae*: Deletion of the *chrAS* Genes Results in Heme Sensitivity and Diminished Heme-Dependent Activation of the *hmuO* Promoter. *Infect Immun* **73**: 7406-7412.
- Bibb, L.A., C.A. Kunkle & M.P. Schmitt, (2007) The ChrA-ChrS and HrrA-HrrS Signal Transduction Systems Are Required for Activation of the *hmuO* Promoter and Repression of the *hemA* Promoter in *Corynebacterium diphtheriae*. *Infect Immun* **75**: 2421-2431.
- Bibb, L.A. & M.P. Schmitt, (2010) The ABC Transporter HrtAB Confers Resistance to Hemin Toxicity and Is Regulated in a Hemin-Dependent Manner by the ChrAS Two-Component System in *Corynebacterium diphtheriae*. *J Bacteriol* **192**: 4606-4617.
- Bloom, K. & A. Joglekar, (2010) Towards building a chromosome segregation machine. *Nature* **463**: 446-456.
- Bott, M. & M. Brocker, (2012) Two-component signal transduction in *Corynebacterium glutamicum* and other corynebacteria: on the way towards stimuli and targets. *Appl Microbiol Biotechnol* **94**: 1131-1150.
- Bott, M. & B.J. Eikmanns, (2013) TCA Cycle and Glyoxylate Shunt of *Corynebacterium glutamicum*. In: *Corynebacterium glutamicum* : biology and biotechnology. H. Yukawa & M. Inui (eds). Heidelberg ; New York: Springer, pp. 281-314.
- Bouchard, J.D., E. Dion, F. Bissonnette & S. Moineau, (2002) Characterization of the two-component abortive phage infection mechanism AbiT from *Lactococcus lactis*. *J Bacteriol* **184**: 6325-6332.
- Bravo, A., G. Serrano-Heras & M. Salas, (2005) Compartmentalization of prokaryotic DNA replication. *FEMS Microbiol Rev* **29**: 25-47.
- Breüner, A., R.B. Jensen, M. Dam, S. Pedersen & K. Gerdes, (1996) The centromere-like *parC* locus of plasmid R1. *Mol Microbiol* **20**: 581-592.
- Bröker, D., M. Arenskötter, A. Legatzki, D.H. Nies & A. Steinbüchel, (2003) Characterization of the 101-Kilobase-Pair Megaplasmid pKB1, Isolated from the Rubber-Degrading Bacterium *Gordonia westfalica* Kb1. *J Bacteriol* **186**: 212-225.
- Brune, I., H. Werner, A.T. Hüser, J. Kalinowski, A. Pühler & A. Tauch, (2006) The DtxR protein acting as dual transcriptional regulator directs a global regulatory network involved in iron metabolism of *Corynebacterium glutamicum*. *BMC Genomics* **7**: 21.

- Bukovska, G., L. Klucar, C. Vlcek, J. Adamovic, J. Turna & J. Timko, (2006) Complete nucleotide sequence and genome analysis of bacteriophage BFK20 - a lytic phage of the industrial producer *Brevibacterium flavum*. *Virology* **348**: 57-71.
- Burgos, J.M. & M.P. Schmitt, (2012) The ChrA response regulator in *Corynebacterium diphtheriae* controls hemin-regulated gene expression through binding to the *hmuO* and *hrtAB* Promoter Regions. *J Bacteriol* **194**: 1717-1729.
- Burkovski, A., (2008) *Corynebacteria: Genomics and molecular biology*. Caister Academic Press, Norfolk UK.
- Busche, T., R. Silar, M. Pičmanová, M. Pátek & J. Kalinowski, (2012) Transcriptional regulation of the operon encoding stress-responsive ECF sigma factor SigH and its anti-sigma factor RshA, and control of its regulatory network in *Corynebacterium glutamicum*. *BMC Genomics* **13**: 445.
- Campbell, A., (1994) Comparative molecular biology of lambdoid phages. *Annu Rev Microbiol* **48**: 193-222.
- Carballido-López, R., (2006) The Bacterial Actin-Like Cytoskeleton. *Microbiol Mol Biol Rev* **70**: 888-909.
- Carballido-López, R. & J. Errington, (2003) The Bacterial Cytoskeleton: *In Vivo* Dynamics of the Actin-like Protein Mbl of *Bacillus subtilis*. *Dev Cell* **4**: 19-28.
- Carballido-López, R., A. Formstone, Y. Li, S.D. Ehrlich, P. Noirot & J. Errington, (2006) Actin Homolog MreBH Governs Cell Morphogenesis by Localization of the Cell Wall Hydrolase LytE. *Dev Cell* **11**: 399-409.
- Casjens, S., (2003) Prophages and bacterial genomics: what have we learned so far? *Mol Microbiol* **49**: 277-300.
- Courcelle, J., A. Khodursky, B. Peter, P.O. Brown & P.C. Hanawalt, (2001) Comparative gene expression profiles following UV exposure in wild-type and SOS-deficient *Escherichia coli*. *Genetics* **158**: 41-64.
- D'Herelle, F., (2007) On an invisible microbe antagonistic toward dysenteric bacilli: brief note by Mr. F. D'Herelle, presented by Mr. Roux. 1917. *Res Microbiol* **158**: 553-554.
- Dam, M. & K. Gerdes, (1994) Partitioning of Plasmid R1. Ten Direct Repeats Flanking the *parA* Promoter Constitute a Centromere-like Partition Site *parC*, that Expresses Incompatibility. *J Mol Biol* **236**: 1289-1298.
- Daniel, R.A. & J. Errington, (2003) Control of cell morphogenesis in bacteria: two distinct ways to make a rod-shaped cell. *Cell* **113**: 767-776.
- Davis, B.M., E.H. Lawson, M. Sandkvist, A. Ali, S. Sozhamannan & M.K. Waldor, (2000) Convergence of the Secretory Pathways for Cholera Toxin and the Filamentous Phage, CTXPHI. *Science* **288**: 333-335.
- Davis, B.M. & M.K. Waldor, (2003) Filamentous phages linked to virulence of *Vibrio cholerae*. *Curr Opin Microbiology* **6**: 35-42.
- Derman, A.I., E.C. Becker, B.D. Truong, A. Fujioka, T.M. Tucey, M.L. Erb, P.C. Patterson & J. Pogliano, (2009) Phylogenetic analysis identifies many uncharacterized actin-like proteins (Alps) in bacteria: regulated polymerization, dynamic instability and treadmilling in Alp7A. *Mol Microbiol* **73**: 534-552.
- Derman, A.I., P. Nonejuie, B.C. Michel, B.D. Truong, A. Fujioka, M.L. Erb & J. Pogliano, (2012) Alp7R Regulates Expression of the Actin-like Protein Alp7A in *Bacillus subtilis*. *J Bacteriol* **194**: 2715-2724.
- Dmitrova, M., G. Younès-Cauet, P. Oertel-Buchheit, D. Porte, M. Schnarr & M. Granger-Schnarr, (1998) A new LexA-based genetic system for monitoring and analyzing protein heterodimerization in *Escherichia coli*. *Mol Gen Genet* **257**: 205-212.
- Dodd, I.B., K.E. Shearwin & J.B. Egan, (2005) Revisited gene regulation in bacteriophage lambda. *Curr Opin Gen & Dev* **15**: 145-152.
- Donovan, C., A. Schauss, R. Krämer & M. Bramkamp, (2013) Chromosome Segregation Impacts on Cell Growth and Division Site Selection in *Corynebacterium glutamicum*. *PLoS one* **8**: e55078.
- Donovan, C., A. Schwaiger, R. Krämer & M. Bramkamp, (2010) Subcellular Localization and Characterization of the ParAB System from *Corynebacterium glutamicum*. *J Bacteriol* **192**: 3441-3451.

- Donovan, C., B. Sieger, R. Krämer & M. Bramkamp, (2012) A synthetic *Escherichia coli* system identifies a conserved origin tethering factor in Actinobacteria. *Mol Microbiol* **84**: 105-116.
- Draper, O., M.E. Byrne, Z. Li, S. Keyhani, J.C. Barrozo, G. Jensen & A. Komeili, (2011) MamK, a bacterial actin, forms dynamic filaments *in vivo* that are regulated by the acidic proteins MamJ and LimJ. *Mol Microbiol* **82**: 342-354.
- Eggeling, L. & M. Bott, (2005) *Handbook of Corynebacterium glutamicum*. Academic Press, Inc., Boca Raton, FL.
- Ehira, S., H. Teramoto, M. Inui & H. Yukawa, (2009) Regulation of *Corynebacterium glutamicum* Heat Shock Response by the Extracytoplasmic-Function Sigma Factor SigH and Transcriptional Regulators HspR and HrcA. *J Bacteriol* **191**: 2964-2972.
- Engels, S., C. Ludwig, J.E. Schweitzer, C. Mack, M. Bott & S. Schaffer, (2005) The transcriptional activator ClgR controls transcription of genes involved in proteolysis and DNA repair in *Corynebacterium glutamicum*. *Mol Microbiol* **57**: 576-591.
- Engels, S., J.E. Schweitzer, C. Ludwig, M. Bott & S. Schaffer, (2004) *clpC* and *clpP1P2* gene expression in *Corynebacterium glutamicum* is controlled by a regulatory network involving the transcriptional regulators ClgR and HspR as well as the ECF sigma factor sigmaH. *Mol Microbiol* **52**: 285-302.
- Eriksson, J.E., T. Dechat, B. Grin, B. Helfand, M. Mendez, H.M. Pallari & R.D. Goldman, (2009) Introducing intermediate filaments: from discovery to disease. *J Clin Invest* **119**: 1763-1771.
- Fackler, O.T. & H.G. Kräusslich, (2006) Interactions of human retroviruses with the host cell cytoskeleton. *Curr Opin Microbiol* **9**: 409-415.
- Friedman, D.I. & D.L. Court, (1995) Transcription antitermination: the lambda paradigm updated. *Mol Microbiol* **18**: 191-200.
- Friedman, S.D., F.J. Genthner, J. Gentry, M.D. Sobsey & J. Vinjé, (2009) Gene Mapping and Phylogenetic Analysis of the Complete Genome from 30 Single-Stranded RNA Male-Specific Coliphages (Family *Leviviridae*). *J Virol* **83**: 11233-11243.
- Frunzke, J., M. Bramkamp, J.E. Schweitzer & M. Bott, (2008) Population Heterogeneity in *Corynebacterium glutamicum* ATCC 13032 Caused by Prophage CGP3. *J Bacteriol* **190**: 5111-5119.
- Frunzke, J., C. Gätgens, M. Bocker & M. Bott, (2011) Control of Heme Homeostasis in *Corynebacterium glutamicum* by the Two-Component System HrrSA. *J Bacteriol* **193**: 1212-1221.
- Gaillard, M., N. Pradervand, M. Minoia, V. Sentchilo, D.R. Johnson & J.R. van der Meer, (2010) Transcriptome analysis of the mobile genome ICE<sub>clc</sub> in *Pseudomonas knackmussii* B13. *BMC Microbiol* **10**: 153.
- Galkin, V.E., X. Yu, J. Bielnicki, D. Ndjonka, C.E. Bell & E.H. Egelman, (2009) Cleavage of bacteriophage lambda cI repressor involves the RecA C-terminal domain. *J Mol Biol* **385**: 779-787.
- Gao, R. & A.M. Stock, (2009) Biological Insights from Structures of Two-Component Proteins. *Ann Rev Microbiol* **63**: 133-154.
- Gayathri, P., T. Fujii, J. Moller-Jensen, F. van den Ent, K. Namba & J. Löwe, (2012) A bipolar spindle of antiparallel ParM filaments drives bacterial plasmid segregation. *Science* **338**: 1334-1337.
- Gayathri, P., T. Fujii, K. Namba & J. Löwe, (2013) Structure of the ParM filament at 8.5 Å resolution. *J Struct Biol*.
- Gerdes, K., M. Howard & F. Szardenings, (2010) Pushing and pulling in prokaryotic DNA segregation. *Cell* **141**: 927-942.
- Gerdes, K., J. Moller-Jensen & R. Bugge Jensen, (2000) Plasmid and chromosome partitioning: surprises from phylogeny. *Mol Microbiol* **37**: 455-466.
- Gerova, M., N. Halgasova, J. Ugorcakova & G. Bukovska, (2011) Endolysin of bacteriophage BFK20: evidence of a catalytic and a cell wall binding domain. *FEMS Microbiol Lett* **321**: 83-91.
- Gerstmeir, R., A. Cramer, P. Dangel, S. Schaffer & B.J. Eikmanns, (2004) RamB, a Novel Transcriptional Regulator of Genes Involved in Acetate Metabolism of *Corynebacterium glutamicum*. *J Bacteriol* **186**: 2798-2809.

- Graumann, P.L., (2007) Cytoskeletal elements in bacteria. *Annu Rev Microbiol* **61**: 589-618.
- Greber, U.F. & M. Way, (2006) A Superhighway to Virus Infection. *Cell* **124**: 741-754.
- Haeusser, D.P. & W. Margolin, (2012) Bacteriophage Tubulins: Carrying Their Own Cytoskeleton Key. *Curr Biol* **22**: R639-641.
- Halgasova, N., I. Mesarosova & G. Bukovska, (2012) Identification of a bifunctional primase–polymerase domain of corynephage BFK20 replication protein gp43. *Virus Res* **163**: 454-460.
- Hatfull, G.F. & R.W. Hendrix, (2011) Bacteriophages and their genomes. *Curr Opin Virol* **1**: 298-303.
- Hayes, S., C. Erker, M.A. Horbay, K. Marciniuk, W. Wang & C. Hayes, (2013) Phage Lambda P Protein: Trans-Activation, Inhibition Phenotypes and their Suppression. *Viruses* **5**: 619-653.
- Herrmann, H., S.V. Strelkov, P. Burkhard & U. Aebi, (2009) Intermediate filaments: primary determinants of cell architecture and plasticity. *J Clin Invest* **119**: 1772-1783.
- Hertel, L., (2011) Herpesviruses and intermediate filaments: close encounters with the third type. *Viruses* **3**: 1015-1040.
- Heyer, A., C. Gätgens, E. Hentschel, J. Kalinowski, M. Bott & J. Frunzke, (2012) The two-component system ChrSA is crucial for haem tolerance and interferes with HrrSA in haem-dependent gene regulation in *Corynebacterium glutamicum*. *Microbiology* **158**: 3020-3031.
- Hochschild, A. & M. Lewis, (2009) The bacteriophage lambda CI protein finds an asymmetric solution. *Curr Opin Struct Biol* **19**: 79-86.
- Huang, K.H., J. Durand-Heredia & A. Janakiraman, (2013) FtsZ Ring Stability: of Bundles, Tubules, Crosslinks, and Curves. *J Bacteriol* **195**: 1859-1868.
- Indest, K.J., C.M. Jung, H.P. Chen, D. Hancock, C. Florizone, L.D. Eltis & F.H. Crocker, (2010) Functional Characterization of pGKT2, a 182-Kilobase Plasmid Containing the *xplAB* Genes, Which Are Involved in the Degradation of Hexahydro-1,3,5-Trinitro-1,3,5-Triazine by *Gordonia* sp. Strain KTR9. *Appl Environ Microbiol* **76**: 6329-6337.
- Jochmann, N., A.K. Kurze, L.F. Czaja, K. Brinkrolf, I. Brune, A.T. Hüser, N. Hansmeier, A. Pühler, I. Borovok & A. Tauch, (2009) Genetic makeup of the *Corynebacterium glutamicum* LexA regulon deduced from comparative transcriptomics and *in vitro* DNA band shift assays. *Microbiology* **155**: 1459-1477.
- Jones, L.J., R. Carballido-Lopez & J. Errington, (2001) Control of cell shape in bacteria: helical, actin-like filaments in *Bacillus subtilis*. *Cell* **104**: 913-922.
- Juhas, M., J.R. van der Meer, M. Gaillard, R.M. Harding, D.W. Hood & D.W. Crook, (2009) Genomic islands: tools of bacterial horizontal gene transfer and evolution. *FEMS Microbiol Rev* **33**: 376-393.
- Kaiser, A.D., (1957) Mutations in a Temperate Bacteriophage Affecting its Ability to Lysogenize *Escherichia coli*. *Virology* **3**: 42-61.
- Kalinowski, J., (2005) The Genomes of Amino Acid Producing Corynebacteria. In: Handbook of *Corynebacterium glutamicum*. CRC Press, pp. 37-56.
- Kalinowski, J., B. Bathe, D. Bartels, N. Bischoff, M. Bott, A. Burkovski, N. Dusch, L. Eggeling, B.J. Eikmanns, L. Gaigalat, *et al.*, (2003) The complete *Corynebacterium glutamicum* ATCC 13032 genome sequence and its impact on the production of L-aspartate-derived amino acids and vitamins. *J Biotechnol* **104**: 5-25.
- Kimsey, H.H. & M.K. Waldor, (2009) *Vibrio cholerae* LexA Coordinates CTX Prophage Gene Expression. *J Bacteriol* **191**: 6788-6795.
- Kinoshita, S., S. Uda & M. Shimono, (1957) Studies on the amino acid fermentation: I. Production of L-glutamic acid by various microorganisms. *J Gen Appl Microbiol* **3**: 193-205.
- Kobiler, O., A. Rokney, N. Friedman, D.L. Court, J. Stavans & A.B. Oppenheim, (2005) Quantitative kinetic analysis of the bacteriophage lambda genetic network. *Proc Natl Acad Sci U S A* **102**: 4470-4475.

- Kobiler, O., A. Rokney & A.B. Oppenheim, (2007) Phage lambda CIII: a protease inhibitor regulating the lysis-lysogeny decision. *PLoS one* **2**: e363.
- Koptides, M., I. Barák, M. Sisová, E. Baloghová, J. Ugorcaková & J. Timko, (1992) Characterization of bacteriophage BFK20 from *Brevibacterium flavum*. *J Gen Microbiol* **138**: 1387-1391.
- Kraemer, J.A., M.L. Erb, C.A. Waddling, E.A. Montabana, E.A. Zehr, H. Wang, K. Nguyen, D.S. Pham, D.A. Agard & J. Pogliano, (2012) A Phage Tubulin Assembles Dynamic Filaments by an Atypical Mechanism to Center Viral DNA within the Host Cell. *Cell* **149**: 1488-1499.
- Lander, E.S., L.M. Linton, B. Birren, C. Nusbaum, M.C. Zody, J. Baldwin, K. Devon, K. Dewar, M. Doyle, W. FitzHugh, *et al.*, (2001) Initial sequencing and analysis of the human genome. *Nature* **409**: 860-921.
- Larsen, R.A., C. Cusumano, A. Fujioka, G. Lim-Fong, P. Patterson & J. Pogliano, (2007) Treadmilling of a prokaryotic tubulin-like protein, TubZ, required for plasmid stability in *Bacillus thuringiensis*. *Genes Dev* **21**: 1340-1352.
- Laub, M.T. & M. Goulian, (2007) Specificity in two-component signal transduction pathways. *Annu Rev Genet* **41**: 121-145.
- Lederberg, E.M., (1951) Lysogenicity in *Escherichia coli* K-12. *Genetics* **36**: 560-560.
- Lee, J.Y., H.J. Kim, E.S. Kim, P. Kim, Y. Kim & H.S. Lee, (2013) Regulatory interaction of the *Corynebacterium glutamicum* *whc* genes in oxidative stress responses. *J Biotechnol*.
- Letek, M., M. Fiuza, E. Ordonez, A.F. Villadangos, A. Ramos, L.M. Mateos & J.A. Gil, (2008a) Cell growth and cell division in the rod-shaped actinomycete *Corynebacterium glutamicum*. *Antonie van Leeuwenhoek* **94**: 99-109.
- Letek, M., M. Fiuza, A.F. Villadangos, L.M. Mateos & J.A. Gil, (2012) Cytoskeletal proteins of actinobacteria. *Int J Cell Biol* **2012**: 905832.
- Letek, M., E. Ordóñez, J. Vaquera, W. Margolin, K. Flärdh, L.M. Mateos & J.A. Gil, (2008b) DivIVA Is Required for Polar Growth in the MreB-Lacking Rod-Shaped Actinomycete *Corynebacterium glutamicum*. *J Bacteriol* **190**: 3283-3292.
- Letunic, I., T. Doerks & P. Bork, (2012) SMART 7: recent updates to the protein domain annotation resource. *Nucleic Acids Res* **40**: D302-305.
- Li, Y. & S. Austin, (2002) The P1 plasmid in action: time-lapse photomicroscopy reveals some unexpected aspects of plasmid partition. *Plasmid* **48**: 174-178.
- Little, J.W., (1984) Autodigestion of *lexA* and phage lambda repressors. *Proc Natl Acad Sci U S A* **81**: 1375-1379.
- Little, J.W., (1991) Mechanism of specific LexA cleavage: autodigestion and the role of RecA coprotease. *Biochimie* **73**: 411-421.
- Little, J.W. & D.W. Mount, (1982) The SOS Regulatory System of *Escherichia coli*. *Cell* **29**: 11-22.
- Lu, T.K. & M.S. Koeris, (2011) The next generation of bacteriophage therapy. *Curr Opin Microbiol* **14**: 524-531.
- Lutkenhaus, J., S. Pichoff & S. Du, (2012) Bacterial cytokinesis: From Z ring to divisome. *Cytoskeleton* **69**: 778-790.
- Lutkenhaus, J.F., H. Wolf-Watz & W.D. Donachie, (1980) Organization of genes in the *ftsA-envA* region of the *Escherichia coli* genetic map and identification of a new *fts* locus (*ftsZ*). *J Bacteriol* **142**: 615-620.
- Lwoff, A., (1953) Lysogeny. *Bacteriol Rev* **17**: 269-337.
- Makarova, K.S., Y.I. Wolf & E.V. Koonin, (2009) Comprehensive comparative-genomic analysis of Type 2 toxin-antitoxin systems and related mobile stress response systems in prokaryotes. *Biol Direct* **4**: 19.
- Meijer, W.J., A. Serna-Rico & M. Salas, (2001) Characterization of the bacteriophage phi29-encoded protein p16.7: a membrane protein involved in phage DNA replication. *Mol Microbiol* **39**: 731-746.

- Moreau, S., V. Leret, C. Le Marrec, H. Varangot, M. Ayache, S. Bonnassie, C. Blanco & A. Trautwetter, (1995) Prophage distribution in coryneform bacteria. *Res Microbiol* **146**: 493-505.
- Muñoz-Espin, D., R. Daniel, Y. Kawai, R. Carballido-López, V. Castilla-Llorente, J. Errington, W.J. Meijer & M. Salas, (2009) The actin-like MreB cytoskeleton organizes viral DNA replication in bacteria. *Proc Natl Acad Sci U S A*.
- Muñoz-Espin, D., I. Holguera, D. Ballesteros-Plaza, R. Carballido-López & M. Salas, (2010) Viral terminal protein directs early organization of phage DNA replication at the bacterial nucleoid. *Proc Natl Acad Sci U S A* **107**: 16548-16553.
- Muñoz-Espin, D., G. Serrano-Heras & M. Salas, (2012) Role of Host Factors in Bacteriophage phi29 DNA Replication. *Adv Virus Res* **82**: 351-383.
- Murray, H. & J. Errington, (2008) Dynamic control of the DNA replication initiation protein DnaA by Soj/ParA. *Cell* **135**: 74-84.
- Ni, L., W. Xu, M. Kumaraswami & M.A. Schumacher, (2010) Plasmid protein TubR uses a distinct mode of HTH-DNA binding and recruits the prokaryotic tubulin homolog TubZ to effect DNA partition. *Proc Natl Acad Sci U S A* **107**: 11763-11768.
- Nickels, B.E., (2009) A New Twist on a Classic Paradigm: Illumination of a Genetic Switch in *Vibrio cholerae* phage CTX Phi. *J Bacteriol* **191**: 6779-6781.
- Niebisch, A. & M. Bott, (2001) Molecular analysis of the cytochrome  $bc_1-aa_3$  branch of the *Corynebacterium glutamicum* respiratory chain containing an unusual diheme cytochrome  $c_1$ . *Arch Microbiol* **175**: 282-294.
- Niebisch, A. & M. Bott, (2003) Purification of a cytochrome  $bc_1-aa_3$  supercomplex with quinol oxidase activity from *Corynebacterium glutamicum*. - Identification of a fourth subunit of cytochrome  $aa_3$  oxidase and mutational analysis of diheme cytochrome  $c_1$ . *J Biol Chem* **278**: 4339-4346.
- Nir, U., H. Ladan, Z. Malik & Y. Nitzan, (1991) *In vivo* effects of porphyrins on bacterial DNA. *J Photochem Photobiol. B* **11**: 295-306.
- Ogino, H., H. Teramoto, M. Inui & H. Yukawa, (2008) DivS, a novel SOS-inducible cell-division suppressor in *Corynebacterium glutamicum*. *Mol Microbiol* **67**: 597-608.
- Ohlendorf, D.H., W.F. Anderson, M. Lewis, C.O. Pabo & B.W. Matthews, (1983) Comparison of the Structures of Cro and lambda Repressor Proteins from Bacteriophage lambda. *J Mol Biol* **169**: 757-769.
- Oliva, M.A., A.J. Martin-Galiano, Y. Sakaguchi & J.M. Andreu, (2012) Tubulin homolog TubZ in a phage-encoded partition system. *Proc Natl Acad Sci U S A* **109**: 7711-7716.
- Oppenheim, A.B., O. Kobiler, J. Stavans, D.L. Court & S. Adhya, (2005) Switches in Bacteriophage Lambda Development. *Annu Rev Genet* **39**: 409-429.
- Ozyamak, E., J. Kollman, D.A. Agard & A. Komeili, (2013) The bacterial actin MamK: *in vitro* assembly behavior and filament architecture. *J Biol Chem* **288**: 4265-4277.
- Pabo, C.O. & M. Lewis, (1982) The operator-binding domain of lambda repressor: structure and DNA recognition. *Nature* **298**: 443-447.
- Pátek, M., J. Ludvík, O. Benada, J. Hochmannová, J. Nesvera, V. Krumphanzl & M. Bucko, (1985) New bacteriophage-like particles in *Corynebacterium glutamicum*. *Virology* **140**: 360-363.
- Plassmeier, J., M. Persicke, A. Pühler, C. Sterthoff, C. Rückert & J. Kalinowski, (2012) Molecular characterization of PrpR, the transcriptional activator of propionate catabolism in *Corynebacterium glutamicum*. *J Biotechnol* **159**: 1-11.
- Quinones, M., H.H. Kimsey & M.K. Waldor, (2005) LexA Cleavage Is Required for CTX Prophage Induction. *Mol Cell* **17**: 291-300.
- Rakonjac, J., N.J. Bennett, J. Spagnuolo, D. Gagic & M. Russel, (2011) Filamentous bacteriophage: biology, phage display and nanotechnology applications. *Current Iss Mol Biol* **13**: 51-76.

- Ramos, A., M. Letek, A.B. Campelo, J. Vaquera, L.M. Mateos & J.A. Gil, (2005) Altered morphology produced by *ftsZ* expression in *Corynebacterium glutamicum* ATCC 13869. *Microbiology* **151**: 2563-2572.
- Reinhard, F., R. Miyazaki, N. Pradervand & J.R. van der Meer, (2013) Cell differentiation to "mating bodies" induced by an integrating and conjugative element in free-living bacteria. *Curr Biol* **23**: 255-259.
- Roberts, K.L. & J.D. Baines, (2011) Actin in Herpesvirus Infection. *Viruses* **3**: 336-346.
- Rokney, A., O. Kobiler, A. Amir, D.L. Court, J. Stavans, S. Adhya & A.B. Oppenheim, (2008) Host responses influence on the induction of lambda prophage. *Mol Microbiol* **68**: 29-36.
- Salje, J., P. Gayathri & J. Löwe, (2010) The ParMRC system: molecular mechanisms of plasmid segregation by actin-like filaments. *Nat Rev Microbiol* **8**: 683-692.
- Salje, J. & J. Löwe, (2008) Bacterial actin: architecture of the ParMRC plasmid DNA partitioning complex. *EMBO J* **27**: 2230-2238.
- Salje, J., F. van den Ent, P. de Boer & J. Löwe, (2011) Direct Membrane Binding by Bacterial Actin MreB. *Mol Cell* **43**: 478-487.
- Sberro, H., A. Leavitt, R. Kiro, E. Koh, Y. Peleg, U. Qimron & R. Sorek, (2013) Discovery of Functional Toxin/Antitoxin Systems in Bacteria by Shotgun Cloning. *Mol Cell* **50**: 136-148.
- Schäfer, A., A. Tauch, N. Droste, A. Pühler & J. Kalinowski, (1997) The *Corynebacterium glutamicum* *cglIM* gene encoding a 5-cytosine methyltransferase enzyme confers a specific DNA methylation pattern in an McrBC-deficient *Escherichia coli* strain. *Gene* **203**: 95-101.
- Schmitt, M.P., (1997) Transcription of the *Corynebacterium diphtheriae* *hmuO* gene is regulated by iron and heme. *Infect Immun* **65**: 4634-4641.
- Schröder, J. & A. Tauch, (2010) Transcriptional regulation of gene expression in *Corynebacterium glutamicum*: the role of global, master and local regulators in the modular and hierarchical gene regulatory network. *FEMS Microbiol Rev* **34**: 685-737.
- Schubert, R.A., I.B. Dodd, J.B. Egan & K.E. Shearwin, (2007) Cro's role in the CI-Cro bistable switch is critical for lambda's transition from lysogeny to lytic development. *Genes Dev* **21**: 2461-2472.
- Schumacher, M.A., (2008) Structural biology of plasmid partition: uncovering the molecular mechanisms of DNA segregation. *Biochem J* **412**: 1-18.
- Schumacher, M.A., T.C. Glover, A.J. Brzoska, S.O. Jensen, T.D. Dunham, R.A. Skurray & N. Firth, (2007) Segrosome structure revealed by a complex of ParR with centromere DNA. *Nature* **450**: 1268-1271.
- Sengupta, M., H.J. Nielsen, B. Youngren & S. Austin, (2010) P1 plasmid segregation: accurate redistribution by dynamic plasmid pairing and separation. *J Bacteriol* **192**: 1175-1183.
- Sievers, F., A. Wilm, D. Dineen, T.J. Gibson, K. Karplus, W. Li, R. Lopez, H. McWilliam, M. Remmert, J. Soding, *et al.*, (2011) Fast, scalable generation of high-quality protein multiple sequence alignments using Clustal Omega. *Mol Syst Biol* **7**: 539.
- Smith, G., (2012) Herpesvirus Transport to the Nervous System and Back Again. *Annu Rev Microbiol* **66**: 153-176.
- Smits, W.K., O.P. Kuipers & J.W. Veening, (2006) Phenotypic variation in bacteria: the role of feedback regulation. *Nat Rev Microbiol* **4**: 259-271.
- St-Pierre, F. & D. Endy, (2008) Determination of cell fate selection during phage lambda infection. *Proc Natl Acad Sci U S A* **105**: 20705-20710.
- Stauff, D.L., D. Bagaley, V.J. Torres, R. Joyce, K.L. Anderson, L. Kuechenmeister, P.M. Dunman & E.P. Skaar, (2008) *Staphylococcus aureus* HrtA is an ATPase Required for Protection against Heme Toxicity and Prevention of a Transcriptional Heme Stress Response. *J Bacteriol* **190**: 3588-3596.
- Sullivan, N.L., K.A. Marquis & D.Z. Rudner, (2009) Recruitment of SMC by ParB-*parS* organizes the origin region and promotes efficient chromosome segregation. *Cell* **137**: 697-707.

- Svenningsen, S.L., N. Costantino, D.L. Court & S. Adhya, (2005) On the role of Cro in lambda prophage induction. *Proc Natl Acad Sci U S A* **102**: 4465-4469.
- Szambowska, A., M. Pierechod, G. Wegrzyn & M. Glinkowska, (2011) Coupling of transcription and replication machineries in lambda DNA replication initiation: evidence for direct interaction of *Escherichia coli* RNA polymerase and the lambdaO protein. *Nucleic Acids Res* **39**: 168-177.
- Szwedziak, P., Q. Wang, S.M. Freund & J. Lowe, (2012) FtsA forms actin-like protofilaments. *EMBO J* **31**: 2249-2260.
- Tao, L., X. Wu & B. Sun, (2010) Alternative Sigma Factor sigmaH Modulates Prophage Integration and Excision in *Staphylococcus aureus*. *PLoS Pathog* **6**: e1000888.
- Thanbichler, M. & L. Shapiro, (2006) MipZ, a spatial regulator coordinating chromosome segregation with cell division in *Caulobacter*. *Cell* **126**: 147-162.
- Tomasz, M., (1995) Mitomycin C: small, fast and deadly (but very selective). *Chem Biol* **2**: 575-579.
- Tu, A.H., L.L. Voelker, X. Shen & K. Dybvig, (2001) Complete Nucleotide Sequence of the *Mycoplasma* Virus P1 Genome. *Plasmid* **45**: 122-126.
- Twort, F.W., (1915) An investigation on the nature of ultra-microscopic viruses. *Lancet* **186**: 1241-1243.
- van den Ent, F., L.A. Amos & J. Löwe, (2001) Prokaryotic origin of the actin cytoskeleton. *Nature* **413**: 39-44.
- van den Ent, F., C.M. Johnson, L. Persons, P. de Boer & J. Löwe, (2010) Bacterial actin MreB assembles in complex with cell shape protein RodZ. *EMBO J* **29**: 1081-1090.
- Veening, J.W., W.K. Smits & O.P. Kuipers, (2008) Bistability, epigenetics, and bet-hedging in bacteria. *Annu Rev Microbiol* **62**: 193-210.
- Waldor, M.K. & D.I. Friedman, (2005) Phage regulatory circuits and virulence gene expression. *Curr Opin Microbiol* **8**: 459-465.
- Wennerhold, J. & M. Bott, (2006) The DtxR Regulon of *Corynebacterium glutamicum*. *J Bacteriol* **188**: 2907-2918.
- Wieschalka, S., B. Blombach, M. Bott & B.J. Eikmanns, (2013) Bio-based production of organic acids with *Corynebacterium glutamicum*. *Microb Biotechnol* **6**: 87-102.
- Wozniak, R.A. & M.K. Waldor, (2010) Integrative and conjugative elements: mosaic mobile genetic elements enabling dynamic lateral gene flow. *Nat Rev Microbiol* **8**: 552-563.

## 6 Appendix

### 6.1 Additional Figures – AlpC

MAQ**KQ**D**T**THV**S**ED**D**AP**W**R**N**V**R**M**R**F**P**ET**D**A**I**VE**R**F**L**ET**Q**G**A**R**G**I**S**L**A**M**R**Q**L**I**Y**L  
 F**V**A**E**Y**G**D**V**E**V**AT**V**I**G**L**K**L**V**E**S**L**Q**A**G**A**E**G**S**D**L**F**A**Q**L**A**A**G**V**A**D**V**D**A**V**T**T**R**K**K**A**P**Q**  
 Q**I**A**P**P**S**T**T**T**R**A**P**D**Q**V**N**E**F**V**A**E**A**E**S**Q**P**V**E**E**S**V**V**E**A**K**V**P**K**Q**Q**V**A**P**Q**P**A**Q**K**P**E**Q**K**P  
 E**Q**K**S**A**Q**P**A**Q**S**E**P**D**D**G**F**D**M**D**D**V**M**G**Q**A**F**G**R**

**Fig. 6.1.1 Amino acid sequence of AlpA (Cg1891) with charged residues.** AlpA (187 amino acids) contains 26% charged residues (aspartat (D) and glutamate (E) in red, lysine (K) and arginine (R) in blue). ParR (117 amino acids) contains 28% charged residues.

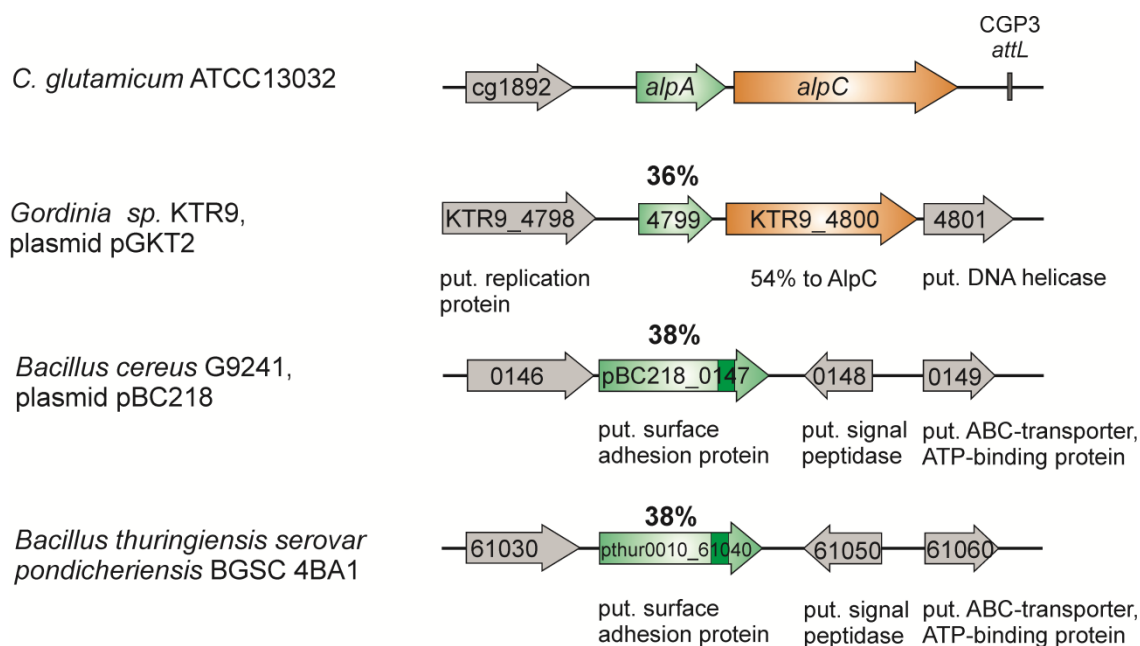


**Fig. 6.1.2 Genetic organization of the alpAC locus.** Alignment of the amino acid sequence of AlpC and AlpA was conducted by BLAST (NCBI, <http://blast.ncbi.nlm.nih.gov/>). The genes with similarity to AlpA are shown in green; in the genes coding for a putative adhesion protein the overlapping region sharing similarities with AlpA is indicated in dark green. The gene KTR9\_4799 from plasmid pGKT2 in *Gordinia* sp. KTR9 showed 36% sequence identity. The genes pBC218\_0147 from plasmid pBC218 in *Bacillus cereus* G9241, and pthur0010\_61040 from *Bacillus thuringiensis* serovar *pondicheriensis* BGSC 4BA1 showed 38% sequence identity to AlpA. The gene annotation is indicated below the respective gene.

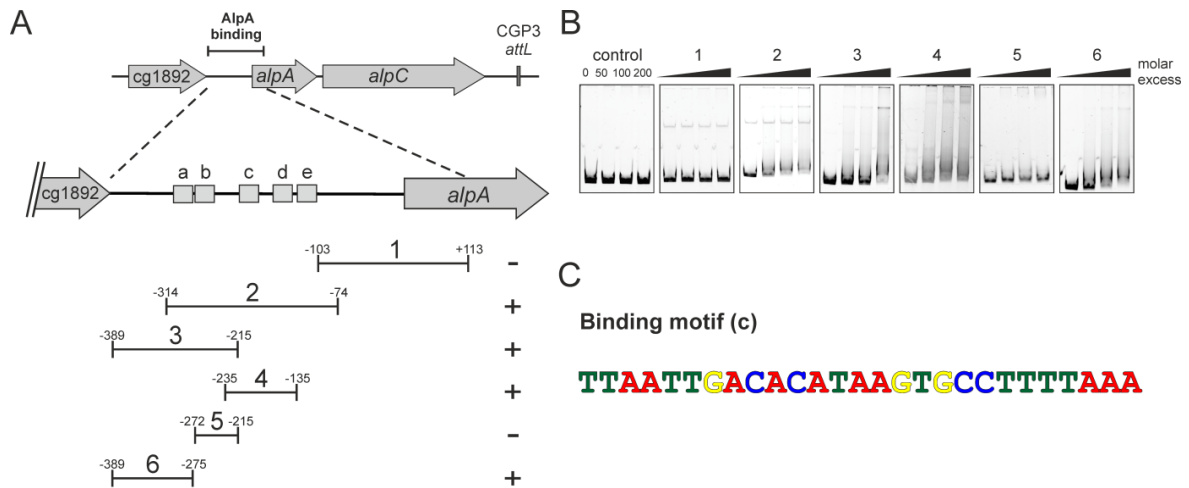


**Fig. 6.1.3 Search of the DNA-binding region of AlpA in the upstream promoter region of *alpAC* (designated as *alpS* site).** (A) Overview of the tested subfragments covering the upstream promoter region of *alpAC*. (B) Corresponding EMSA study to (A). To test for AlpA-DNA interaction, the DNA fragments were incubated with varying molar excess of AlpA. A detailed description is included in the manuscript for *alpC* (see 3.2 in this work). (C) Sequence of binding motif c (30 bp) that was shifted by AlpA in the promoter region of *alpAC*. Motif prediction of an AlpA binding site revealed five putative binding motifs in the upstream region of *alpAC* (grey boxes a-e in (A)). The promoter region has high AT-nucleotide content and revealed many motifs. However, only motif c was shifted. The motifs were predicted by the program MEME suite (<http://meme.nbcr.net/meme/>).

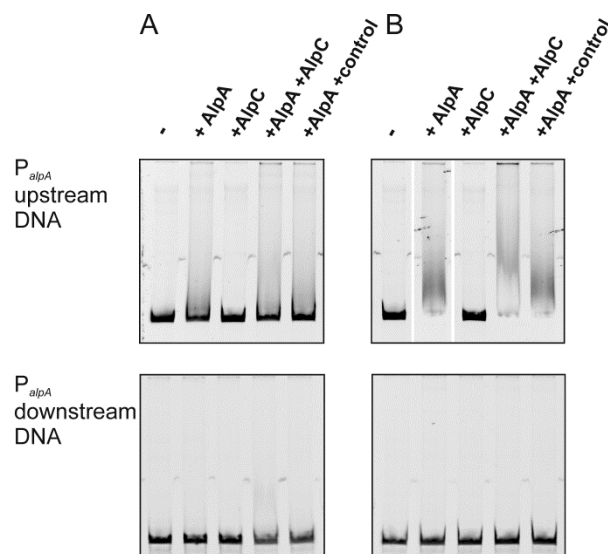


**Fig. 6.1.4 Evidence for an interaction of AlpA and AlpC in the presence of the upstream region of *alpAC*.** 100 ng DNA of the upstream region of *alpAC* (500bp) containing the binding site of AlpA, *alpS*, were incubated with AlpA (200-fold molar excess) as indicated without ATP (A) or with ATP (B). AlpC (30-fold molar excess) or the control protein HrrA (2-fold molar excess) were added as indicated. (B) To induce polymerization of AlpC filaments ATP was added to the reaction mixture. The downstream region of the *alpAC* operon (500 bp) was used as control fragment in both experiments. After 20 min of incubation the samples were separated on a 10% non-denaturing polyacrylamide gel and stained with SYBR green I. No difference was observed without ATP, but the addition of ATP to induce AlpC filament formation resulted in a different shift. This provide first evidence of an interaction of AlpC filaments with AlpA in the presence of *alpS* DNA.

## 6.2 Supplemental Material – Cg2040

**Tab. S1** Oligonucleotides used in this study

Oligonucleotide	Sequence 5' – 3' <sup>1)</sup>	Application <sup>2)</sup>
Dcg2040-1	CCGGAATTCGAAGAGAAAGTATGTCTTCAATATG ( <i>EcoRI</i> )	Fw for upstream flanking region of Dcg2040
Dcg2040-2	CCCATCCACTAAACTTAAACAGAGTTTTACCTTATAT CCTTCATT	Rv for upstream flanking region of Dcg2040
Dcg2040-3	TGTTTAAGTTTAGTGGATGGGGTTGATTGGGAAAA GCCCATTTTG	Fw for downstream flanking region of Dcg2040
Dcg2040-4	CGCGGATCCGGATCTGCGTGTGGAATGCAC ( <i>BamHI</i> )	Rv for downstream flanking region of Dcg2040
Dcg2040-5	CTGCTCTGATAACCATATTGAAGAA	Fw for verification of the deletion of cg2040
Dcg2040-6	AGGCCGTCGATTTACTAAAAACC	Rv for verification of the deletion of cg2040
cg2040-RBS-fw	CGCGGATCCAAAGGAGATATAGATATGAGAGGATA TAAGGTAAAACCTC ( <i>BamHI</i> )	Fw for cg2040, adding a ribosome binding site
cg2040-Sac-rv	GCGCGAGCTCCTACGCCAAAATGGGCTTTTC ( <i>SacI</i> )	Rv for cg2040 of pEKEx2-cg2040
Cg2040_Nde_fw	CGCCATATGAGAGGATATAAGGTAAAACCTCATG ( <i>NdeI</i> )	Fw for cg2040 in pET-TEV-cg2040
Cg2040_Xho_rv	CCGCTCGAGCTACGCCAAAATGGGCTTTTCC ( <i>XhoI</i> )	Rv for cg2040 in pET-TEV-cg2040
cg2040-TEV-fw	GCGCGAGCTCCGAGAACCTGTATTTTCAGGGCCAT ATG ( <i>SacI</i> )	Fw for cg2040, inserting a TEV cleavage site (template: pET-TEV-cg2040)
cg2040-Xba-rv	TGCTCTAGACTACGCCAAAATGGGCTTTTC ( <i>XbaI</i> )	Rv for cg2040 of pMBP-TEV-cg2040 (template: pET-TEV-cg2040)
Cg2033_prom_fw	CATCCCACAACCTGGTTTCAGGT	Fw for EMSA- fragment 500 bp cg2033
<b>Oligonucleotides for EMSA</b>		
Cg2033_prom_rv	CAAACATCAGCGTACTGACAGC	Rv for EMSA- fragment 500 bp cg2033
Cg2036_prom_fw	CACTTCCAAGGAAGATACACGC	Fw for EMSA- fragment 500 bp cg2036
Cg2036_prom_rv	ATGTTAAGAGCGTAACGGATATCA	Rv for EMSA- fragment 500 bp cg2036
Cg2038_prom_fw	CTGAAGCAATCTATTTGATTCCTG	Fw for EMSA- fragment 500 bp cg2038
Cg2038_prom_rv	TCCCCTTGATAAGTAAGCCTCAA	Rv for EMSA- fragment 500 bp cg2038
Cg2039_prom_fw	CAACGAACTACCCCATGGCGAG	Fw for EMSA- fragment 500 bp cg2039
Cg2039_prom_rv	CTGCACTAACTCATCATGATGAG	Rv for EMSA- fragment 500 bp cg2039
Cg2040_prom_fw	GAAGAGAAAGTATGTCTTCAATATG	Fw for EMSA- fragment 500 bp cg2040
Cg2040_prom_rv	CATCGCTTTCTTACTGTGCGTC	Rv for EMSA- fragment 500 bp cg2040
Cg2041_prom_fw	GTTGCTGGGTTAGTCAGGCGA	Fw for EMSA- fragment 500 bp cg2041
Cg2041_prom_rv	CGTTTCGGTCAACATATTGAAGA	Rv for EMSA- fragment 500 bp cg2041
Hmp-fw	CGACGGCTTCGCAGCGGTCGTC	Fw for EMSA- fragment 500 bp <i>hmp</i> (control)
Hmp-rv	GGAAGCGTTGCTTTGATCACCTC	Rv for EMSA- fragment 500 bp <i>hmp</i> (control)
Cg2040p_1_rv	GACTGGAAATACTCTTAACATGCT	Fw for EMSA- subfragment 125 bp cg2040-1
Cg2040p_2_fw	AGCATGTTAAGAGTATTTCCAGTC	Rv for EMSA- subfragment 125 bp cg2040-2
Cg2040p_2_rv	GCATCAATATTGAGTATCCATCAC	Fw for EMSA- subfragment 125 bp cg2040-2
Cg2040p_3_fw	GTGATGGATACTCAATATTGATGC	Rv for EMSA- subfragment 125 bp

---

<b>Cg2040p_3_rv</b>	CTCGGTGTTTTGACGGTGTGTTG	cg2040-3 Fw for EMSA- subfragment 125 bp cg2040-3
<b>Cg2040p_4_fw</b>	CAAACACCGTCAAAACACCGAG	Rv for EMSA- subfragment 125 bp cg2040-4
<b>Cg2040p_4_rv</b>	GAATTAATCTACTGGTGATCCATC	Fw for EMSA- subfragment 125 bp cg2040-4
<b>Cg2040p_5_fw</b>	GATGGATCACCAGTAGATTAATTC	Rv for EMSA- subfragment 125 bp cg2040-5
<b>2040-motif-M1-fw</b>	GATGGATCACCAGTAGATTAATTCGTCTTAA CAT	Fw for EMSA-motif 30 bp cg2040
<b>2040-motif-M1-rv</b>	ATGTTAAGACGAATTAATCTACTGGTGATCC ATC	Rv for EMSA-motif 30 bp cg2040
<b>2040-motif-M2-fw</b>	CAACGAACTACCCCATGGCGAGTTTTTA	Fw for EMSA-motif 30 bp cg2040
<b>2040-motif-M2-rv</b>	TAAAACTCGCCAATGGGGGTAGTTCGTTG	Rv for EMSA-motif 30 bp cg2040
<b>2040-motif-M3-fw</b>	GAAAAAATTGAATGAGAGGATATAAGGTAA	Fw for EMSA-motif 30 bp cg2040
<b>2040-motif-M3-rv</b>	TTACCTTATATCCTCTCATTCAATTTTTTC	Rv for EMSA-motif 30 bp cg2040
<b>2040-motif-M4-fw</b>	AACTCATGACGCACAGTAAGAAAGCGATG	Fw for EMSA-motif 30 bp cg2040
<b>2040-motif-M4-rv</b>	CATCGCTTCTTACTGTGCGTCATGAGTT	Rv for EMSA-motif 30 bp cg2040
<b>2040-motif-M5-fw</b>	CCATTGGCGAGTTTTTAGAAAAAATTGAAT	Fw for EMSA-motif 30 bp cg2040
<b>2040-motif-M5-rv</b>	ATTCATTTTTTCTAAAACTCGCAATGG	Fw for EMSA-motif 30 bp cg2040
<b>2040-motif-M6-fw</b>	GAGAGGATATAAGGTAAAACTCATGACGCA	Rv for EMSA-motif 30 bp cg2040
<b>2040-motif-M6-rv</b>	TGCGTCATGAGTTTTACCTTATATCCTCTC	Fw for EMSA-motif 30 bp cg2040
<b>2040-M6-mut1-fw</b>	CTCAGGATATAAGGTAAAACTCATGACGCA	Fw for EMSA-mutated motif 30 bp cg2040-M6
<b>2040-M6-mut1-rv</b>	TGCGTCATGAGTTTTACCTTATATCCTGAG	Rv for EMSA-mutated motif 30 bp cg2040-M6
<b>2040-M6-mut2-fw</b>	GAGTCCATATAAGGTAAAACTCATGACGCA	Fw for EMSA-mutated motif 30 bp cg2040-M6
<b>2040-M6-mut2-rv</b>	TGCGTCATGAGTTTTACCTTATATGGACTC	Rv for EMSA-mutated motif 30 bp cg2040-M6
<b>2040-M6-mut3-fw</b>	GAGAGGTATTAAGGTAAAACTCATGACGCA	Fw for EMSA-mutated motif 30 bp cg2040-M6
<b>2040-M6-mut3-rv</b>	TGCGTCATGAGTTTTACCTTAATACCTCTC	Rv for EMSA-mutated motif 30 bp cg2040-M6
<b>2040-M6-mut4-fw</b>	GAGAGGATAATTGGTAAAACTCATGACGCA	Fw for EMSA-mutated motif 30 bp cg2040-M6
<b>2040-M6-mut4-rv</b>	TGCGTCATGAGTTTTACCAATTATCCTCTC	Rv for EMSA-mutated motif 30 bp cg2040-M6
<b>2040-M6-mut5-fw</b>	GAGAGGATATAACCAAAAACTCATGACGCA	Fw for EMSA-mutated motif 30 bp cg2040-M6
<b>2040-M6-mut5-rv</b>	TGCGTCATGAGTTTTGGTTATATCCTCTC	Rv for EMSA-mutated motif 30 bp cg2040-M6
<b>2040-M6-mut6-fw</b>	GAGAGGATATAAGGTTTTACTCATGACGCA	Fw for EMSA-mutated motif 30 bp cg2040-M6
<b>2040-M6-mut6-rv</b>	TGCGTCATGAGTAAACCTTATATCCTCTC	Rv for EMSA-mutated motif 30 bp cg2040-M6
<b>2040-M6-mut7-fw</b>	GAGAGGATATAAGGTAAATGACATGACGCA	Fw for EMSA-mutated motif 30 bp cg2040-M6
<b>2040-M6-mut7-rv</b>	TGCGTCATGTCATTTACCTTATATCCTCTC	Rv for EMSA-mutated motif 30 bp cg2040-M6
<b>2040-M6-mut8-fw</b>	GAGAGGATATAAGGTAAAACTGTAGACGCA	Fw for EMSA-mutated motif 30 bp cg2040-M6
<b>2040-M6-mut8-rv</b>	TGCGTCTACAGTTTTACCTTATATCCTCTC	Rv for EMSA-mutated motif 30 bp cg2040-M6

---

<b>2040-M6-mut9-fw</b>	GAGAGGATATAAGGTA <del>AAACTCATCTGGCA</del>	Fw for EMSA-mutated motif 30 bp cg2040-M6
<b>2040-M6-mut9-rv</b>	TGCCAGATGAGTTTTACCTTATATCCTCTC	Rv for EMSA-mutated motif 30 bp cg2040-M6
<b>2040-M6-mu10-fw</b>	GAGAGGATATAAGGTA <del>AAACTCATGACCGT</del>	Fw for EMSA-mutated motif 30 bp cg2040-M6
<b>2040-M6-mu10-rv</b>	ACGGTCATGAGTTTTACCTTATATCCTCTC	Rv for EMSA-mutated motif 30 bp cg2040-M6

- 1) Some oligonucleotides were designed to introduce restriction sites (underlined), a TEV cleavage site (*italic, underlined*), ribosome binding sites (**bold**) or as a complementary sequence (*italic*) for overlap PCR.
- 2) Fw, forward oligonucleotide; Rv reverse nucleotide for amplification by PCR (Sambrook *et al.*, 2001).

**Tab. S2** Transcriptome analysis of strain ATCC 13032/ pEKEx2-cg2040 in comparison to ATCC 13032/ pEKEx2. <sup>1)</sup>

Gene	Gene name	Annotation	Average	n	p-value
cg0404		Nitroreductase family	0.26	3	0.000
cg0487		Conserved hypothetical protein, possibly secreted	0.44	3	0.008
cg0488	ppx1	Exopolyphosphatase	0.44	3	0.000
cg0728	phr	Deoxyribodipyrimidine photolyase	0.34	3	0.002
cg0803	thtR	Thiosulfate sulfurtransferase	0.33	3	0.003
cg0806		Hypothetical protein	0.48	3	0.004
cg0807		Hypothetical protein	0.49	3	0.008
cg0809	maf	Maf-like protein	0.45	3	0.003
cg0810		Hypothetical protein	0.47	3	0.005
cg0811	dtsR2	Acetyl/propionyl CoA carboxylase, beta subunit	0.48	3	0.000
cg0816	purK	Phosphoribosylaminoimidazole carboxylase	0.50	3	0.001
cg0817	kup	K <sup>+</sup> potassium transporter	0.47	3	0.001
cg0821		Hypothetical protein	0.50	3	0.006
cg0826		Hypothetical protein	0.47	3	0.000
cg0828		Putative dihydrofolate reductase	0.49	3	0.000
cg0829		Lactoylglutathione lyase or related lyase	0.48	3	0.001
cg0830		Membrane protein	0.39	2	0.012
cg0831		Sugar ABC transporter, permease protein	0.32	3	0.001
cg0832		ABC transporter, membrane spanning protein	0.40	3	0.001
cg0838		Helicase	0.46	3	0.005
cg0839		Hypothetical protein	0.38	3	0.002
cg0961		Homoserine O-acetyltransferase	0.49	3	0.000
cg0985	citE	Citryl-CoA lyase beta subunit homolog	0.49	3	0.009
cg1159		Putative secreted protein	0.39	3	0.009
cg1180		Glycosyltransferase, probably involved in cell wall biogenesis	2568.11	3	0.002
cg1292		Flavin-containing monooxygenase 3	6.69	3	0.000
cg1293		Putative secreted protein	7.47	3	0.000

<b>cg1294</b>		Predicted esterase of the alpha-beta hydrolase superfamily	5.82	3	0.001
<b>cg1336</b>		Putative secreted protein	0.39	3	0.038
<b>cg1484</b>		Putative secreted protein	0.44	3	0.012
<b>cg1782</b>		Tnp13b(ISCg13b), transposase	0.07	3	0.001
<b>cg1935</b>	gntR2	Gluconate-responsive repressors of genes involved in gluconate catabolism and the pentose phosphate pathway	0.25	3	0.004
<b>cg2004</b>		Similar to 232 protein-lactobacillus bacteriophage g1e	0.48	2	0.007
<b>cg2033</b>		Putative secreted protein	0.35	3	0.007
<b>cg2036</b>		Putative secreted protein	0.33	3	0.001
<b>cg2038</b> <sup>2)</sup>		Hypothetical protein predicted by Glimmer	0.10	3	0.024
<b>cg2039</b>		Hypothetical protein	0.13	3	0.002
<b>cg2040</b>		Putative transcriptional regulator	6059.84	3	0.002
<b>cg2155</b>		Hypothetical protein	0.24	3	0.011
<b>cg2183</b>		ABC-type peptide transport system, permease component	0.04	3	0.001
<b>cg2184</b>		ATPase component of peptide ABC-type transport system, contains duplicated ATPase domains	0.02	3	0.000
<b>cg2804</b>		Tnp21a(ISCg21a), transposase	0.14	3	0.000
<b>cg2808</b>		Tnp13a(ISCg13a), transposase	0.06	3	0.001
<b>cg2893</b>		Permease of the major facilitator superfamily	0.01	3	0.001
<b>cg2894</b>		Drug resistance-related transcriptional repressor	0.08	3	0.001
<b>cg2956</b>		Putative secreted protein	0.19	3	0.000
<b>cg3138</b>	ppmA	Putative membrane-bound protease modulator	2.41	3	0.006
<b>cg3139</b>		Hypothetical protein	2.01	3	0.000
<b>cg3140</b>	tagA1	Probable DNA-3-methyladenine glycosylase I protein	2.20	3	0.012
<b>cg3267</b>		Hypothetical protein	0.47	3	0.014
<b>cg3282</b>		Cation transport ATPase	2.05	3	0.010
<b>NCgl1518</b>		No annotation	0.07	3	0.001

1) For the transcriptome analysis the strains ATCC 13032/ pEKEx2-cg2040 and ATCC 13032/ pEKEx2 were cultivated in BHI with kanamycin (25 µg/ml) before a second preculture (CGXII with kanamycin) was grown. The main culture (CGXII with kanamycin) was inoculated with an OD<sub>600</sub> of 1. To induce the expression of cg2040 0.5 mM IPTG was added to the cultures. The transcriptome analysis was performed as described for Δcg2040 vs. wild type in Tab. 2.

2) The altered mRNA level of cg2038 was only detected with a signal-to-noise ratio of ≥ 3.

### 6.3 Supplemental Material – AlpC

**Table S1:** Bacterial strains, plasmids and oligonucleotides.

Strains or plasmids	Relevant characteristics	Source or reference
<b>Strains</b>		
<b>C. glutamicum ATCC 13032</b>	Biotin-auxotrophic wild type	[1]
<b>C. glutamicum <math>\Delta</math>alpC</b>	In-frame deletion of cg1890	This study
<b>CDC020</b>	ATCC 13032 with <i>ecfp-alpC</i>	This study
<b>CDC021</b>	ATCC 13032, IPTG-inducible extra-chromosomal copy of <i>alpC-cfp</i> , Kan <sup>r</sup>	This study
<b>CDC022</b>	ATCC 13032, IPTG-inducible extra-chromosomal copy of <i>alpCD<sup>301A</sup>-cfp</i> , Kan <sup>r</sup>	This study
<b>13032::pLAU44-CGP3-Spec</b>	13032 derivative containing plasmid pLAU44-CGP3-Spec integrated into the cg1905-cg1906 intergenic region	[34]
<b>CDC023</b>	CDC20, 13032 derivative containing plasmid pLAU44-CGP3-Spec integrated into the cg1905-cg1906 intergenic region	This study
<b>ATCC13032 <math>\Delta</math>alpA</b>	In-frame deletion of cg1891 ( <i>alpA</i> )	This study
<b>ATCC13032 <math>\Delta</math>alpA <i>alpC::cfp-alpC</i></b>	In-frame deletion of cg1891 ( <i>alpA</i> ) in the strain CDC020 with an allelic replacement of <i>alpC</i> to <i>cfp-alpC</i>	This study
<b>E. coli DH5<math>\alpha</math></b>	<i>supE44 <math>\Delta</math>lacU169 (<math>\phi</math>80lacZDM15) hsdR17 recA1 endA1 gyrA96 thi-1 relA1</i>	Invitrogen
<b>E. coli BL21 (DE3) pLysS</b>	F <sup>-</sup> <i>ompT hsdS(r<sub>B</sub><sup>-</sup> m<sub>B</sub><sup>-</sup>) gal dcm <math>\lambda</math>(DE3) pLysS (Cam<sup>r</sup>) (<math>\lambda</math>(DE3): <i>lacI, lacUV5-T7 gene 1, ind1, sam7, nin5</i>)</i>	Promega
<b>Plasmids</b>		
<b>pK19mobsacB</b>	Kan <sup>r</sup> ; vector for allelic exchange in <i>C. glutamicum</i> ; (pK18 <i>oriV<sub>E.c.</sub>, sacB, lacZ</i> )	[2]
<b>pK19mob-sacB-<math>\Delta</math>alpA</b>	Kan <sup>r</sup> ; pK19mobsacB derivative containing a crossover PCR product covering the up- and downstream regions of <i>alpA</i> (cg1891)	This study
<b>pK19mobsacB<math>\Delta</math>alpA-<i>cfp-alpC</i></b>	Kan <sup>r</sup> ; pK19mobsacB derivative containing a crossover PCR product covering the flanking regions of <i>alpA</i> (cg1891) in strain CDC020 ( <i>alpC</i> replaced by <i>cfp-alpC</i> )	This study
<b>pK19mobsacB-<math>\Delta</math>alpC</b>	Kan <sup>r</sup> ; pK19mobsacB derivative containing a crossover PCR product covering the up- and downstream regions of <i>alpC</i> (cg1890)	This study
<b>pCD127</b>	Integration vector, <i>ori pUC, Kan<sup>r</sup>, mob sacB eCFP-alpC</i>	This study
<b>pEKEx2</b>	Kan <sup>r</sup> ; <i>C. glutamicum</i> / <i>E. coli</i> shuttle vector for regulated gene expression ( <i>P<sub>tac</sub>, lacI<sup>q</sup>, pBL1 oriV<sub>Cg</sub>, pUC18 oriV<sub>Ec</sub></i> )	[3]
<b>pCD129</b>	Kan <sup>r</sup> , <i>P<sub>tac</sub> lacI<sup>q</sup> pBL1 oriV<sub>C.g.</sub> pUC18 oriV<sub>E.c.</sub> AlpC<sup>+</sup>-CFP</i>	This study
<b>pCD130</b>	Kan <sup>r</sup> , <i>P<sub>tac</sub> lacI<sup>q</sup> pBL1 oriV<sub>C.g.</sub> pUC18 oriV<sub>E.c.</sub> AlpC<sup>D301A+</sup>-CFP</i>	This study
<b>pEKEx2-<i>yfp-tetR</i></b>	Kan <sup>r</sup> , pEKEx2 derivative containing <i>yfp-tetR</i> under control of the <i>P<sub>tac</sub></i> promoter	[4]
<b>pET16(b)</b>	<i>bla PT7lac-10his lacI</i>	Novagen
<b>pCD115</b>	<i>bla PT7lac-10his-alpC lacI</i>	This study
<b>pCD116</b>	<i>bla PT7lac-10his-alpCD301A lacI</i>	This study
<b>pET-TEV</b>	Kan <sup>r</sup> ; pET28b derivative for overexpression of genes in <i>E. coli</i> (pBR322 <i>oriV<sub>E.c.</sub>, PT7, lacI</i> )	[5]
<b>pET-TEV-<i>alpA</i></b>	Kan <sup>r</sup> , pET-TEV derivative to overproduce AlpA with an N-terminal His <sub>10</sub> tag	This study
<b>pJC1</b>	Kan <sup>r</sup> , Amp <sup>r</sup> , <i>E. coli</i> – <i>C. glutamicum</i> shuttle vector	[6]
<b>pJC1-P<sub>alpA</sub>-<i>alpA-eyfp</i></b>	Kan <sup>r</sup> , pJC1 derivative containing <i>alpA-eyfp</i> , encoding an AlpA-eYFP protein fusion under the control of the native promoter <i>P<sub>alpA</sub></i>	This study

Oligonucleotide	Sequence (5' → 3') and properties <sup>a</sup>
<b>DalpC-1</b>	ATATATGAATTCTTGTGGTTCGCTGAATACGGTG (EcoRI)
<b>DalpC-2</b>	CCCATCCACTAAACTTAAACACACATTCACAGCGCTGGTCATAATC
<b>DalpC-3</b>	TGTTTAAGTTTAGTGGATGGGCGCTCGATTGCAGCGAAAGCACG
<b>DalpC-4</b>	TATATAGGATCCAGCGCGCCAAAGAAAACACAGAG (BamHI)
<b>DalpA-1</b>	TATATAGAATTCCCATTTTCGGGGTGATGGTTAC (EcoRI)
<b>DalpA-2</b>	CCCATCCACTAAACTTAAACACGTGTCCTGTTTTGAGCCATGTG
<b>DalpA-3</b>	TGTTTAAGTTTAGTGGATGGGGATGTCATGGGCCAAGCGTTCCG
<b>DalpA-4</b>	TATATAGGATCCTCGTGCAGACAAGCTGCGCGTGCC (BamHI)
<b>DalpA-cfp-<i>alpC</i>-4</b>	TATATAGGATCCGTCCTCCTTGAAGTCGATGCC (BamHI)
<b><i>alpA</i>-NdeI-fw</b>	CGCCATATGGCTCAAAAACAGGACACGAC (NdeI)
<b><i>alpA</i>-EcoRI-rv</b>	CCGGAATTCCTAGCGACCGAACGCTTGG (EcoRI)
<b>PalpA-BamHI-fw</b>	CGCGGATCCGTCATGGTGGGGCTCCATTAG (BamHI)
<b><i>alpA</i>-link-rv</b>	GCCAGCAGCGCCGCGACCGAACGCTTGGCC
<b><i>eyfp</i>-link-fw</b>	GGCGCTGCTGGCATGGTGGAGCAAGGGCGAGG
<b><i>eyfp</i>-Sall-rv</b>	CGCGTCGACTTATCTAGACTTGTACAGCTCGTC (Sall)
<b><i>alpA</i>-up-fw</b>	TGTCATGGTGGGGCTCCATTA
<b><i>alpA</i>-up-rv</b>	TGTGTTTCCAAAACCGCTCAAC
<b><i>alpC</i>-down-fw</b>	AAGGACTTATGATTGCGGCAC
<b><i>alpC</i>-down-rv</b>	CTGGGGGCTAGAGCGCGCCAA
<b>Cg2036-up-fw</b>	CACTTCCAAGGAAGATACACGC
<b>Cg2036-up-rv</b>	ATGTTAAGAGCGTAACGGATATCA
<b>Phage-LC-for</b>	CCCACGTTCACCCCACAAACG
<b>Phage-LC-rev</b>	CTAAAATGAAGCCATCGCGACC
<b><i>ddh</i>-LC-for</b>	ACGTGCTGTTCTGTGCATGG
<b><i>ddh</i>-LC-rev</b>	GCTCGGCTAAGACTGCCGCT
<b>Alp-up-Hind-F</b>	CAGAAAGCTTTGTGGGTGAAGGTACT (HindIII)
<b>Alp-up-Sal-R</b>	CAGGTCGACCTTGCGTGCTTTCGC (Sall)
<b>Alp-D-Xba-F</b>	CAGTCTAGATAATTAATACCTAGTT (XbaI)
<b>Alp-D-Bam-R</b>	CATGGATCCCACTCATTACCGCC (BamHI)
<b>eCFP-Sall-F</b>	CATGTCGACATGGTGAGCAAGGGC (Sall)
<b>eCFP-Xba-R</b>	CATCTCGAGCTTGTACAGCTCGTC (XbaI)
<b>AlpC-Sall-F</b>	CAGGTCGACATGACCAGCGCTGTGAAT (Sall)
<b>AlpC-BamHI-os-R</b>	CAGGGATCCCTTGCGTGCTTTCGCTGC (BamHI)
<b>CFP-SacI-F</b>	CAGGAGCTCATGGTGAGCAAGGGCGAG (SacI)
<b><i>cfp</i> EX2 Eco R mS</b>	GCGGAATTCTTACTTGTACAGCTCGTC (EcoRI)
<b>1890-D301A-F</b>	CGCCACACAATCGGTGTGGCCGTGGGTGAAGGTACTG
<b>1890-D301A-R</b>	CAGTACCTTCACCCACGCCACACCGATTGTGTGGCG
<b>AlpC-et-F</b>	CAGCTCGAGATGACCAGCGCTGTG (XhoI)
<b>AlpC-et-R</b>	CAGGGATCCTTACTTGCCTGCTTTCGC (BamHI)

<sup>a</sup> In some cases oligonucleotides were designed to introduce recognition sites for restriction endonucleases (recognition sites underlined, restriction endonucleases indicated in parentheses) or complementary 21mer sequences for generating overlap PCR products (*italics*). Amino acid mutations on mutagenesis primers are indicated in grey boldfacing.

### Legend to supplemental movies

**Movie S1. AlpC assembles into filaments.** Z-stack through *C. glutamicum* cells expressing AlpC-CFP. Cells were grown to logarithmic growth phase and imaged using a Zeiss Axioimager M1 as described in material and methods.

**Movie S2. AlpC filaments are dynamic.** Time lapse image series of *C. glutamicum* cells expressing AlpC-CFP. Cells were grown to logarithmic growth phase and imaged using a Zeiss Axioimager M1 as described in material and methods.

**Movie S3. AlpC filament dynamics need nucleotide hydrolysis.** Time lapse image series of *C. glutamicum* cells expressing AlpC<sup>D301A</sup>-CFP. Cells were grown to logarithmic growth phase and imaged using a Zeiss Axioimager M1 as described in material and methods. Many cells only show foci or patches of AlpC-CFP, but no filaments. Indeed only 1.6 % of all cells expressing AlpC<sup>D301A</sup>-CFP show clear filaments. Time lapse analysis shows that these filaments are not as dynamic as wild type AlpC-CFP filaments.

### Supplemental material references

1. Kinoshita, S., Udaka, S., and Shimono, M. (1957). Studies on the amino acid fermentation: I. Production of L-glutamic acid by various microorganisms. *J. Gen. Appl. Microbiol.* 3, 193-205.
2. Schäfer, A., Tauch, A., Jäger, W., Kalinowski, J., Thierbach, G., and Pühler, A. (1994). Small mobilizable multi-purpose cloning vectors derived from the *Escherichia coli* plasmids pK18 and pK19: selection of defined deletions in the chromosome of *Corynebacterium glutamicum*. *Gene* 145, 69-73.
3. Eikmanns, B.J., Kleinertz, E., Liebl, W., and Sahm, H. (1991). A family of *Corynebacterium glutamicum/Escherichia coli* shuttle vectors for cloning, controlled gene expression, and promoter probing. *Gene* 102, 93-98.
4. Frunzke, J., Bramkamp, M., Schweitzer, J.E., and Bott, M. (2008). Population Heterogeneity in *Corynebacterium glutamicum* ATCC 13032 caused by prophage CGP3. *J Bacteriol* 190, 5111-5119.
5. Bussmann, M., Baumgart, M., and Bott, M. (2010). RosR (Cg1324), a hydrogen peroxide-sensitive MarR-type transcriptional regulator of *Corynebacterium glutamicum*. *J Biol Chem* 285, 29305-29318.
6. Cremer, J., Eggeling, L., and Sahm, H. (1990). Cloning the *dapA dapB* cluster of the lysine-secreting bacterium *Corynebacterium glutamicum*. *Mol Gen Genet* 220, 478-480.

## 6.4 Supplementary Material – ChrSA

### Cloning techniques

In-frame deletion mutants of the operons *hrtBA*, *chrSA*, and *hrrSA* were constructed *via* the two-step homologous recombination method as described before (Niebisch & Bott, 2001). Therefore, the corresponding upstream region covering the first 30 bp of the gene *hrtB* was amplified by PCR using the oligonucleotides DhrtBA-1 and DhrtBA-2. Amplification of the downstream region with the last 30 bp of *hrtA* was performed with the oligonucleotides DhrtBA-3 and DhrtBA-4. Subsequently, the up- and downstream flanking region of *hrtBA* and *chrSA* were fused *via* an overlap of 21 bp by overlap extension PCR with the oligonucleotides DhrtBA-1/DhrtBA-4 and DchrSA-1/DchrSA-4, respectively. PCR products were ligated into pK19*mobsacB* at the *Bam*HI and *Sal*I restriction sites. The pK19*mobsacB* inserts for the deletion of *chrSA* and *hrrSA* were created analogously using the oligonucleotides DchrSA-1/DchrSA-2 plus DchrSA-3/DchrSA-4 and DhrrSA-1/DhrrSA-2 plus DhrrSA-3/DhrrSA-4, respectively.

The resulting plasmids pK19*mobsacB*- $\Delta$ *hrtBA*, pK19*mobsacB*- $\Delta$ *chrSA*, and pK19*mobsacB*- $\Delta$ *hrrSA* were used for the deletion of the corresponding genes in *C. glutamicum* by homologous recombination as described (Schäfer *et al.*, 1994). Successful deletion was verified by colony PCR and DNA sequencing (oligonucleotides: DhrtBA-fw/DhrtBA-rv, DchrSA-fw/DchrSA-rv, or DhrrSA-fw/DhrrSA-rv respectively).

For complementation of the phenotype of  $\Delta$ *hrtBA* and  $\Delta$ *chrSA*, DNA fragments covering the respective operon were amplified with the oligonucleotides *hrtBA*-RBS-fw/*hrtBA*-rv and *chrSA*-fw/*chrSA*-rv, respectively. The DNA fragment of *chrSA* and its native promoter was cloned after an *Nhe*I digestion, into the low-copy vector pJC1 (Cremer *et al.*, 1990), while the *hrtBA* DNA fragment without the native promoter but with an additional ribosome binding site was ligated into the *Pst*I restriction site of the pEKEx2 vector under the control of the IPTG-inducible promoter  $P_{tac}$ . The *C. glutamicum* wild type and the deletion strains  $\Delta$ *hrtBA* and  $\Delta$ *chrSA* were transformed with the resulting plasmids according to a standard protocol (van der Rest *et al.*, 1999).

For overproduction of ChrA with an N-terminal hexa-histidine tag (addition of 20 amino acids [MGSSHHHHHSSGLVPRGSH] at the N-terminus of the protein ChrA), the coding region *chrA* (cg2200) was amplified by PCR with the oligonucleotides *chrA*-*Nde*I-fw and *chrA*-*Hind*III-rv thereby inserting *Nde*I and *Hind*III restriction sites. The purified PCR product was cloned into pET28b (Novagen) resulting in the vector pET28b-*chrA*.

For the construction of promoter fusions of the promoter of *chrSA* and *hrtBA* with *eyfp*, encoding the yellow fluorescent protein eYFP, 235 bp of the intergenic region of *chrSA* and *hrtBA* were amplified with the oligonucleotides PchrS-*Bam*HI-fw/PchrS-8C-RBS-*Nde*I-rv and PhrtB-*Bam*HI-fw/PhrtB-8C-*Nde*I-rv, respectively, thereby covering the promoter region and the first 24 bp of the respective gene. After 8 codons, a stop codon, a ribosome binding site and *Bam*HI and *Nde*I restriction sites were inserted by the designed oligonucleotides. As N-terminal peptide-tags may affect protein stability, we used this strategy to translate unaltered eYFP, but to include the first 24

bp of the leaderless transcripts of *chrS* and *hrtB*. The resulting fragments were ligated in front of *eyfp* by exchanging the *brnF* promoter cassette within the vector pJC1-*lrp-brnF'-eyfp* (Mustafi *et al.*, 2012), resulting in the plasmids pJC1-P<sub>*chrSA*</sub>-*eyfp* and pJC1-P<sub>*hrtBA*</sub>-*eyfp*. For the promoter fusion of *hmuO* and *eyfp*, the *hmuO* upstream region was amplified by using the oligonucleotides PhmuO-NheI-fw and PhmuO-RBS-rv, while *eyfp* was amplified with the oligonucleotides eyfp-RBS-fw and eyfp-NheI-rv. To combine both fragments a cross-over PCR was performed with PhmuO-NheI-fw and eyfp-NheI-rv. The final construct consists of 494 bp of the upstream region, the first 41 codons of the *hmuO* gene followed by a stop codon, a ribosome binding site and a *NheI* restriction site. The cross-over PCR was ligated in the *NheI* restriction site of pJC1, resulting in the plasmid pJC1-P<sub>*hmuO*</sub>-*eyfp*.

### Identification of transcription start sites (TSS) and promoter regions by RNAseq

A 5'-end enriched RNAseq library was constructed according to the following procedures. 1) Depletion of stable rRNA and enrichment of mRNA molecules were performed using the Ribo-Zero™ rRNA Removal Kit for Gram-positive Bacteria (Epicentre Biotechnologies). 2) The enriched mRNA was fragmented by magnesium oxaloacetate (MgKOAc) hydrolysis. Four volumes of RNA solution were mixed with one volume of MgKOAc solution (100 mM KOAc and 30 mM MgOAc in 200 mM Tris-HCl, pH 8.1) and the mixture was incubated for 2.5 min at 94 °C. The reaction was stopped by adding an equal volume of 1 x TE (10 mM Tris, 1 mM EDTA, pH 8) and chilling on ice for 5 min. 3) The fragmented RNA was precipitated by addition of three volumes 0.3 M NaAc in ethanol with 2 µl glycogen and incubation over night at -20 °C. 4) The precipitated RNA fragments were dissolved in water and the 5'-end RNA fragments were enriched by using Terminator™ 5'-Phosphate-Dependent Exonuclease (Epicentre Biotechnologies). 5) After RNA precipitation (as above), the triphosphates were removed using RNA 5' polyphosphatase (Epicentre Biotechnologies). 6) After RNA precipitation (as above), the 5'-enriched, monophosphorylated RNA fragments were used to construct a cDNA library by using the Small RNA Sample Prep Kit (Illumina).

The fragmentation of RNA molecules (fragment sizes were 200-500 bp) and RNA concentration were monitored using the RNA 6000 Pico Assay on an Agilent 2100 Bioanalyzer (Agilent). Sequencing of the cDNA library was carried out on the GA IIx platform (Illumina). Resulting reads were aligned to the *C. glutamicum* genomic sequence using the mapping software SARUMAN (Blom *et al.*, 2011). TSS and promoter regions were deduced by combining published information about promoter regions in *C. glutamicum* (Patek & Nesvera, 2011) with 5'-end enriched RNAseq data.

**Table S1.** Bacterial strains and plasmids used in this study.

Strains	Characteristics	Reference
<i>Escherichia coli</i>		
<i>E. coli</i> DH5 $\alpha$	supE44 $\Delta$ lacU169 ( $\phi$ 80lacZDM15) hsdR17 recA1 endA1 gyrA96 thi-1 relA1	Invitrogen
<i>E. coli</i> BL21(DE3)	F <sup>-</sup> <i>ompT hsdS<sub>B</sub>(r<sub>B</sub><sup>-</sup> m<sub>B</sub><sup>-</sup>) gal dcm</i> (DE3)	(Studier & Moffatt, 1986)
<i>C. glutamicum</i>		
ATCC13032	Biotin-auxotrophic wild type	(Kinoshita <i>et al.</i> , 1957)
ATCC13032 $\Delta$ <i>chrSA</i>	In-frame deletion of the genes <i>chrS</i> (cg2200) and <i>chrA</i> (cg2201)	This study
ATCC13032 $\Delta$ <i>hrtBA</i>	In-frame deletion of the genes <i>hrtB</i> (cg2202) and <i>hrtA</i> (cg2204)	This study
ATCC13032 $\Delta$ <i>hrrSA</i>	In-frame deletion of the genes <i>hrrS</i> (cg3248) and <i>hrrA</i> (cg3247)	This study
Plasmids		
pK19 <i>mobsacB</i>	Kan <sup>r</sup> ; vector for allelic exchange in <i>C. glutamicum</i> (pK18 <i>oriV<sub>E. coli</sub></i> <i>sacB lacZ<math>\alpha</math></i> )	(Schäfer <i>et al.</i> , 1994)
pK19 <i>mobsacB</i> - $\Delta$ <i>chrSA</i>	Kan <sup>r</sup> , pK19 <i>mobsacB</i> derivative with an overlap extension PCR product of the up- and downstream regions of <i>chrS</i> (cg2201) and <i>chrA</i> (cg2200)	This study
pK19 <i>mobsacB</i> - $\Delta$ <i>hrtBA</i>	Kan <sup>r</sup> , pK19 <i>mobsacB</i> derivative with an overlap extension PCR product of the up- and downstream regions of <i>hrtB</i> (cg2202) and <i>hrtA</i> (cg2204)	This study
pJC1	Kan <sup>r</sup> , Amp <sup>r</sup> ; <i>C. glutamicum</i> shuttle vector.	(Cremer <i>et al.</i> , 1990)
pJC1- <i>chrSA</i>	pJC1 derivative containing the 1.6 kbp fragment of the genes <i>chrA</i> and <i>chrS</i> and their native promoter region (250 bp)	This study
pEKEx2	Kan <sup>r</sup> ; expression vector with <i>lacI<sup>q</sup></i> , P <sub>tac</sub> and <i>pUC18</i> multiple cloning site	(Eikmanns <i>et al.</i> , 1994)
pEKEx2- <i>hrtBA</i>	pEKEx2 containing the <i>Pst</i> I fragment of <i>hrtB</i> and <i>hrtA</i> under control of P <sub>tac</sub>	This study
pET28b	Kan <sup>r</sup> ; vector for heterologous gene expression in <i>E. coli</i> , adding an N-terminal or a C-terminal hexa-histidine tag to the synthesized protein (pBR322 <i>oriV<sub>E. coli</sub></i> , P <sub>T7</sub> , <i>lacI</i> )	Novagen
pET28b- <i>chrA</i>	Kan <sup>r</sup> , pET28b-Streptag derivative containing an <i>Nde</i> I, <i>Hind</i> III insert of cg2200 for over-production of ChrA (Cg2200) with an N-terminal hexa-histidine tag.	This study
pJC1-P <sub><i>hrtBA</i></sub> - <i>eyfp</i>	pJC1 derivative containing the promoter region (235 bp) of the genes <i>hrtBA</i> with an translational fusion to <i>eyfp</i> . The insert includes the first 24bp of <i>hrtB</i> , a stop codon and an additional ribosome binding site in front of <i>eyfp</i> .	This study
pJC1-P <sub><i>chrSA</i></sub> - <i>eyfp</i>	pJC1 derivative containing the promoter region (235 bp) of the genes <i>chrSA</i> with an translational fusion to <i>eyfp</i> . The insert includes the first 24bp of <i>chrS</i> , a stop codon, and an additional ribosome binding site in front of <i>eyfp</i> .	This study
pJC1-P <sub><i>hmuO</i></sub> - <i>eyfp</i>	pJC1 derivative containing the upstream region (494 bp) of the gene <i>hmuO</i> with an transcriptional fusion to <i>eyfp</i> . The insert includes the first 123 bp of <i>hmuO</i> , a stop codon, and an additional ribosome binding site in front of <i>eyfp</i> .	This study

Table S2. Oligonucleotides used in this study<sup>a</sup>

Oligonucleotide	Sequence 5' -> 3'	Restriction site
<b>Primer for deletion plasmids</b>		
DhrtAB-1	CGCGGATCCCGCCGTCAGTATTGCAATGATGA	BamHI
DhrtAB-2	CCCATCCACTAAACTTAAACATGCGGTGAGTCTTTTAGTCCTTG	
DhrtAB-3	TGTTTAAGTTTAGTGATGGGGTCCACCTCTCACACCCAC	
DhrtAB-4	ACGCGTCCGACCGTCTTTGGTCTGCAATGACAC	Sall
DhrtBA-fw	GACCGGTGACAACGCCAACAG	
DhrtBA-rv	GATGACTGGTGGGAACGTGAG	
DchrSA-1	TATAGTCGACCACTACATCATGCGCAGTAGCG	Sall
DchrSA-2	CCCATCCACTAAACTTAAACAAATTCGGGCGATGGTCGCTTGGC	
DchrSA-3	TGTTTAAGTTTAGTGATGGGCAGCGCGGAATTATCTAGACGC	
DchrSA-4	TATACTGCAGGTGCTGGTTGGCGCCAGTTTGG	PstI
DchrSA-fw	TTCATCAATACCACGGGCAGGTG	
DchrSA-rv	TTACGTTGGCTCGCTGCGCTTC	
DhrrSA-1	TATACCCGGGATGTGGCCTTCTAATAGTTAGA	XmaI
DhrrSA-2	CCCATCCACTAAACTTAAACACAGCGAGGCTGTCAAATGTGGA	
DhrrSA-3	TGTTTAAGTTTAGTGATGGGCTCGGCGTGCAGTACGTACC	
DhrrSA-4	TATATATCTAGATGTGTATGGTACACATTTTGTGC	XbaI
DhrrSA-fw	CTCCTCATGGATGTTGTGTTCC	
DhrrSA-rv	AATCAATACACCGCCAAGCAGG	
<b>Oligonucleotides used for complementation</b>		
chrSA-fw	TCTAGCTAGCGCGGTGAGTCTTTTAGTC	NheI
chrSA rv	TCTAGCTAGCCTAGATAATTCGCGCTGTC	NheI
hrtBA-RBS-fw	AAAACCTGCAGAAGGAGATATAGATATGTTTCAAGGACTAAAAGAAGCTC	PstI
hrtAB-rv	TATACTGCAGCTACAGGTGTGGGGTGTGAG	PstI
<b>Oligonucleotides for overproduction of ChrA</b>		
chrA-NdeI-fw	TATACATATGATCCGTATTCTGTTGGCTGAT	NdeI
chrA-HindIII-rv	TATAAAGCTTCTAGATAATTCGCGCTGTCTGG	HindIII
<b>Oligonucleotides for promoter fusion studies</b>		
PchrS-BamHI-fw	CGCGGATCCCGGTGAGGGCAGAGAGGAAAG	BamHI
PchrS-8C-RBS-NdeI-rv	CGCCATATGATATCTCCTTCTTAAAGTTCAGATGGTCGCTTGGCTAGTTTTAC	NdeI
PhrtB-BamHI-fw	CGCGGATCCACACACCCCAATGGCTGG	BamHI
PhrtB-8C-RBS-NdeI-rv	CGCCATATGATATCTCCTTCTTAAAGTTCAGATGTTCTTTTAGTCCTGAAACAT	NdeI
PhmuO-NheI-fw	CTA GCTAGCGAAGTCTTGAAGTGTGGAAAAGC	NheI
PhmuO-RBS-rv	CCATATATCTCCTTCTTAAAGTTCATCGAGCTTCCCGGTGAGCAGATCA	
eyfp-RBS-fw	TGAACTTAAAGAAGGAGATATGGTGTGAGCAAGGGCGAGGAG	
eyfp-NheI-rv	CTAGCTAGCTTATCTAGACTTGTACAGCTCG	NheI
<b>Oligonucleotides for electrophoretic mobility shift assays</b>		
gntK-control-fw	ATGGTGGCGTCATGCTCGGCCG	

---

<b>gntK-control-rv</b>	GGATTTGCCGCAGCCAGAAACGC
<b>chrS-hrtB-fw</b>	GTGTCTGCTACTCGGTCGCGGAC
<b>chrS-hrtB-rv</b>	CACCAACACCAACAAAACGGC
<b>hmuO-fw</b>	ATGCGCTTGTGCTGGTCAGGGG
<b>hmuO-rv</b>	TCGGCCTCTTCATGGGCCTGCGC
<b>hrrA-fw</b>	TAACTACGAAGACACAGAAG
<b>hrrA-rv</b>	AGACTTCGCCCACCACTTCAATG
<b>chrS-hrtB-motif-fw</b>	TTCTTGCACTACGACCAAAGTCGGATTCGC
<b>chrS-hrtB-motif-rv</b>	GCGAATCCGACTTTGGTCGTAAGCAAGAA
<b>hrrA_motif_fw</b>	AAGGCTAGACTAAAGTACGATTCATCTGCT
<b>hrrA_motif_rv</b>	AGCAGATGAATCGTACTTTAGTCTAGCCTT
<b>hmuO-motif-fw</b>	AATTGTTCCAATAAGGGACTATATGTAGG
<b>hmuO-motif-rv</b>	CCTACATATAGTCCCTTAGTTGGAACAATT
<b>CgtR8_M1_for</b>	TTCAACGAGTACGACCAAAGTCGGATTCGC
<b>CgtR8_M1_rev</b>	TTCTTGCACTACGACCAAAGTCGGATTCGC
<b>CgtR8_M2_for</b>	TTCTTGCTCATCGACCAAAGTCGGATTCGC
<b>CgtR8_M2_rev</b>	GCGAATCCGACTTTGGTCGATGAGCAAGAA
<b>CgtR8_M3_for</b>	TTCTTGCACTAGCTGCAAAGTCGGATTCGC
<b>CgtR8_M3_rev</b>	GCGAATCCGACTTTGCAGCTACTGCAAGAA
<b>CgtR8_M4_for</b>	TTCTTGCACTACGACGTTTGTGCGATTCGC
<b>CgtR8_M4_rev</b>	GCGAATCCGACAAACGTCGTAAGCAAGAA
<b>CgtR8_M5_for</b>	TTCTTGCACTACGACCAAACAGCGATTCGC
<b>CgtR8_M5_rev</b>	GCGAATCGCTGTTTGGTCGTAAGCAAGAA
<b>CgtR8_M6_for</b>	TTCTTGCACTACGACCAAAGTCGCTAACGC
<b>CgtR8_M6_rev</b>	GCGTTAGCGACTTTGGTCGTAAGCAAGAA
<b>CgtR8_M7_for</b>	TTCTTGCACTACGACCAAAGTCGGATTGCG
<b>CgtR8_M7_rev</b>	CGCAATCCGACTTTGGTCGTAAGCAAGAA
<b>CgtR8_M8_for</b>	AAGTTGCACTACGACCAAAGTCGGATTCGC
<b>CgtR8_M8_rev</b>	GCGAATCCGACTTTGGTCGTAAGCAACTT

---

<sup>a</sup> Some oligonucleotides were designed with restriction sites (underlined) as indicated or with complementary sequences for overlap PCR, shown in italics.

**Table S3.** Promoters of putative ChrA target genes.

Gene ID	Gene <sup>a</sup>	Promoter sequence	TS position <sup>b</sup>
cg2201- cg2200	chrS, chrA	agtacgaccaaagtcggaTTcgCgttcatacttagttgatcTATcgTggtggcG	nt 2.095.028, leaderless
cg2202- cg2204	hrtB, hrtA	gaatcgaccagagcccgaTTaAaAaatgccccgcgcaacgAaAcTagtaatcA	nt 2.095.139, leaderless
cg2445	hmuO	ttgtccaactaagggactatatgtaggtgtgggtaacctaaGtTAatcTttgtgA	nt 2.331.195
cg3247	hrrA	gaggttgaactaagttctccaactgacgatgag <u>taaggc</u> TAGACTaaagtacG	nt 3.109.880
cg3248	hrrS	caagcggtagcatgatggaagcagcgaggatagtaggTAATGTacgacgcA	nt 3.111.231

<sup>a</sup> Operon structures controlled by the same promoter are shown in one box. The -10 and -35 regions are highlighted in bold, conserved bases in capitals. The stop codon of cg3248 (*hrrS*) is underlined. The end of the sequence represents the first base of the start codon.

<sup>b</sup> For the position of the transcriptional start the coryneregnet annotation ([www.coryneregnet.de](http://www.coryneregnet.de)) for *C. glutamicum* ATTC 13032 was used.

## References

- Blom, J., T. Jakobi, D. Doppmeier, S. Jaenicke, J. Kalinowski, J. Stoye & A. Goesmann, (2011) Exact and complete short-read alignment to microbial genomes using Graphics Processing Unit programming. *Bioinformatics* **27**: 1351-1358.
- Cremer, J., L. Eggeling & H. Sahm, (1990) Cloning the *dapA dapB* cluster of the lysine-secreting bacterium *Corynebacterium glutamicum*. *Mol Gen Genet* **220**: 478-480.
- Eikmanns, B. J., N. Thumschmitz, L. Eggeling, K. U. Lüdtke & H. Sahm, (1994) Nucleotide sequence, expression and transcriptional analysis of the *Corynebacterium glutamicum gltA* gene encoding citrate synthase. *Microbiology* **140**: 1817-1828.
- Kinoshita, S., S. Uda & M. Shimono, (1957) Studies on the amino acid fermentation: I. Production of L-glutamic acid by various microorganisms. *J Gen Appl Microbiol* **3**: 193-205.
- Mustafi, N., A. Grünberger, D. Kohlheyer, M. Bott & J. Frunzke, (2012) The development and application of a single-cell biosensor for the detection of L-methionine and branched-chain amino acids. *Metabolic Engineering*: doi:10.1016/j.ymben.2012.1002.1002.
- Niebisch, A. & M. Bott, (2001) Molecular analysis of the cytochrome *bc<sub>1</sub>-aa<sub>3</sub>* branch of the *Corynebacterium glutamicum* respiratory chain containing an unusual diheme cytochrome *c<sub>1</sub>*. *Arch Microbiol* **175**: 282-294.
- Patek, M. & J. Nesvera, (2011) Sigma factors and promoters in *Corynebacterium glutamicum*. *J Biotechnol* **154**: 101-113.
- Schäfer, A., A. Tauch, W. Jäger, J. Kalinowski, G. Thierbach & A. Pühler, (1994) Small mobilizable multi-purpose cloning vectors derived from the *Escherichia coli* plasmids pK18 and pK19: selection of defined deletions in the chromosome of *Corynebacterium glutamicum*. *Gene* **145**: 69-73.
- Studier, F. W. & B. A. Moffatt, (1986) Use of bacteriophage T7 RNA polymerase to direct selective high-level expression of cloned genes. *J Mol Biol* **189**: 113-130.
- van der Rest, M. E., C. Lange & D. Molenaar, (1999) A heat shock following electroporation induces highly efficient transformation of *Corynebacterium glutamicum* with xenogeneic plasmid DNA. *Appl Microbiol Biotechnol* **52**: 541-545.



Contents lists available at SciVerse ScienceDirect

Plasmid

journal homepage: [www.elsevier.com/locate/yplas](http://www.elsevier.com/locate/yplas)

Short Communication

## A tetracycline inducible expression vector for *Corynebacterium glutamicum* allowing tightly regulable gene expression

Frank Lausberg\*, Ava Rebecca Chattopadhyay, Antonia Heyer, Lothar Eggeling, Roland Freudl\*

Institut für Bio- und Geowissenschaften, IBG1: Biotechnologie, Forschungszentrum Jülich GmbH, D-52425 Jülich, Germany

## ARTICLE INFO

## Article history:

Received 19 March 2012

Accepted 5 May 2012

Available online 12 May 2012

Communicated by Richard Calendar

## Keywords:

*Corynebacterium glutamicum*

Expression vector

Anhydrotetracycline

TetR

Promoter

## ABSTRACT

Here we report on the construction of a tetracycline inducible expression vector that allows a tightly regulable gene expression in *Corynebacterium glutamicum* which is used in industry for production of small molecules such as amino acids. Using the green fluorescent protein (GFP) as a reporter protein we show that this vector, named pCLTON1, is characterized by tight repression under non-induced conditions as compared to a conventional IPTG inducible expression vector, and that it allows gradual GFP synthesis upon gradual increase of anhydrotetracycline addition.

© 2012 Elsevier Inc. All rights reserved.

## 1. Introduction

*Corynebacterium glutamicum* is a Gram-positive soil bacterium that has been used for industrial amino acid production for decades (Yamada et al., 1972; Aida et al., 1986; Leuchtenberger, 1996; Ikeda, 2003). Besides that it has become a platform organism for the production of different chemicals and fuels (Becker and Wittmann, 2011; see also references therein), as well as for the secretory production of heterologous proteins (Liebl et al., 1992; Kikuchi et al., 2006; Meissner et al., 2007). In addition, it serves as a model organism for the investigation of cell envelope biogenesis and composition in *Actinobacteria* (Hoffmann et al., 2008; Bansal-Mutalik and Nikaido, 2011; Marchand et al., 2011).

Both for basic and applied research it is essential to have genetic tools which allow controlled expression of homologous and heterologous genes. Accordingly, a variety of such vectors have been developed for *C. glutamicum*.

**Abbreviations:** IPTG, isopropyl- $\beta$ -D-thiogalactopyranoside; ATc, anhydrotetracycline.

\* Corresponding authors. Fax: +49 2461 612710.

E-mail addresses: [f.lausberg@fz-juelich.de](mailto:f.lausberg@fz-juelich.de) (F. Lausberg), [r.freudl@fz-juelich.de](mailto:r.freudl@fz-juelich.de) (R. Freudl).

Most of these are IPTG inducible (Eikmanns et al., 1991; Jakoby et al., 1999; Kirchner and Tauch, 2003), but also heat inducible (Tsuchiya and Morinaga, 1988; Park et al., 2008) and carbon source inducible (Okibe et al., 2010) expression vectors have been constructed. A great disadvantage of the so far available regulable expression vectors is the leaky expression of the target gene in the absence of an inducer (Pátek et al., 2003 and our own unpublished observations).

An expression system which is known to allow tightly regulated gene expression is the tetracycline inducible Tet repressor (TetR) based expression system derived from the *Escherichia coli* Transposon Tn10 (Hillen and Berens; 1994). This system has been employed successfully in a variety of Gram-positive bacteria (Geissendörfer and Hillen, 1990; Bateman et al., 2001; Ehrt et al., 2005; Fagan and Fairweather, 2011). In fact, a previous report has shown that a TetR based expression system allows controlled expression of a chromosomally encoded gene in *C. glutamicum* (Radmacher et al., 2005).

To also allow the use of the TetR-dependent, tetracycline inducible expression system for regulated expression of plasmid encoded genes, we have constructed a tetracycline inducible expression vector for *C. glutamicum*. The vector is based on the ColE1 replicon of *E. coli*, the pBL1 replicon of *C.*

*glutamicum*, it carries the *tetR* gene under the control of a strong constitutive *C. glutamicum* promoter (Radmacher et al., 2005) and a TetR controllable promoter derived from *Bacillus subtilis* (Kamionka et al., 2005). It could be shown that this newly constructed expression vector allows a gradual induction of a reporter protein and shows a tightly repressed basal expression under non-induced conditions.

## 2. Material and methods

### 2.1. Bacterial strains, plasmids, and culture conditions

The bacterial strains and plasmids used in this study are listed in Table 1. *E. coli* was grown at 37 °C in Luria Bertani medium (Miller, 1972). *C. glutamicum* was grown at 30 °C in BHI medium (Difco). If required, isopropyl- $\beta$ -D-thiogalactopyranoside (IPTG) was used at a concentration of 1 mM, anhydrotetracycline (ATc) was used at concentrations ranging from 10 to 250 ng/ml. Antibiotic supplements were at the following concentrations: kanamycin, 50 mg/l (*E. coli*); 25 mg/l (*C. glutamicum*). *E. coli* was transformed with plasmid DNA by the CaCl<sub>2</sub> method (Cohen et al., 1972). *C. glutamicum* was transformed with plasmid DNA by electroporation as described previously (Reyes and Eggeling, 2005).

### 2.2. DNA manipulation and plasmid construction

All DNA manipulations followed standard procedures (Sambrook et al., 1989). The following oligonucleotides were used as PCR primers (restriction enzyme recognition sites are underlined):

Primer1 (AACTGCAGAAAGGAGATATAGATATGAGTAAAGGAGAAGAACTTTTCACTG),  
Primer 2 (CGGAATTCTTATTTGTAGAGCTCATCCATGCC),  
Primer 3 (AGAGAGCGTACGCGTTTGTGAACCTAATGGTGCTTTAG),

Primer 4 (CTCTCTCTGCAGGTGTATCAACAAGCTGGGGA TCTTAAG).

Plasmid pEKEx2-GFP was constructed by amplifying the *gfp* gene via PCR using primers 1 and 2 and vector pCGTorA-GFP (Meissner et al., 2007) as the template. The PCR product was digested with *Pst*I and *Eco*RI and ligated into the *Pst*I/*Eco*RI digested pEKEx2 vector. pTc105-GFP was constructed by replacing the *lacI<sup>q</sup>* and *ptac* regions from pEKEx2-GFP by a TetR controllable promoter from pWH105 (Kamionka et al., 2005). The promoter was amplified via PCR using primers 3 and 4 and pWH105 as the template, digested with *Bsi*WI and *Pst*I and ligated with the 6.9 kb fragment of the *Bsi*WI/*Pst*I digested pEKEx2-GFP. Plasmid pCLTON1-GFP was constructed by incorporating the *tetR* gene under control of the strong *C. glutamicum* promoter of the glyceraldehyde-3-phosphate dehydrogenase (*pgap*) from the vector pJC1-*pgap-tetR* (Radmacher et al., 2005) into pTc105-GFP vector. Therefore, the 1.4 kb *Bam*HI/*Dra*I fragment from pJC1-*pgap-tetR* was filled in using the Klenow fragment of DNA polymerase and ligated into the pTc105-GFP vector which had been digested with *Bsi*WI and was also filled in using the Klenow fragment of DNA polymerase. After ligation and transformation of *E. coli*, different clones were checked by an asymmetric digestion with *Xba*I. *Xba*I cuts once at the beginning of the *tetR* gene and once elsewhere in the vector. Thus a clone could be selected in which the *pgap* promoter was oriented in opposite direction to the pWH105 promoter. The pCLTON1 empty vector was constructed by replacing the 3.3 kb *Pst*I/*Pvu*I fragment encompassing the *gfp* gene with the 2.6 kb *Pst*I/*Pvu*I fragment of pEKEx2, thus restoring the pEKEx2 multiple cloning site.

### 2.3. Preparation of whole cell extracts

For protein analysis, *C. glutamicum* was grown overnight in BHI medium. The overnight culture was washed

**Table 1**  
Bacterial strains and plasmids.

Bacterial strains and plasmids	Relevant properties <sup>a</sup>	Source
<b>Bacterial strains</b>		
<i>E. coli</i> XL1-Blue	<i>recA1 endA1 gyrA96 thi-1 hsdR17 supE44 relA1 lac</i> [ <i>f<sup>+</sup> proAB lacI<sup>q</sup> ZAM15 Tn10 (Tet<sup>r</sup>)</i> ]	Stratagene (Heidelberg)
<i>C. glutamicum</i> ATCC13032	Wild-type	Abe et al. (1967)
<b>Plasmids</b>		
pEKEx2	<i>ptac</i> , <i>lacI<sup>q</sup></i> , Km <sup>r</sup>	Eikmanns et al. (1991)
pWH105	pWH102 derivative with second <i>tetO</i> cloned in <i>Bam</i> HI site; Ap <sup>r</sup> , Cm <sup>r</sup>	Kamionka et al. (2005)
pJC1- <i>pgap-tetR</i>	pJC1 containing the <i>tetR</i> gene under control of <i>pgap</i> promoter from <i>C. glutamicum</i> ; Km <sup>r</sup>	Radmacher et al. (2005)
pCGTorA-GFP	pEKEx2 containing a <i>torA-gfp</i> hybrid gene	Meissner et al. (2007)
pEKEx2-GFP	pEKEx2 containing the <i>gfp</i> gene	This study
pTc105-GFP	<i>ptac</i> and <i>lacI<sup>q</sup></i> deficient variant of pEKEx2-GFP with the <i>B. subtilis</i> derived <i>ptet</i> promoter from pWH105	This study
pCLTON1-GFP	pTc105-GFP with <i>pgap-tetR</i> from pJC1- <i>pgap-tetR</i>	This study
pCLTON1	<i>C. glutamicum</i> expression vector with the <i>B. subtilis</i> derived <i>ptet</i> promoter from pWH105 and the <i>tetR</i> gene under control of <i>C. glutamicum</i> <i>pgap</i> promoter from pJC1- <i>pgap-tetR</i> ; Km <sup>r</sup>	This study

<sup>a</sup> Ap<sup>r</sup>, ampicillin resistance; Km<sup>r</sup>, kanamycin resistance; Cm<sup>r</sup>, chloramphenicol resistance; Tet<sup>r</sup>, tetracycline resistance.

once with fresh BHI medium and used to inoculate a BHI medium induction culture to an  $OD_{600}$  of 1.0. Gene expression was induced at 30 °C for 4 h by the addition of IPTG or ATc, respectively, as indicated in the results and discussion section. Cells were separated from the supernatant by centrifugation. Cells were washed in 30 mM Tris/HCl pH 8.0 and resuspended in the same buffer. *C. glutamicum* cells were disrupted with 0.1 mm zirconia/silica beads (BioSpec Products, Inc.; Bartlesville, USA) using a MM2 mixer mill (Retsch GmbH; Haan, Germany). Cell debris and glass beads were removed from the whole cell lysate by centrifugation.

#### 2.4. Miscellaneous procedures

SDS-PAGE and Western blotting were done as described earlier (Kreutzenbeck et al., 2007). Immunological detection of GFP derived polypeptides was performed by using a polyclonal anti-GFP antibody. Visualization was done using an ECL Western blotting detection kit (GE Healthcare; Buckinghamshire, UK) according to the manufacturer's instructions. The chemoluminescent protein bands were recorded using a Fujifilm LAS-3000 Mini CCD camera and image analyzing system (Fuji Photo Film Europe GmbH; Düsseldorf, Germany) together with the software AIDA 4.15 (Raytest GmbH; Straubenhardt, Germany).

#### 2.5. Fluorescence spectroscopy

*C. glutamicum* cells were induced for 4 h as described above. Cells corresponding to an  $OD_{600}$  of 0.5 were taken from cultures, harvested by centrifugation, washed with 30 mM Tris/HCl pH 8.0 and resuspended in 1 ml 30 mM Tris/HCl pH 8.0. The suspension was incubated at 4 °C for further 3.5 h. The relative fluorescence intensity was measured using a FP-6500 Spectrofluorometer (Jasco Germany

GmbH; Groß-Umstadt, Germany) in the “emission spectrum” measurement mode together with a precision cell made of Quartz Suprasil (Hellma GmbH & Co. KG; Mühlheim, Germany) with a 10 mm light path. The excitation wavelength was set to 395.0 nm. The emission spectrum was measured between 410 and 650 nm. The data were recorded and evaluated with the “spectra manager” software 1.53.01 (Jasco Germany GmbH; Groß-Umstadt, Germany).

### 3. Results and discussion

#### 3.1. Construction of a *C. glutamicum* vector containing a heterologous promoter with two tet-operator sites and a constitutively expressed tetR gene

Expression of target genes from vectors with controllable promoters is an important tool for studying gene function. Throughout our work with *C. glutamicum* we often observed leaky expression of genes cloned into expression vectors with IPTG inducible promoters. Leaky expression of target genes is often an undesired trait e.g. in a situation where a low amount of the target gene product is sufficient to develop a phenotype. As the tetracycline inducible TetR based expression system has proven its suitability concerning tight expression control in a number of Gram-positive bacteria (Bateman et al., 2001; Ehart et al., 2005; Kamionka et al., 2005; Fagan and Fairweather, 2011), we addressed the question whether it can also be used advantageously for *C. glutamicum*. Therefore, we constructed the vector pCLTON1, containing a TetR controllable promoter and the *tetR* gene itself, with its detailed construction outlined in the Section 2. Briefly, the plasmid backbone consists of the *C. glutamicum* expression vector pEKEx2 (Eikmanns et al., 1991) lacking its *laqI*<sup>q</sup> and *ptac* regions. It contains a multiple cloning site, transcriptional terminators, a kanamycin resistance gene and the origins of

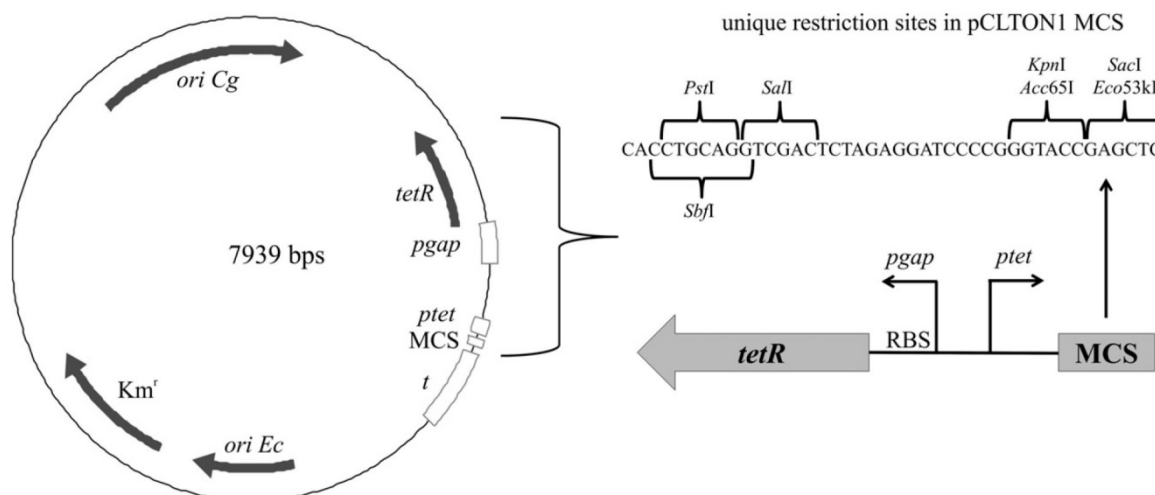


**Fig. 1.** Schematic drawing of the tetracycline inducible expression vector pCLTON1. On the left side the entire plasmid is shown including its transcriptional terminator (*t*), a kanamycin resistance marker (*Km<sup>r</sup>*), the origins of replication for maintenance in *E. coli* (*ori Ec*) and *C. glutamicum* (*ori Cg*) and the Tet-Repressor based expression system, which is displayed enlarged on the right side. It consists of the *tetR* gene with its ribosome binding site (RBS) under control of the promoter *pgap* and the *B. subtilis* derived TetR-controllable promoter from pWH105 with two TetR binding sites (*ptet*). The multiple cloning site (MCS) with its unique restriction enzyme recognition sites is also presented in detail.

replication for maintenance in *E. coli* and *C. glutamicum*. The TetR-controllable promoter is derived from the *B. subtilis* vector pWH105 (Kamionka et al., 2005), has two *tet*-operator sites and is functional in *C. glutamicum* (Heyer and Eggeling, unpublished data). The *tetR* gene is constitutively expressed by the strong *C. glutamicum* promoter of the glyceraldehyde-3-phosphate dehydrogenase as described by Radmacher et al. (2005). A schematic drawing of pCLTON1 is given in Fig. 1.

### 3.2. The expression of GFP from pCLTON1-GFP is tightly repressed under non-induced conditions and can gradually be induced by increasing inducer concentrations

In order to analyze the functionality of the newly constructed tetracycline inducible *C. glutamicum* expression vector pCLTON1, we chose a variant of GFP (GFPuv) from the jellyfish *Aequorea victoria* as reporter protein (Chalfie et al., 1994; Cramer et al., 1996). The gene encoding GFP(uv) was cloned into pCLTON1 and into the parental IPTG inducible expression vector pEKEx2 as outlined in the Section 2. The resulting vectors pCLTON1-GFP and pEKEx2-GFP were used to transform *C. glutamicum*. As a control, *C. glutamicum* was also transformed with the empty pCLTON1 vector. GFP

expression was induced with anhydrotetracycline (ATc) concentrations ranging from 10 to 250 ng/ml culture. The strain harboring the empty pCLTON1 vector was cultivated either uninduced or induced with 250 ng/ml ATc. The strain containing the pEKEx2-GFP vector was also cultivated uninduced or induced with 1 mM IPTG.

The Western-blot presented in Fig. 2A clearly shows that pCLTON1 is functional as GFP is expressed in an ATc dependent manner. The GFP expression from pCLTON1-GFP is tightly repressed under non-induced conditions, here only a faint band is visible. GFP expression gradually increases at ATc concentrations between 25 and 150 ng/ml. At ATc concentrations of 150 ng/ml and higher the GFP expression from pCLTON1-GFP is fully induced. When comparing the GFP expression of the strain harboring the newly constructed, ATc inducible pCLTON1-GFP with the GFP expression of the strain with the IPTG inducible pEKEx2-GFP vector under fully induced conditions, it is evident that the GFP expression level is somewhat lower in the case of the ATc inducible pCLTON1 vector. As a consequence of this observation, pCLTON1 is probably not the vector of choice when high levels of a desired target protein are required. However, it is also evident from the Western-blot that the GFP expression is much

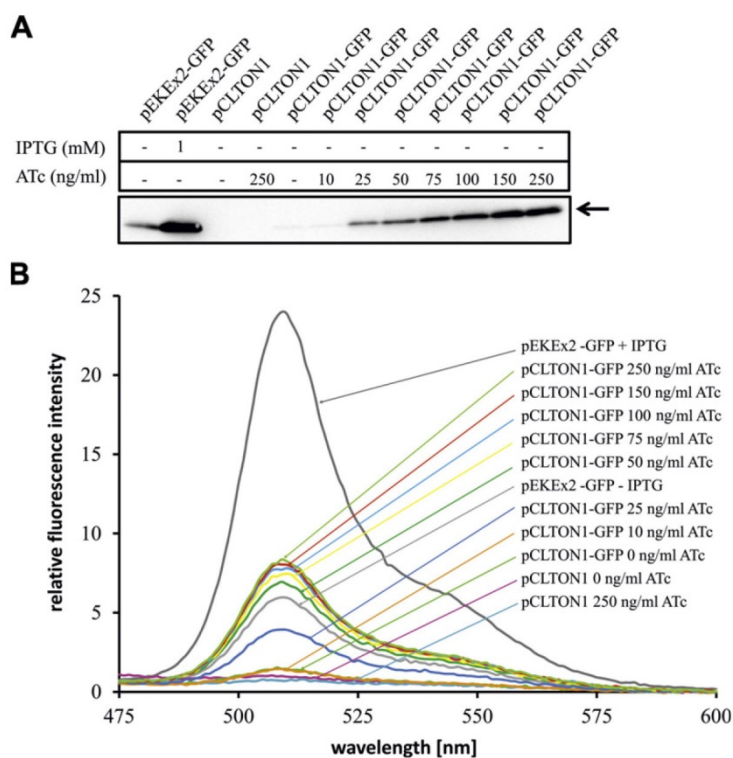


**Fig. 2.** pCLTON1 based expression of GFP in *C. glutamicum*. (A) Analysis of GFP expression on protein level. Whole cell lysates of induction cultures from *C. glutamicum* containing plasmids pEKEx2-GFP (lanes 1 and 2), pCLTON1 (lanes 3 and 4) or pCLTON1-GFP (lanes 5–12) were prepared. Of each strain, whole cell lysates from 1 ml culture with an  $OD_{600}$  of 0.25 were used for SDS-PAGE and Western blotting using GFP-specific antibodies. IPTG was used to induce GFP expression of the strain containing pEKEx2-GFP. ATc was used to induce GFP expression of the strains containing pCLTON1 and pCLTON1-GFP. The respective inducer concentrations are indicated above the corresponding lane. Arrow = GFP. (B) Analysis of GFP expression by fluorescence measurement. Cells corresponding to an  $OD_{600}$  of 0.5 were taken from the same cultures described in (A), treated as explained in the Section 2 and used for measurement of the fluorescence emission of whole *C. glutamicum* cells. The emission spectrum from 475 to 600 nm is shown. The strains and the used inducer concentrations are assigned to the respective emission curve by arrows.

tighter repressed in the case of pCLTON1-GFP in comparison to pEKEx2-GFP under uninduced conditions. As mentioned above, the strain carrying pCLTON1-GFP only shows a faint GFP-band without ATc (Fig. 2A), whereas the strain with the pEKEx2-GFP vector shows a clear GFP protein band due to leaky expression of GFP in the uninduced state from the IPTG controllable promoter.

Furthermore, we also determined the GFP-fluorescence of the strains carrying the different expression vectors (Fig. 2B). In agreement with the protein data from Fig. 2A, a clear ATc dependent gradual increase of the GFP fluorescence was observed within the strains carrying pCLTON1-GFP. The measurement also confirms that gene expression from pCLTON1 is tightly repressed under uninduced conditions as there is only a very low fluorescence peak at 509 nm whereas the strain carrying the pEKEx2-GFP vector shows a clear fluorescence peak even without inducer. Due to the tight repression of gene expression under uninduced conditions, pCLTON1 will be very useful for studies that demand tight repression of the target gene.

#### 4. Conclusion

In the present work we have implemented a tetracycline inducible, plasmid based expression system consisting of the tetracycline controllable transcriptional repressor TetR and a heterologous promoter with two TetR binding sites for use in *C. glutamicum*. The newly constructed expression vector allows a gradual expression of a target gene and clearly outperforms a representative of IPTG inducible *C. glutamicum* expression vectors concerning the level of repression of gene expression under non-induced conditions.

This vector can be especially beneficial, when the experimental setup demands tight repression of the expression substrate e.g. when studying the function of genes by conditional gene knockdown or for the expression of toxic gene products.

Besides the potential benefits of pCLTON1 concerning the tightly repressible target gene expression, it also expands the range of tools for the genetic manipulation of *C. glutamicum* in another way. pCLTON1 is the first described ATc inducible *C. glutamicum* expression vector and it can be of great advantage when the experimental strategy demands the use of two differentially controllable expression vectors in one host.

#### Acknowledgments

We are very grateful to W. Hillen for the generous gift of the plasmid pWH105. We thank D. Oertel for critical reading of the manuscript and M. Bott for ongoing support.

#### References

- Abe, S., Takayama, K.I., Kinoshita, S., 1967. Taxonomical studies on glutamic acid-producing bacteria. *J. Gen. Appl. Microbiol.* 13, 279–301.
- Aida, K., Chibata, I., Nakayama, K., Takinami, K., Yamada, H., 1986. *Biotechnology of Amino Acid Production*. Progress in Industrial Microbiology. Kodansha Ltd., Tokyo; Elsevier, Amsterdam-Oxford-New York-Tokyo.
- Bansal-Mutalik, R., Nikaido, H., 2011. Quantitative lipid composition of cell envelopes of *Corynebacterium glutamicum* elucidated through reverse micelle extraction. *Proc. Natl. Acad. Sci. USA* 108, 15360–15365.
- Bateman, B.T., Donegan, N.P., Jarry, T.M., Palma, M., Cheung, A.L., 2001. Evaluation of a tetracycline-inducible promoter in *Staphylococcus aureus* in vitro and in vivo and its application in demonstrating the role of sigB in microcolony formation. *Infect. Immun.* 69, 7851–7857.
- Becker, J., Wittmann, C., 2011. Bio-based production of chemicals, materials and fuels – *Corynebacterium glutamicum* as versatile cell factory. *Curr. Opin. Biotechnol.* (Epub ahead of print).
- Chalfie, M., Tu, Y., Euskirchen, G., Ward, W.W., Prasher, D.C., 1994. Green fluorescent protein as a marker for gene expression. *Science* 263, 802–805.
- Cohen, S.N., Chang, A.C., Hsu, L., 1972. Nonchromosomal antibiotic resistance in bacteria: genetic transformation of *Escherichia coli* by R-factor DNA. *Proc. Natl. Acad. Sci. USA* 69, 2110–2114.
- Cramer, A., Whitehorn, E.A., Tate, E., Stemmer, W.P., 1996. Improved green fluorescent protein by molecular evolution using DNA shuffling. *Nat. Biotechnol.* 14, 315–319.
- Ehrt, S., Guo, X.V., Hickey, C.M., Ryou, M., Monteleone, M., Riley, L.W., Schnappinger, D., 2005. Controlling gene expression in mycobacteria with anhydrotetracycline and Tet repressor. *Nucleic Acids Res.* 33, e21.
- Eikmanns, B.J., Kleinertz, E., Liebl, W., Sahm, H., 1991. A family of *Corynebacterium glutamicum*/*Escherichia coli* shuttle vectors for cloning, controlled gene expression, and promoter probing. *Gene* 102, 93–98.
- Fagan, R.P., Fairweather, N.F., 2011. *Clostridium difficile* has two parallel and essential Sec secretion systems. *J. Biol. Chem.* 286, 27483–27493.
- Geissendörfer, M., Hillen, W., 1990. Regulated expression of heterologous genes in *Bacillus subtilis* using the Tn10 encoded tet regulatory elements. *Appl. Microbiol. Biotechnol.* 33, 657–663.
- Hillen, W., Berens, C., 1994. Mechanisms underlying expression of Tn10 encoded tetracycline resistance. *Annu. Rev. Microbiol.* 48, 345–369.
- Hoffmann, C., Leis, A., Niederweis, M., Plitzko, J.M., Engelhardt, H., 2008. Disclosure of the mycobacterial outer membrane: cryo-electron tomography and vitreous sections reveal the lipid bilayer structure. *Proc. Natl. Acad. Sci. USA* 105, 3963–3967.
- Ikeda, M., 2003. Amino acid production processes. *Adv. Biochem. Eng.* 79, 2–35.
- Jakoby, M., Ngouoto-Nkili, C.-E., Burkovski, A., 1999. Construction and application of new *Corynebacterium glutamicum* vectors. *Biotechnol. Tech.* 13, 437–441.
- Kamionka, A., Bertram, R., Hillen, W., 2005. Tetracycline-dependent conditional gene knockout in *Bacillus subtilis*. *Appl. Environ. Microbiol.* 71, 728–733.
- Kikuchi, Y., Date, M., Itaya, H., Matsui, K., Wu, L.F., 2006. Functional analysis of the twin-arginine translocation pathway in *Corynebacterium glutamicum* ATCC 13869. *Appl. Environ. Microbiol.* 72, 7183–7192.
- Kirchner, O., Tauch, A., 2003. Tools for genetic engineering in the amino acid producing bacterium *Corynebacterium glutamicum*. *J. Biotechnol.* 104, 287–299.
- Kreutzenbeck, P., Kröger, C., Lausberg, F., Blaudeck, N., Sprenger, G.A., Freudl, R., 2007. *Escherichia coli* twin arginine (Tat) mutant translocases possessing relaxed signal peptide recognition specificities. *J. Biol. Chem.* 282, 7903–7911.
- Leuchtenberger, W., 1996. Amino acids – technical production and use. In: Rehm, H.J., Pühler, A., Reed, G., Stadler, P.J.W. (Eds.), *Biotechnology*, vol. 6. VCH Verlagsgesellschaft, Weinheim, Germany, pp. 465–502.
- Liebl, W., Sinskey, A.J., Schleifer, K.H., 1992. Expression, secretion, and processing of staphylococcal nuclease by *Corynebacterium glutamicum*. *J. Bacteriol.* 174, 1854–1861.
- Marchand, C.H., Salmeron, C., Bou Raad, R., Méniche, X., Chami, M., Masi, M., Blanot, D., Daffé, M., Tropis, M., Huc, E., Le Maréchal, P., Decottignies, P., Bayan, N., 2011. Biochemical disclosure of the mycolate outer membrane of *Corynebacterium glutamicum*. *J. Bacteriol.* 194, 587–597.
- Meissner, D., Vollstedt, A., van Dijk, J.M., Freudl, R., 2007. Comparative analysis of twin-arginine (Tat)-dependent protein secretion of a heterologous model protein (GFP) in three different Gram-positive bacteria. *Appl. Microbiol. Biotechnol.* 76, 633–642.
- Miller, J.H., 1972. *A Short Course in Bacterial Genetics. A Laboratory Manual and Handbook for Escherichia coli and related Bacteria*. Cold Spring Harbor Laboratory, Cold Spring Harbor, NY.
- Okibe, N., Suzuki, N., Inui, M., Yukawa, H., 2010. Isolation, evaluation and use of two strong, carbon source-inducible promoters from *Corynebacterium glutamicum*. *Lett. Appl. Microbiol.* 50, 173–180.

- Park, J.U., Jo, J.H., Kim, Y.J., Chung, S.S., Lee, J.H., Lee, H.H., 2008. Construction of heat-inducible expression vector of *Corynebacterium glutamicum* and *C. ammoniagenes*: fusion of lambda operator with promoters isolated from *C. ammoniagenes*. *J. Microbiol. Biotechnol.* 18, 639–647.
- Pátek, M., Nešvera, J., Guyonvarch, A., Reyes, O., Leblon, G., 2003. Promoters of *Corynebacterium glutamicum*. *J. Biotechnol.* 104, 311–323.
- Radmacher, E., Stansen, K.C., Besra, G.S., Alderwick, L.J., Maughan, W.N., Hollweg, G., Sahm, H., Wendisch, V.F., Eggeling, L., 2005. Ethambutol, a cell wall inhibitor of *Mycobacterium tuberculosis*, elicits L-glutamate efflux of *Corynebacterium glutamicum*. *Microbiology* 151, 1359–1368.
- Reyes, O., Eggeling, L., 2005. Experiments. In: Eggeling, L., Bott, M. (Eds.), *Handbook of Corynebacterium glutamicum*. CRC Press/Taylor & Francis Group, Boca Raton, Florida, pp. 535–566.
- Sambrook, J., Fritsch, E.F., Maniatis, T., 1989. *Molecular Cloning: A Laboratory Manual*, second ed. Cold Spring Harbor Laboratory, Cold Spring Harbor, New York.
- Tsuchiya, M., Morinaga, Y., 1988. Genetic control systems of *Escherichia coli* can confer inducible expression of cloned genes in coryneform bacteria. *Nat. Biotechnol.* 6, 428–430.
- Yamada, K., Kinoshita, S., Tsunoda, T., Aida, K., 1972. *The Microbial Production of Amino Acids*. Kodansha Ltd., Tokyo.

Name of the journal:	Plasmid
Impact factor:	1.516 (5- year: 1.744)
Contribution of own work:	15%
3. Author:	Experimental work and assistance in writing of the manuscript.

# ***Curriculum vitae***

Name	Antonia Heyer
Date of birth	15.05.1985
Place of birth	Neuss
1996-2004	Marie Curie Gymnasiums Neuss, Germany Abitur
2004-2005	Heinrich-Hertz-Berufskolleg Düsseldorf, Germany Qualification: Certified chemical technical assistant
2005-2010	Studies of Biology at the Heinrich-Heine-Universität Düsseldorf
2009-2010	Diploma thesis in the group "Amino acids und cell wall" of Dr. Lothar Eggeling at the Institute of Biotechnology IBT-1, Forschungszentrum Jülich, Germany "Silencing of essential genes in <i>Corynebacterium glutamicum</i> "
2010-2013	PhD thesis in the group "Population heterogeneity and signal transduction" of Jun.-Prof. Dr. Julia Frunzke at the Institute of Bio- and Geosciences, IBG-1: Biotechnology, Forschungszentrum Jülich "Characterization of a novel phage-encoded actin-like protein and the function of the ChrSA two-component system in <i>Corynebacterium glutamicum</i> "
Jülich, 23 May 2013	Antonia Heyer



# Danksagung

Ein ganz besonderer Dank gilt Jun.-Prof. Dr. Julia Frunzke, für Überlassung des spannenden Themas und die Ermöglichung der Doktorarbeit, sowie für die exzellente Betreuung und die vielen Ideen.

Des Weiteren möchte mich bei Professor Wagner für die Übernahme des Zweigutachtens bedanken und erinnere mich gerne an die Zeit der Grundvorlesung bei ihm zurück.

Bei Catriona Donovan und Marc Bramkamp in München möchte ich mich für die effektive und motivierende Zusammenarbeit trotz der größeren Entfernung bedanken.

Zudem möchte ich mich herzlich bei allen jetzigen und ehemaligen Mitgliedern meiner Arbeitsgruppe für die schöne Zeit, die vielen guten Ratschläge und die lustigen Momente im Labor bedanken. Dabei möchte ich besonders meiner Master-Studentin Kim Gärtner für ihre Arbeit zu den Integrasen unseres Prophagens danken, Nuriye Mustafi für den gemeinsamen Laboraufbau in unserer Anfangszeit und Meike Baumgart für ihre Hilfe am Maldi und wertvolle Tipps.

Außerdem möchte ich mich bei Cornelia Gätgens und Eva Hentschel für die sehr gute Zusammenarbeit im Häm Projekt bedanken. Natürlich gilt mein Dank auch dem restlichen Häm-Team, Christina Mack und Melanie Brocker. Zudem möchte ich unserem interdisziplinären DFG-Team, Arun Nanda, Stefan Helfrich, Christina Krämer, Alexander Grünberger, Katharina Nöh, Dietrich Kohlheyer, sowie Wolfgang Wiechert und Julia Frunzke für die schöne und produktive Zeit danken, insbesondere in München.

Weiterhin möchte ich mich allen Mitgliedern des IBG-1 für die freundliche, offene und hilfsbereite Arbeitsatmosphäre bedanken, vor allem bei Katharina Raasch für ihre Tipps und Tricks sowie Alexander Grünberger und Jennifer Pahlke für die aufschlussreiche Fachsimelei.

Auch möchte ich mich bei allen Jülicher Doktoranden und Postdocs für die netten Abende bedanken, die das Leben in Jülich versüßt haben.

Natürlich danke ich auch meinen Freunden in Neuss, Düsseldorf und Solingen, die für gute Abwechslung, schöne Stunden und Aufmunterungen gesorgt haben.

Von ganzem Herzen danke ich auch meinem Freund Toni, der immer für mich da war und mich liebevoll und geduldig unterstützt und motiviert hat.

Abschließend möchte ich mich bei meinen Eltern Albrecht und Anemone und meinen Schwestern Annika und Amelie ganz herzlich für die liebevolle Unterstützung und den Rückhalt bedanken.



# Erklärung

Ich versichere an Eides Statt, dass die vorgelegte Dissertation von mir selbständig und ohne unzulässige fremde Hilfe unter Beachtung der „Grundsätze zur Sicherung guter wissenschaftlicher Praxis an der Heinrich-Heine-Universität Düsseldorf“ erstellt worden ist. Die Dissertation wurde in der vorgelegten oder in ähnlicher Form noch bei keiner anderen Institution eingereicht. Ich habe bisher keine erfolglosen Promotionsversuche unternommen.

---

Jülich, den 23.05.2013